THE UNIVERSITY OF HULL

ON-LINE MONITORING OF WATER QUALITY PARAMETERS

being a Thesis submitted for the Degree of

DOCTOR OF PHILOSOPHY

in the University of Hull

by

RICHARD LYNN BENSON

B.Sc., M.Sc.

November, 1991

ACKNOWLEDGEMENTS

I would like to thank my supervisor, Professor Paul Worsfold, for his invaluable encouragement, advice and guidance throughout the course of this work.

My thanks also to Frank Sweeting, for providing me with useful practical advice, suggestions and discussion.

I would like to acknowledge Wessex Water for financial support.

I also gratefully acknowledge the technical assistance generously given to me by Dick Middleton and Adrian Hopkins, and all the staff in the Department of Chemistry, University of Hull and latterly the Department of Environmental Sciences, Polytechnic South West.

Finally, I extend my special thanks to all my friends and colleagues in Hull and Plymouth, and in particular to Paul MacLaurin and Simon Lewis for their unfaltering support and friendship during the past year.

To my parents, for their continuing love, support and encouragement.

ABSTRACT

Chapter one summarises the development of UK legislation for the protection of the aquatic environment, and highlights current EC legislative requirements for water quality. The need for on-line water quality monitoring and the alternative instrumental approaches to it are discussed, together with the philosophy of "easy care instrumentation" and water industry requirements for on-line analysers. A simple spectrophotometric FI system is proposed for the on-line determination of a range of water quality parameters.

The following chapter details instrumentation used in the FI system, emphasising the solid-state photometric detector.

Development of an FI manifold for the determination of aluminium in potable and treated waters is covered in the next chapter. The method, based on complexation of aluminium with pyrocatechol violet is compared with a standard Driscoll procedure. Details of the construction and testing of a fully automated FI instrument are also given.

Chapter four describes the development of a modular automated FI monitor with a PC compatible STEbus based computer system. Successful operation of this monitor is illustrated by its application to the determination of residual coagulants (aluminium and iron). Full details of software routines for control, processing and validation are given together with results from a tap water trial for dissolved aluminium.

The FI determination of residual iron by its complexation with ferene S, and the application of the optimised method in the STEbus based monitor is detailed in chapter five.

In the final chapter the use of on-line FI oxidation procedures for the determination of dissolved organic carbon are examined. The oxidation of a wide range of organic species to carbon dioxide using a silver catalysed persulphate reaction, enhanced with UV irradiation and a stopped-flow procedure is described. The sequential determination of inorganic and organic carbon without separation of the fractions is also investigated.

CONTENTS

Chapter One

Introduction

Most of the world's water, 99.3 %, exists in either saline form or in glaciers and ice caps, only 0.7 % is found as fresh water [1]. Unfortunately, the world wide demand for water at 1 $x10^{15}$ gallons/year necessitates the reuse of a large proportion of the fresh water reserves with only a small fraction of the 1 $x10^{18}$ gallons of stored fresh water being available. In countries where resources of water are limited, its control creates the potential for political power, authority and influence. In developed countries increasing public and political pressure on environmental issues dictates greater and more effective control and management of our aquatic resources.

In 1973 the UK water consumption was some 17,040 megalitres per day, equivalent to 317 litres daily per capita consumption. This water was supplied to the 99 % of homes in England, Scotland and Wales which were recorded as being connected to the public supply [2]. By 1989/90 this had risen to 17,211 megalitres per day [3], with an additional 33,333 megalitres per day abstracted from surface and ground waters for supply to industry. The increase in the demand for water is coupled with increasing recorded water pollution incidents which rose from 12,600 in 1981 to 26,926 in 1988. Of these 38 % were the result of industrial discharges, 17 % from farm pollution and 19 % from sewage and sewerage.

It is clear that an effective mechanism for both the control, protection and management of our water resources and the aquatic environment as a whole is required. To this end the implementation of water quality monitoring schemes has now become of considerable importance in our modern water conscious society.

1.1. LEGISLATION

1.1.1. The History of Pollution Control and Water Management in the UK

Legislation to protect the environment by preventing pollution can be traced back as far as 1388 [4], with the introduction of the "Act for punishing nuisances which cause corruption of the air near cities and great towns". But it was not until the industrialisation of Britain that legislation specific to the protection

of the aquatic environment was introduced, for example the "Industrial Pollution Act", 1830, and the "Clauses" Acts of 1847. Legislation protecting the quality of water for human consumption came about with the "Waterworks Clauses Act", authorising the establishment of waterworks supplying water for domestic and industrial consumption. This act, details certain activities to be regarded as offences in causing the water of "water undertakers" to be polluted.

The "Public Health Act" of 1848 set about the formation of a framework for the improvement of sanitary conditions, placing water supply, sewerage, drainage and cleansing in the control of a single local management body, which was subject to general supervision at a national level. In 1876 an Act emerged that was exclusively concerned with the prevention of pollution - "The Rivers (Prevention of Pollution) Act". However, it was not until the present century that attempts were made towards the formation of administrative bodies for water pollution control and legislation enforcement.

River Boards, established under an Act in 1948 were conferred comprehensive responsibility for the prevention of pollution. Under the "Rivers (Prevention of Pollution) Act", 1951, they were granted key legal powers to prohibit the use of any water "stream" for the disposal of polluting matter, to grant consents for the discharge of trade effluent and to take pre-emptive action to prevent pollution.

In the "Water Resources Act", 1963, national policy was extended to promote conservation and the proper use of water resources by the introduction of twenty-seven new "river authorities". Responsibility for the provision of water supplies, sewage treatment and protection of the aquatic environment was transferred, by the "Water Act" of 1973, from a collection of public authorities to ten multipurpose regional water authorities [5]. These new authorities found themselves in the position of being both the pollution control agency and a major discharger of effluent into rivers. Therefore provisions were included in the act to make new outlets and discharges by a water authority subject to the control of the Secretary of State for the Environment. Existing legislation for the control of

pollution was almost entirely repealed and re-enacted under the "Control of Pollution Act", 1974, [6].

The privatisation of the water industry required major revisions in legislation, with the "Public Utility Transfers and Water Charges Act", 1988, including provisions for the restructuring of the water authorities [7]. The "Water Act", 1989 Part I, provided the basis for the establishment of a National Rivers Authority. The "Authority" took over the former responsibilities of the water authorities in England and Wales in relation to the functions of water pollution, water resource management, flood defence, fisheries, recreation and navigation. The responsibility for the general regulation of water supply and sewage services by the water and sewage undertakers lying with the Secretary of State for the Environment and a Director General of Water Services.

1.1.2. European Community Legislation and UK Practice

The implementation of European Community legislation laid the foundations for the refinement of water quality legislation in England and Wales [8]. Traditionally there had been a reluctance to impose quantitative legislative standards for the quality of water and the discharge of effluent; any standards being of an imprecise character, falling short of explicit specifications. This required "persons" to adopt "the best practical means within a reasonable cost". The stated duty of the Secretary of State, was to secure effective execution of so much of that policy relating to the restoration and maintenance of the wholesomeness (ie conducive to health or physical well-being) of rivers and other inland waters. It could be argued that this approach had the advantage of setting no restraints on the ability of regional authorities, allowing them to take whatever action was necessary to control the quality of the water in the light of local knowledge.

Part II of the "Water Act", 1989, covers the regulations for preserving the quality of the water supplied to domestic premises, as well as the function of local authorities in relation to the wholesomeness of domestic water. The standards of

wholesomeness prescribe specific requirements as to the substances that are to be present in or absent from the water, and as to the concentration of these substances. Part III of the Act deals with the protection and management of rivers and other waters, including territorial, coastal, inland and ground waters. In order to maintain and improve the quality of these controlled waters a framework of "Water Quality Objectives" has been established [9].

EEC Environmental Policy for water can largely be divided into two broad categories [10]: 1/ Control of water pollution; and 2/ the quality of water for specified uses.

Pollution Control

Central to the prevention of pollution of the aquatic environment is the "Dangerous substances in water" directive [11], this with several daughter directives seeks to control the discharge of certain substances, List I (Grey List) or List II (Black List). List I substances are selected on the basis of their toxicity, persistence and bioaccumulation e.g. organohalogen and organophosphorus compounds, carcinogenic substances and mercury and cadmium compounds. List II includes potentially less dangerous substances such as zinc, copper and lead compounds. The directive requires Member States to introduce pollution reduction programmes for List II substances, establishing emission standards based on quality objectives. In addition, pollution "elimination" programmes for List I substances are to be introduced; where pollution is not defined by the presence of the substance, but to its effects on the aquatic environment. For the control of List I substances two alternative regimes are defined, where emission standards are set by: a/ Reference to Community limit values and b/ Reference to quality objectives. The use of uniform emission standards (UESs) or environmental quality objectives (EQOs) has led to a disagreement between the European Community and Britain. Britain argues that it should be allowed to take advantage of its geography and site industry in positions where acute pollution problems are less likely to arise. This follows the adoption of "quality objectives" where the type

and quantity of the discharge is related to the ability of the water course to cope with it, as well as the intended use of that water resource. With the adoption of such an approach it is necessary to monitor the whole aquatic environment. This, it is argued, will have the benefit of taking diffuse or non-point discharges into account. Discharges are then only controlled where necessary and financial resources can be directed to priority areas for maximum benefit. The advantages of uniform emission standards are that they can be easily administered and monitored to ensure compliance, while it is not necessary to take account of the quality of the water into which the effluent is being discharged. Despite this disagreement, Britain has adopted a dual approach for List I substances on a "Red List" where either a limit value or an environmental quality standard is applied; where the more stringent measure is selected.

Quality of Water for Specified Uses

The quality of water for specified uses is defined in four separate directives [11]: 1/ Abstraction for drinking water (75/440/EEC) (for which a further directive (79/869/EEC) specifies the sampling and analytical requirements); 2/ use for bathing (76/160/EEC); 3/ protection of freshwater (78/659/EEC); and 4/ protection of shellfish (79/923/EEC). These contain Guide (G) and Imperative (I) values for seventy-two physical, chemical, microbiological and bacteriological parameters. Member States are required to set values no less stringent than the I values and using the G values as guidelines. They must then ensure that 95 % of the "surface water" samples meet these values. Examples of these I and G values are given in Table 1.1.

Drinking Water

The "Drinking Water Directive" (80/778/EEC) [12] lays down sixty-two quality standards for water intended for drinking water, and water used in food and drink manufacture. The parameters are defined in six categories:

1. Organoleptic, e.g. colour, odour, taste.

2. Physico-chemical, e.g. pH, conductivity.
3. Those concerning toxic substances undesirable in excessive amounts, e.g. nitrates, nitrites.
4. Those concerning toxic substances, e.g. mercury, lead, pesticides.
5. Microbiological, e.g. coliforms, faecal steptococci.
6. Minimum required concentration for softened water, e.g. hardness, alkalinity.

TABLE 1.1

Standards for Quality of Water for Direct Abstraction to the Public Supply.

Parameter	Unit	G*	I*
A/ General Physico-Chemical			
Ammonia	mg N l^{-1}	0.04	-
Dissolved oxygen	% saturation	>70	-
B/ Inorganic Anions			
Arsenic	mg As l^{-1}	0.01	0.05
Nitrate	mg N l^{-1}	5.65	11.3
C/ Metals			
Copper	μg Cu l^{-1}	20	50
Iron	μg Fe l^{-1}	100	300
D/ Organic Substances			
Hydrocarbons	μg l^{-1}	-	50
Phenols	μg l^{-1} as C_6H_5OH	-	1
E/ Microbiological			
Faecal streptococci	/100 ml	20	-

Note: * For A1 Treatment

Three types of standards are used in quantifying these parameters: The Guide Level (GL), the Maximum Admissible Concentration (MAC) and the Minimum Required Concentration (MRC) standards for quality of water for direct abstraction to the public supply. Member States are required to set values for all parameters with MAC or MRC values and ensure that they are met. These values should be set with reference to the GL value and must not breach the MAC or

MRC value. Examples of these standards are given in Table 1.2. Until the introduction of this legislation the Department of the Environment (DoE) did not recommend or impose precise standards for the quality of drinking water, however most water authorities used guidelines proposed by The World Health Organisation [13]. Since its introduction guidance has been issued by The Welsh Office of the DoE to water authorities and companies, for example to safeguard the quality of public water supplies [14].

Formal compliance with EC legislation has necessitated a review of UK legislation, with some amendments being made to statutes in the Water Act 1989. Water companies are now obliged to adhere to EC legislation or risk prosecution.

TABLE 1.2

Quality Standards for Drinking Water.

Parameter	Unit	GL	MAC
A/ General Physico-Chemical			
Ammonia	mg N l^{-1}	0.04	0.39
Dissolved oxygen	% saturation	>75	-
B/ Inorganic Anions			
Arsenic	mg As l^{-1}	-	0.05
Nitrate	mg N l^{-1}	5.65	11.3
C/ Metals			
Aluminium	μg Al l^{-1}	50	200
Copper	μg Cu l^{-1}	100	3000
Iron	μg Fe l^{-1}	50	200
D/ Organic substances			
Hydrocarbons	μg l^{-1}	-	10
Phenols	μg l^{-1} as C_6H_5OH	-	0.5
E/ Microbiological			
Total bacteria	/ml	10	-

1.2. WATER QUALITY MONITORING

Chemical, physical and biological information is required for the efficient protection and management of freshwater resources. These resources are not only the source of water for domestic and industrial consumption but also the home for a large aquatic biota. Most information is currently obtained by the manual collection of samples and their subsequent analysis in a remote laboratory. The provision of frequent periodic or continuous information for all natural, drinking and industrial waters could prove to be very valuable.

Water quality objectives (WQOs) for the regulation and control of discharges can only be sensibly, and effectively met if extensive and reliable information on the current status of the water is available [15]. The establishment of regional and nationally coordinated monitoring schemes, with on-line instrumentation, would provide the data required for the economic management of pollution control. With such a monitoring network the early detection of transient pollution incidents due to accidental discharges could be quickly controlled, thereby limiting the damage to the aquatic environment.

Further benefits could be gained from the deployment of on-line instrumentation for both supply intake protection and efficient control of water treatment processes. In the first example, pollution could be detected upstream to river based abstraction points by deployment of such an instrument, thereby preventing water of an undesirable quality from entering the treatment plant. In the second example it would allow the effective treatment of potable water in the production of drinking water, while also preventing the release of unwholesome water to the public supply.

1.2.1. Principles

The planning of any measurement program must address the following seven questions [16]:

1. What are the objectives of the program, and what chemical, physical or biological information is required ?
2. What are the determinands of interest ? Are they specific or non-specific, for example a metal species or chemical oxygen demand.
3. Where and when are the samples to be taken ? A carefully defined sampling location and minimal sampling frequency must be identified. This should ensure that the analytical data adequately represents the quality of the water during the sampling period [17,18].
4. What are the analytical methods to be used ? These must meet the sensitivity, accuracy and precision requirements [19].
5. How are the samples to be taken and subsequently handled [20] ? The maximum tolerable period between sampling and generation of the result will have an important bearing on the selection of both the sampling and analytical procedure, and as to whether on-line analysis is justifiable.
6. How are the results to be reported ? The units and the accuracy to which the results are given will be dependent on the method of measurement.
7. What is to be done with the results ? This is largely dictated by the main objectives of the measurement program. For example, whether the result is used in a control process or accumulated for statistical trend analysis.

Examples of analytical procedures for the sampling and preservation of waters and wastewaters are given in a standard text published by the American Public Health Association [21]. The analytical method may be manual, semi-automatic, automatic or on-line [16] and selected appropriately for the sampling strategy and the chemical information required.

The traditional approach involves the collection of a series of grab-samples, transportation to a central laboratory and subsequent manual analysis. However, there are several major limitations with such a procedure:

1. Delay between sample collection and generation of an analytical response may be too slow to allow effective control of the water "process".
2. Difficulties may arise in sampling outside of normal working hours.
3. Human resources and laboratory facilities may be insufficient to allow collection and analysis of all the required samples.
4. Accuracy of the result is dependent on the skill and care of the analyst (less so for automatic analysis).
5. The sample may deteriorate during transport and require stabilisation.
6. The sampling location may be remote or hazardous, where access must be restricted to infrequent visits.
7. The cost per analysis is likely to be high.

Some of these disadvantages may be overcome by the use of semi-automatic and automatic methods, where higher sample throughputs and an increase in analytical precision may be achieved. The inherent problem of the time delay between sampling and analysis cannot easily be overcome whilst the analysis is restricted to a laboratory remote to the sampling point, and this may lead to short term variations passing unobserved.

The use of on-line instrumentation [22,23] has increased in the last twenty years; here a sample line is used to withdraw a discrete or continuous sample directly into the instrument. This type of instrument vastly reduces the sampling and analytical resources required, while increasing the speed with which an analytical response can be generated after sampling.

The application of on-line instrumentation can be justified when the overall cost is less than that of the laboratory based analysis, either because of the remote sampling location or the high sampling frequency. Their deployment can

also often be justified because of their ability to provide continuous and immediate information, for example for the control of water treatment processes.

1.2.2. Monitor Requirements

The critical performance and design features of an on-line monitor will include most, if not all, of those associated with standard laboratory instrumentation. These standard requirements of accuracy, precision, sensitivity and selectivity are primarily concerned with the performance of the analytical method. However, it is also necessary to address other instrumental requirements. The specification of an on-line instrument is dependent on several factors including the frequency of the analysis, the length of the period of unattended operation, the intended location and the output or feedback that is required.

The water industry has produced specifications, and guideline notes relating to the design and operation of on-line monitoring instruments [24]. This document should enable manufacturers to develop analysers that meet an industry-wide standard, and that can be evaluated against Water Industry specification.

This document also addresses the problems that are encountered and must be overcome in order to achieve reliable operation in "field" situations:

1. Biological, organic and mineral fouling of sensors and sampling systems.
2. Moisture ingress into instrument electronics.
3. Electrical and magnetic interference.
4. Poor accuracy due to sample variability and the presence of interferents.
5. Influence of environmental factors.

1.2.3. Easy Care Instrumentation

The critical performance requirements are embraced in the philosophy of "easy care instrumentation" [25]:

1. *Reagent stability*, no degradation of reagents and subsequent loss of performance during the period of unattended operation.
2. *Hardware and software flexibility*, to allow easy adaption of the analyser for the determination of different parameters. For example, plug-in "manifold" cartridges and software with access to user-defined control and alarm parameters.
3. *Internal diagnostics*, self-checking facilities capable of identifying faults in various instrument areas and providing remote indication of these failures.
4. *Stay-clean properties*, to minimise attention due to fouling of the sensor or flow system.
5. *Modular construction*, allowing simple testing, repair or replacement of individual components with a minimum of instrument down-time.
6. *Long-term unattended operation*, extended operational periods between manual calibration & scheduled maintenance.
7. *Periodic automatic recalibration*, when required to ensure adherence to performance requirements.
8. *Easy on-site maintenance*, routine maintenance not requiring the instrument to be off-line for longer than 1 hour.

The purpose of these requirements is to maintain the quality and validity of the analytical data and to ensure the reliability of the instrument operation, whilst the overall cost and thus cost per analysis is kept to a minimum. These requirements are encompassed in three sections: General (e.g. construction, calibration and maintenance), Electrical (e.g. output signal and supply) and Environmental (e.g. magnetic and electrical interference). One key feature is to reduce the interaction of personnel with the instrument, frequently the most

expensive component of a monitoring scheme. Therefore it is specified that the instrument shall be so designed as to allow unattended operation for a minimum of 35 days. To ensure the accuracy of the analytical result during these extended operational periods, automatic recalibration becomes a necessity [16], as does the detection of malfunction.

1.2.4. Types of Monitor

Ion-Selective Electrode Monitors

Traditionally, electrochemical techniques have been those most widely applied to the on-line analysis of waters. The most common is that of a probe-type sensor [16] which can be placed directly in the sample stream, or "in-situ", providing an electrical signal the size of which is governed by the determinand concentration. These types of sensor can be used to measure a range of parameters, for example a simple glass electrode for pH determination. Alternatively, a complex liquid ion-exchanger or gas-transfer ion-selective electrode (ISE) [26] may be applied to the measurement of for example nitrate [27] and ammonia [28].

The major advantages of ISEs for continuous monitoring are as follows:

1. Speed and simplicity of analytical procedure.
2. Small sample volume.
3. No extensive sample pre-treatment required.
4. Responds only to uncomplexed ions.
5. Ease of adaption to on-line/in-situ measurement.

The precision of these ISEs can be attributed to the standardised way in which the sample is presented to the sensor [29]. Therefore crucial to the design of the instrument is the flow cell which must be kept small to minimize hold-up volume and maximise sample velocity across the sensor membrane.

Unfortunately, several disadvantages are encountered when ISEs are applied to the on-line analysis of freshwaters:

1. They respond only to free ions, often a major advantage, but also a disadvantage when ions of interest are bound-up in complexes, for example fluoride complexation of H^+, Al^{3+} and Fe^{3+}.
2. Their non-Nernstian behaviour can lead to problems with the accuracy of this method. This may be due to, for example, interference from other ionic species, properties of the membrane or the variation in the ionic strength of the sample.
3. The potential of the ISE is temperature dependent and therefore careful temperature control of the solutions during analysis is required.
4. Some ions of interest cannot be directly determined, for example aluminium.
5. Fouling, degradation and physical abrasion of the electrode/membrane surface limits the lifetime of the probe and necessitates frequent chemical or mechanical cleaning.

Some of these problems can be overcome, for example the addition of a biocide to the reagents will prevent the formation of a biological "slime" on the membrane surface. A wider range of analytes may be determined by the introduction of new and universal electrodes, for example the "Selectrode" [30]. In this type of electrode, the membrane was replaced by an activated teflon hydrophobised graphite rod. This rod could be easily cut to the appropriate size and shape for any particular application, and in addition its simple construction allowed the provision of reproducible and renewable surfaces. However, because of the drawbacks associated with ISEs, they have only been applied to the determination of a limited number of chemical species. Therefore there is still considerable interest in the development of versatile and robust on-line instrumentation.

Biological Monitors

In recent years considerable effort has been directed to the development and application of biological monitors for the on-line measurement of "total pollution" [31]. These are based on the chronic toxicity of the water as a whole, without selective identification or quantification of any individual analytes. The development of a biological early warning system (BEWS) [32] outlines the important criteria that must be met. It is essential that the change in the physiological or behavioural parameter of the organism should be reliable, rapid and readily quantifiable through computer analysis. The measurement of this change should be achieved with a minimum of direct interference, and thus avoid placing undue stress on the aquatic organism. This organism, used as the sensor, should be fairly inexpensive, easily acquired and of consistent "strain" so as to minimise the within species variation in response.

The components of an automated BEWS, Fig. 1.1, are analogous to those required for any on-line system. A "sensor" (either an organism, ISE or other device) generates a response or signal when a certain analyte is present. This signal is then received and processed by a computer, which also controls any functions of the instrument and outputs a result to the user or control mechanism.

The selection of the aquatic organism is largely made on the basis of its suitability to "respond" to the analytes of interest. A wide variety of fish, including crayfish and green sunfish were tested for a "fish monitor" [33-35], where the activity or ventilatory movement of an array of fish was processed to identify unusual behaviour. Rainbow trout were selected as the basis for a commercial monitor (WRc Fish Monitor, pHOX Systems Ltd.). Other, simpler aquatic organisms, for example daphnia (water fleas), have also been proposed for incorporation in effluent biomonitoring instrumentation [36,37].

The major problems associated with biological monitors are the high costs associated with purpose built facilities and the employment of skilled personnel. The poor reliability of such systems and the lack of consistency in the response between organisms can also cause operational problems, and in addition the

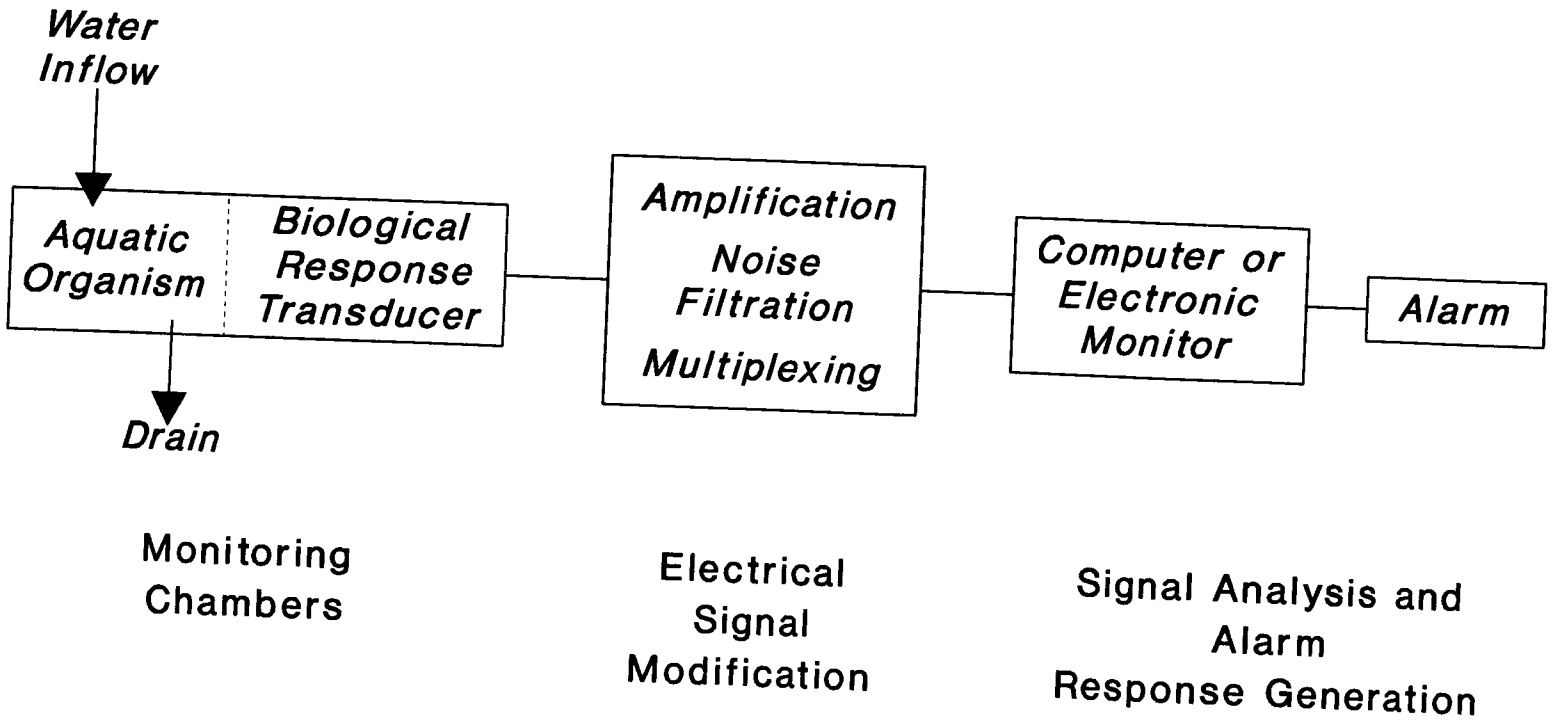

Fig. 1.1 Schematic Diagram of an Automated Biological Early Warning System (BEWS).

"exposure-effect-response" delay for some species is too slow [38]. A biomonitoring system is useful in indicating a water quality hazard, possibly due to a combination of toxic species. However, this will only provide limited qualitative information, and thus it is necessary to simultaneously deploy physico-chemical monitors to correlate the response with the concentration of specific analytes.

Spectrophotometric Monitors

With the development of spectrophotometric analysers many of the disadvantages normally associated with ISE monitors have been overcome. One such analyser is a direct UV monitor for nitrate [39] which claims to offer sensitive and selective determination, coupled with high reliability and low operating costs. Spectrophotometric methods have the advantage that well proven and documented procedures already exist for most organic and inorganic species [40]; with a wide range of selective and sensitive chromogenic reagents also being available [41]. Traditionally however, the drawbacks to colorimetric analysis have been high reagent consumption, and the relatively high cost and fragile nature of the instrumentation. Two types of analyser, discrete and continuous (segmented and non-segmented), have been developed which essentially overcome the first disadvantage. These also improve both the sample throughput and the accuracy compared with a manual method.

Discrete analysers operate on the principle of the injection of an aliquot of sample together with appropriate reagents into a sample cell, where colour development and measurement take place. This type of analyser is therefore cheap and simple to construct with high reliability offered by the use of simple syringe pumps. Unfortunately difficulty in sample manipulation, together with carryover and the need for frequent cleaning of the sample cell limit their usefulness for on-line analysis. The generation of an analytical response is also relatively slow, an analytical measurement is not usually taken until a steady-state for the sample-reagent reaction has been established.

Continuous Analysers

Continuous analysers [42] overcome the problem of slow analytical response and thus increase sample throughput, while still maintaining most of the advantages associated with discrete analysers. Segmented flow analysers (SFAs) and continuous flow analysers (CFAs) both allow measurement of the analytical response before a steady-state is reached. This is possible because of the reproducible sample-reagent flow pattern through the analyser to the measurement cell. In an SFA air bubbles are introduced into the sample stream in order to maintain sample integrity whilst promoting efficient mixing. However, in early instruments variation in the bubble pattern affected the precision of the method. Because of the nature of the analyser and the sample introduction method, sample pre-treatment prior to reagent addition is relatively straightforward.

The disadvantages of SFA, i.e. relatively high reagent consumption and complex instrumentation can be overcome, and the primary advantages of the utilisation of flowing streams and rapid analyses can be maintained, and even improved upon by using the continuous flow technique of flow injection analysis (FIA) [43,44]. This technique is based on the injection of a sample into a continuous unsegmented carrier stream, this zone is then transported to a detector where a changing physical or chemical parameter is continuously recorded. The characteristics of a typical FIA system are given in Table 1.3; the advantages of such a system are well documented [45] and with particular reference to on-line analysis include:

1. Reproducible sample handling and therefore high precision.
2. Easy sample manipulation and pre-treatment, for example on-line reduction, oxidation, pre-concentration and separation.
3. Rapid response, typically 30 s to 1 min between sample injection and generation of an analytical signal, allowing high sample throughput without loss of precision.

4. Very low reagent consumption, resulting from the combination of the use of small bore tubing and low flow rates.
5. Small sample volumes.
6. Simple construction.
7. Low purchase and operational costs.
8. Ease of automation, with only a small number of components to control.

TABLE 1.3

FIA Characteristics.

Parameter	Range
Sample volume	5 - 200 μl
Tube diameter	0.4 - 1.0 mm
Flow rates	0.4 - 2.0 ml min^{-1}
Coil lengths	0 - 2.0 m
Sample throughput	30 - 300 hr^{-1}

The versatile and economic nature of FIA has led to the widespread recognition of its use as "a sample handling technique" [46], and as a means to achieve near real-time process/on-line monitoring and control [47-52]. The use of traditional spectrophotometric detectors in on-line FIA analysers is not practical. As an alternative, solid-state photometers [53] with light emitting diode (LED) light sources and photodiode light detectors, can easily be incorporated into such a system. These offer a suitably cheap, robust and reliable alternative and have already been successfully applied in the flow-injection (FI) determination of phosphate, nitrate and ammonia [54-56] in natural waters.

1.3. RESEARCH OBJECTIVES

To develop a flow-injection based analyser for the remote on-line analysis of freshwaters. Certain target applications have been identified, where the determination of the analytes on a pseudo-continuous basis would prove advantageous.

1. The determination of residual metal coagulants, iron and aluminium, in treated and potable waters. The information providing a means for the effective management and control of treatment processes.
2. The determination of dissolved organic carbon, and the supply-intake protection and control of river water abstracted to the public supply.

The determination of these analytes using on-line spectrophotometric FI techniques will also necessitate the development of system hardware and software. This development work should ensure that the "monitoring system" meets industry specification with regards to versatility, reliability and operational performance. The system should also be validated and tested in order that its operational suitability can be assessed.

Chapter Two

Instrumentation

2.1. MANUAL FI SYSTEM

Throughout this work a manual FIA system has been used for the laboratory based development, optimisation and validation (including calibration) of the reaction manifolds for each of the analytes. These manifolds were all based on the formation of a coloured complex, or the measurement of a colour change. A schematic diagram of a two channel FIA manifold, Fig. 2.1, serves to illustrate the arrangement of the key components.

A peristaltic pump (1) propels the reagent (R) and carrier (C) streams through PTFE tubing (0.8 mm i.d., 1.5 mm o.d.). The standard and sample solutions are injected via a six port PTFE rotary valve (2) into the carrier stream. These injected "slugs" are then mixed with the chromogenic reagent in the reaction coil (3) (constructed from the same PTFE tubing). The absorbance of the coloured complex is measured with an in-house solid-state photometric detector (4), of which further details are given below.

A summary of the components and suppliers is given in Table 2.1.

2.1.1. Solid-State Detector Design

The use of light emitting diodes (LEDs) and phototransistors in photometric modules was first reported by Flaschka et al. [57] which illustrated the advantages of their compact size, low power consumption and negligible warm up time. Photodiodes as light detectors have also been reported [58], having the advantage of rapid response to a wide range of transmitted light. This response range is three to four times that typically found for phototransistors. Several papers describe the use of solid-state photometers as detectors for FIA [59-64], in all these a flow-through design is utilised to minimise the dispersion and disruption of the sample slug as it passes through the detector flow cell. A useful summary of these ideas is given in a review by Trojanowicz et al. [53].

The solid-state detector used in part of this work is of the same design as that proposed by Worsfold et al. [54] for the FI determination of phosphate. This original detector design will be designated as "DETECTOR A". The double-beam

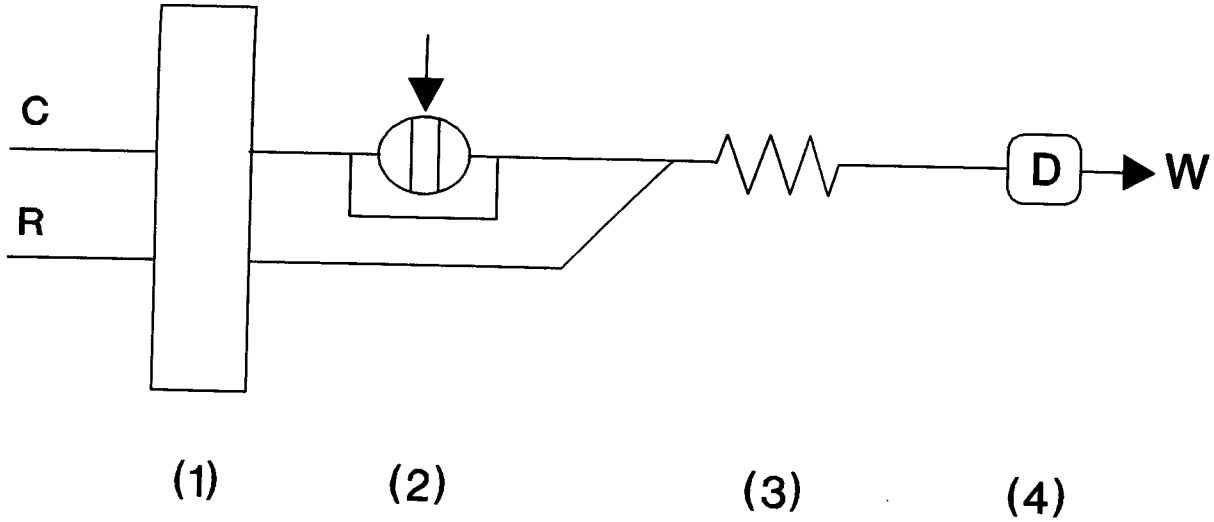

Fig. 2.1 Schematic Diagram of a Flow-Injection Manifold.

Key: (1) Peristaltic pump
(2) Rotary injection valve
(3) Reaction coil
(4) Detector

TABLE 2.1

Manual FIA System Components.

Component	Supplier
Peristaltic pump(s):	
Ismatec Mini S-820 4 channel / 8 roller / fixed speed (20 rpm)	Ismatec UK Ltd., Carshalton
Gilson Minipuls 3 4 channel / 10 roller / variable speed (0.01-48 rpm)	Anachem, Luton
PVC bridged pump tubing, (0.38-1.14 mm i.d.)	Labsystems Group (UK) Ltd., Basingstoke
Injection valve:	
Rheodyne 5020 PTFE, six port	Anachem
Reaction manifold:	
PTFE tubing (0.8 mm i.d.)	Anachem
Perspex "T"/"Y" mixing pieces	In-house
Acetal resin nuts (1/4"-28 flanged fitting)	Anachem
Tefzel coupling bodies (1/4"-28 threads)	
Detector:	In-house

configuration of this detector minimises the drift associated with changes in temperature, and the transmittance of the flow stream. These effects are compensated for by comparison of the response from the sample cell with that from the reference cell.

Light Source and Light Detector

The output of the light source was restricted to the visible region, and fixed at a wavelength determined by the type of LED selected. The LEDs covered the range between 550 and 650 nm, the three available colours were: red, 635 nm; yellow, 583 nm; and green, 565 nm (RS Components Ltd., Corby). Each of these LEDs exhibited a spectral bandwidth of 30 - 40 nm, allowing a degree of flexibility when selecting the chromogenic reagent. These particular ultrabright LEDs were selected because of their advantageous operating characteristics: 1/ low power consumption (typically 20 mA at 2 V); 2/ ambient temperature operation; 3/ long lifetimes (20000 - 100000 hr); and 4/ compact (5 mm in diameter, 9 mm in length) and robust design.

The light detector employed was an integrating silicon PIN photodiode, the amplifier exhibiting high gain and low noise characteristics. Both the photodiode and the amplifier were housed in a small, single package (8 mm in diameter, 6 mm in length). This photodiode was sensitive to visible and infrared radiation, with a broad spectral response (250 - 1050 nm), Fig. 2.2.

The associated detector circuitry, shown in Appendix A, was divided into two parts: 1/ the photodiode output and 2/ the LED power supply:

1. The two photodiode outputs were fed into a low noise operational amplifier, configured in differential mode. This subtracted the reference signal from the sample signal, producing an output proportional to the transmittance of the sample stream. This output passed through a low band-pass filter, removing high frequency noise, before being fed into another operational amplifier to provide a

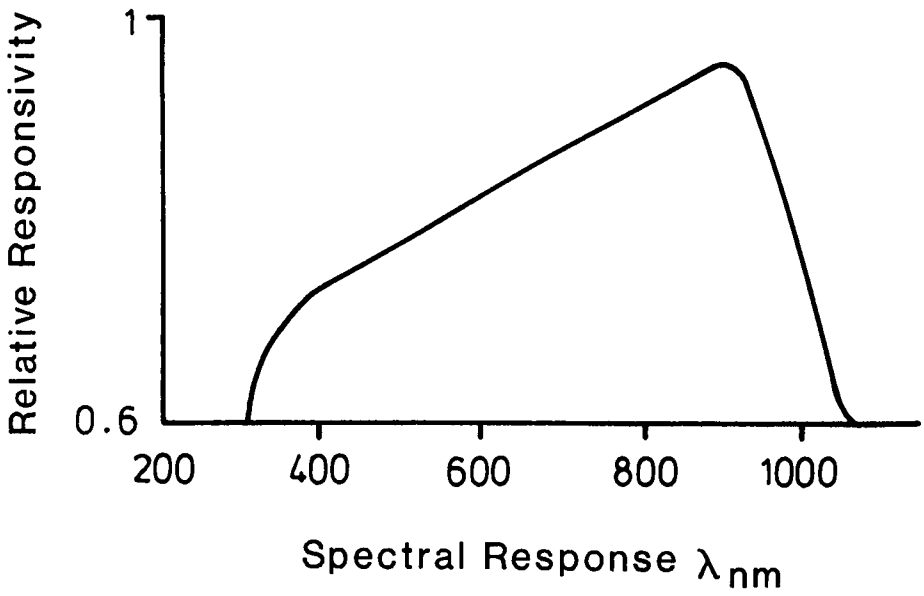

Fig. 2.2 Spectral Response of Integrating Photodiode.

low impedance output. This output signal was capable of driving a chart recorder or could be fed directly into an A/D converter.

2. The LEDs were driven from constant current sources to maintain a regular output. One of these current sources was variable, so that the reference channel signal could be adjusted to zero the detector output.

The simple construction and compact nature of the solid-state detector is illustrated in Fig. 2.3.

2.1.2. Flow Cell Design

The flow cell housing [65] was constructed from an aluminium block with two parallel 1.8 mm diameter holes drilled through one side of the cube. PTFE tubing (1.5 mm o.d., 0.8 mm i.d.) was passed through each hole, one tube being the sample cell and the other the reference cell. Holes were drilled perpendicular to these to house the two LEDs and the two photodiodes. The path length of the sample and reference beams was therefore 0.8 mm. An illustration of the flow cell housing, with dimensions, is given in Appendix A.

2.1.3. Detector Modifications

Two changes were made to the design of the solid-state detector in an attempt to achieve higher sensitivity by increasing light throughput. These modifications were incorporated into the design of a new detector, "DETECTOR B", where either or both of the following modifications were made:

1/ Replacement of the ultrabright LEDs of the original design by higher intensity versions which had become commercially available in the same clear mounting package. Table 2.2 compares the specification of these new LEDs with those used in detector A. This modification did not require any changes to the electronic circuitry of the detector.

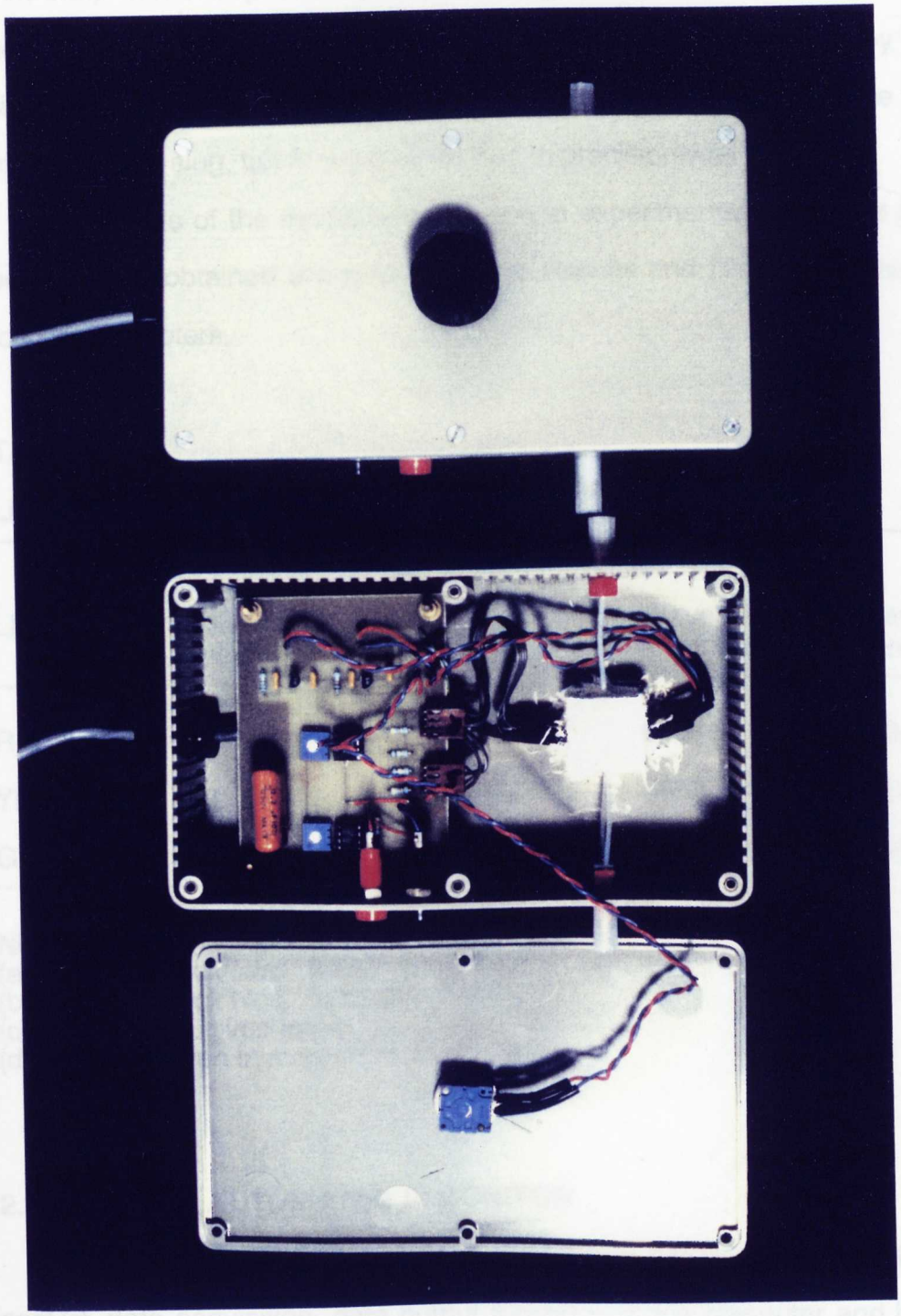

Fig. 2.3 Solid-State Detector.

2/ Replacement of the material used for the detector flow cells. The PTFE tubing used in the original design was replaced by glass capillaries (1.35 mm i.d., 1.96 mm o.d.). These capillaries (40 mm in length) were passed through the flow cell housing, and coupled to the PTFE tubing of the reaction manifold by means of a silicon rubber sleeve. This modification caused some disruption to the flow pattern of the sample slug, but in practice no loss in precision was observed.

Details of the modifications made in experimental trials, and the superior performance obtained are detailed in the Results and Discussion sections of the following chapters.

TABLE 2.2

LED Peak Wavelength and Intensity Data.

	Detector A[a]		Detector B[b]	
LED	Wavelength maximum[c]	Intensity maximum[d]	Wavelength maximum[c]	Intensity maximum[d]
RED	635	125	650	200
YELLOW	583	120	585	250
GREEN	565	140	563	200

Notes:
(a) LED RS stock Nos. 590-519/531/525
(b) LED RS stock Nos. 590-480/503/496
(c) Wavelength given in nm
(d) Intensity given in mcd @ 20 mA

2.2. THE AUTOMATED FI MONITOR

A schematic diagram of the automated monitor, Fig. 2.4, illustrates the control, data acquisition, data output functions of the computer and its interaction with the five other major components. A brief description of each of these is given below.

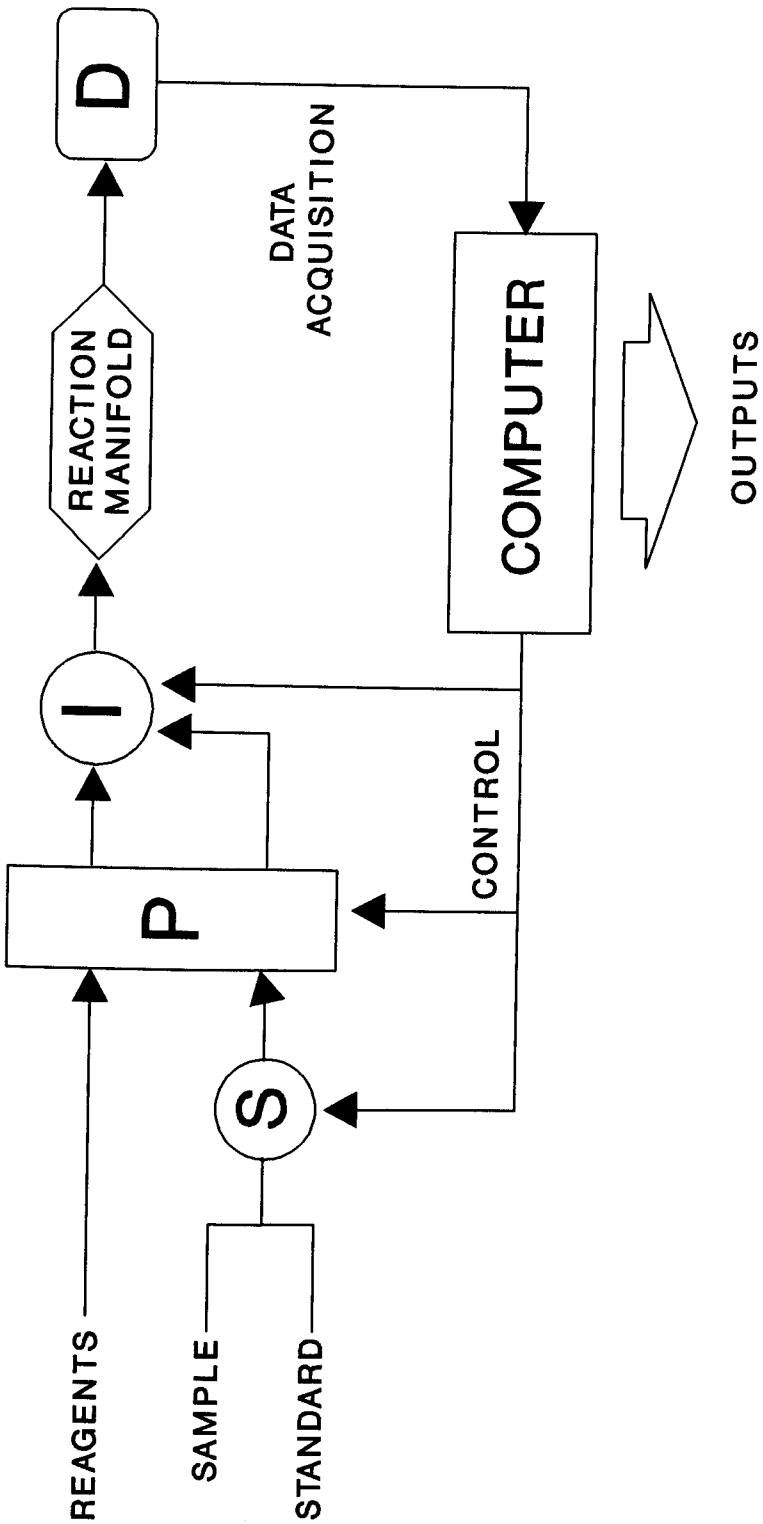

Fig. 2.4 Schematic Diagram of Automated FI Monitor.

KEY: S = SWITCHING VALVE
P = PUMPS
I = INJECTION VALVE
D = DETECTOR

1. *Pump Unit*: housing twin, independently controlled, peristaltic pumps (Ismatec Mini S-820). Power supply units for the detector and injection/switching valves, and the interface between the computer and the rest of the "system".
2. *Detector*: solid-state design, described above.
3. *Manifold*: the reaction manifold unchanged from the manual FI method.
4. *Injection valve*: initially a 12 V solenoid operated six port sliding valve (Chemlab Instruments Ltd., Cambridge), later replaced by a 12 V six port rotary valve (Burkard Scientific, Uxbridge).
5. *Switching valve(s)*: either a 12 V solenoid operated 3-way isolation valve (Neptune Research, 161T031: PhaseSep, Queensferry) or 12 V solenoid operated 2 channel pinch valve (Neptune Research, 2258091-21: Caldy Science Associates, Liverpool).

2.2.1. Computer Hardware

This system was designed and constructed around a single board computer. Additional cards were added to facilitate the capture of the analogue signal from the detector, and output the processed result to a local display and printer. The computer hardware and system software were supplied by Control Universal (Cambridge). The individual "function" cards are described below:

1. *Control and data processing*: EuroBEEB with 6502 8-bit, 2 MHz microprocessor, 8 Kb RAM for software development or 16 Kb EPROM for debugged control software.
2. *Data storage*: CU-MEM Selecta with 32 Kb RAM for the storage of raw analytical data prior to processing.
3. *Signal capture*: CUBAN-12A, 16 channel analogue to digital converter with 13 bit accuracy and 1 mV resolution.

4. *Output*: JOBBER interface allowing data output to VIEWLINE, 24 character by 2 row liquid crystal display, and RACKPRINT, 24 character per line miniature impact printer.

2.2.2. Computer Software and Monitor Operation

The programming language used was an extended version of BBC BASIC, MosB4, which included features for instrument control and data acquisition. The structure of the software divided the operational functions of the system into three main sections: analysis, data processing and validation. Each of these sections contained the necessary routines to fulfil particular operations which together comprised the "measurement cycle". This cycle was defined as the operation of the monitor for the analysis of the sample, and the generation of a validated analytical result. This cycle was repeated every thirty minutes, on the hour and half hour; but was software controllable to allow adjustment for individual monitor applications.

Monitor Protocol

One complete measurement cycle consisted of duplicate injections of sample followed by duplicate injections of an appropriate standard. The means of each pair of injections were then ratioed to calculate the analyte concentration in the sample. The advantage of this approach was that every result was automatically calibrated, compensating for any signal drift due to changes in physical or instrumental parameters. For example, the change in the rate of formation of the coloured complex as a result of falling air or sample temperature, and the subsequent decrease in detector response.

Analysis: The peristaltic pumps, injection valve and switching valve were controlled by a pattern of instructions. These followed the monitor protocol defining duplicate sample and standard injections. Sufficient "flushing" delays were included to eliminate carryover from sample to standard solutions and vice versa.

Data Processing: The analogue signal generated by the solid-state detector was converted to a digital value and stored in memory until the injections of both sample and standard were completed. After this, an algorithm was used to process the raw data and isolate four "peaks", searching for minimum and maximum values corresponding to the baseline and the "top" of the signal or peak. The analyte concentration was then calculated by ratioing the mean peak values obtained for the known and unknown solutions. This was output together with time, date and validation information to the local display, printer and appropriate feedback mechanism.

Validation: In order to check the validity of the calculated result, a software routine compared the signals obtained from each pair of duplicate injections. If there was a size discrepancy greater than that defined in the software as acceptable, for example > 10 %, an error message was output to indicate where the error had occured. If the result failed during this validation procedure a repeat measurement cycle was immediately initiated.

A remarked software listing for a typical monitor application is given in Appendix B.

2.2.3. Sample Presentation

An important consideration in the "field" deployment and operation of the monitor was that of the provision of the water sample. Ideally this sample should be "clean" and free from suspended particulate matter. In the water industry anything remaining in the water sample after filtration through a 0.45 μm filter is arbitrarily regarded as dissolved. The level of sample "clean-up" or treatment prior to analysis being dependent on the source of the sample. If for example the sample was abstracted from a river a more complex clean-up procedure would be required than if it were drawn from the treated domestic supply.

A typical pre-treatment and presentation unit is schematically illustrated in Fig. 2.5. With this system, the sample is drawn from the river and passed through a course filter to remove any large debris. It is then passed through a series of wedge-wire stainless steel filters with progressively smaller pore sizes, the last filter being in the range 10-15 μm. The sample is then piped to a small constant head device, with a typical hold-up volume of 100 ml. From this constant head device, often positioned immediately adjacent to the monitor, a sample aliquot is withdrawn from the continuously replenished supply. Because of the potential for blockages in the filter assembly, a remote tap water/compressed air backflush mechanism is included to facilitate remote cleaning.

2.2.4. Data Transmission

The output of the analytical result together with validation and alarm information was another important consideration. The format of this output is dependent on the particular application of the monitor. For example on intake supply protection it would be necessary to relay the response (or alarm signal) to a control mechanism that would stop the abstraction process; whereas for nutrient budget studies a data logging device would probably be all that would be required. The more common output features of the monitor are illustrated in Fig. 2.6; usually a link to a laboratory based or central computer would be included so that the operational status of the monitor could be remotely observed.

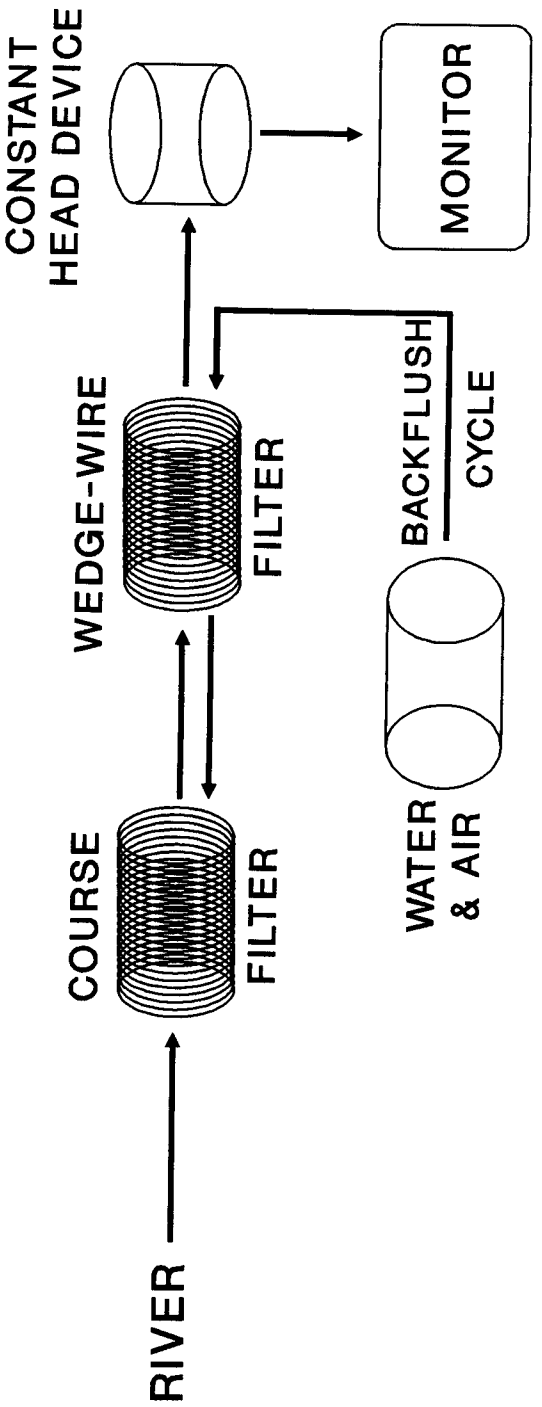

Fig. 2.5 Schematic Diagram of Sample Presentation Unit.

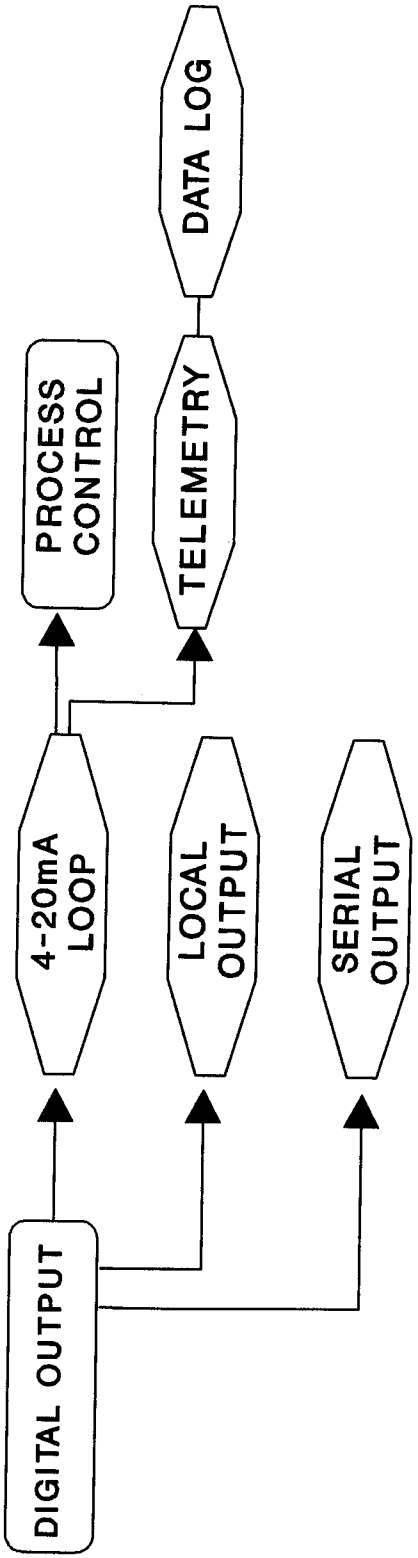

Fig. 2.6 Data Transmission Options from FI Monitor.

Chapter Three

On-Line FI Determination of Aluminium

3.1. INTRODUCTION

3.1.1. Water Treatment

The production of aesthetically pleasing and palatable drinking water often necessitates the treatment of raw turbid water to remove suspended particulate, colloidal matter and coloured humic substances. Traditionally, aluminium and iron salts (in particular aluminium sulphate and iron(III) chloride) have been used as both primary coagulants and flocculants for water clarification [66].

This clarification procedure can be divided into two separate processes, requiring different conditions. The first is "coagulation" where a chemical coagulating agent is added to the raw water with rapid mixing. The second process of "flocculation" is brought about with slow mixing, often without the addition of any further chemicals. The coagulation process is one of charge neutralisation, where the positively charged species of the chemical reagent neutralise the negative charges on the suspended colloidal matter. The formation of flocs is then enhanced by rapid mixing which increases particulate collisions. Further slow mixing brings about the formation of larger settleable agglomerates (flocculation), which can then be removed from the clarified water. The chemical flocculant improves this agglomeration process by acting as a bridge between the floc particles, allowing the formation of a "net". However, these metal coagulants are sensitive to pH changes and if the pH falls outside of the ideal range, pH 6-7, the clarification process is inefficient. This may result in the solubilisation of the metals, allowing them to be carried out of the treatment plant into the public supply.

The use of alternative coagulants and in particular cationic polyelectrolytes [67] has been investigated. Unfortunately, and with few exceptions, they are poor coagulants without the addition of finely divided clay or silica. The required dose is critical, although this dose is generally less than that of conventional coagulants. It is unlikely that water companies will voluntarily switch to using these alternative coagulants unless a substantial saving in cost can be

proven, and the consumer appreciates the need for chemically "clean" as opposed to "clear" water.

3.1.2. Natural Sources of Aluminium

Aluminium is a ubiquitous element being the third most abundant in the earth's crust [68] (which contains 8.8 % by mass [69]), and is the most abundant metal. Most of this aluminium, in the only natural stable valence state of +3, is found in rocks and minerals, with the average Al_2O_3 content of rock being 15.61 % [70]. Consequently, the largest natural source of "free" aluminium in the environment is due to the weathering of rocks, where aluminium is leached out by percolating water despite being less soluble than other rock elements e.g. sodium and potassium.

Weathering under temperate conditions gives rise to clay minerals [70]. Aluminium has a dual role in the complex aluminosilicates as both an octahedrally and tetrahedrally coordinated cation [68]. Only certain aluminosilicate minerals can be easily weathered, usually those with a tetrahedral structure (e.g. amphiboles and pyroxenes). Octahedrally coordinated minerals (e.g. gibbsite) are often the end-point of the weathering process. Examples of such weathering reactions [71] are given below, the structural breakdown of aluminium silicate is accompanied by release of cations and silicic acid.

I. Congruent Dissolution Reaction

$$Al_2O_3.3H_2O\ (s) + 2H_2O = 2Al(OH)_4^- + 2H^+$$

gibbsite

II. Incongruent Dissolution Reactions

$$CaAl_2Si_2O_8\ (s) + 2H_2CO_3 + H_2O = Ca^{2+} + 2HCO_3^- + Al_2Si_2O_5(OH)_4\ (s)$$

anorthite kaolinite

$$Al_2Si_2O_5(OH)_4\ (s) + 5H_2O = 2H_4SiO_4 + Al_2O_3.3H_2O\ (s)$$

kaolinite gibbsite

A study has been conducted by Johnson et al. [72] into the geochemical response to "acid rain" on the process of chemical weathering, and the influence that modern industry may have on the availability of aluminium.

3.1.3. Aqueous Chemistry of Aluminium

The aqueous chemistry of aluminium is extremely complex and diverse. The principle area of uncertainty concerns the exact nature of the hydrolysed aluminium species and whether they are monomeric or polynuclear [73,74]. This is largely due to the difficulty in making measurements of very slowly equilibrating aluminium solutions.

The form of the aluminium species in aquatic systems will be dependent on several factors including the pH of the solution, the type and concentration of complexing and chelating agents and the oxidation states of the mineral components. When aluminium salts first dissolve in water (in the absence of complexing agents) the free metal ion Al^{3+} first hydrates, coordinating six water molecules in an octahedral configuration. The first step in the hydrolysis of this hydroxy complex is:

$$Al(H_2O)_6^{3+} + H_2O = Al(H_2O)_5OH^{2+} + H_3O^+$$

The second step in monomeric hydrolysis involves the formation of the dihydroxo-aluminium(III) species $Al(OH)_2^+$. The solubility and stability of this hydroxide precipitate is strongly pH dependent.

The principal ionic aluminium(III) species in aqueous solutions are likely to be: Al^{3+}, $AlOH^{2+}$, $Al_8(OH)_{20}^{4+}$ and $Al(OH)_4^-$ [73]. In general most aluminium in natural water occurs as complexes of either fluoride or hydroxide [75], except in

waters of low pH where polymerised hydroxide aggregates of colloidal and subcolloidal size may exist.

3.1.4. Aluminium and Health

The toxic effects of aluminium were not appreciated until the late 1970s, when it was established that elevated levels were the cause of a progressive dementia in some sufferers of chronic renal disease [76]. The causes of "dialysis dementia" were recognised to be twofold. Firstly, due to the diffusion of aluminium into the patients bloodstream during dialysis therapy, and secondly the oral administration of large quantities of aluminium hydroxide to balance inorganic phosphate metabolism.

In recent years concern has been voiced as to the potential role of aluminium in other human pathological conditions including: Alzheimer senile and presenile dementia, Down syndrome with Alzheimer's disease, Parkinsonia dementia of Guam and osteomalacia [77,78]. Further studies have highlighted the possible role of aluminium in the development of brain disease and in particular neurofibrillary degeneration [79-82], (the degeneration of the fine fibres within the cytoplasm of nerve cells). The exact role of aluminium in the pathogenesis of these conditions has not been established. It has been hypothesised that elevated levels in damaged brain tissue are the result of an increase in cation binding sites available because of degenerating neurons. Alternatively, it has been suggested that aluminium plays an active role in molecular disorders, resulting in altered function, cell death and the formation of senile plaques [82]. The key to the role of aluminium is its bioavailability which will be subject to many factors [83,84]:

1. pH.
2. Counter-ions and buffers.
3. Dietary factors.
4. Formation of aluminium-lipid complexes.
5. Damage to membrane barriers.

6. Multiple chemical states of aluminium salts.
7. Route of exposure and vehicle.

Absorption of aluminium in the gut is likely to increase where there is a calcium, magnesium or zinc deficiency and decrease in the presence of fluoride [81]. Most of the aluminium that is absorbed into the bloodstream is likely to be quickly complexed by plasma proteins or silicic acid and thus excreted by renal and bile processes. It has also been proposed that aluminium may bind with inositol phosphate within cells and thus interfere with the cell-messenger system [85]. There is however little information as to the extent to which aluminium can cross biological membranes and most importantly the blood-brain barrier. The latter is the last protective mechanism to prevent the passage of harmful substances into brain tissue. It is likely that any damage to this membrane would allow aluminium bound with proteins or bio-organic phosphates to enter the brain resulting in neurone damage [86].

A study of human exposure to aluminium reveals several major sources:

1. Drinking water.
2. Residues in foods.
3. Cooking utensils.
4. Food and beverage packaging.
5. Antacid formulations.
6. Antiperspirant formulations.
7. Acidic leaching into ground water.

Most concern surrounds the dietary intake of some foodstuffs which contain high residues of aluminium [87]. Table 3.1 lists some of these as examples.

An epidemiological study in the UK [88] has shown a correlation between the aluminium content of drinking water and the occurrence of Alzheimer's

disease. This has led to renewed calls for the improvement of water quality and to abandon the use of aluminium salts in water treatment. Primarily because of the concern for the role of aluminium in human health, the EC has set GL and MAC levels of 50 and 200 $\mu g\ l^{-1}$ respectively for total aluminium in drinking water [12].

TABLE 3.1

Aluminium Content of Some Foods, Beverages and Ingestibles.

Substance	Al Content	Unit
1% extract, Earl Grey tea	1268	$\mu g\ l^{-1}$
1% extract, Camomile tea	1065	$\mu g\ l^{-1}$
1% solution, Nescafe coffee	20	$\mu g\ l^{-1}$
Diet coke	2064	$\mu g\ l^{-1}$
Mateus rose wine	886	$\mu g\ l^{-1}$
Stilton cheese	6010	$\mu g\ kg^{-1}$
Post's raisin bran	29330	$\mu g\ kg^{-1}$
Gaviscon antacid	240	$\mu g\ kg^{-1}$

3.1.5. Methods for the Determination of Aluminium

Many methods have been successfully developed for the determination of aluminium, with procedures and methodologies for a wide variety of matrices including water [89,90], steel [91], soils and minerals [92-94]. Traditionally, these methods have been based on colorimetric techniques, but in recent years other spectrometric techniques, for example inductively coupled plasma and DC arc emission spectrometry have found more widespread use [21,95]. Electrochemical methods are not widely used for the determination of aluminium in water, but a differential-pulse polarographic method has been proposed as the basis of a standard method [95]. The key to the selection of the analytical method is the form of the aluminium to be quantified, for example an atomic spectrometric method will allow the direct determination of total aluminium (including colloidal and

complexed aluminium), whereas most spectrophotometric methods will only determine free or weakly bound aluminium without sample pretreatment. Recently, an ion-chromatographic method has been proposed for the speciation of aluminium in natural and potable waters [96]. In such waters various forms of aluminium will be present, but it is unlikely that colloidal and particulate aluminium will be: 1/ Present after coagulation and flocculation processes and 2/ Bioavailable (and therefore toxic). Thus a method by which it is possible to determine free or dissolved aluminium is appropriate in the determination of residual coagulants.

The selection of a colorimetric FIA method as the basis of the instrumentation made it necessary to select a suitable chromogenic reagent both selective and sensitive for aluminium. The method must meet the analytical specification, where the range of interest is defined by current EC and UK legislation i.e. around the GL and MAC levels, 50-200 μg Al l^{-1}. An additional requirement is that the chemistry is stable for the duration of the operational period of the monitor. Marczenko [41] lists seven particularly useful reagents: aluminon, chrome azurol S [92], eriochrome cyanine R (ECR), 8-hydroxyquinoline, methylthymol blue, pyrocatechol violet (PCV) [97] and xylenol orange [93]. Other reagents that have been used include bromopyrogallol red [98] and 2,2'-dihydroxyazobenzene [99]. In a detailed study of several of the above chromogenic reagents Dougan and Wilson [100] confirmed the suitability of PCV for the determination of aluminium in water in preference to the then standard methods using aluminon and ECR. In a more recent comparison Royset [101] used four chromogenic reagents for the FIA determination of aluminium in water and concluded that the performance of the PCV method was satisfactory, and should be the reagent of choice for routine determinations.

Pyrocatechol Violet

It was decided to use the formation of the blue PCV-Al complex to quantify residual dissolved aluminium in potable and treated water. The flow-injection manifolds of Royset [102] and Henshaw et al. [103] and the UK "blue-book"

method [95] and US [11] standard method give a convenient starting point for the development of a suitable "field" method and instrumentation. The structure of PCV is shown in Fig. 3.1. PCV in it's trianionic state forms a 3:1 complex with aluminium that exhibits maximum absorbance at 580 nm (see Fig. 3.2). Good sensitivity should be achieved by the use of yellow LEDs in the solid-state detector, which exhibit maximum intensity at 583-585 nm. This complex has an ill-defined structure and is best described as a colloidal lake where the PCV molecule is either bound to the surface of, or incorporated into, the gelatinous aluminium hydroxy complexes that are likely to be prevalent in natural waters.

3.2. EXPERIMENTAL

3.2.1. Reagents

Flow-Injection (FI) Methods: All solutions were prepared in distilled/deionised or Milli-Q water in polyethylene plasticware. All reagents were of GPR (or equivalent) grade unless otherwise stated. The three reagent streams used were as follows: R1, hydroxylammonium chloride (HYD) (Aldrich) and 1,10-phenanthroline (PHE) (Fluka); R2, pyrocatechol violet (PCV) (BDH); and R3, hexamine (HEX) (Aldrich). Reagent concentrations are given in text of the discussion where appropriate. Aluminium and iron(III) 100 mg l^{-1} stock solutions were prepared by dilution of 1000 mg l^{-1} standard solutions (SpectrosoL, BDH).

Standardised Driscoll Method: All solutions were prepared in Milli-Q water and all reagents were of AnalaR (or equivalent) grade unless otherwise stated. The three reagent solutions were as follows: R1, 1.0 g l^{-1} 1,10-phenanthroline (Fluka) and 100 g l^{-1} hydroxylammonium chloride (Aldrich); R2, 0.375 g l^{-1} pyrocatechol violet (BDH); R3, 300 g l^{-1} hexamine (Aldrich) and 16 ml l^{-1} 30 % ammonia solution (AristaR, BDH). Sodium chloride (BDH) solutions were prepared by serial dilution of a 1.0 M stock solution and a 1.0 M hydrochloric acid working solution from concentrated acid (AristaR, BDH). A 0.01 M nitric acid solution was

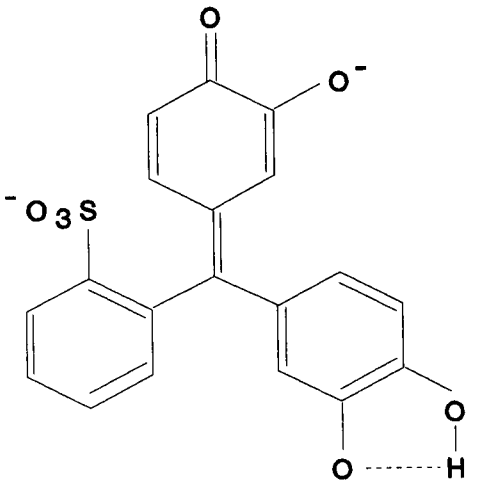

Fig. 3.1 Pyrocatechol Violet.

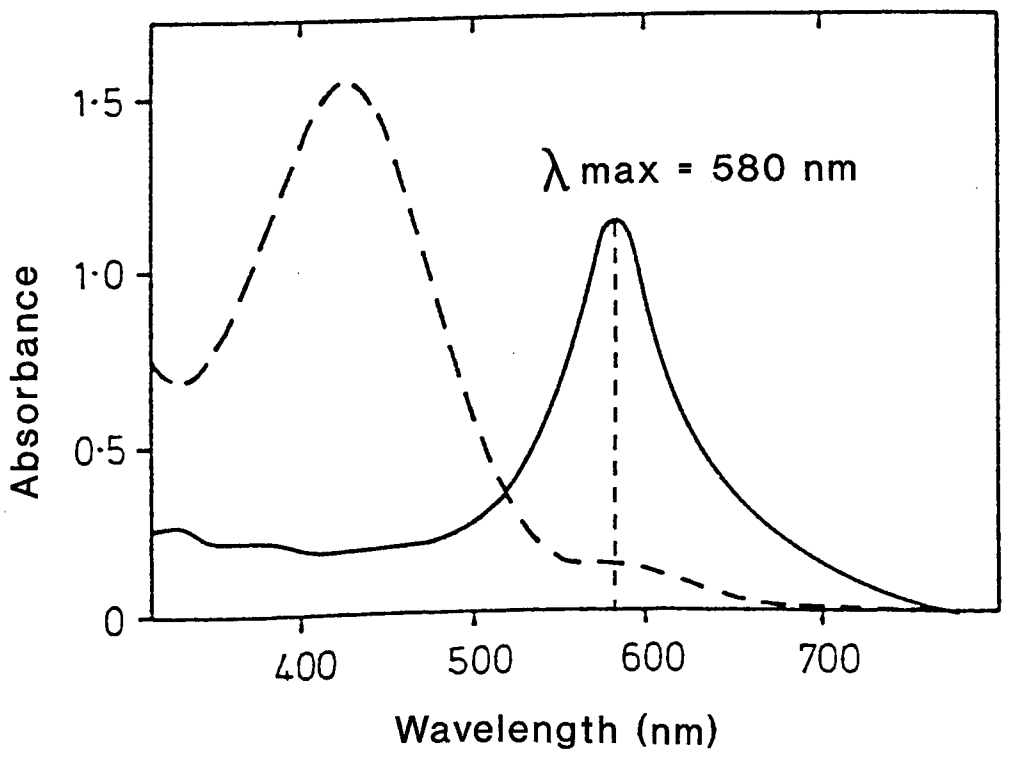

Fig. 3.2 Absorbance Spectra of PCV and PCV-Al Complex.

Key: ····· PCV —— PCV-Al

prepared from concentrated acid (AnalaR, BDH) and used to prepare the aluminium standards by dilution of a 1000 mg l^{-1} stock solution, this stock solution being prepared from high purity metal (Aldrich). A non-metal column (100 mm long and 3.5 mm i.d.) was dry packed with "Amberlite" IR - 120 (H) resin (BDH) and used in the separation of aluminium fractions in the water samples.

3.2.2. Instrumentation

Flow-Injection Methods: A manual system was used for the development, optimisation and calibration of the flow-injection manifolds. The manifolds were then incorporated into the automated FI monitor prior to its testing and validation. Variable flow rates were achieved by using a Gilson Minipuls 3 variable speed peristaltic pump. The coloured PCV-Al colloidal complex was measured with a solid-state detector fitted with either red (reagent injection manifold), or yellow (sample injection manifold) light emitting diodes. The construction details and specifications of the manual/automated systems and the solid-state detector are described in detail in Chapter 2.

Standardised Driscoll Method: All absorbance measurements for this manual batch analysis were made with a Lambda 7 double beam UV/visible spectrophotometer (Perkin Elmer). A Gilson Minipuls 3 peristaltic pump was used to propel the preparatory reagents and water samples through the ion exchange column.

3.2.3. Procedures

Flow-injection methods: A simplex optimisation procedure was used to optimise the experimental conditions both to maximise the response due to aluminium and minimise that due to iron. A modified simplex software package (for the BBC microcomputer) allowed the optimisation of a response with respect to a matrix containing up to ten elements or variables, for which each of the following conditions were specified:

Range: Boundary conditions for the variable i.e. minimum and maximum values.

Percentage of range: Maximum value, as a function of the total range, over which each variable could increase between consecutive experiments. Unless otherwise stated set to 30 %. (Maximum step size)

Precision: The smallest value or increment that could be measured. (Minimum step size)

Initial Condition: The starting point for the simplex.

The simplex matrices containing the experimental variables and the initial and final conditions for each optimisation procedure are given in the Results and Discussion section. The variables included in the simplex matrix were chosen on the basis of those most likely to interact with each other, whereas variables that were considered to be independent from the effects of other variables were excluded. The initial conditions and the range of each of the variables were derived from initial pre-optimisation experiments. These experiments were used to assess the basic suitability of a manifold and establish conditions where a reasonable performance was obtained.

During the course of these experiments a newer version of the software designed to operate on a PC compatible computer became available. The operation of this version was the same except that a maximum step size was defined as opposed to a percentage range.

Reagent Injection Manifold: Unless otherwise stated, all experiments were based around the FI manifold schematically illustrated in Fig. 3.3, where the variable parameters were: FR, the flow rate of the sample (ml min^{-1}); RV, the reagent injection volume (μl); LC, the reaction coil length (cm) and the composition of the reagent streams R1, which had a fixed flow rate of 0.7 ml min^{-1}, and R2 and R3 with fixed flow rates of 0.35 ml min^{-1} each.

Sample Injection Manifold: All experiments were based around the FI manifold schematically illustrated in Fig. 3.4, where the variable parameters were: SV, the sample injection volume (μl); C1, C2 and C3, mixing and reaction coil lengths (cm) and the composition of the reagent streams R1, R2 and R3. During

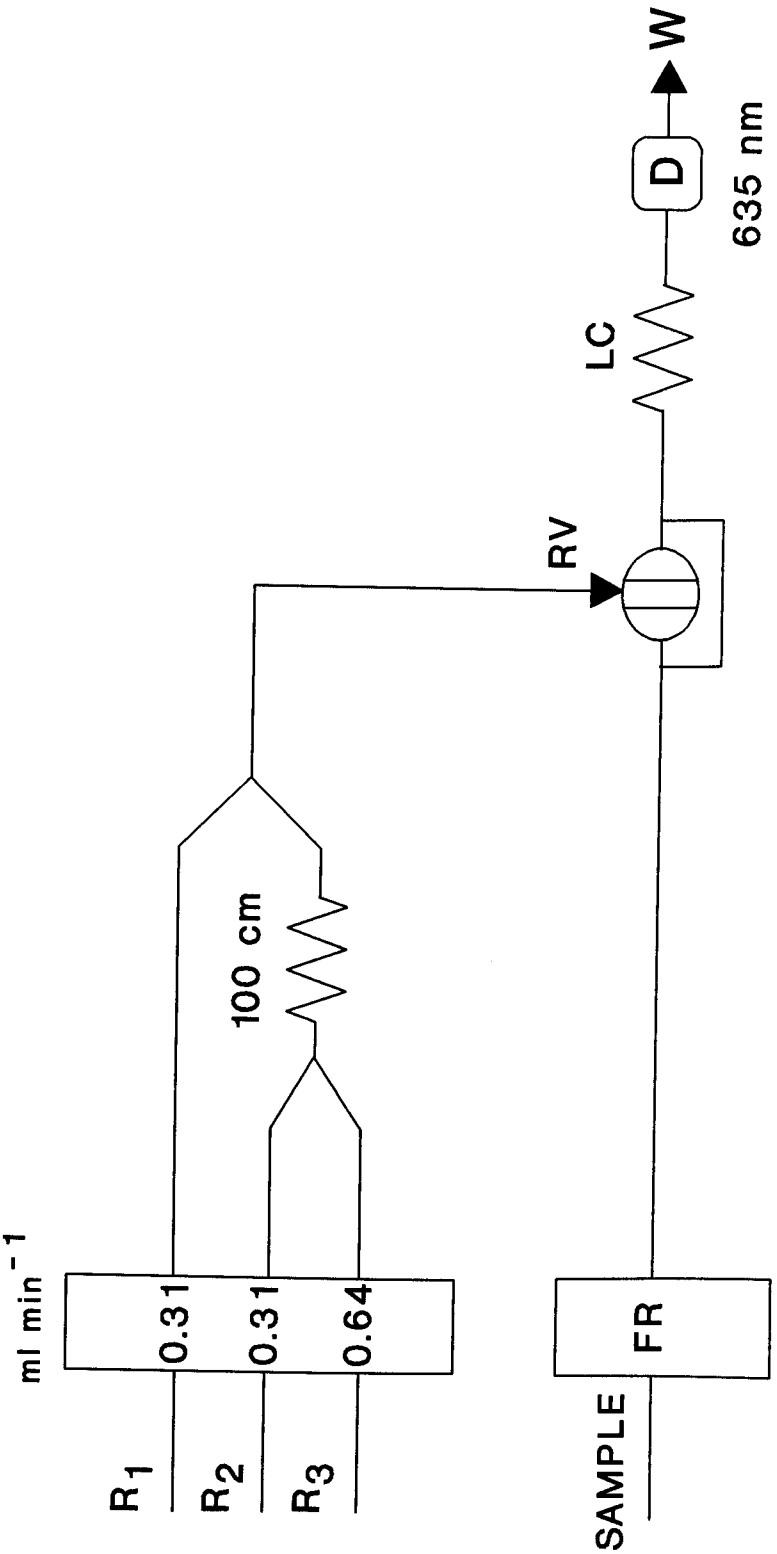

Fig. 3.3 Reagent Injection Manifold.

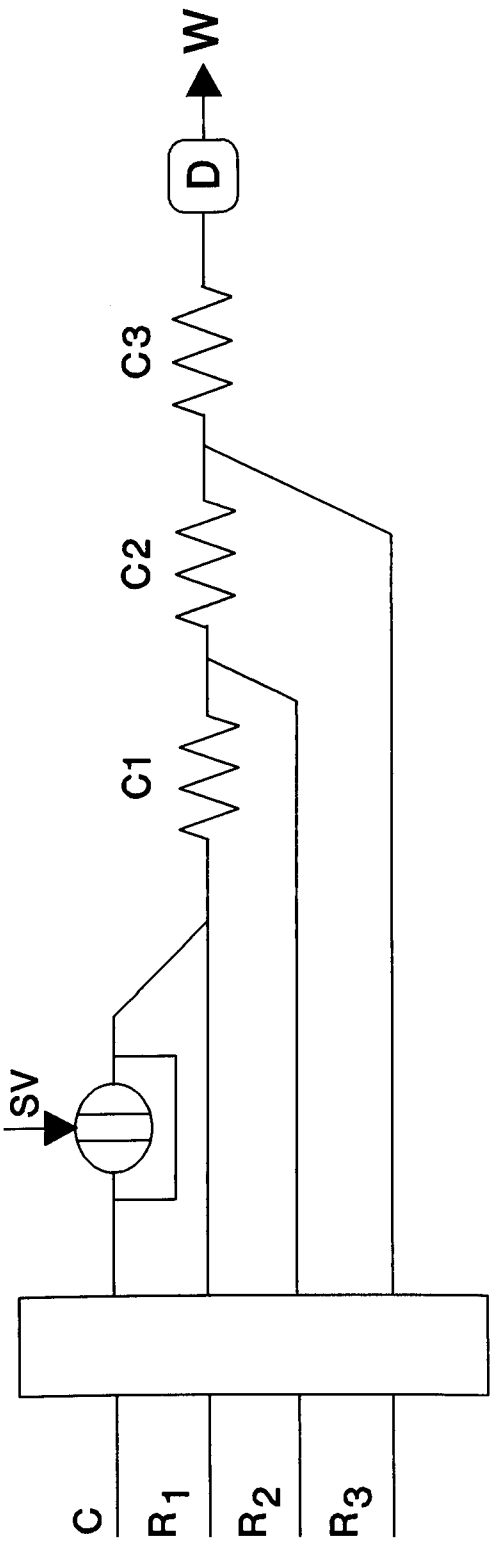

Fig. 3.4 Sample Injection Manifold.

the initial optimisation of the manifold with respect to aluminium response, the concentrations of the components of R1: hydroxylammonium chloride and 1,10-phenanthroline remained fixed at 7.6 g l^{-1} and 0.56 g l^{-1} respectively, and the mixing coil C1 remained fixed at 12 cm. The flow rates for the deionised water carrier stream (C), R1, R2 and R3 were fixed at 3.5, 0.8, 0.8 and 1.8 ml min^{-1} and at 1.45, 0.31, 0.31 and 0.64 ml min^{-1} for the manual and automated systems respectively.

Standardised Driscoll Method: The different aluminium fractions in natural waters: acid reactive (Al_r), total monomeric (Al_{tm}) and non-labile monomeric (Al_{nl}) were determined by a PCV detection method coupled with appropriate sample pretreatment.

The PCV detection method relied on the formation and measurement of the PCV-Al complex and was carried out according to the following protocol:

1. To 3.5 ml of sample, standard or blank in a 10 ml disposable polystyrene test tube (all being acidified to pH 1 for 1 hour except Al_{tm} samples, by the addition of 0.025 ml of concentrated hydrochloric acid), the following were added: 1/ 0.1 ml of R1 and 2/ 0.2 ml of R2.
2. These solutions were mixed well prior to the addition of 1.0 ml of R3.
3. After thorough mixing the reagent/sample mixture was set aside and after 10 minutes the absorbance measured at 581 nm against a Milli-Q water reference.
4. The absorbance zero was set with water in both the reference and sample cuvettes.
5. For the Al_{tm} fraction, 0.025 ml of concentrated hydrochloric acid was added simultaneously with R3 to avoid extreme sample pH variations.
6. Six replicate determinations were carried out for the blank and each sample and standard.
7. Quartz cuvettes were used for all measurements and the sample cuvette was rinsed three times with Milli-Q water and then with a small fraction of the next sample before filling with the sample and subsequent measurement.

8. All containers for stock solutions and those used during the analysis (except the test tubes) were made from high density polyethylene and cleaned before use by soaking in 10 % nitric acid for 48 hours.

The Al_{nl} fraction was separated using a cationic exchange column according to the following procedure:

1. The analytical column, as described in section 3.2.1., was cleaned with 5 ml of 1.0 M hydrochloric acid.
2. The resin was then reconverted to the sodium form with 30 ml of 1.0 M sodium chloride solution.
3. A weak sodium chloride solution, the ionic strength of which matched that of the sample to be analysed, was passed through the column until the effluent pH was within 0.2 pH units of the eluent pH (approximately 35 ml).
4. The untreated sample was then passed through the column with a flow rate of 3.5 ml min^{-1}. After discarding the first 10 ml of the exchanged sample, 3.5 ml aliquots were collected and analysed for aluminium by the PCV detection method.
5. This process was repeated for each of the six water samples.

3.3. RESULTS AND DISCUSSION

3.3.1. Optimisation of Reagent Injection FI Manifold with Respect to Aluminium Response

A reagent injection manifold was selected for two reasons: 1/ To minimise the use of reagents, and 2/ To ensure that the flow cell of the detector remained clean and free from reagent deposits by being flushed with sample. This reagent injection manifold was based on one proposed by Clinch [65]. In this work a red LED was selected for the solid-state detector, on the basis that its greater intensity

(albeit at a higher wavelength of 635 nm) would provide better sensitivity than a yellow LED. A simpler version of this manifold with the iron masking reagent stream (R1) removed, was optimised with respect to the response generated by a 500 $\mu g\ l^{-1}$ aluminium signal. The simplex matrix for this optimisation procedure is given in Table 3.2 together with the initial and final conditions. The response variable was defined as the numerical difference between the signal corresponding to 500 $\mu g\ l^{-1}$ aluminium and that corresponding to a deionised water blank, the mean of three injections for each was used.

A 20 % increase in the response variable was achieved after only 4 experiments, after which no further improvement was obtained, and the procedure was terminated after 15 experiments.

TABLE 3.2

Optimisation of Reagent Injection Manifold with Respect to Aluminium Response.

Variable	Range	Precision	Conditions	
			Initial	Final
FR (ml min^{-1})	0.17 - 1.78	0.01	0.63	0.96
LC (cm)	0 - 500	50	300	250
PCV (g l^{-1})	0.5 - 3.0	0.25	1.5	2.0
HEX (g l^{-1})	50 - 300	20	200	200
RV (μl)	10 - 300	5	15	15

3.3.2. Calibration

Five standards in the range 0 - 1000 $\mu g\ l^{-1}$ aluminium were analysed with the simplified manifold using the final conditions given in Table 3.2. The results, Table 3.3, were linear over this range (r = 0.9959) and were described by the regression equation:

$$\text{Signal (mV)} = 0.83\ [Al]\ (\mu g\ l^{-1}) + 282.30$$

The limit of detection, defined as the mean blank signal + 3σ of the blank, was calculated to be 30 μg l^{-1}.

TABLE 3.3

Calibration Data for Simplified and Optimised Reagent Injection Manifold.

Aluminium (μg l^{-1})	Signal (mV)	RSD[a] (%)
0	247.5	2.3
50	297.5	2.5
100	396.9	3.2
200	477.5	2.3
500	710.6	3.5
1000	1095.0	1.1

[a] n = 8

3.3.3. Minimising Iron Interference

Because iron(III) interferes with the PCV-Al reaction, it was necessary to minimise this interference. Ideally, up to a twenty-fold excess of iron(III) over 50 μg l^{-1} aluminium should be suppressed, although it is very unlikely that such high concentrations of iron would occur in natural waters. In North American rivers the typical dissolved iron concentration varies between 6 and 90 μg l^{-1} [73]. The masking of iron interference was achieved by the addition of an iron masking reagent stream, R1, to the FIA manifold. The two components of this reagent, hydroxylammonium chloride and 1,10-phenanthroline, are used to reduce any iron(III) to iron(II) and then remove it by complexation respectively.

The manifold was optimised with respect to iron interference; the simplex matrix including the initial and final conditions is given in Table 3.4. To reduce the

iron interference over the aluminium response, the response variable was calculated as the reciprocal value of the numerical difference between the responses given by a 50 μg l^{-1} aluminium standard and a similar standard spiked with 500 μg l^{-1} iron(III). The mean values obtained from 3 separate injections were used when calculating the difference in the responses. The simplex procedure then maximised the response variable and thereby changed the conditions to minimise the difference between the two responses.

TABLE 3.4

Optimisation of Reagent Injection Manifold to Reduce Iron Interference.

Variable	Range	Precision	Conditions	
			Initial	Final
FR (ml min^{-1})	0.89 - 4.27	0.01	0.96	1.48
LC (cm)	100 - 300	25	250	150
PHE (g l^{-1})	0.5 - 3.0	0.25	2.0	1.75
HYD (g l^{-1})	50 - 300	20	100	80
PCV (g l^{-1})	1.5 - 3.0	0.25	2.0	1.75
HEX (g l^{-1})	100 - 300	20	200	160
RV (μl)	15 - 100	5	15	15

The simplex procedure succeeded in reducing the difference in the response between the spiked and unspiked aluminium standards by > 65 %. Further reductions in the iron interference were achieved by increasing the reductant concentration from 80 to 160 g l^{-1} as illustrated in Table 3.5. The blank value increases with increasing reductant concentration, but despite this, at 50 μg l^{-1} aluminium a ten-fold excess of iron(III) gives only a small positive bias of 3 %, equivalent to 1.5 μg l^{-1} aluminium.

TABLE 3.5

Effect of Reductant Concentration on Iron Interference.

Reductant	Signal (mV)			
(g l^{-1})	Blank	Al[a]	Al/Fe[b]	Interference (%)
80	237.5	274.2	294.2	54.5
100	261.7	292.5	304.2	38.0
120	291.7	326.7	336.7	28.6
140	311.7	345.0	341.7	9.9
160	342.5	373.3	374.2	2.9

[a] Al = 50 μg l^{-1}, [b] Al = 50 μg l^{-1}, Fe = 500 μg l^{-1}

3.3.4. Calibration

The optimum manifold was calibrated to ensure that it was suitable for application in the automated system. For example that linear calibration (50 - 200 μg Al l^{-1}) and LOD (< 50 μg Al l^{-1}) requirements for the analytical method were met.

Aluminium standards in the range 0 - 500 μg l^{-1} and an equivalent range spiked with 500 μg l^{-1} iron(III) were analysed. The final conditions were stated in Table 3.4, with the exception of the reductant concentration (HYD) which was increased to 160 μg l^{-1}. The calibration data for both unspiked and spiked aluminium standards are given in Table 3.6. The responses were described by the following regression equations:

$$\text{Unspiked,} \quad \text{Signal (mV)} = 0.62\,[\text{Al}]\ (\mu\text{g } l^{-1}) + 339.04$$

$$\text{Spiked,} \quad \text{Signal (mV)} = 0.60\,[\text{Al}]\ (\mu\text{g } l^{-1}) + 337.15$$

In both cases the response was linear across the range with correlation coefficients of 0.9997 and 0.9982 respectively. The theoretical limit of detection (blank + 3σ) was calculated to be 13 μg l^{-1} from the regression equation for the

unspiked calibration. It was also apparent from this calibration data that a tenfold excess of iron was successfully masked. Therefore this manifold, having achieved suitable performance criteria, was selected as the basis of the automated FI analyser.

TABLE 3.6

Calibration Data for Automated Monitor-Optimised Reagent Injection Manifold.

	No Iron(III)		500 $\mu g\ l^{-1}$ Iron(III)	
Aluminium ($\mu g\ l^{-1}$)	Signal (mV)	RSD[a] (%)	Signal (mV)	RSD[a] (%)
0	342.5	0.4	346.3	0.2
50	370.0	0.2	370.0	0.1
100	398.0	0.2	387.9	0.5
200	458.3	0.3	448.3	0.2
400	589.2	0.5	574.6	0.2
500	645.8	0.7	640.0	0.1

[a] n = 6

3.3.5. Application of Reagent Injection Manifold to Automated Monitor

The construction and component details of the automated monitor are given in Chapter 2. The conditions for the reagent injection manifold (Fig. 3.3) are summarised in Table 3.7.

Because of the nature of the manifold it was not possible to avoid a blank signal (due to uncomplexed PCV). Therefore it was necessary that the automated monitor be able to obtain responses for a blank as well as a suitable standard, so that the aluminium concentration in the sample could be calculated. This necessitated the sequential operation of two switching valves connected in series, the first valve selecting either the standard or blank stream and the second valve selecting either the stream from the first valve or the sample stream. Duplicate

reagent injections were subsequently made into each of these three streams and the mean responses generated by each of these duplicate injections used in the calculation algorithm. The aluminium concentration in the sample, expressed as $\mu g\ l^{-1}$, together with time and date information were output to a local printer and display.

TABLE 3.7

Reagent Injection Manifold - Monitor Experimental Conditions.

Reagent Stream	Concentration ($g\ l^{-1}$)	Flow Rate ($ml\ min^{-1}$)
R1, HYD	80	
PHE	1.75	0.31
R2, PCV	1.75	0.31
R3, HEX	160	0.64
Parameter	**Value**	
FR	1.48 $ml\ min^{-1}$	
LC	150 cm	
RV	15 μl	

Development of the Automated Monitor

Two major problems were encountered in the application of the manual reagent injection manifold to the automated system:

1. The ingress of air into and/or the degassing of the "sample" stream during its passage through the flow system, i.e. the stream carrying either blank, standard or sample solutions.

2. The poor accuracy of the analytical response.

The first problem resulted in the disruption of the detector output. The passage of air through the flow cell caused a false peak, which was not readily distinguished from a genuine signal by the peak finding algorithm. The poor accuracy of the result was partly attributable to the lack of reproducibility within each pair of duplicate injections. Both of these problems were established as resulting from the operation and connection of the two switching valves.

Air Ingress and "Sample" Degassing

The ingress of air into the "sample" flow stream was found to be preventable by the careful selection of air-tight connectors between the valves and the PTFE tubing. This prevented air being "pulled into" the flow system, although air bubbles continued to be observed when either the blank or standard streams were selected. This indicated that these two solutions were degassing (at least partially), during their passage through the flow tubing of the manifold. This was later confirmed by degassing both the blank and standard solutions with helium prior to use, which alleviated the problem. The sample solution which was only pulled through one valve did not degass, therefore it was concluded that a pressure difference between the two switching valves was causing the solution degassing. No advantages were obtained by substitution of the 3-way solenoid valves with a 2-channel pinch valve. However, the fitting of a back pressure regulator to the "sample" waste line resulted in a significant reduction in the frequency with which air bubbles were observed. This in-house device comprised of a barclip around a short piece of silicone tubing, which when compressed, restricted the flow of the stream. This back pressure regulator was later replaced with a commercial version (Anachem #02-0175), with an adjustable back pressure (15 - 60 psi). Satisfactory performance was achieved with it adjusted to give minimum back pressure, while too high a pressure resulted in manifold joints being forced apart.

Accuracy of the Analytical Result

The analogue output from the solid-state detector for a complete analytical cycle of the monitor is illustrated in Fig. 3.5. Each analytical cycle comprised of a sequence of duplicate injections: 1/ Blank; 2/ sample; and 3/ standard. This analogue output showed there was carryover from the blank to the sample and sample to the standard. This problem led to a difference between the signals for duplicate injections and was thought to arise from "leakage" from the switching valve ports immediately after the transition from open to closed. The severity of this problem was highlighted by the substitution and analysis of three different "sample" solutions. The concentration of aluminium in each of these solutions was established by comparison with a 500 $\mu g\ l^{-1}$ standard. The results of this procedure, Table 3.8, highlighted the poor analytical accuracy of the monitor. Attempts were made to rectify this problem and bring the specification up to that required by the water industry of overall accuracy of ± 10 %.

TABLE 3.8

Accuracy of Aluminium FI Monitor.

Aluminium ($\mu g\ l^{-1}$)	Calculated Value ($\mu g\ l^{-1}$)	Difference (%)
50	33	34
100	83	17
200	170	15

Software Modifications

Although moderate success had been achieved by some of the hardware alterations it was decided that software modifications were required to improve the accuracy of the analytical response, reliability and general operational performance characteristics of the monitor.

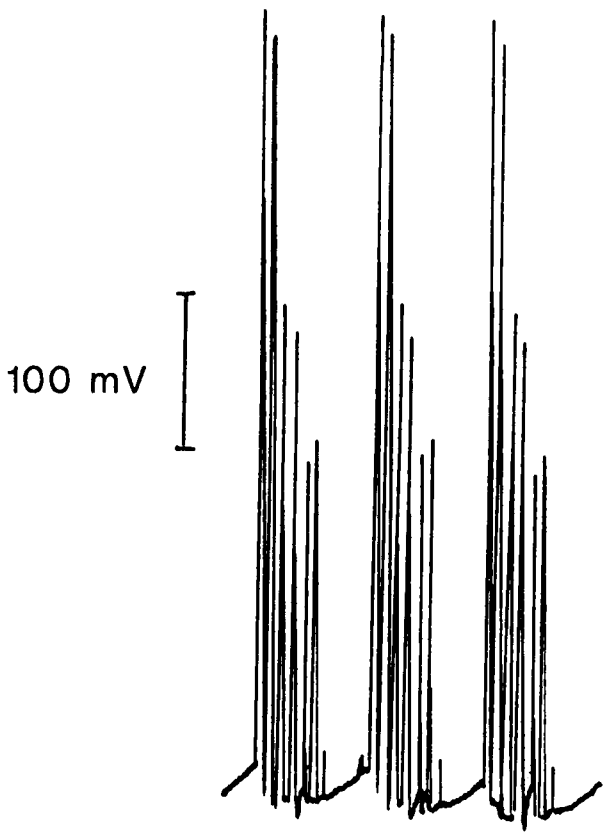

Fig. 3.5 Analogue Output from FI Monitor.

The timing intervals and sequencing of the injections and pump operation were adjusted, but no significant improvements could be made to reduce the carryover effect, and thus the overall accuracy of the calculated result. Further software modifications, detailed below, were made so that the monitor could provide reliable trend information. Error checking routines were introduced into the data processing software to isolate erroneous signals caused by air spikes. These modifications attempted to identify the air spikes by establishing when a maximum signal was achieved. If the rate at which the signal increased was greater than expected for a "normal" flow-injection peak (i.e. a different peak profile), an error was reported. The analytical result calculated using this signal was rejected and an error message transmitted to the local display and printer. The modified software was evaluated in a laboratory-based trial for aluminium in tap water. During a typical period of operation over 32 hours, 15 of the 64 results were identified as erroneous by studying the analogue output from the detector; 10 of which were identified by the software. The calculated overall success rate of the monitor was therefore > 76 %, while > 60 % of the erroneous results were positively identified. The final monitor specifications, including reagent consumption and performance characteristics are summarised in Table 3.9. The advantages associated with using a reagent-injection FI manifold, i.e. low reagent consumption, were outweighed by the disadvantages associated with the blank signal, and in particular the use of two switching valves in series. An alternative sample-injection manifold was therefore developed to simplify the automated monitor.

TABLE 3.9

Performance Characteristics for Reagent-Injection FI Monitor.

Parameter	Value
Overall Accuracy	± 34 % at 50 $\mu g\ l^{-1}$ ± 15 % at 200 $\mu g\ l^{-1}$
Response Time	18 min
Nominal Range	0 - 1000 $\mu g\ l^{-1}$
Limit of Detection	15 $\mu g\ l^{-1}$
Reliability	> 70 %
Reagent Consumption[a] (l)	
Iron Mask	1.0
PCV	0.5
HEX	0.5
Standard	2.7
Blank	4.0

[a] For twice hourly determinations over a 7 day period

3.3.6. Selection and Optimisation of a Sample Injection Manifold with Respect to Aluminium Response

To overcome the drawbacks of the reagent injection manifold, a sample injection manifold was developed for incorporation into the automated system. This type of manifold removes the need for two switching valves because it can be configured so that no blank signal is observed.

The sample injection manifold proposed by Henshaw et al. [103] was adopted and eight aluminium standards covering the range 0 - 1000 $\mu g\ l^{-1}$ were analysed using the set of conditions which were subsequently used as the initial simplex conditions. The response was linear ($r = 0.9999$) and was described by the regression equation:

$$\text{Signal (mV)} = 0.09\ [\text{Al}]\ (\mu g\ l^{-1}) + 0.21$$

The manifold exhibited a wide linear range and a practical limit of detection, defined as twice the peak-to-peak baseline noise, of < 25 $\mu g\ l^{-1}$. This definition for the LOD was used instead of (blank + 3σ) because of the absence of a measurable blank signal.

This manifold was then optimised with respect to the mean response of six injections of a 50 $\mu g\ l^{-1}$ aluminium standard. The simplex optimisation matrix containing the five variables is given in Table 3.10, this table also includes two sets of "final" conditions at which increases of 77 % and 112 % respectively over the initial response were achieved. These conditions were designated as Manifold (A) and (B) and their performance characteristics were studied; details are given in the following section.

A plot of the response against experiment number, Fig. 3.6, illustrates the pattern of the modified simplex optimisation procedure. The plot reveals three distinct "groups" of data. In each case a sharp rise in the response is followed by a slow decrease before a new set of conditions were located which produced a significantly higher response. This large change in response appeared to be due

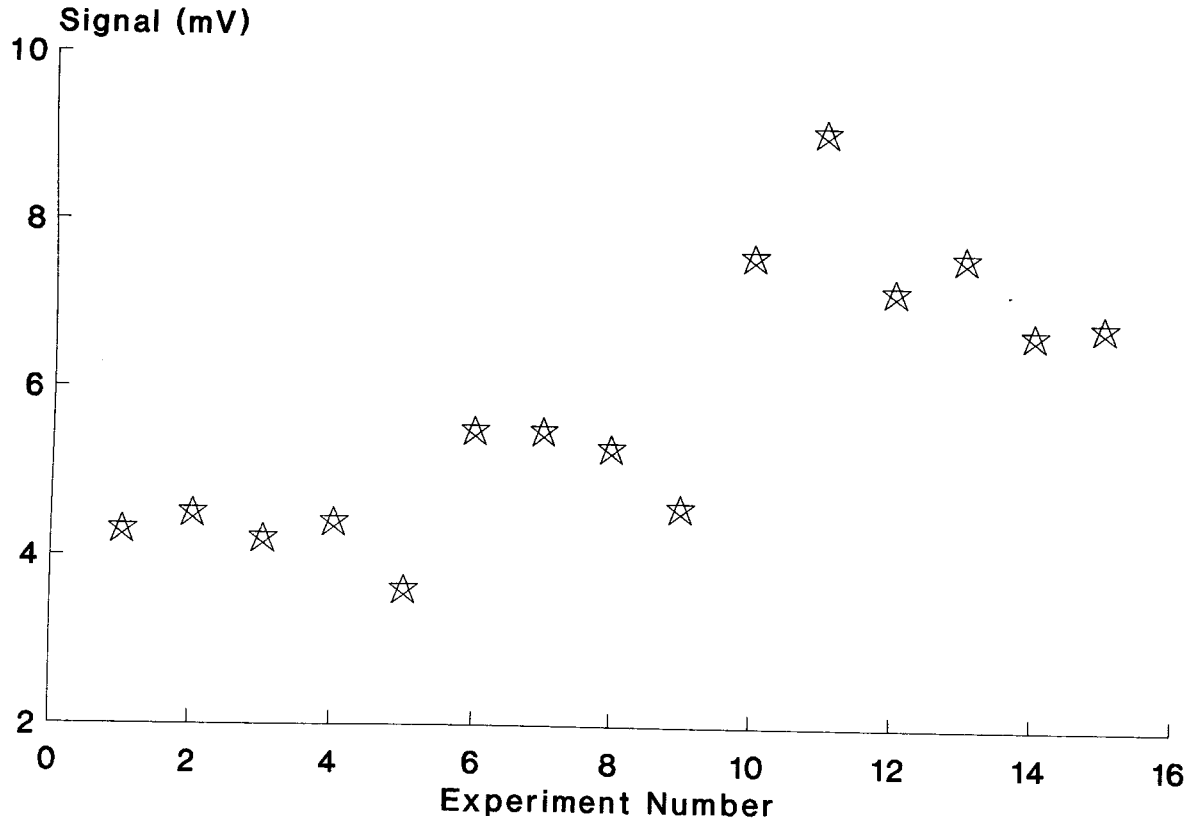

Fig. 3.6 Simplex Optimisation to Maximise Aluminium Response.

to an expansion of the simplex resulting in a significant increase in injection volume. This might be expected to give rise to an increase in the response because of the higher aluminium loading.

TABLE 3.10

Optimisation of Sample Injection Manifold with Respect to Aluminium Response.

Variable	Range	Precision	Conditions		
			Initial	Final (A)	(B)
PCV ($g\ l^{-1}$)	0.1 - 1.0	0.1	0.4	0.4	0.2
HEX ($g\ l^{-1}$)	70 - 100	2	84	82	80
C2 (cm)	0 - 100	10	60	20	0
C3 (cm)	0 - 200	10	100	40	30
SV (μl)	10 - 200	10	100	160	200

A two dimensional variable-size simplex with three vertices is illustrated in Fig. 3.7. The rules for the optimisation procedure for reflection, contraction and expansion are as follows [104,105]:

1. The initial simplex is labelled BNW and after measurement, vertex B was found to have the best response, N the next best and W the worst. P is the centroid of the face remaining when W is eliminated from the full simplex.

2. A *reflection* is accomplished by extending the line segment WP beyond P to generate the new vertex R, where:

$$R = P + (P - W)$$

3. The response at this new vertex R is measured, the three possibilities for the response will each generate a different new vertex:

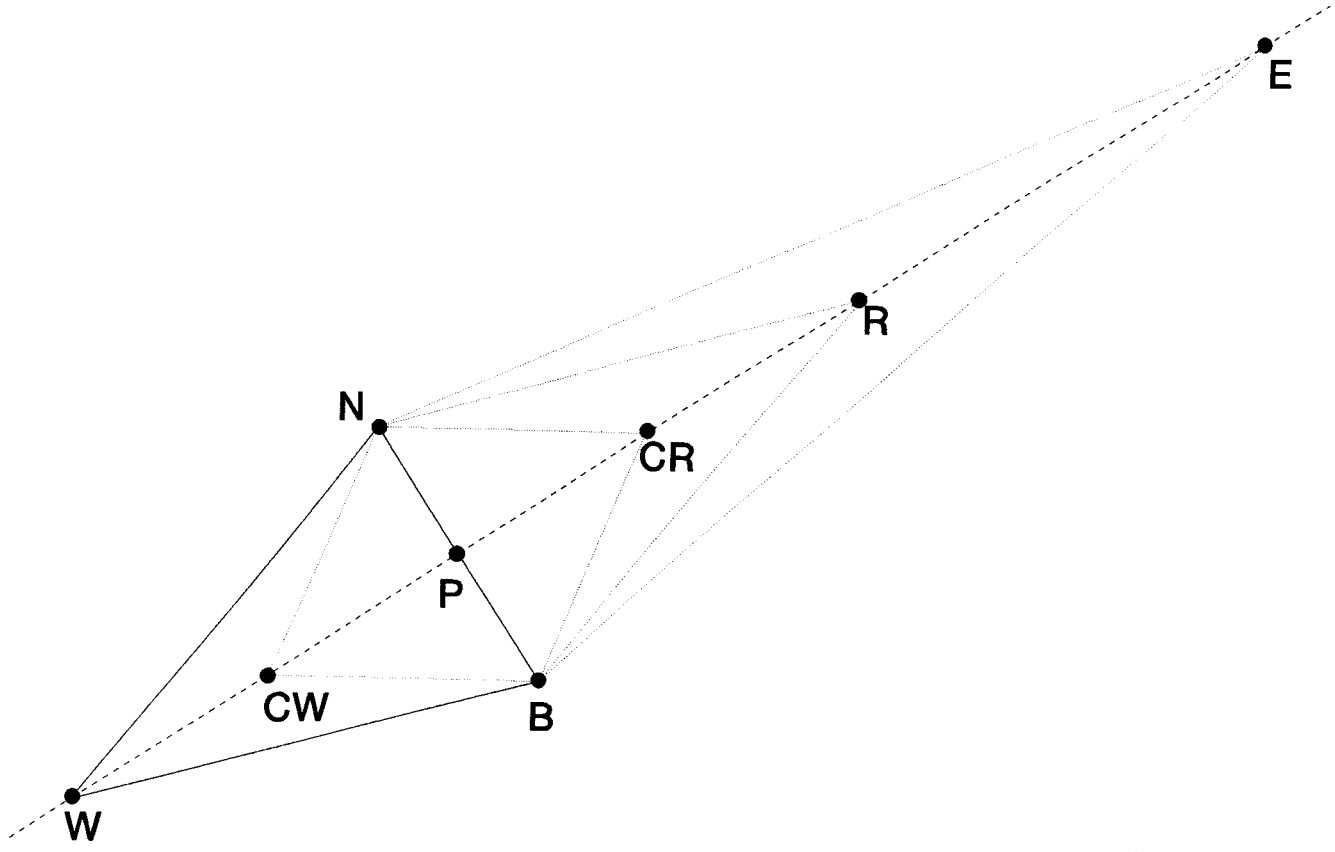

Fig. 3.7 Schematic Illustration of a Variable Size Simplex.

(a) If the response at R is better than that at B an *expansion* is performed and the new vertex E is generated, where:

$$E = R + (P - W)$$

If the response at E is: 1/ Better than the response at B then the new simplex is BNE. 2/ Worse than at B, the expansion has failed and BNR is the new simplex. The algorithm then iterates using the new simplex BNE or BNR and its vertexes ranked from best to worse.

(b) If the response at R is between that of B and N neither expansion or contraction is recommended and the algorithm continues with the new simplex BNR.

(c) If the response at R is worse than the response at N, a step in the wrong direction has been made and the simplex should be *contracted*. One of two possible vertexes must be generated.

i/ If the response at R is worse than the response at N but not worse than the response at W, the new vertex should lie closer to R than to W.

$$C_r = P + (P - W)/2$$

The algorithm then continues using the new simplex BNC_r

ii/ If the response at R is worse than the previous worst vertex W, the new vertex should be closer to W than R.

$$C_W = P - (P - W)/2$$

The algorithm then continues using the new simplex BNC_W.

Alternative Manifolds

The selection of the most suitable manifold conditions from those established during the optimisation procedure was carried out on the basis of the response achieved for the analysis of a range of aluminium standards, 0 - 1000 μg l^{-1}, using both Manifolds (A) and (B). The response was linear across the range for both manifolds ((A): r = 0.9998, (B): r = 0.9990) and described by the regression equations:

$$\text{(A):} \quad \text{Signal (mV)} = 0.15\ [\text{Al}]\ (\mu g\ l^{-1}) + 0.08$$

$$\text{(B):} \quad \text{Signal (mV)} = 0.19\ [\text{Al}]\ (\mu g\ l^{-1}) - 2.38$$

The practical limit of detection, twice the peak-to-peak noise was 10 μg l^{-1} for (A) and 18 μg l^{-1} for (B). Both manifolds exhibited the necessary performance requirements but (A) was chosen as the optimum manifold because of the lower noise and therefore lower limit of detection. Manifold (A) was used for all other investigations unless otherwise stated.

3.3.7. Minimising Iron Interference

Table 3.11 illustrates the effect of the presence of a 1000 μg l^{-1} spike of iron(III) on the response to aluminium standards in the range 50 - 600 μg l^{-1}. At 50 μg l^{-1} aluminium a twenty-fold excess of iron led to a 50 % increase in the signal, while at 200 μg l^{-1} aluminium a five-fold excess of iron gave only a small positive bias of 6 %.

To reduce the level of iron interference observed at low concentrations of aluminium, a simplex optimisation procedure was used with a three variable matrix. This matrix included variables for the component concentrations of the iron masking reagent (R1) and the length of the reagent/carrier stream mixing coil. Fig. 3.8(a) illustrates the changing response difference between the unspiked and spiked aluminium standards with experiment number. In the simplex the response

variable was defined as the reciprocal of the numerical difference in the responses observed for a spiked (1000 μg l^{-1} Fe (III)) and an unspiked 50 μg l^{-1} aluminium. The simplex was terminated after 10 experiments after which the simplex fell outside of the boundary conditions. No significant decrease in the level of iron interference was observed without an accompanying decrease in the signal observed for the unspiked aluminium standard, which decreased the sensitivity of the method. Fig. 3.8(b) illustrates the change in the concentration of 1,10-phenanthroline during the optimisation procedure. Comparison of Fig. 3.8(a) and Fig. 3.8(b) reveals that when the simplex expands to reduce the 1,10-phenanthroline concentration the response difference increases. The simplex then compensates for this by contracting again.

TABLE 3.11

Effect of 1000 μg l^{-1} Iron(III) on Aluminium Signal - Sample Injection Manifold (A).

	Unspiked		Spiked		
Aluminium (μg l^{-1})	Signal (mV)	RSD[a] (%)	Signal (mV)	RSD[a] (%)	Increase (%)
50	7.3	5.4	11.0	2.0	+ 50.7
100	14.4	3.1	15.8	1.4	+ 9.7
200	28.3	2.0	30.0	0.4	+ 6.0
400	59.0	0.8	57.1	0.8	- 3.2
600	88.0	0.6	91.1	0.9	+ 3.5

[a] n = 6

It was not possible to reduce the iron interference further using either simplex optimisation or univariate optimisation techniques. This manifold was however used as the basis for the FI monitor, where in the intended application for the monitoring of residual coagulants the iron levels will be low. The iron suppression capabilities would be sufficient to suppress any natural iron present, usually < 100 μg Fe l^{-1}.

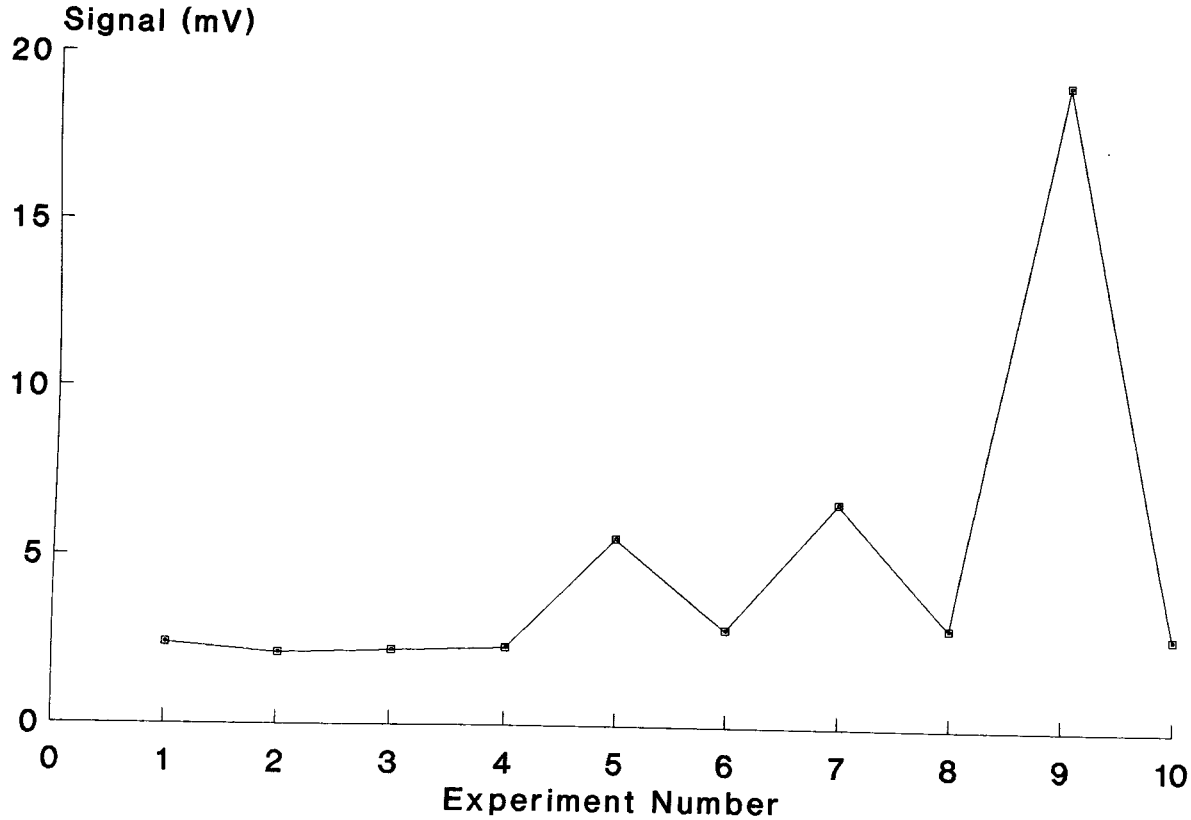

Fig. 3.8(a) Simplex Optimisation to Reduce Iron Interference.

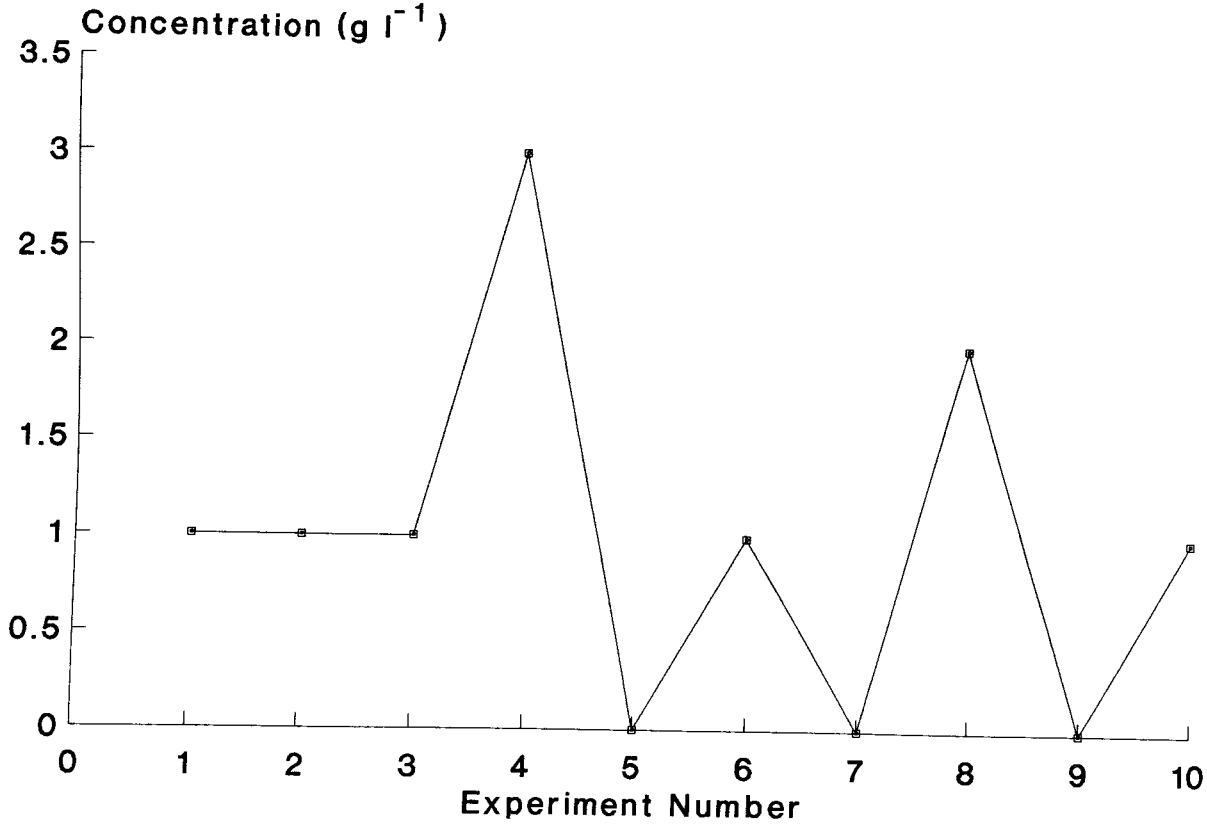

Fig. 3.8(b) Simplex Optimisation - Changing Phenanthroline Concentration.

3.3.8. Application of Sample Injection Manifold to Automated FI Monitor and Method Stability

The application of the previously optimised manifold to the monitor was relatively straightforward with only one switching valve required to select either a standard or sample, although consideration was given to the flow rates of the carrier and reagent streams:

1. The economical use of the reagents was considered to be important to allow for extended unattended operation of the monitor. Therefore, lower flow rates were selected in preference to those used in the manual FI manifold, without significantly decreasing sample throughput.

2. The peristaltic pumps utilised in the automated system had a fixed head speed of 20 rpm, which coupled with the most suitable pump tubing restricted the available flow rates to between 0.2 ml min^{-1} and 1.45 ml min^{-1}.

It was anticipated that any reduction in the flow rates of the carrier or reagent streams would not lead to a significant change in the overall performance of the manifold, provided that the relative flow rates between the different reagent streams remained unchanged.

The experimental conditions for the FI manifold are given in Table 3.12. These conditions were unchanged from Manifold (A) except that the flow rates were reduced to achieve a decrease in reagent consumption while maintaining the same reagent ratios. The performance characteristics of this manifold together with the stability of the method are examined below.

TABLE 3.12

Sample Injection Manifold - Monitor Experimental Conditions.

Reagent Stream	Concentration ($g\ l^{-1}$)	Flow Rate ($ml\ min^{-1}$)
C, Deionised Water	-	1.45
R1, HYD	7.6	-
PHE	0.56	0.31
R2, PCV	0.4	0.31
R3, HEX	82	0.64
Parameter	**Value**	
C1	12 cm	
C2	20 cm	
C3	40 cm	
SV	160 μl	

Method Stability and Performance

In order to assess the stability of the method a batch of reagents were prepared and used to analyse seven aluminium standards over a 16 day period. The aluminium standards, 0 - 1000 $\mu g\ l^{-1}$, were prepared immediately prior to each analysis. The calibration data collected during the stability trial is summarised in Table 3.13, over which time the calibration remained linear. From the calculated regression equations given below the practical limits of detection, defined as twice the peak-to-peak noise, were 46, 51 and 44 $\mu g\ l^{-1}$ on days 1, 3 and 17 respectively.

Day 1, Signal (mV) = 0.043 [Al] ($\mu g\ l^{-1}$) - 0.250 ($r = 0.9988$)

Day 3, Signal (mV) = 0.045 [Al] ($\mu g\ l^{-1}$) - 0.290 ($r = 0.9994$)

Day 17, Signal (mV) = 0.043 [Al] ($\mu g\ l^{-1}$) + 0.106 ($r = 0.9999$)

This trial illustrated that the reagents and hence the method were stable over a period of at least 16 days, confirming the work of Dougan and Wilson [100] who found that the reagents were stable for up to 11 weeks.

TABLE 3.13

Sample Injection Method Stability Trial - Calibration Data.

	Day 1		Day 3		Day 17	
Aluminium ($\mu g\ l^{-1}$)	Signal (mV)	RSD[a] (%)	Signal (mV)	RSD[a] (%)	Signal (mV)	RSD[a] (%)
0	0	0	0	0	0	0
50	2.4	8.9	2.5	12.0	2.6	12.1
100	4.6	5.2	4.2	8.1	4.3	6.8
200	8.9	4.7	8.6	5.5	8.4	3.7
400	17.8	2.4	16.7	2.2	17.1	2.8
600	26.7	2.0	25.7	1.1	25.6	1.9
800	32.9	1.9	35.4	1.3	34.4	1.2
1000	44.0	1.6	45.1	0.6	42.6	1.2

[a] n = 10

To ensure that the monitor FI manifold with the lower flow rates still adequately suppressed iron interference, four spiked aluminium standards were prepared and analysed using a manual manifold with the same experimental conditions as outlined in Table 3.12. The results from these analyses are given in Table 3.14 and show that a twenty-fold excess at the GL level (50 $\mu g\ l^{-1}$) gave rise to only a small positive bias. It was concluded that without major revision of the standard method it was unlikely that any further reduction in the level of iron interference could readily be achieved.

The method fulfilled the requirements for the determination of dissolved aluminium, with a wide linear range and a practical limit of detection below the GL level.

TABLE 3.14

Interference of Iron(III) on Aluminium Signal[a] (mV) - FI Monitor.

Aluminium	Iron(III) ($\mu g\ l^{-1}$)				
($\mu g\ l^{-1}$)	0	50	100	200	1000
0	0	0	0	0	0
50	2.2	2.3	2.6	2.6	2.6
100	4.6	4.2	4.2	5.2	5.4
200	8.2	8.5	8.3	9.6	10.4
1000	44.0	44.3	44.3	44.6	45.8

[a] n = 6

3.3.9. Monitor Performance and Field Trials

The PCV method for aluminium only allows the quantitative determination of a particular fraction of the total aluminium (see discussion in following sections) and consequently the monitor is best suited to applications where trend information is required, rather than absolute values.

Monitor Accuracy

The accuracy of the quantitative determination of dissolved aluminium, in the absence of iron(III), was assessed by the substitution of the "sample" with an aluminium standard. Three solutions were each analysed for a minimum of 24 hours against the same 200 $\mu g\ l^{-1}$ aluminium standard, the results of this trial are given in Table 3.15. As expected, with increasing concentration and increasing response (with the subsequent improvement in the signal-to-noise ratio), the accuracy and precision of the measurement improved. The FI monitor met the industry specification for accuracy at both the GL and MAC levels.

TABLE 3.15

Accuracy and Precision of the FI Monitor.

Aluminium ($\mu g\ l^{-1}$)	Response ($\mu g\ l^{-1}$)	Difference (%)	σ ($\mu g\ l^{-1}$)	RSD (%)
50	45.4	- 9.2	4.9	10.8[a]
150	157.9	+ 5.3	7.4	4.7[b]
200	203.9	+ 2.0	5.8	2.8[c]

[a] n = 135, [b] n = 58, [c] n = 60

Field Trials and System Evaluation

During a series of field trials, in which the monitor was applied to the determination of dissolved aluminium in tap water, hardware and software modifications were evaluated. These modifications were made to improve response precision and optimise rejection and operation thresholds. These modifications were all made to ensure the validity of the analytical response. A summary of the major changes is given below; the resulting performance characteristics are given in Table 3.16. The performance of the monitor was assessed in terms of both initial failure rate and overall success rate after one repeat determination.

System Modifications:

1. Back pressure regulators fitted on sample line and reagent waste line (set to minimum backpressure). (ALMON2E).
2. Monitor software unchanged, but regulators adjusted to increase backpressure.
3. New version of software evaluated which featured a new pattern of valve and pump operation to avoid sample/standard carryover. (ALMON6.1E).
4. Software further modified to include repeat function if < 4 peaks isolated from acquired data, Brij 35 (0.3 % w/v) added to the carrier stream to prevent adhesion of PCV-Al colloidal lake to detector flow tubing. (ALMON6.6E).

5. Software further modified to initiate repeat determination if standard "peaks" did not fall within defined threshold limits. (ALMON6.7E).
6. Repeat trials with specification as (5).
7. Repeat trials with specification as (5).
8. Threshold value for peak rejection lowered from 5 to 2 mV (expected noise ≈1 mV), new error message to indicate aluminium concentration below limit of detection if <4 peaks detected. (ALMON6.8E).

TABLE 3.16

Performance Characteristics for FI Monitor Trials.

		Failures		Repeats	
Trial	Cycles	No.	Rate (%)	No.	Rate[a] (%)
(1)	142	42	29.6	-	-
(2)	149	16	10.7	-	-
(3)	109	15	13.8	-	-
(4)	197	33	16.8	3	84.8
(5)	180	34	18.9	31	98.3
(6)	229	78	34.1	54	89.5
(7)	145	18	12.4	12	95.9
(8)	86	4	4.7	4	100.0

[a] Overall success rate

Fitting back pressure regulators and adding surfactant to the carrier stream, and the refinement of the software improved monitor operation. Although errors were not completely avoided, good overall performance was achieved. A fully remarked program is given in Appendix B, with user defined thresholds highlighted.

Response and Monitor Protocol

The overall timing of the operational cycle was reduced to a minimum by careful adjustment of the flush periods, but still ensuring that sample/standard carryover was prevented and that fresh sample was drawn into the manifold for each determination. The analytical cycle took nine minutes and was repeated every thirty minutes (on the hour and half hour). This framework allowed two repeat determinations while still remaining within the thirty minute schedule. A repeat was initiated if the difference between the two standard signals fell outside of the predefined margin. This margin was set so that random noise did not cause the rejection of an otherwise valid result.

Reagent Consumption

The reagent consumption, Table 3.17, was calculated on the basis of a 35 day operational cycle, i.e. unattended operation between scheduled routine maintenance periods; these consumption figures also allowed for a 10 % repeat of the analytical cycle. The repeat rate was set at this value assuming that the monitor provided valid results on the basis of first determinations for 90 % of the operational period.

TABLE 3.17

Reagent Consumption for Sample Injection FI Aluminium Monitor.

Stream	Litres
Carrier	18.8
Iron mask reagent	8.0
Colour reagent	8.0
Buffer	16.6
Standard	12.2

Overall Monitor Performance

This was assessed by comparison of the performance characteristics for the FI monitor (from field trials) and those detailed by the water industry [24], Table 3.18. The proposed aluminium monitor met the specification detailed by the water industry for analysers, for clarified water monitoring. For this application significant changes are expected to occur within a period of thirty to sixty minutes [25], within which the monitor must respond.

TABLE 3.18

Monitor Specification and Performance.

Parameter	Industry specification	Proposed monitor
Overall accuracy	± 10 %	± 9 % (at 50 $\mu g\ l^{-1}$)[a] ± 2 % (at 200 $\mu g\ l^{-1}$)[b]
Repeatability	± 10 %	± 10 % (at 50 $\mu g\ l^{-1}$)[a] ± 3 % (at 200 $\mu g\ l^{-1}$)[b]
Response time	< 15 min	9 min
Nominal range	0-1000 μg l-1	0-1000 $\mu g\ l^{-1}$
Limit of detection		45 $\mu g\ l^{-1}$
Reliability		> 90 %

[a] n = 135, [b] n = 60

3.3.10. Detector Design and Comparison between Manual and FI Procedures

To improve the sensitivity of the method a modification was made to the detector, whereby the PTFE flow tubing in the detector flow cell was substituted with glass capillaries (see Chapter 2 for full details). Calibration data for the two different detectors is given in Table 3.19, the responses were linear using both detectors across the range (0 - 1000 $\mu g\ l^{-1}$) and were described by the following regression equations:

(A) Signal (mV) = 0.040 [Al] (μg l^{-1}) + 1.251 (r = 0.9996)

(B) Signal (mV) = 0.26 [Al] (μg l^{-1}) + 2.88 (r = 0.9996)

A blank solution was obtained because, in this experiment, the standards were prepared in dilute nitric acid (to be consistent with the Driscoll method). This signal, was more likely to be due to changing refractive index than aluminium contamination of the blank solution. The limits of detection, calculated as the blank + 3σ, were 73 μg l^{-1} for the unmodified detector (A) and 14 μg l^{-1} for the modified detector (B). The modification to the detector greatly enhances the sensitivity of the method. At 40 μg l^{-1} an increase of > 390 % was achieved, while maintaining the linearity of the calibration over the range of interest. This improvement was due to the higher light transmission properties of the glass capillaries. Unfortunately these capillaries, may not be suitable for all applications and were not as robust as the PTFE tubing. An alternative would be to use a more transparent fluoropolymer tubing thereby maintaining the advantages of the PTFE tubing, i.e. flexibility and durability but with greater light throughput.

To check this theoretical limit of detection a range of 10 aluminium standards, 10 - 60 μg l^{-1}, were analysed with the modified detector (B). The response was linear, Table 3.20, and was described by the regression equation:

Signal (mV) = 0.25 [Al] (μg l^{-1}) + 4.21 (r = 0.9976)

Although the response for a 10 μg l^{-1} standard was discernable above the blank signal, a practical limit of detection (blank + 3σ) of 18 μg l^{-1} could more realistically be measured in a "field" application.

TABLE 3.19

Comparison Data for Solid-State Detectors.

Aluminium ($\mu g\ l^{-1}$)	Detector (A) Signal (mV)	Detector (A) RSD[a] (%)	Detector (B) Signal (mV)	Detector (B) RSD[b] (%)
0	2.0	33.3	4.5	12.2
10	-	-	4.8	8.5
20	-	-	6.7	7.8
40	2.4	21.5	11.8	6.4
60	3.3	25.0	17.0	3.7
80	4.5	15.7	22.2	3.4
100	5.1	28.4	28.3	2.9
200	8.8	9.0	52.5	1.0
300	13.1	5.6	79.8	0.9
400	16.9	1.9	105.5	0.5
500	21.4	3.3	133.8	0.6
600	25.5	2.1	161.2	0.7
800	33.1	2.2	206.8	1.5
1000	40.4	1.3	252.8	0.8
Noise	0.8	10.0	1.0	66.7

[a] n = 10, [b] n = 6

TABLE 3.20

Validation of Limit of Detection for Modified Detector.

Aluminium ($\mu g\ l^{-1}$)	Signal (mV)	RSD[a] (%)
0	5.1	21.6
10	6.4	8.1
15	7.7	11.3
20	9.0	7.4
25	10.4	5.1
30	11.5	4.6
35	12.2	6.5
40	14.1	7.8
45	15.8	7.8
50	16.5	5.9
60	19.7	7.2
Noise	1.0	-

[a] n = 10

Comparison of Methods

As part of a European Community BCR programme (Project No. 5311/1/9/351/90/02-BCR-(10)) the fractionation of aluminium in three tap and three lake water samples was established by the use of a standardised Driscoll method. The results of three separate analyses carried out over a period of four months are given in Table 3.21. The values for the aluminium fractions: Al_{tm} (total monomeric), Al_{nl} (non-labile), Al_r (total reactive) were established directly by analysis, while Al_{lb} (labile) and Al_{sl} (acid soluble) fractions were calculated by difference. A schematic representation of the different aluminium fractions is given in Fig. 3.9. The non-labile fraction contains monomeric alumino-organic complexes and the labile fraction free aquo aluminium and inorganic complexes. The acid soluble fraction contains colloidal aluminium and extremely non-labile organic complexes [106]. Table 3.22 compares the calculated values from the Driscoll method for the labile and total monomeric aluminium fractions, with those calculated for the same samples using the manual FI method. The labile aluminium fraction best matches the values calculated from the FI method. Therefore, it would appear likely that this fraction, which should the be most readily available for complexation, was that which was being determined by the FI method. The labile fraction correlates strongly with pH while the non-labile fraction correlates to dissolved organic carbon. Thus small changes in pH may significantly change the balance of the aluminium fractions.

This comparison confirmed that the FI method was only determining a small fraction of the total aluminium. However, any residual coagulant is most likely to exist in an uncomplexed monomeric form, but dependant on the presence of complexing species, for example fluoride and humic substances. The calculated aluminium values should therefore only be used as a guide to changing aluminium levels and not absolute values.

TABLE 3.21

Aluminium Fractions ($\mu g\ l^{-1}$) - Driscoll Method.

	pH	Al_r	Al_{nl}	Al_{tm}	Al_{lb}	Al_{sl}
Event One, Day 1						
A	7.9	11.0	39.6	9.5	-	1.5
B	8.0	79.4	8.8	72.6	63.8	6.8
C	6.4	286.7	11.0	29.8	18.8	256.9
D	8.2	8.0	11.8	7.3	-	0.7
E	7.9	104.2	10.3	98.2	87.9	6.0
F	7.3	42.6	9.5	26.0	16.5	16.6
Event Two, Day 36						
A	7.8	11.3	8.5	12.7	4.2	-
B	7.9	60.1	12.7	57.9	45.2	2.2
C	-	139.3	10.6	23.3	12.7	116.0
D	8.0	11.3	7.8	11.3	3.5	-
E	7.8	101.0	12.7	97.5	84.8	3.5
F	7.2	50.9	8.5	37.4	28.9	13.5
Event Three, Day 124						
A	8.1	12.1	5.7	11.5	5.8	0.6
B	8.1	62.4	5.1	56.7	51.6	5.7
C	6.2	111.5	4.5	17.8	13.3	93.7
D	8.3	7.6	3.8	8.3	4.5	-
E	8.3	98.0	14.0	94.8	80.8	3.2
F	7.5	44.6	3.8	41.4	37.6	3.2

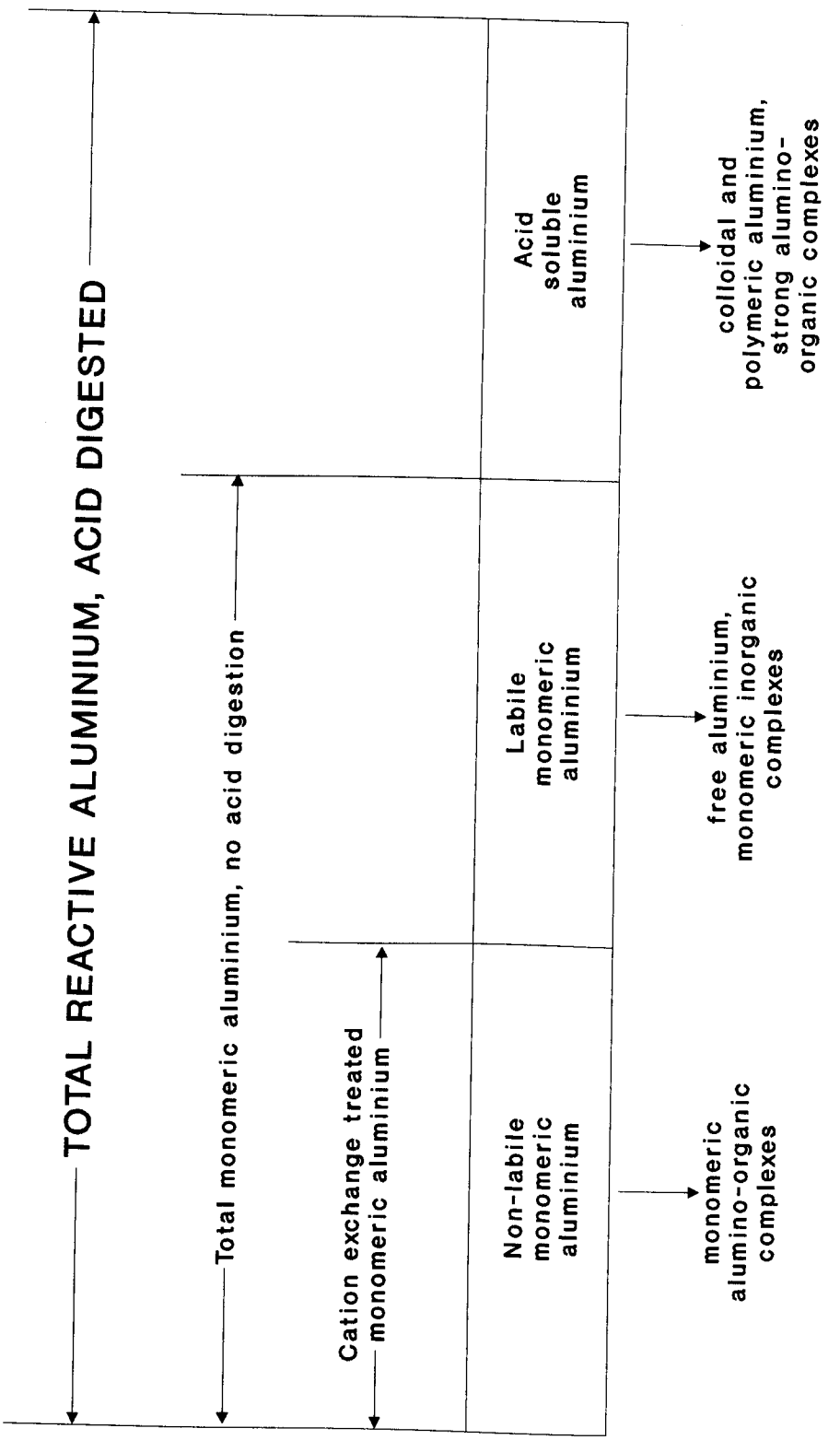

Fig. 3.9 Fractionation of Aluminium in Natural Waters.

TABLE 3.22

Comparison of Manual Driscoll Method and FI Method.

	Calculated Aluminium Concentration ($\mu g\ l^{-1}$)[a]		
	Driscoll (Event Two)		FI
	Al_{tm}	Al_{lb}	
A	12.7 ± 0.9	4.2 ± 2.1	11.0 ± 2.5
B	57.9 ± 3.7	45.2 ± 6.4	53.0 ± 1.9
C	23.3 ± 4.0	12.7 ± 6.5	11.0 ± 2.5
D	11.3 ± 5.7	3.5 ± 6.2	9.9 ± 1.8
E	97.5 ± 2.8	84.8 ± 3.5	85.5 ± 3.8
F	37.4 ± 2.2	28.9 ± 3.1	30.6 ± 2.5

[a] All errors calculated in $\mu g\ l^{-1}$ for 95 % confidence limits.

3.4. CONCLUSIONS

The operation of the FI monitor is more successful with a sample injection manifold than a reagent injection manifold. The proposed aluminium FI monitor meets water industry specifications and is sufficiently rugged and reliable for "field" use.

Chapter Four

Development of STEbus Based FI Monitor

4.1. INTRODUCTION

The suitability of FI for water quality monitoring was illustrated in the previous chapter. The main drawbacks of the FI monitor previously described were concerned with the computer system. This offered only limited expansion possibilities and required a purpose built interface between it and the main monitor components. A new monitor design was proposed to fulfil certain manufacturing and operational criteria:

1. Simplified construction to enable widespread ease of use, e.g. the use of direct connection of the monitor components to the computer system.
2. Industrial standard computer system with widely available replacement parts.
3. Simple maintenance using "plug-in" units, i.e. modular construction.
4. Full PC compatibility, with versatile software.
5. Capacity to allow the control of several manifolds or "chemistry" modules from one computer system.

This chapter describes the construction, development and testing of a new FI monitor which embraces the principles of easy care instrumentation [24] and fulfils the above criteria.

4.2. INSTRUMENTATION

The monitor was designed as two separate modules in order to provide system flexibility and to keep production costs to a minimum. The computer module, comprising of the computer system and the associated electronics for the control and operation of the wet chemistry module. The other module, containing all the FI instrumentation, was housed so as to eliminate the possibility of water ingress into the detector electronics or the computer system.

4.2.1. Computer Module

The computer system was constructed around a modular bus, with the central processing unit (CPU), memory and input/output (I/O) devices selected to give the most appropriate configuration. The bus selected was of an STE type (STandard Eurocard bus) as defined by IEEE P1000 (1988), and was both manufacturer and processor independent. Central to the operation of this bus is the protocol defining the transfer of data between the CPU or "master" and the other devices or "slaves". The transfer cycle is initiated by the master, and only terminated when an acknowledge signal is received from the slave device after valid information has been placed on the data lines of the bus. This protocol is known as asynchronous data transfer [107]. The main advantage of this procedure (commonly known as handshaking) is that it is independent of processor and device operational speed, so that any speed of device can be accommodated by the bus. As newer and faster devices become available the system can be easily upgraded. This overcomes the lifetime limitations normally associated with systems dependent on matching the individual speeds of the separate devices. Another major advantage of this type of bus based system is the ease with which it can be configured from a wide range of manufacturer's products. This provides optimum operational characteristics, and allows easy modifications to fulfil changing control and data processing requirements. The STE bus was designed to provide reliable, robust and flexible low cost systems where very high performance is not required, e.g. process control applications.

The computer system for the FI monitor was configured to provide the necessary input/output and data handling features:

1. Independent control of the individual components in the wet chemistry module.
2. Acquisition and processing of the analogue signal from the solid-state detector.
3. Calculation and validation of the analytical result.
4. Output of analyte and system information.

5. Straightforward system development.

The bus, CPU and peripheral card connections are schematically illustrated in Fig. 4.1, and a technical description of each of the cards, supplied by ARCOM Control Systems Ltd., Cambridge, is given below.

Central Processing Unit

SC88T: 8 MHz 80188 CPU, low cost target and development card with serial communication facilities, 64 Kb RAM and up to 128 Kb EPROM on board.

Memory

SCRAM: 48 Kb of battery-backed RAM on board with an access time of < 400 ns, used for data logging or as pseudo EPROM during software development. Battery backed realtime clock providing hours, minutes, seconds, day-of-week, date, month and year information.

Communications

SERCOM 4: 4 channel serial output, RS232 compatible with synchronous and asynchronous data transmission. When used in conjunction with loop interface card, *SCB20*, it provides analogue output to the 20 mA standard for telemetry and control mechanisms.

Analogue Input

SADC 12/16: high resolution A/D converter with 12 bit plus sign resolution (0.025%), and a conversion time of 30 ms. Input voltage range of ± 4.096 V (1 mV per bit), which is shielded to eliminate electrical noise.

Digital Output

SPIBB: 40 lines of digital I/O (2 x 8255 devices), all direction and enable commands software programmable, of which 32 are fully buffered. When coupled

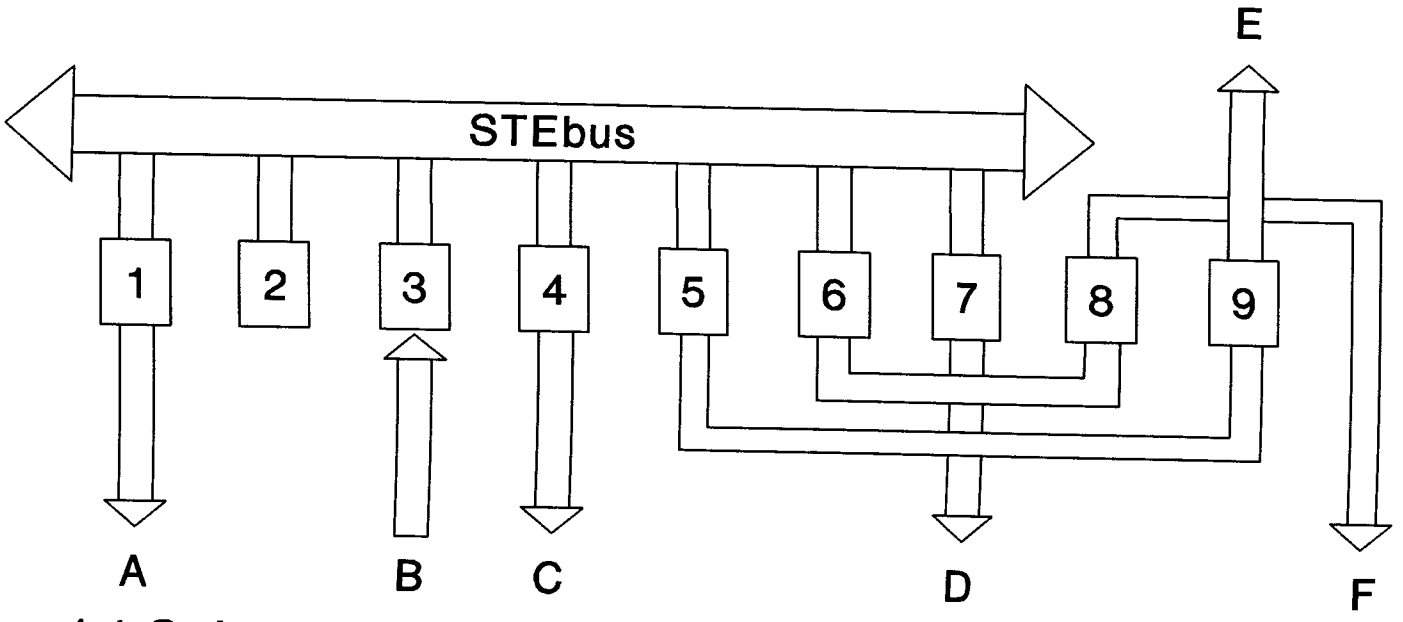

Fig. 4.1 Schematic Illustration of STEbus Computer System.

Key:
- A : Serial communication
- B : Data acquisition
- C : Local output
- D : System development
- E : Telemetry & feedback
- F : Control

1. Central processor unit
2. RAM & realtime clock
3. A/D converter
4. Local display & printer interface
5. Serial output
6. Parallel I/O
7. EPROM programmer
8. Relay output
9. Analogue loop output

with relay output card, *SCB11*, it provides 8 channels of 240 V a.c., 5 A rated output, up to 4 relay cards may be daisy-chained together to provide up to 32 relay outputs.

Utilities

Syscon: Provision of parallel I/O and system watch-dog facilities (e.g. power-line monitor), together with centronics output and liquid crystal display (LCD) interface for multi-line displays.

SEPD: Versatile EPROM programmer, which is fully software driven. Selectable for device and programming voltage with EPROM verification.

These individual cards were mounted in a standard 19" 3U subrack unit which was fitted with an STEbus 10-slot backplane (SBPL10), and a multi-output high stability power supply (PSU14T). A regulated low voltage power supply for the solid-state detector and solenoid switching and injection valves was also mounted within this subrack unit. On the front of the computer module two local output devices were mounted: 1/ A 40 character x 2 line alphanumeric liquid crystal display, and 2/ a 24 character miniature dot matrix printer (both supplied by RS Components Ltd., Corby).

4.2.2. Wet Chemistry Module

This was built within the frame of an aluminium 19" 6U subrack unit, similar to that of the computer module. The major components of the system were selected on the basis of their proven reliability. These were housed so as to maintain their individual integrity, and to facilitate easy removal and replacement. All the components except the detector electronics, were mounted on/around an aluminium panel towards the front of the subrack unit, and over a fibreglass drip tray (to contain and channel away any liquid spillages).

Many of the components were common to the manual FI system and the previous FI monitor. Twin peristaltic pumps (Ismatec Mini S-820, Ismatec UK, Carshalton) were used to propel reagent, sample and standard solutions. The sample and standard solutions, selected using a 12 V solenoid switching valve (Phase Sep, Queensferry), were injected into the reagent stream via a 12 V automated rotary injection valve (Burkard, Uxbridge). A remote detector flow cell was mounted adjacent to the FI manifold, with the detector electronics mounted in a separate protective housing. The power supply to the detector was electronically regulated to prevent the disruption of the analogue signal.

The wet chemistry and computer modules were connected via two independent cables, Fig. 4.2 : 1/ Low voltage lines, including the power supply lines for the detector, switching valve and injection valve and signal lines into and out of the computer module; 2/ High voltage power lines to the peristaltic pumps. As a safety feature, differently configured multi-way connectors were used for the high and low voltage lines to prevent accidental incorrect connection.

Fig. 4.3 illustrates the FI monitor. The components in the wet chemistry module were positioned to allow easy access for routine maintenance and the FI manifold was designed to allow simple conversion between "chemistries", with sufficient space to permit the inclusion of on-line/pretreatment units e.g. gas diffusion cell(s) or reductor column(s).

The specification for the outer cabinet of the FI monitor would be dependent on the harshness of the operating location. For most water treatment applications a GRP cabinet to IP65 would be specified, i.e. to provide total protection from dust and resistance to low pressure water jets. The cabinet would have to be large enough to allow the storage of sufficient reagents for the desired unattended operational period.

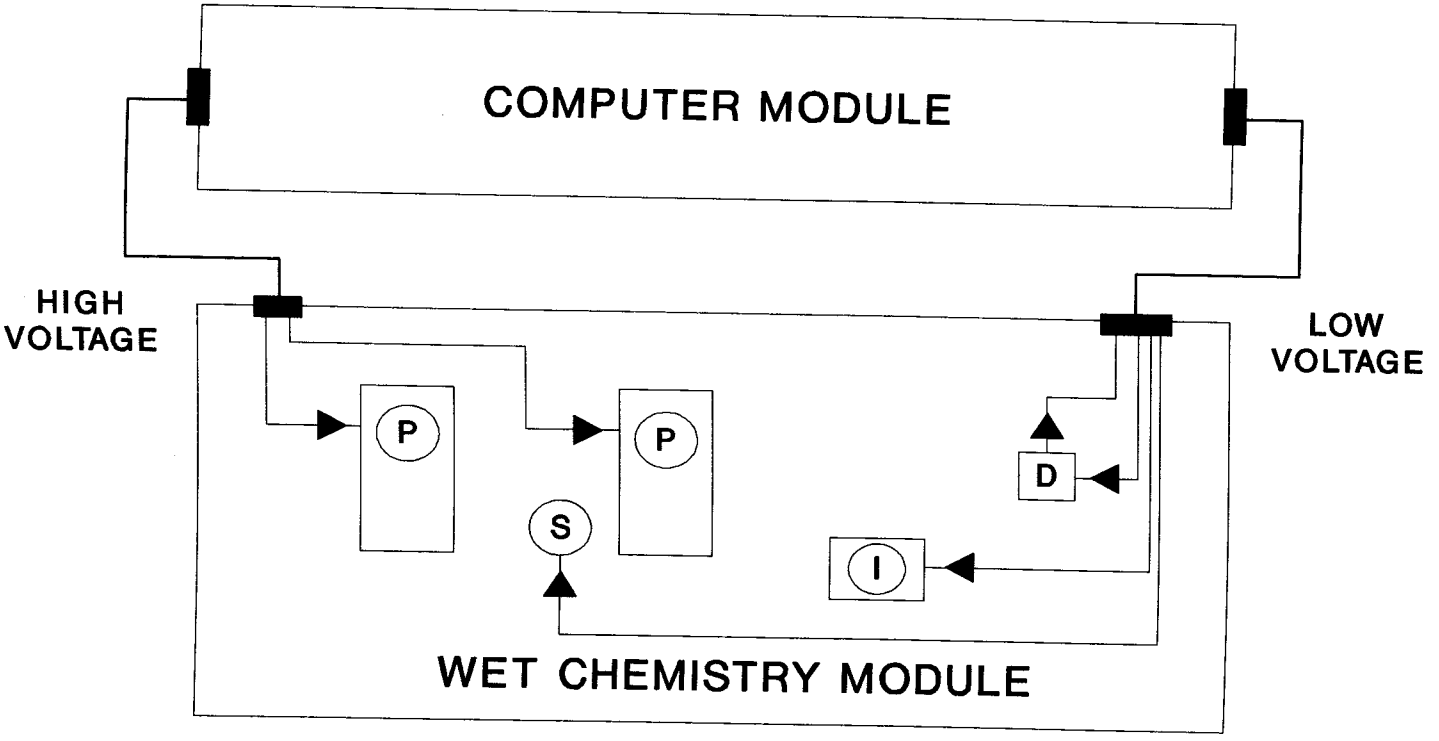

Fig. 4.2 Schematic Illustration of FI Monitor Module Connections.

Key: P = Peristaltic pump
S = Switching valve
I = Injection valve
D = Detector

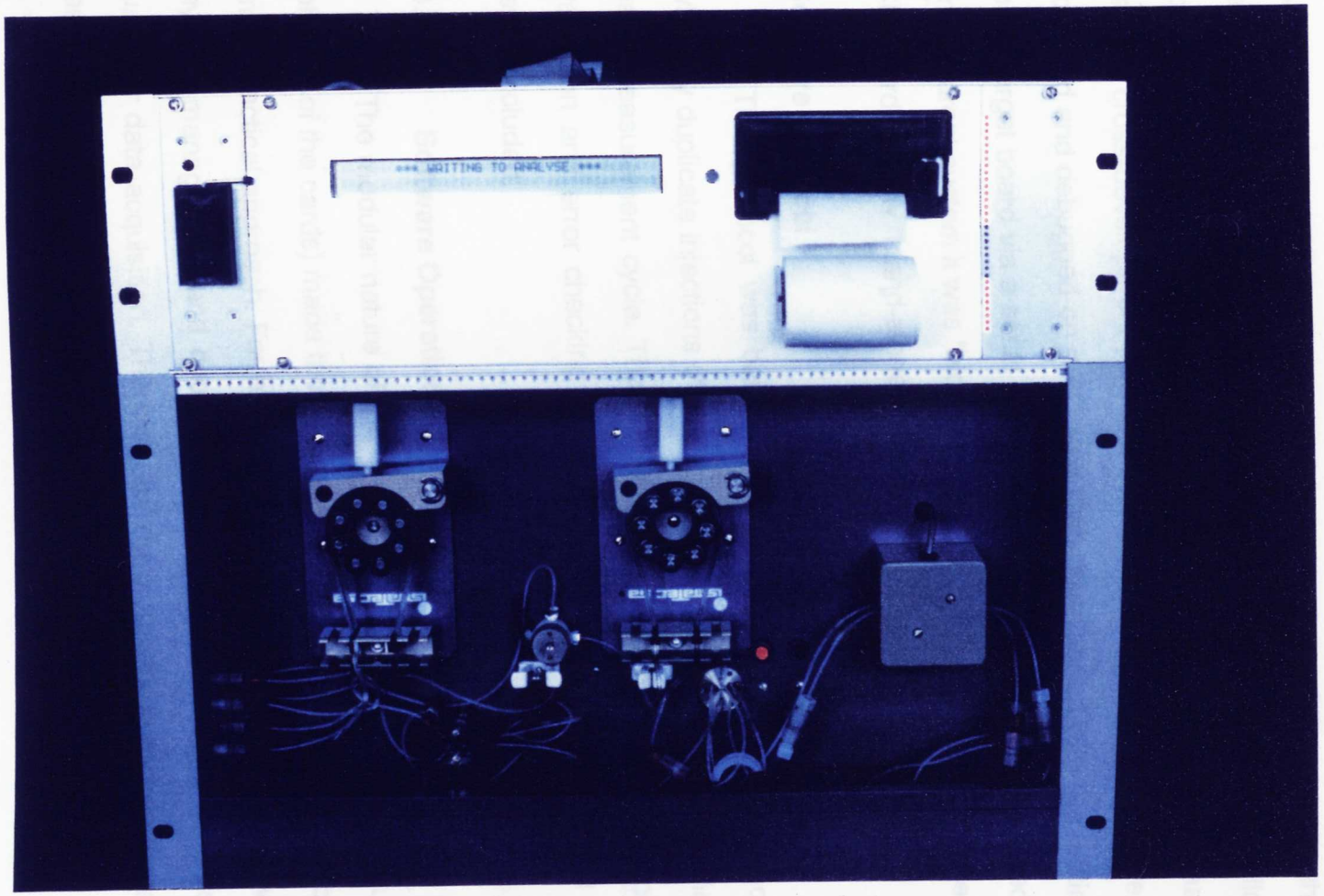

Fig. 4.3 STEbus Based FI Monitor.

4.3. SOFTWARE DEVELOPMENT AND OPERATION

The MS-DOS operating environment of the CPU permits the use of a variety of languages; in this application the system was controlled using a compiled BASIC (AB88, Arcom). The development of the software was carried out using a cross-development package (XPC+, Arcom); this allowed the code to be compiled and debugged on a PC, and then downloaded with the runtime package to the target board via a serial link. When the code was fully debugged and tested on the target system it was "blown" into an EPROM, this was then inserted into the CPU card to allow "stand-alone" operation.

Software Protocol

This protocol was based on that established for the previous monitor, whereby duplicate injections of standard were used to calibrate the monitor during each measurement cycle. The protocol was extended to include more rigourous validation and error checking routines, with both alarm "high" and alarm "low" levels included.

4.3.1. Software Operation

The modular nature of the computer system (and the individual operation of each of the cards) made the separate development of these functional units the most practical approach. For example the processor card operation was central to system management and coordination, and the A/D converter card was solely used for data acquisition. Therefore for development purposes the software was assembled in seven separate sections, each with individual functions:

1. Initialisation
2. Timing
3. Control
4. Data Acquisition

5. Data Processing
6. Data Validation
7. Data Output

These sections were then merged together to give the total "system" operational software. Figs. 4.4(a) and 4.4(b) schematically illustrate the overall operation of the program, including the protocol to ensure calibration. These individual operational functions are described below.

System Intialisation

The initialisation of the input/output card (SPIBB) and the LCD prior to the operation of the main program was necessary in order to ensure their correct operation.

The two 8255s used in the SPIBB are versatile input/output devices which, because they can be used in a number of different ways must be configured before use. This was achieved by writing a control byte to the control register of each device (to select either input or output) and, in addition, a control byte was sent to set the direction of, and enable the input/output buffers. In order to fulfil the control functions of the system all the channels of Port A were set as outputs (for system control via the relay outputs of SCB11), while all the channels of Port B were set as inputs (allowing manual interaction with software). This code was run immediately after system power up to prevent any damage to the computer module.

The LCD was operated from the driver port of the SYSCON card, and because of the variety of LCDs available appropriate intialisation of the display characteristics was required. The port was first initialised for a two line display, and then set to give the required type of cursor and direction of display. The final step was carried out to clear any erroneous data from the display and return the cursor to its starting position.

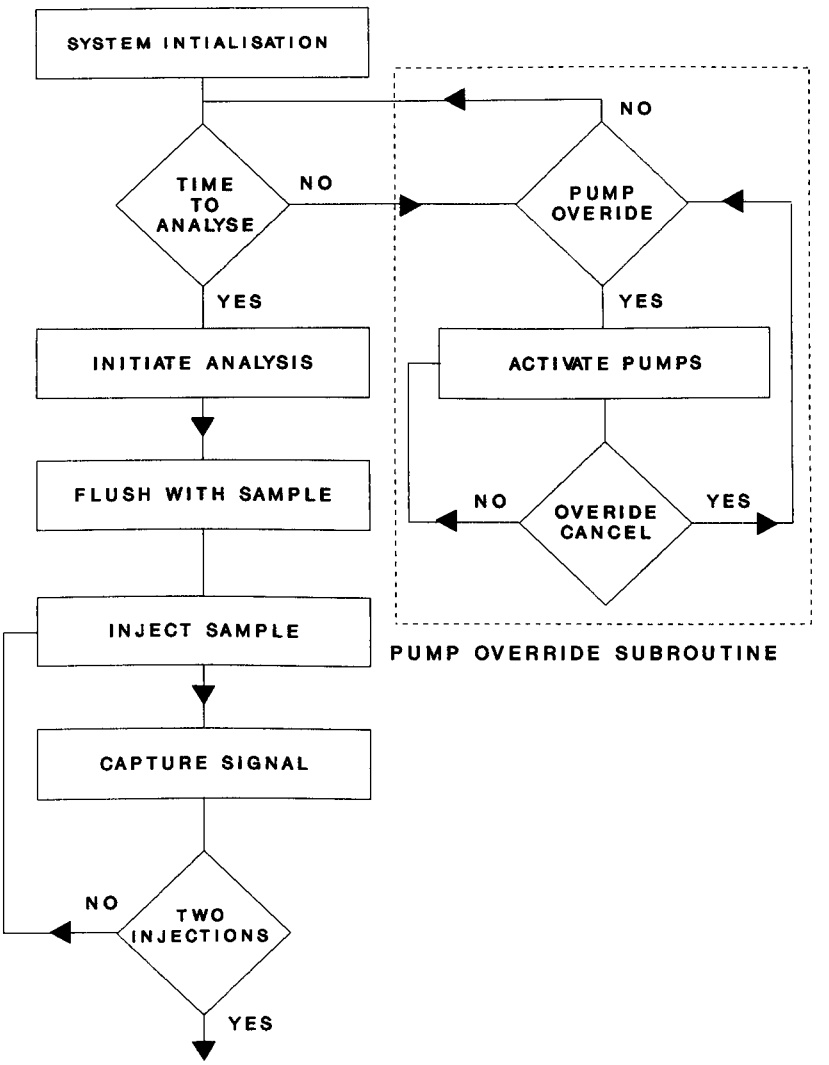

Fig. 4.4(a) Flow Diagram for FI Monitor Software

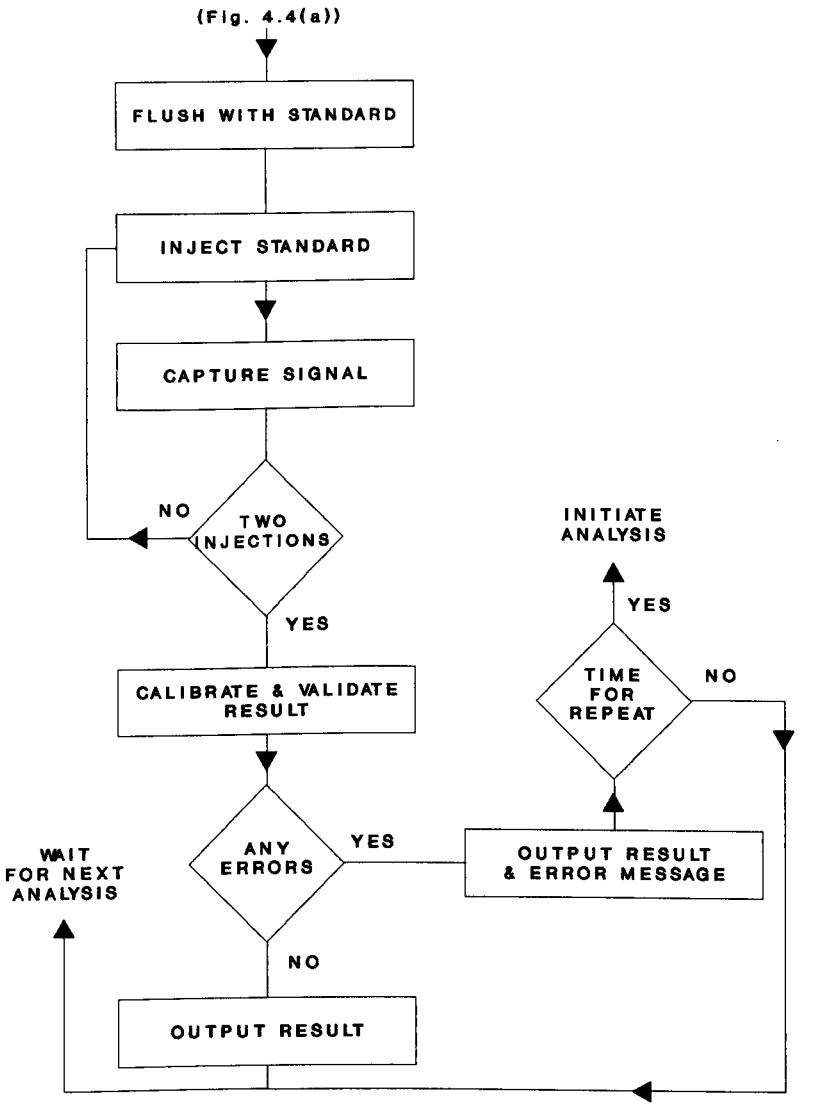

Fig. 4.4(b) Flow Diagram for FI Monitor Software

This section of the program also included all the user-defined parameters which were used in the control of the monitor, validation of the data and calculation of the analytical result. These parameters, described below, allowed the operation of the monitor to be tailored to any specific application.

Control/Analysis

Sampling interval, *sampint%*, the frequency with which the measurement cycle was activated. For example sampint% = 30 initiates a cycle every 30 minutes.

Cycle time, *cycletime%*, total running time for the measurement cycle. This was used to ensure that sufficient time remained before the next scheduled measurement in the event of a repeat determination being required.

Flush delay, *flushdel%*, the time delay that allowed sufficient sample and standard to be drawn through the flow system so that carryover was prevented. This also ensured that a fresh sample was injected for each determination.

Fill delay, *filldel%*, the time delay that was required in order to flush out and refill the sample loop of the injection valve.

Inject delay, *injdel%*, the time delay required between an injection being made and data capture being initiated. This was necessary to ensure that the peak generated appeared in a known "window" (to simplify peak finding) and that the captured signal was free from spurious electronic noise, which would otherwise have to be "filtered out" from the bulk data.

Calculation

Standard concentration, *standconc*, the concentration of the standard solution used for the single point calibration and hence calculation of the analyte concentration.

Validation

Sensitivity threshold, *sensthresh*, this acted as a check on the overall performance of the system. It was defined as the factor or percentage by which the standard signal was permitted to decrease before an error was flagged. The action of this check was two-fold, with a decrease in signal size being due to either reagent degradation or a decrease in detector performance. In the event of a loss of performance an error was flagged but was not included in the general failure tally for auto-shutdown.

Sample check, *mvdiff*, the maximum difference that was permitted between two sample signals before an error was flagged. This parameter was defined in terms of the size difference, in mV, between the duplicate peaks.

Maximum analyte concentration expected, *maxexpect*, an alarm "high" level indicating a potential hazard, above which a warning was initiated.

Minimum analyte concentration, *minexpect*, an alarm "low" level indicating that the analyte was at a concentration below the detection limit, or that a system failure had occurred (when flagged with a reduction in sensitivity).

Maximum fails, *maxfails%*, the maximum number of consecutive failures due to gross system irregularities before automatic shut-down of the system.

System Timing

All the timing functions of the monitor were controlled by the real time clock (RTC) onboard the SCRAM card. A simple timing function was used to initiate the measurement cycle, whereby if the modulus of the current minutes value and the sampling interval was equal to zero, a cycle was initiated. (MOD is a

mathematical logical operator where the remainder of a division is obtained, e.g. 5 MOD 2 = 1).

The RTC was also used to generate a series of interrupts at a known frequency and as a delay function (which was used for the timed operation of the pumps and valves). For each delay, in seconds, the program was halted while the appropriate number of interrupts (at 16 Hz) were counted, after which the program was allowed to proceed.

Control

The electronic control of the components in the FI monitor was achieved by using the I/O capabilities of the SPIBB card coupled with the relay outputs of SCB11. The electrical power to the peristaltic pumps and the switching valve was routed via these relays, such that their remote control was possible. A low voltage signal line (12 V d.c.) was also activated/deactivated by one of the relays for the control of the injection valve.

The control of the monitor components was achieved by sending an appropriate pattern of bits (representing each of the channels) to the SPIBB card. This was carried out in such a way as to allow the simultaneous operation and activation/deactivation of the individual components. Logical operators [108] were used to produce a decimal number representing the binary byte of the output port. An example of the bit masking and merging procedure is illustrated below.

Bit Pattern Configuration - Example

Problem: Activate Pump (2) without deactivating Pump (1).

1. Pump (1) = Channel 0 = 00000001 (Binary)
   Pump (2) = Channel 1 = 00000010 (Binary)
2. rflag% = current bit pattern = 00000001
3. i% = masking bit pattern for Pump (2)
   $i\% = 255 - 2^{no\%}$ (no% = Channel No.)
   i% = 253 = 11111101

4. rflag% AND i% = i%, current bit pattern

   i% = 00000001

5. i% OR no% = rflag%, new bit pattern

   rflag% = 00000011

6. Output new bit pattern to activate Pump (2) and leave the status of Pump (1) unchanged.

Initially, the current status of the port was read using the operator "AND", establishing which bits were currently set. Then the operator "OR" was used to merge the current bit pattern with the new bit pattern describing which pumps and valves were to be activated.

The pump manual override facility, software controlled, was introduced to allow the peristaltic pumps to be operated independently of the main control program. This operation allowed the flow system to be "purged" or flushed after reagent or pump tubing replacement and prior to normal operation. Purging was only possible during the "standby" period of the monitor, and activated by pressing a facia mounted button. This drew an input line on the SPIBB card to earth via a resistor, thus changing its status. A software routine searched every second for this change, and continued to search during the purging procedure.

Data Acquisition

The analogue signal from the solid-state detector was fed into one of the channels of the A/D converter. This channel was selected and enabled by sending the appropriate bit to the control latch. This conversion initiated sampling (frequency of 8 Hz), with the data read into memory until a predefined number of individual elements had been recorded.

Data Processing

The signal generated by the solid-state detector was stored as bulk digital data, which was processed immediately after signal capture was completed. The

mean of the numerical values for the first eight elements of the recorded data was taken as a "background" value. The remaining data was then searched to elucidate the maximum numerical value, equivalent to the peak maximum. This used a simple comparative procedure where each subsequent element was compared with the previous maximum value established (at the beginning of each search this maximum value was initially set to -1). Once the maximum value had been found, and the value of the elements started to fall, a mean value including the maximum element and four values either side of this was taken as the maximum signal. The background signal was then subtracted from this value to give a peak maximum. Four values were accumulated, one for each of the individual sample and standard injections. The mean values were then ratioed and this value multiplied by the standard concentration to calculate the analyte concentration.

Validation

The analytical result was validated by examining the variation in the peak size within each duplicate pair of peaks, and by comparison of the mean standard value with the highest previously recorded value (obtained when no errors were reported). Failures during any of these validation procedures were indicated by an error code, which was output with the calculated result where appropriate. The validation process was carried out as described by the following sequence: (where U1/U2 and S1/S2 were the calculated signals for the sample and standard solutions respectively).

1. STANDARD REPRODUCIBILITY: If the difference between the standard peaks S1 and S2 was greater than 10 %, Flag (2) was set true (i.e. to 1) to indicate a standard reproducibility error.

2. LOW STANDARD: If the sum of the standard peaks was greater than a maximum previously recorded value for this sum (maxpeak, initially set to 0) and

Flag (2) was false, then this sum was assigned as the new value of maxpeak. However, if this sum was less than a predefined percentage of maxpeak (sensthresh) then Flag (1) was set true to indicate a low standard reading.

3. SAMPLE REPRODUCIBILITY: If the absolute value of the difference between the sample peaks U1 and U2 was greater than a predefined threshold value (mvdiff), Flag (3) was set true to indicate a sample reproducibility error.

4. ALARM LEVELS: If the calculated analyte concentration in the sample exceeded a predefined upper limit or fell below a predefined lower limit an alarm flag was set true. (Flag (4) = Alarm Low, Flag (5) = Alarm High).

If a true status was set for any of the above Flags, a repeat determination was initiated. If a predefined number of consecutive measurement cycles failed during the validation procedure (maxfails%), excluding Flag (1), then the monitor was automatically shut-down until maintenance had been undertaken.

4.4. APPLICATION OF THE FI MONITOR TO THE DETERMINATION OF RESIDUAL DISSOLVED ALUMINIUM IN TAP WATER

4.4.1. Experimental

Reagents

All solutions were prepared in Milli-Q water in polyethylene plasticware, and all reagents were of GPR grade (Aldrich). The three reagent streams used were as follows: R1, 7.6 g l^{-1} hydroxylammonium chloride and 0.56 g l^{-1} 1,10-phenanthroline; R2, 0.4 g l^{-1} pyrocatechol violet; and R3, 82 g l^{-1} hexamine. Brij 35 (0.3 % (w/v)) was added to the Milli-Q water carrier stream, C. A 1000 mg l^{-1} aluminium stock solution prepared from pure metal, was diluted to provide working aluminium standard solutions.

Instrumentation

The construction and specification of the FI monitor has been detailed above in sections 4.2.1. and 4.2.2. The solid-state detector, type B, incorporated capillary glass flow cells and the more intense yellow LEDs.

A remarked listing of the monitor control software is given in Appendix C. This listing excludes values for the user-defined parameters, which are given in the Results and Discussion section.

The calculated analytical result was logged on a local printer for all the performance and tap water trials.

Tap Water Trial

The instrumental set-up is schematically illustrated in Fig. 4.5. During this trial the monitor withdrew the water sample from a constant head device which was connected directly to the public supply. This device had a hold-up volume of approximately 100 ml and a flow rate of water through it of 500 ml min^{-1}, thus ensuring the rapid "turnover" of the sample.

Procedures

The FI method was the same as that used in the trials of the previous FI monitor (Chapter 3), the FI manifold is schematically illustrated in Fig. 4.6. The monitor was operated on a 30 minute measurement cycle for both the performance trials and the analysis of tap water.

4.4.2. Results and Discussion

The monitor was operated with two different sets of user-defined parameters, these were assigned version names of RLB9 and RLB10. The parameters for RLB10 are given in Table 4.1, which were the same as those for RLB9 except that a standard concentration of 200 $\mu g\ l^{-1}$ was used in the latter.

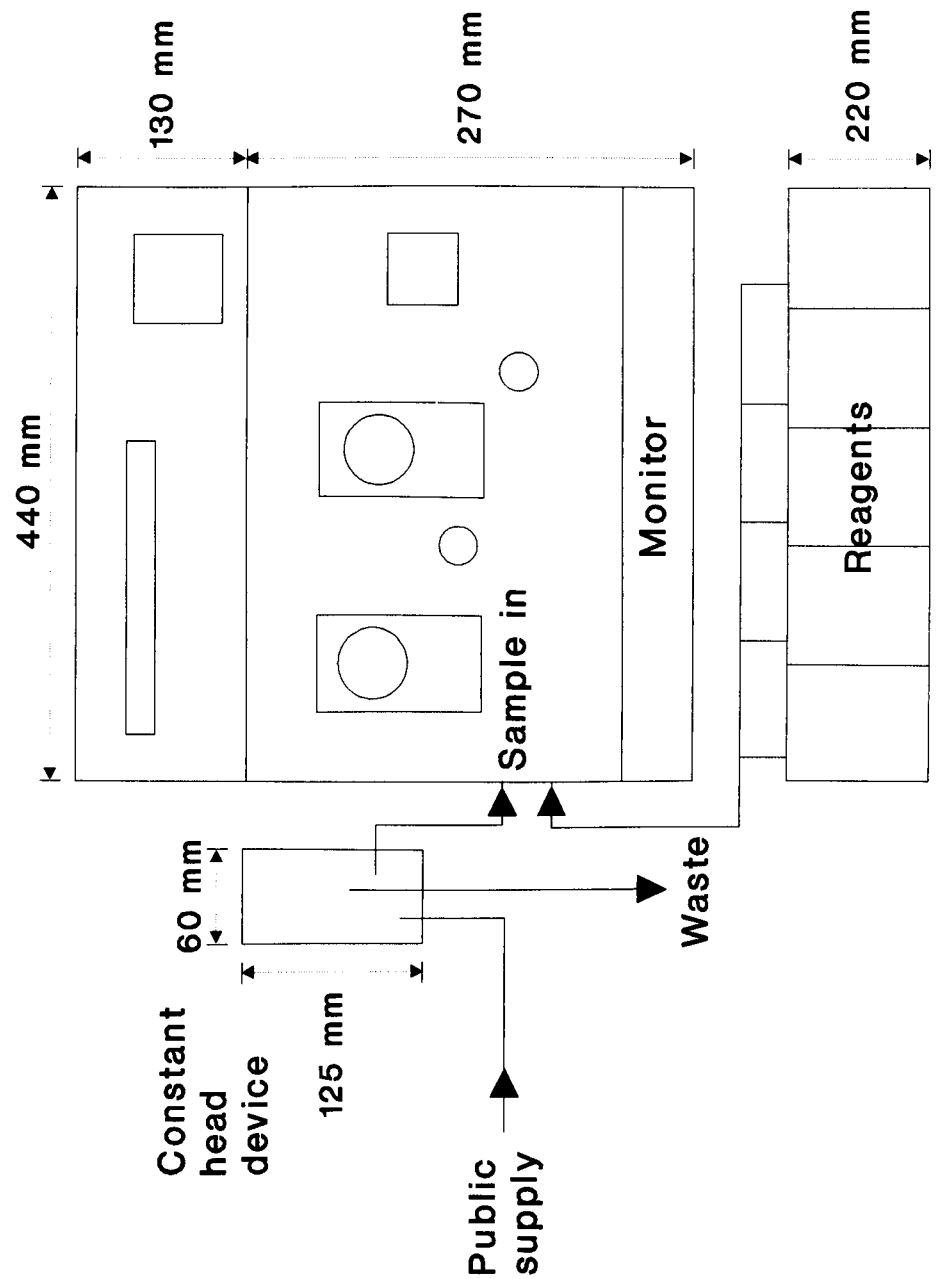

Fig. 4.5 FI Monitor Set-Up for Tap Water Trials.

(Not To Scale, All Dimensions Approximate)

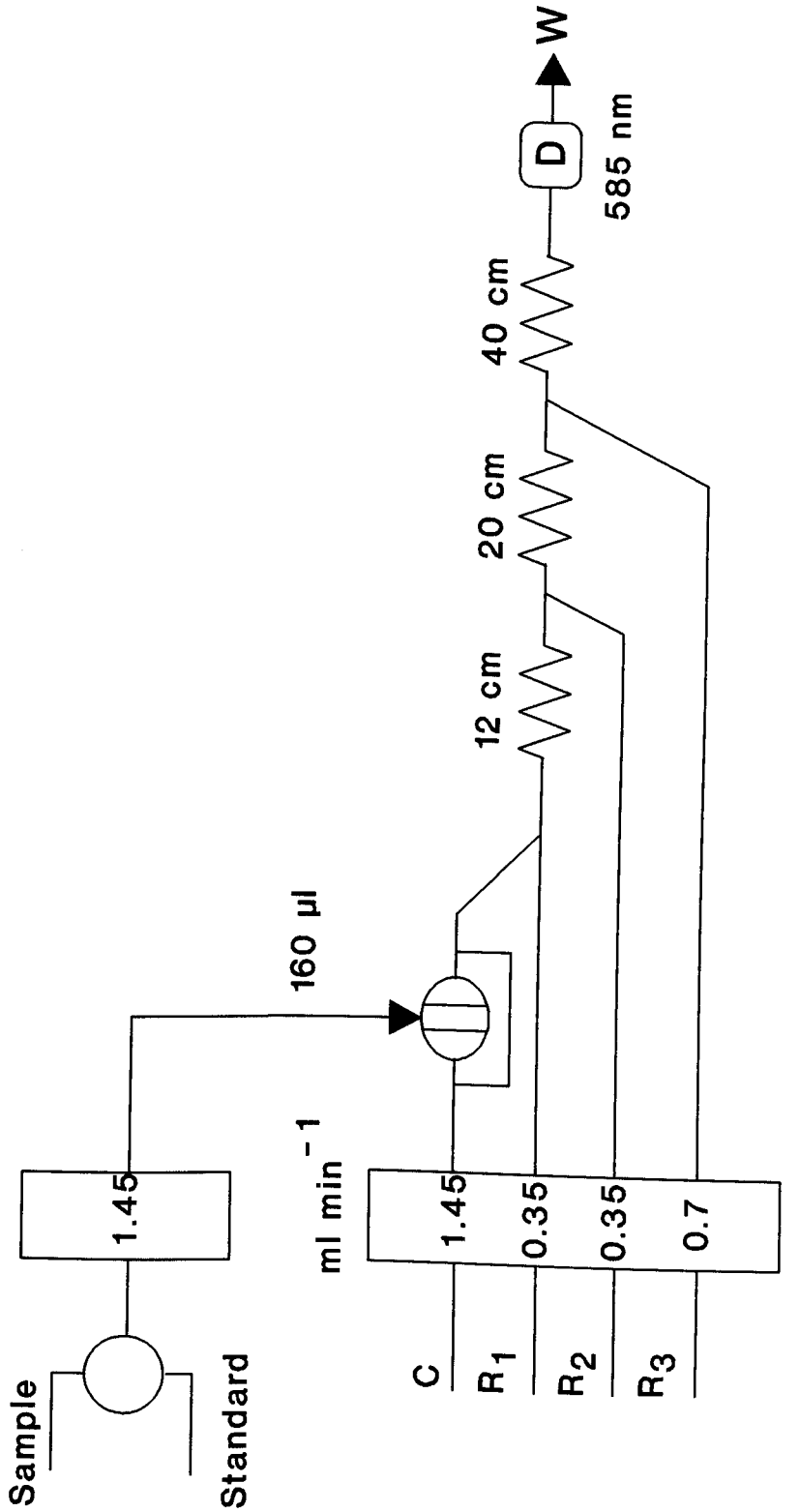

Fig. 4.6 FI Manifold for the Determination of Aluminium.

TABLE 4.1

User-Defined Parameters for FI Aluminium Monitor Software, Version RLB10.

Parameter	Unit	Setting
sampint%	min	30
cycletime%	min	11
flushdel%	s	60
filldel%	s	35
injdel%	s	20
sensthresh	--	0.75
maxfails%	--	3
mvdiff	mV	10
maxexpect	$\mu g\ l^{-1}$	250
minexpect	$\mu g\ l^{-1}$	0
standconc	$\mu g\ l^{-1}$	100

Monitor Accuracy and Performance

The accuracy of the analytical result was assessed by replacing the "sample" solution with one of known aluminium concentration. Two different standard solutions were used for the single point calibration (200 $\mu g\ l^{-1}$ with RLB9, and 100 $\mu g\ l^{-1}$ with RLB10), the results of these trials are given in Table 4.2.

TABLE 4.2

FI Aluminium Monitor Performance Trial.

Parameter	RLB9[a]	RLB10[a]	RLB9[b]	RLB10[b]
Number of measurements	336	192	336	48
Calculated concentration	56.7	53.9	204.6	192.8
Standard deviation ($\mu g\ l^{-1}$)	1.8	2.1	3.0	26.2
RSD (%)	3.1	3.9	1.5	13.6
Total number of failures	4	10	4	2
Initial success rate (%)	98.8	94.8	98.8	95.8
Overall success rate (%)	100	100	100	100

[a] 50 μg Al l^{-1} "sample" solution
[b] 200 μg Al l^{-1} "sample" solution

These trials showed that to ensure that the required analytical accuracy was met for the determination of aluminium at the GL level (50 $\mu g\ l^{-1}$), it was necessary to select a 100 $\mu g\ l^{-1}$ calibration standard. This lower calibration standard also achieved acceptable accuracy for a standard at the MAC level (200 $\mu g\ l^{-1}$). To assess the repeatability of the analytical result a 50 $\mu g\ l^{-1}$ "sample" was analysed against a 100 $\mu g\ l^{-1}$ standard over a period of > 90 hours, the results of this trial are graphically illustrated in Fig. 4.7. The majority of the analytical results fell within 1 σ of the mean value and > 98 % fell within 3 σ.

The repeatability of the analytical result was very good, typically being < 4 %. The reliability of the monitor was also very good, in all trials being ≥ 95 %, as calculated on the basis of successful initial determinations. In every example

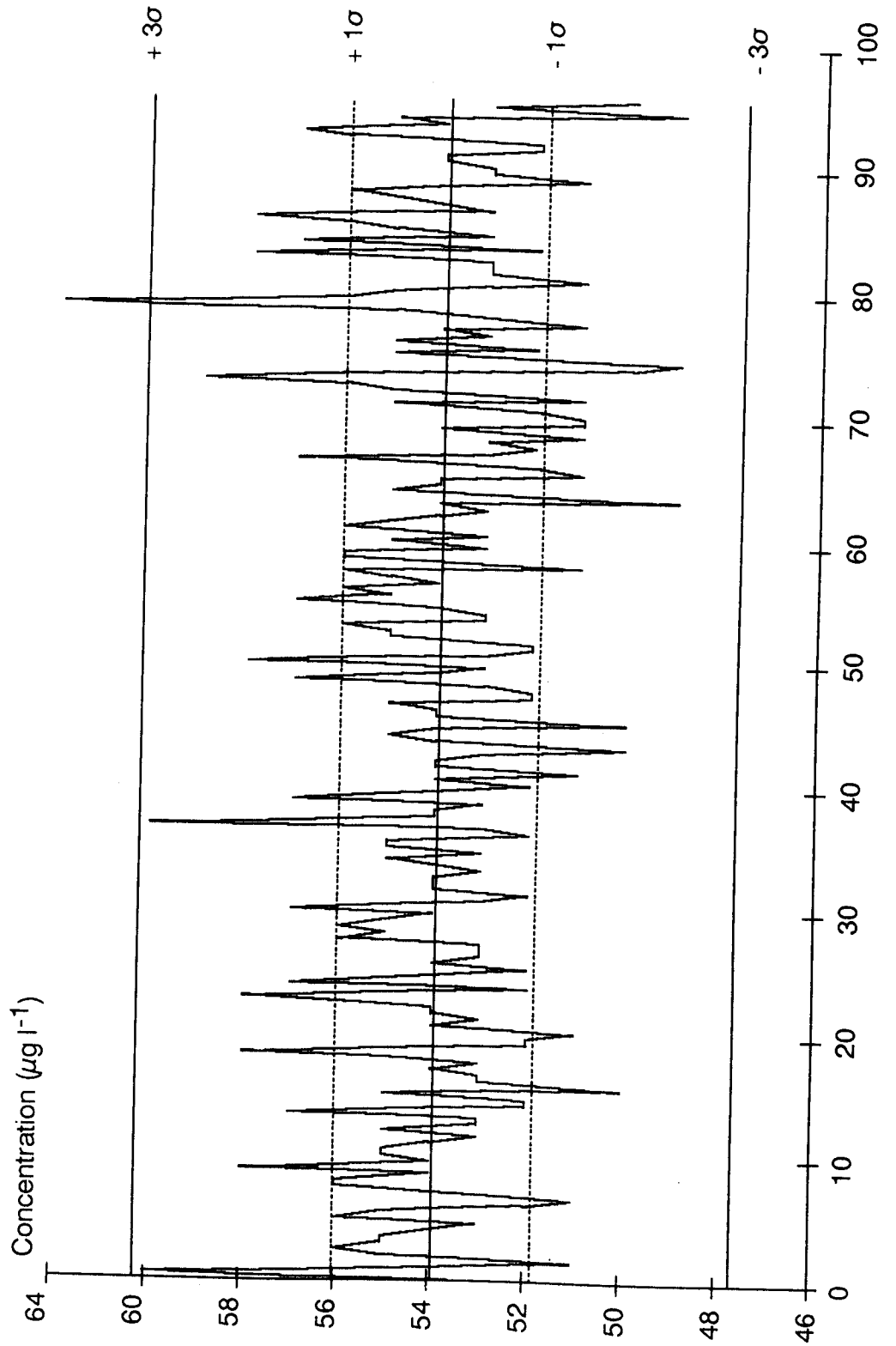

Fig. 4.7 Repeatability of 50 $\mu g\ l^{-1}$ Aluminium Standard.

where an error was flagged and measurement cycle subsequently repeated the second (or repeat) determination was successful, and therefore the overall reliability was 100 %.

Tap Water Trial

An extended trial was undertaken to monitor the aluminium concentration in the public supply. Typical examples of uninterrupted operation are given in Table 4.3; these serve to illustrate the high reliability of the system (> 97 %).

TABLE 4.3

FI Aluminium Monitor Tap Water Trial.

Parameter	(1)	(2)	(3)
Number of measurements	299	231	342
Total number of failures	9	4	8
Initial success rate (%)	97.0	98.3	97.7
Overall success rate (%)	100	100	100

The fluctuation in dissolved aluminium concentration over a period of > 280 hours is illustrated in Fig. 4.8. The bold line of the plot represents the moving average for ten determinations, and the extremity of each broken line represents an individual analytical response. The moving average plot clearly illustrates a downward trend in the level of aluminium during the analysis period.

Monitor Performance

The overall monitor performance characteristics, summarised in Table 4.4, compare very favourably with those detailed in the water industry specification [24] for the monitoring of residual coagulants after water treatment. The reagent consumption figures and operational costs, for a 35 day unattended operational cycle, are given in Table 4.5. These figures have been calculated to allow for the measurement cycle to be repeated in the event of an error being reported.

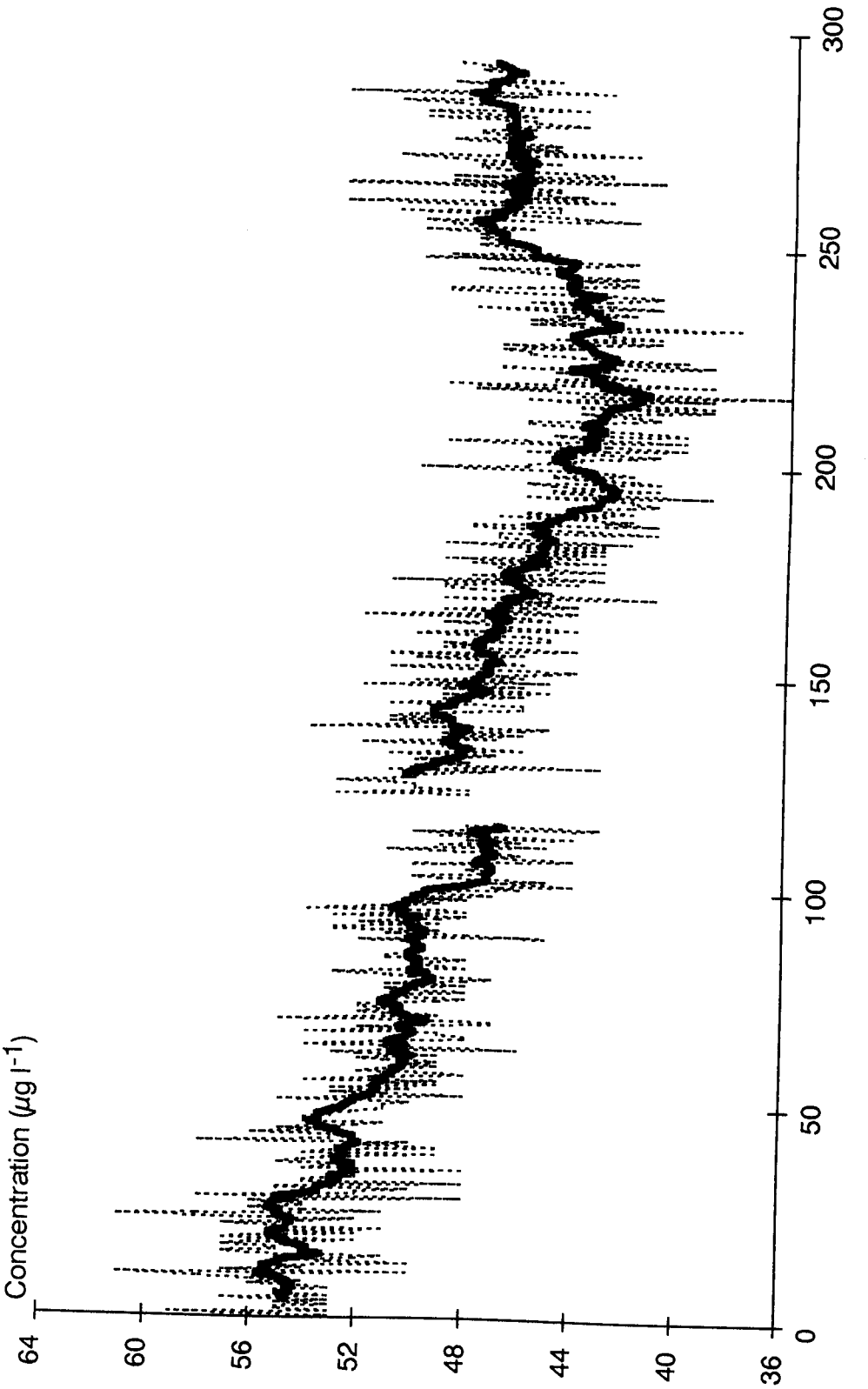

Fig. 4.8 Fluctuation in Dissolved Aluminium Concentration in Potable Water over a 12 Day Period.

TABLE 4.4

FI Aluminium Monitor Specification and Performance

Parameter	Industry specification	Proposed monitor
Overall accuracy	± 10 %	± 8 % (at 50 $\mu g\ l^{-1}$)[a] ± 2 % (at 200 $\mu g\ l^{-1}$)[b]
Repeatability	± 10 %	± 4 % (at 50 $\mu g\ l^{-1}$)[a] ± 2 % (at 200 $\mu g\ l^{-1}$)[b]
Response time	< 15 min	10 min
Nominal range	0-1000 $\mu g\ l^{-1}$	0-1000 $\mu g\ l^{-1}$
Limit of detection		13 $\mu g\ l^{-1}$
Reliability		> 97 %
Unattended operation	35 days	35 Days

[a] n = 192, 100 $\mu g\ l^{-1}$ standard
[b] n = 336, 200 $\mu g\ l^{-1}$ standard

TABLE 4.5

FI Aluminium Monitor Reagent Consumption and Running Costs.

Reagent	Consumption (l)
Pyrocatechol violet	4.1
Iron mask	4.1
Hexamine	8.4
Carrier	19.2
Standard	8.4
Costs	**£**
Reagent cost:	13
Pump tubing:	3
Total Cost:	16

The value for the repeat rate was set at 5 %, assuming that the monitor provided validated results on a first determination basis for 95 % of the period of operation.

The timing parameters for the monitor control were tailored such that the consumption of any one reagent was not greater than 20 l over the 35 day period. Further reductions would be possible by reducing the frequency of: (a) the measurement cycle or (b) the calibration.

4.5. CONCLUSIONS

The FI aluminium monitor operated successfully during an extended on-line trial and met industry specifications for the analysis of residual aluminium in treated water. The STE bus based computer system is well suited to the control of field instrumentation.

Chapter Five

On-Line FI Determination of Iron

5.1. INTRODUCTION

5.1.1. Iron in the Environment

Iron is the fourth most abundant element and second most abundant metal in the earth's crust [66]. Its geochemistry largely determined by its variable valence state which changes in response to physico-chemical conditions. It is widely found in the form of oxides, sulphides, phosphates and silicates in rocks, clays and minerals [68]. With magnesium, for example, it plays an important role in the formation of a number of rock-forming silicates e.g. fayalite (an olivine) and hedenbergite (a pyroxene) [109]. High concentrations of iron are found in coal seams (e.g. as sulphur bearing minerals), sedimentary rocks (e.g. shale and sandstone) and also in plutonic sediments (e.g. basaltine). The weathering of ferromagnesians [70], one of the principle mineral series in igneous rock, releases iron(II) from the crystal lattice which is oxidised to form iron(III) oxides such as haematite, a major iron bearing ore. The weathering of these iron silicates and carbonates gives rise to a series of insoluble iron(III) hydroxides and hydrous oxides, with both soluble and insoluble iron(II) and iron(III) species being found in aquatic systems [110]. However, in natural surface waters iron(III) will be the predominant species due to the thermodynamic instability of iron(II) in the presence of oxygen [73].

5.1.2. Aquatic Iron Chemistry and Health Implications

The hydrolysis of iron(III) is initially governed by the following equilibria [69]:

$$[Fe(H_2O)_6]^{3+} = [Fe(H_2O)_5(OH)]^{2+} + H^+$$

$$[Fe(H_2O)_5(OH)]^{2+} = [Fe(H_2O)_4(OH)_2]^{+} + H^+$$

$$2[Fe(H_2O)_6]^{3+} = [Fe(H_2O)_4(OH)_2.Fe(H_2O)_4]^{4+} + 2H^+$$

The majority of iron complexes are octahedral, but tetrahedral and square

pyramidal complexes also exist; the hydrolysis products of these complexes may be both monomeric and polymeric [71].

The iron(II) - iron(III) system plays an important role in the aquatic environment, acting as a catalyst for the oxidation of organic material by oxygen and chelating with organic acids and humic substances. It is also active in plant metabolism, affecting the iron-porphyrin-protein oxygen carrying complex.

Iron in water has no physiological risks associated with it and the restraints placed upon it are largely for aesthetic reasons. Iron imparts an unpleasant flavour, turbid aspect and red coloration to the water. Heavily contaminated water will stain laundry and encourage the growth of ferrobacteria leading to the corrosion and "furring-up" of pipe work [111]. There is some evidence to suggest that certain concentrations of iron in natural freshwaters may affect the development of fish. Different species are sensitive at different stages of their life cycle, for example Brook trout during their adult life stage, and for fathead minnows at the egg and larval stage [110]. However, the relative importance of particulate and dissolved iron and their toxicity towards the aquatic environment has not been fully established. Although fish and shellfish are known to accumulate iron, it is thought that the risk to human health is negligible [110]. The European Community has set GL and MAC levels of 50 and 200 $\mu g\ l^{-1}$ for total iron in drinking water [12]. It is to these levels that current UK legislation is directed and therefore the levels at which monitoring is required.

Iron, and in particular iron(III) chloride, is used as a primary coagulant and flocculant (see Section 3.1.1); the rapid formation of insoluble ferric hydroxides allowing the effective precipitation and removal of many trace substances [66]. Consequently, there is a need for the routine measurement of iron in potable and treated waters to maintain effective control of water treatment processes. In addition, the determination of iron in natural waters can provide valuable information for nutrient budget studies, e.g. iron uptake by phytoplankton. Iron is routinely analysed in a wide variety of matrices from environmental, clinical and

industrial sources and subsequently a wide range of methods have been developed.

5.1.3. Methods for the Determination of Iron

Many sensitive and selective reagents have been synthesised for the spectrophotometric determination of iron(II) at sub mg l^{-1} levels. A selection of eleven of the more common reagents are listed below:

1. 1,10-Phenanthroline, [112-120].
2. 2,Pyridyl-3'-sulphophenylmethanone-2-pyrimidylhydrazone (PSPmH), [121,122].
3. 4-Hydroxy-1,10-phenanthroline, [123].
4. 4,7-Diphenyl-1,10-phenanthroline (Bathophenanthroline), [124,125].
5. 2,4,6-Tri-(2-pyridyl)-1,3,5-triazine (TPTZ), [126-130].
6. 3-(2-Pyridyl)-5,6-bis(4-phenyl sulphonic acid)-1,2,4-triazine (Ferrozine), [131-140].
7. 3-(4-Phenyl-2-pyridyl)-5,6-diphenyl-1,2,4-triazine (PPDT), [141,142].
8. 3-(2-Pyridyl)-5,6-bis(2-furyl)-1,2,4-triazine (Ferene Triazine), [143].
9. Ammonium 3-(4-phenyl-2-pyridyl)-5-phenyl-1,2,4-triazine-disulphonate (PPTS), [144].
10. 3-(2-Pyridyl)-5,6-bis(2-(5-furyl sulphonic acid))-1,2,4-triazine (Ferene S), [145-148].
11. 2-Amino-5-bromopyridylazo resorcinol (Br-PAR), [149].

The wavelengths at which the maximum absorbance of the reagent-iron(II) complexes are exhibited and the molar absorptivity values of these complexes are given in Table 5.1. A traditional reagent for iron(III) is potassium thiocyanate, but this does not compare favourably with the more recently developed reagents with respect to both specificity and sensitivity. In addition, it will not allow the determination of any iron(II) present.

Ferroin-type reagents have traditionally been observed to react with metal ions including iron(II), copper(II) and cobalt(II) to give highly coloured complex species. Most of the reagents listed in Table 5.1 include the bidentate ferroin ligand, which is illustrated in Fig. 5.1 together with the structures of six ferroin-type reagents.

TABLE 5.1

Chromogenic Reagents for the Determination of Iron(II).

Reagent	(A)	(B)
1,10-Phenanthroline	510	11,100
PSPmH	580	11,800
4,Hydroxy-1,10-phenanthroline	545	11,900
Bathophenanthroline	533	22,230
TPTZ	593	22,600
Ferrozine	562	27,500
PPDT	561	28,700
Ferene triazine	577	32,000
PPTS	565	33,200
Ferene S	593	34,530
Br-PAR	510	66,500

Fe (II):Reagent Complex
(A): Wavelength of maximum absorption (nm)
(B): Molar absorptivity (l mol^{-1} cm^{-1})

These reagents have been applied to the determination of iron in a wide variety of matrices, for example raw, potable and fresh waters [113,119,126,129,135,136,144], waste waters [125], marine waters [141,144], plant matter [119,144] and serum [143,145]; some of these determinations have been based on flow-injection procedures [115-120,122,125,138,140,150-152]. Flow injection analysis has also been used as the basis for the determination of

iron using alternative detection methods, for example atomic absorption spectrometry [153,154], electrochemical [155] and chemiluminescence [156].

The chromogenic reagents used in this work for a spectrophotometric flow-injection procedure for the determination of iron in potable and treated waters were chosen on the basis of three main factors:

1. Wavelength at which maximum absorption of the coloured complex was observed, preferably close to the wavelength of maximum intensity for one of the available LEDs.

2. The molar absorptivity of the complex, the larger this value the more sensitive the method.

3. The selectivity of the reagent, avoiding chromogenic species which suffer interference from analytes commonly occurring in natural waters.

Applying these criteria the choice of reagent was limited to three alternatives: TPTZ, ferrozine and ferene S. The use of 1,10-phenanthroline, previously proposed as the standard method for iron in water [114], was discounted primarily because the maximum absorption of the reagent-iron(II) complex is observed outside of the range of the available LEDs. The same restriction applied to Br-PAR, which although exhibiting a very favourable molar absorptivity, also suffered interference from copper and zinc [149].

TPTZ is used as the standard reagent by the water industry [129] and does not suffer from any serious interferences. The two other potential reagents, ferrozine and ferene S, both exhibit high molar absorptivities at wavelengths appropriate to the solid-state detection system. Ferrozine was proposed by Stookey [131] as a cheap and sensitive reagent, with the rapid AutoAnalyser method described by Gibbs [135]. Hennessy et al. [146] synthesised a new reagent, ferene S, which they proposed for the interference free determination of

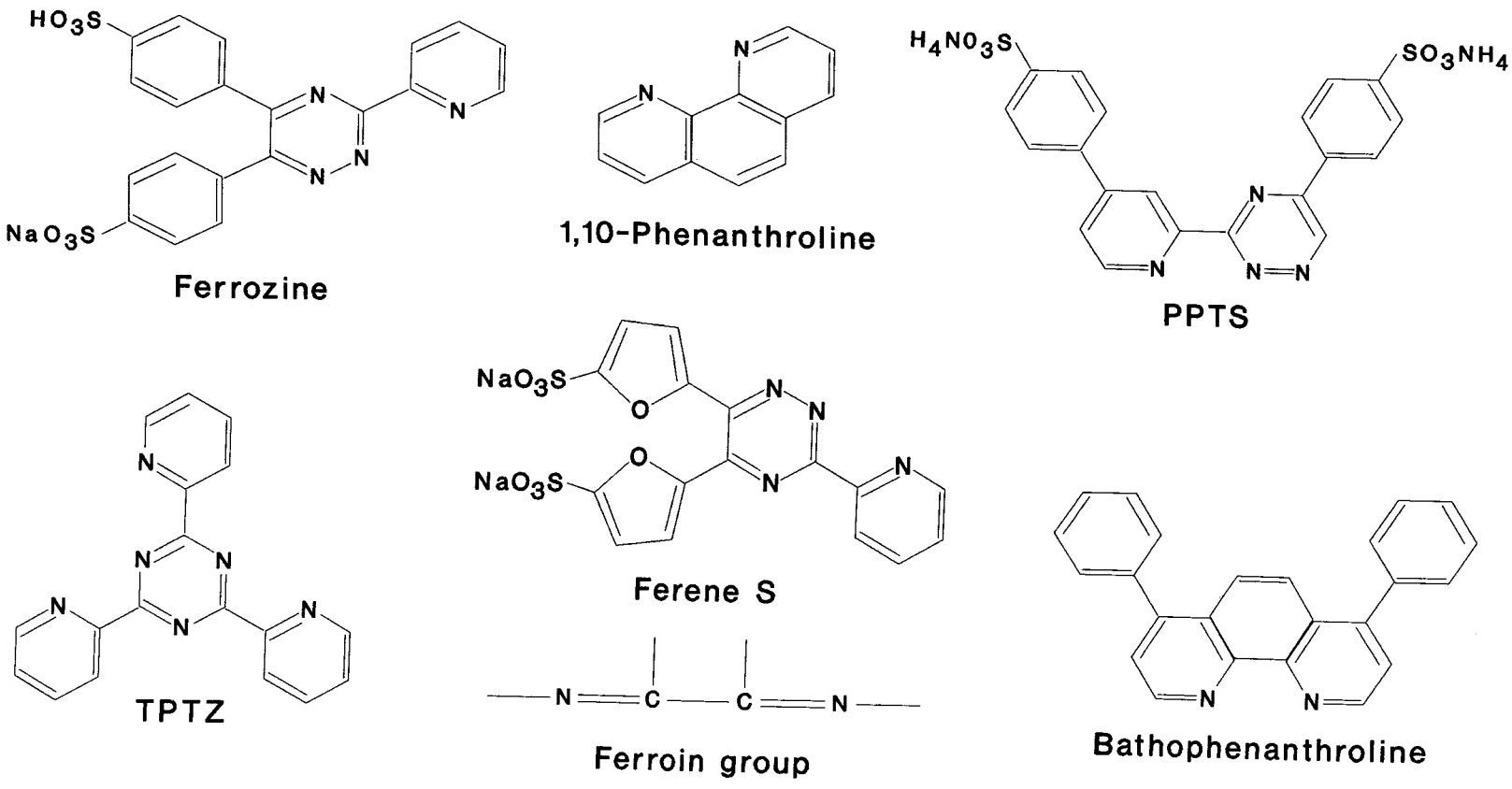

Fig. 5.1 Ferroin-Type Reagents for the Determination of Iron(II).

iron(II) in serum. Spectra for the complexed reagents are given in Fig. 5.2. No absorbance for the uncomplexed reagents was observed above 450 nm. The final selection of the reagent from the three proposed is dependent on the experimental performance of each, with reference to the analytical requirements:

1. That the method should have a linear range embracing both the GL and MAC levels (50 - 200 $\mu g\ l^{-1}$).

2. That the method has adequate sensitivity below the guide level.

Reduction of Iron(III) to Iron(II)

All the proposed reagents are selective for iron(II). A reduction step will therefore be required to reduce iron(III) (the most common species in surface waters) to iron(II). A commonly used universal reducing reagent is hydroxylammonium chloride. An alternative, proposed for the selective reduction of iron(III) in natural waters, is pentacyanoamine ferroate [148]. Both reductants are soluble in aqueous solution and provide a means for the rapid and simple reduction of iron(III) without harsh conditions being required for the reduction process.

5.2. EXPERIMENTAL

5.2.1. Reagents

Flow-Injection (FI) Methods: All solutions were prepared in distilled/deionised water or Milli-Q water, in polypropylene plasticware (Aldrich). All reagents were of GPR (or equivalent) grade unless otherwise stated. The three reagent streams used were as follows: R1, reductant, either hydroxylammonium chloride (HYD) (Aldrich) or pentacyanoamine ferroate, ammonium disodium salt (PCAF) (Aldrich); R2, colour reagent, either TPTZ (Aldrich), ferrozine (Sigma) or ferene S (Sigma); and R3, buffer, either ammonium acetate (NH_4Ac), or a mixed

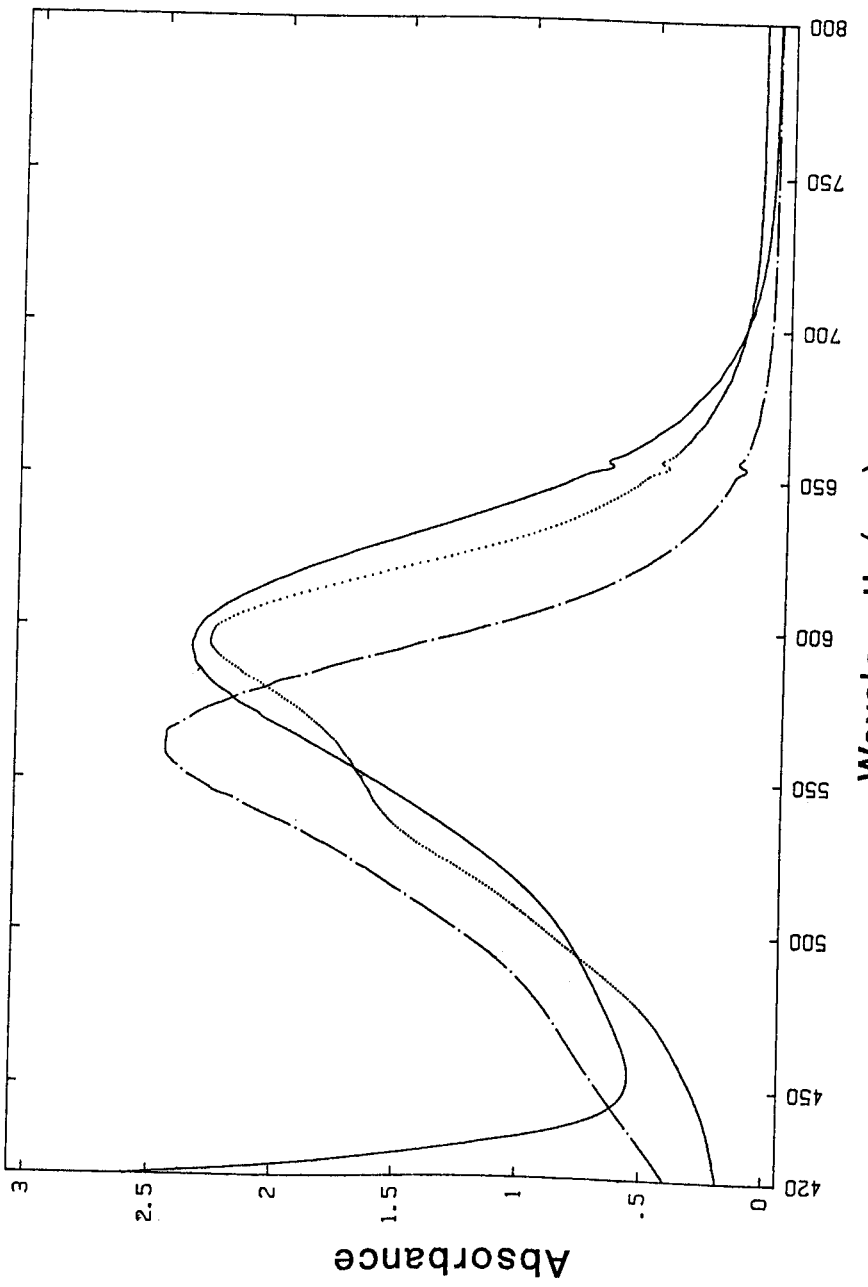

Fig. 5.2 Absorbance Spectra of Iron(II)-Reagent Complexes.

Key: ——— Ferene S
..... TPTZ
—·—·— Ferrozine

solution of sodium acetate (NaAc) (BDH) and acetic acid (HAc) (AnalaR glacial, BDH), with pH adjustment using 0.1 M sodium hydroxide (BDH) where required. Reagent concentrations are given in the results and discussion section where appropriate. Iron(III) standards were prepared by dilution of a 1000 mg l^{-1} standard solution (SpectrosoL, BDH).

Automated FI Monitor: The solutions and standards were prepared as described above. The three reagent streams were as follows: R1, 0.5 g l^{-1} PCAF; R2, 5 g l^{-1} ferene S; and R3, 15.2 ml l^{-1} HAc and 20.5 g l^{-1} NaAc, adjusted to pH 6.0.

Manual Batch Method: All the solutions were prepared in distilled/deionised water and all reagents were of GPR (or equivalent) grade. The three reagents used were as follows: A, reductant, 100 g l^{-1} hydroxylammonium chloride (Aldrich); B, colour reagent, 0.75 g l^{-1} TPTZ (Aldrich); and C, buffer, 287 g l^{-1} sodium acetate (BDH) and 115 ml l^{-1} glacial acetic acid (BDH).

5.2.2. Instrumentation

Flow-Injection Methods: A manual system was used for the development, optimisation and calibration of the flow-injection manifolds, the optimised manifold being used in the automated FI monitor. The coloured reagent-iron complexes were measured with a solid-state detector fitted with red, yellow and green LEDs, or an LKB Ultrospec II uv/visible spectrophotometer (Pharmacia, Milton Keynes). Unless otherwise stated, all measurements of the TPTZ and ferrozine complexes were made using detectors incorporating yellow and green LEDs respectively. The construction details and specifications of the manual FI system were described in Chapter 2.

Automated FI Monitor: The construction details and specifications of the automated FI monitor were given in Chapter 4. A modified solid-state detector

(type B) with the original lower intensity red LEDs fitted, but with glass capillary flow cells was used.

Manual Batch Method: All manual absorbance measurements were made using a diode array spectrophotometer (Hewlett Packard 8451A), and a 10 mm path length quartz cell.

5.2.3. Procedures

FI Methods: Univariate and simplex optimisation procedures were used to optimise the experimental conditions, both being used to maximise the response of the signal due to iron(III). The simplex software package was described in Chapter 3; the simplex matrix and conditions are given in the Results and Discussion section.

All experiments were based around one of four (sample injection) FI manifolds which are schematically illustrated in Figs. 5.3(a)-(d), and designated A, B, C and D respectively. The variable parameters for each manifold were the reagent stream compositions and flow rates; these are given in the Results and Discussion section. For manifold types C and D additional variable parameters were: 1/ the sample injection volume (μl) (SV), and 2/ the reaction coil length (cm) (LC), the latter being fixed at 30 cm except during simplex optimisation.

Automated FI Monitor: For the FI manifold used in the automated monitor, type C, the injection volume (SV) was fixed at 280 μl and the reaction coil length (LC) fixed at 30 cm. The flow rates for the reagent streams were as follows: C, 1.42 ml min^{-1}; R1, 0.2 ml min^{-1}; R2, 0.2 ml min^{-1}; and R3, 0.42 ml min^{-1}.

Manual Batch Method: The TPTZ detection method relied on the formation of the TPTZ-Fe(II) complex and was carried out according to the following protocol:

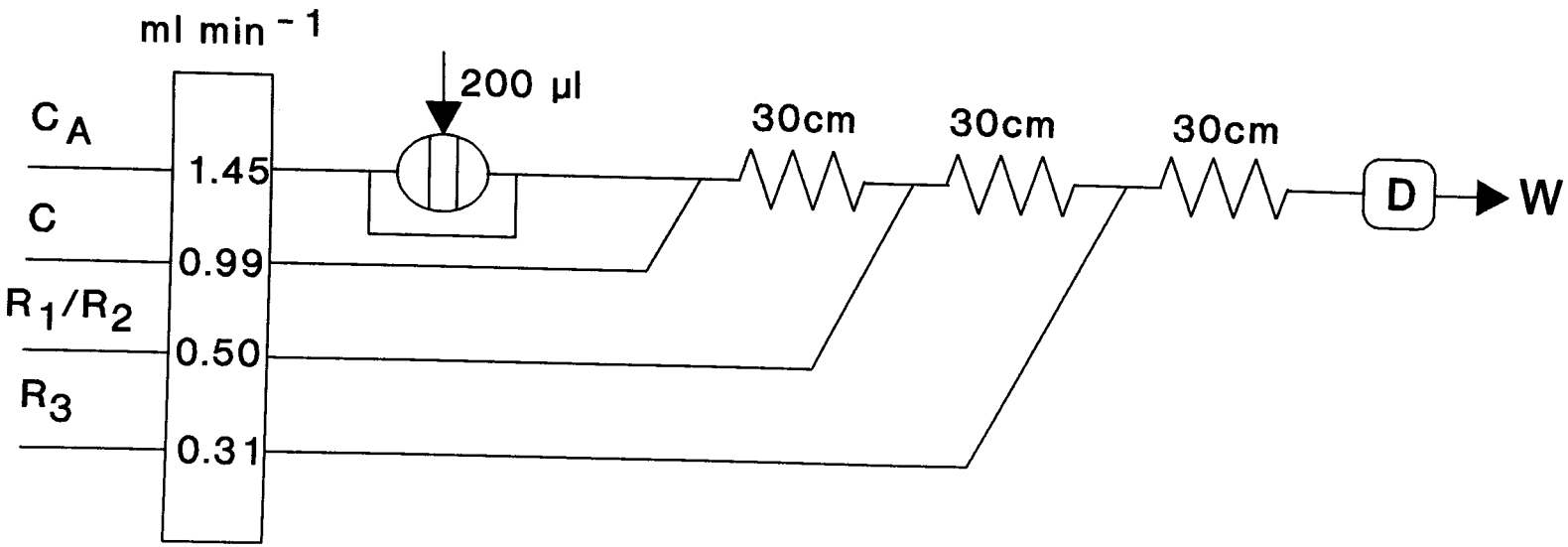

Fig. 5.3(a) FI Manifold for Determination of Iron (III).

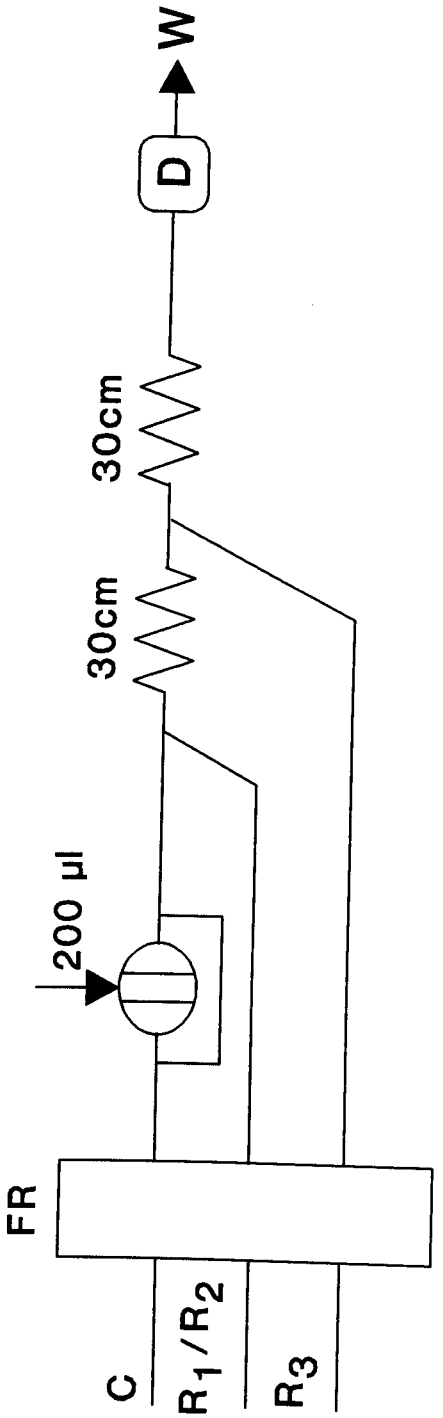

Fig. 5.3(b) FI Manifold for Determination of Iron (III).

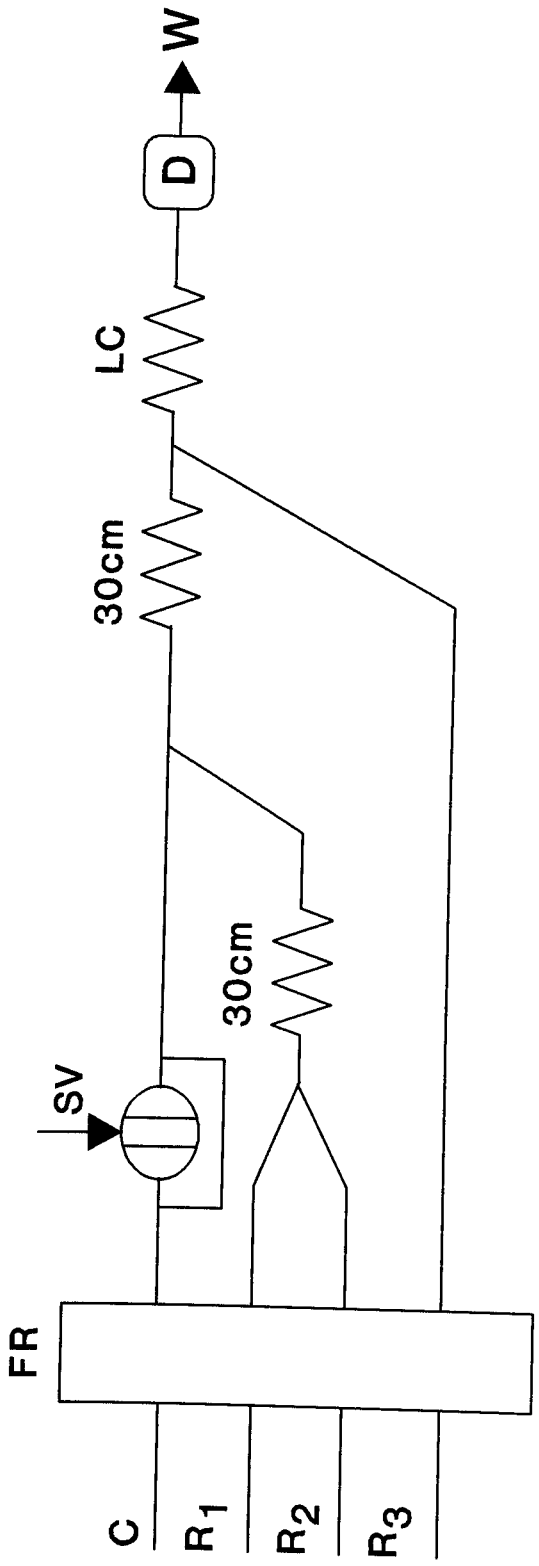

Fig. 5.3(c) FI Manifold for Determination of Iron (III).

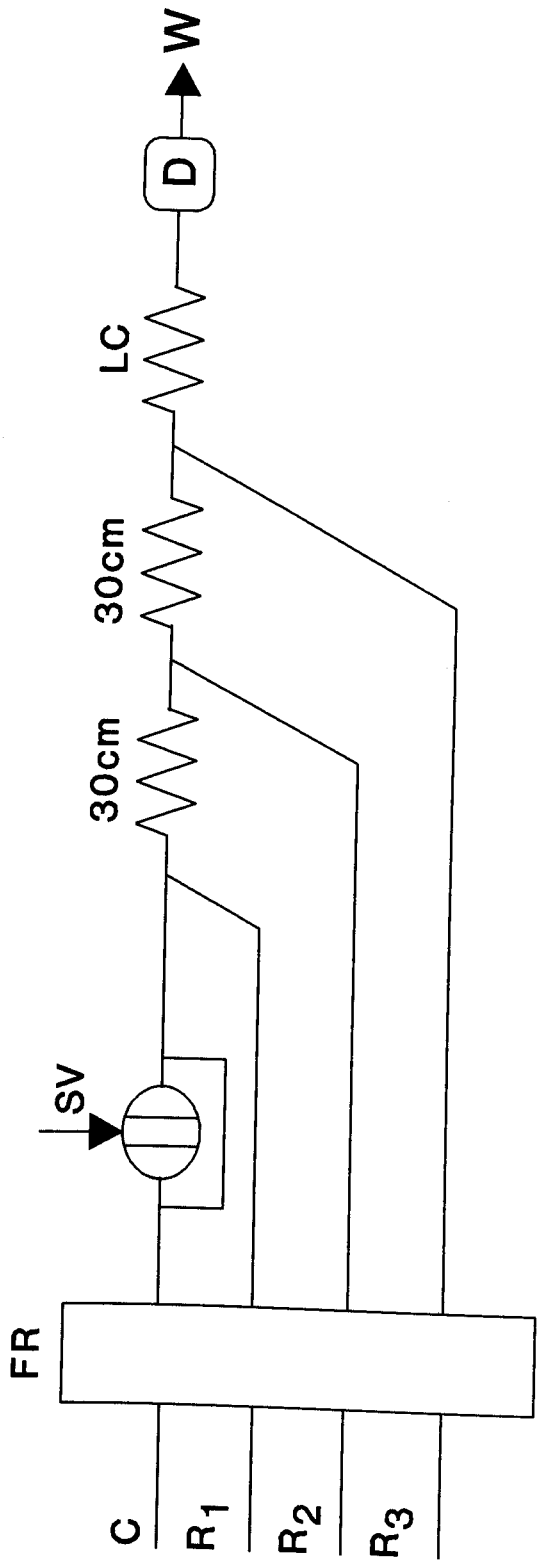

Fig. 5.3(d) FI Manifold for Determination of Iron (III).

1. 20 ml of each standard was pipetted into a 25 ml volumetric flask.
2. Each of the following solutions were added to the flask, mixing after each addition: 1 ml A; 1 ml B and 2.5 ml C. This mixture was then diluted, stoppered and left to stand for 1.5 hours.
3. The absorbance of the homogeneous mixture was measured at 596 nm.

5.3. RESULTS AND DISCUSSION

5.3.1. Determination of Iron(III) Using TPTZ

Manual Batch Method

A standard water industry method for the determination of iron(III) uses the chromogenic reagent TPTZ [129]. Iron(III) standards covering the range 0 - 1000 $\mu g\ l^{-1}$ were analysed by a manual batch method according to the protocol detailed in Section 5.2.3. The response was found to be linear (r = 0.9985) and was described by the following regression equation:

$$\text{Absorbance} = 0.0003\ [Fe]\ \mu g\ l^{-1} + 0.0031$$

The theoretical limit of detection, defined as 3σ of the blank + the blank value, was calculated to be 28 $\mu g\ l^{-1}$. This confirmed that a TPTZ based method could offer sufficient sensitivity for the determination of iron in potable and treated waters.

Sample-Injection FI Method

A FI manifold, type A, using a solid-state detector was developed. This manifold, based on that proposed for a commercial FI analyser [157], utilised a dual carrier stream. The sample was injected into a sulphuric acid carrier stream which was then merged with a deionised water carrier stream, C_A, before addition of the reagents. Reagent concentrations and flow rates are summarised in Table 5.2. A series of iron standards in the range 50 - 1000 $\mu g\ l^{-1}$ were analysed using

this FI procedure. The responses for standards < 400 $\mu g\ l^{-1}$ were not measurable above the inherent noise of the detector and this manifold was abandoned in favour of a simplified version. The simplified manifold, type D, with a single deionised water carrier stream, was based closely on the standard manual method. The sample-injection volume was fixed at 200 μl. The other manifold conditions are summarised in Table 5.3. However, the unstable nature of the baseline with this manifold severely limited the sensitivity of the method, and the response for standards < 600 $\mu g\ l^{-1}$ could not be measured. No significant improvements to the sensitivity of the method were made through manifold modifications, and consequently alternative, more sensitive, reagents were sought.

TABLE 5.2

Conditions for Dual Carrier Stream TPTZ FI Manifold.

Stream	Composition	Flow Rate ($ml\ min^{-1}$)
C1	0.4 M sulphuric acid	1.45
C2	Deionised water	0.99
R1/R2	25 $g\ l^{-1}$ HYD + 0.156 $g\ l^{-1}$ TPTZ	0.50
R3	204 $g\ l^{-1}$ NaAc	0.31

TABLE 5.3

Conditions for Single Carrier Stream TPTZ FI Manifold.

Stream	Composition	Flow Rate ($ml\ min^{-1}$)
C	Deionised water	0.31
R1	100 $g\ l^{-1}$ HYD	0.64
R2	0.75 $g\ l^{-1}$ TPTZ	0.64
R3	287 $g\ l^{-1}$ NaAc + 115 $ml\ l^{-1}$ HAc	1.45

5.3.2. Determination of Iron(III) Using Ferrozine

Reagent-Injection FI Method

A reagent-injection FI manifold using the chromogenic reagent ferrozine was developed. This manifold, based on the AutoAnalyser method proposed by Gibbs [135], was evaluated. This was not adopted because of the high blank response, the occurrence of the blank signal limiting the sensitivity of the method. The use of this manifold in the automated monitor would have necessitated the use of two switching valves in the automated monitor; for the selection of sample, standard or blank.

Sample-Injection FI Manifold: Premixed Reagents

A sample-injection manifold was developed where the colour reagent and reductant were premixed, type B, for which the experimental parameters are given in Table 5.4. This manifold was used to analyse a series of standards in the range 0 - 1000 $\mu g\ l^{-1}$. The coloured ferrozine:iron(II) complex was measured using both an LKB spectrophotometer (570 nm) and a solid-state detector. The responses, Table 5.5, were linear and could be described by the following regression equations for the LKB and solid-state detectors respectively:

$$\text{Signal (mV)} = 0.13\ [\text{Fe}]\ (\mu g\ l^{-1}) - 1.43 \quad (r = 0.9996)$$

$$\text{Signal (mV)} = 0.079\ [\text{Fe}]\ (\mu g\ l^{-1}) - 1.074 \quad (r = 0.9993)$$

The practical limits of detection, defined as twice the peak-to-peak noise, were 12 and 36 $\mu g\ l^{-1}$ respectively. This definition of LOD was used instead of (blank + 3 σ) because of the absence of any measurable blank signals.

TABLE 5.4

Conditions for Ferrozine FI Manifold, Premixed Reagents.

Stream	Composition	Flow Rate ($ml\ min^{-1}$)
C	Deionised water	1.0
R1/R2	35 g l^{-1} HYD + 0.75 g l^{-1} ferrozine	0.2
R3	80 g l^{-1} NaAc	0.2

TABLE 5.5

Calibration Data for Ferrozine FI Determination of Iron(III).

	LKB (570 nm)		Solid-State	
Iron(III) ($\mu g\ l^{-1}$)	Signal[a] (mV)	RSD (%)	Signal[b] (mV)	RSD (%)
0	0	0	0	0
50	3.1	7.2	2.8	10.5
100	10.2	4.4	4.8	6.1
200	23.5	3.0	14.6	4.3
400	50.2	2.1	32.3	2.0
600	73.3	3.0	47.3	2.8
800	100.0	0	62.8	1.0
1000	122.4	0.9	77.9	0.6

[a] n = 5, [b] n = 4

Stability of Premixed Colour and Reducing Reagent

A short term trial was used to establish the stability of the premixed colour/reducing reagent and therefore the frequency at which this reagent would need to be replaced. This mixed reagent was prepared at the beginning of the trial and with a buffer prepared daily was used to analyse fresh 50 and 200 $\mu g\ l^{-1}$ iron(III) standards each day over a four day period. On day one, the response for the 50 $\mu g\ l^{-1}$ standard at 1.9 mV was measurable above the baseline noise of 1 mV. However, after four days it was not possible to distinguish the response for this standard above the background noise. During the four day trial the response for the 200 $\mu g\ l^{-1}$ standard remained constant at $\approx$ 13 mV. The trial indicated that the premixed colour/reducing reagent was not sufficiently stable to allow long term unattended operation if the expected iron concentration was at or near the GL level of 50 $\mu g\ l^{-1}$.

Sample-Injection Manifold: On-line Mixing/Merging of Reagents

Because of the instability of the premixed reagents used in the previous FI manifold and the need for long term operational stability of the method, the performance of two alternative FI manifolds were examined. These manifolds utilised different reagent mixing procedures: a/ On-line mixing of colour and reducing reagents prior to merging with the carrier stream; b/ Sequential merging of colour reagent, reductant and buffer with the carrier stream. These manifolds were schematically represented as Types (C) and (D) in Figs. 5.2(c) and 5.2(d). The sample-injection volume was fixed at 200 μl, all the other experimental conditions are given in Table 5.6. A comparison of the performance of these two manifolds was undertaken by analysing the same set of iron(III) calibration standards, 50 - 1000 $\mu g\ l^{-1}$, with each manifold. The responses obtained from both manifolds were linear, Table 5.7, and were described by the following regression equations:

$$\text{(C)} \quad \text{Signal (mV)} = 0.085\ [\text{Fe}]\ (\mu g\ l^{-1}) - 1.943 \quad (r = 0.9985)$$

TABLE 5.6

Conditions for Ferrozine FI Manifold, On-line Mixing and Merging of Reagents.

Stream	Composition	Flow Rate ($ml\ min^{-1}$)
C	Deionised water	1.00
R1	70 g l^{-1} HYD	0.20
R2	1.5 g l^{-1} ferrozine	0.20
R3	80 g l^{-1} NaAc	0.20

TABLE 5.7

Alternative Reagent Addition Patterns for FI Ferrozine Determination of Iron(III).

	Mixing on-line		Merging on-line	
Iron(III) ($\mu g\ l^{-1}$)	Signal[a] (mV)	RSD (%)	Signal[b] (mV)	RSD (%)
0	0	0	0	0
50	2.8	18.2	-	-
100	4.9	9.8	6.4	16.7
200	14.8	3.4	13.7	1.9
400	33.0	2.1	27.9	2.1
600	47.4	1.0	41.6	1.8
800	64.3	1.0	56.0	0
1000	85.9	0.9	65.9	1.1

[a] $n = 4$, [b] $n = 6$

(D) Signal (mV) = 0.067 [Fe] (μg l^{-1}) + 0.306 (r = 0.9990)

The theoretical limits of detection, twice the peak-to-peak noise, were 54 and 23 μg l^{-1} iron(III) for the on-line mixing (C) and merging (D) manifolds respectively. However, with the latter manifold it was not practically possible to measure the response for a 50 μg l^{-1} standard above the inherent system noise. For this reason, the manifold utilising on-line reagent mixing was selected as the method to which modifications were made to improve sensitivity.

A univariate optimisation procedure failed to produce any significant improvement in the sensitivity of the manifold. It was concluded that the method was not limited by the sensitivity of the manifold or the ferrozine colour reagent, but by the solid-state detector. This was confirmed by earlier work using a commercial spectrophotometer (LKB, Ultrospec II), where a lower detection limit was easily achieved. Therefore a chromogenic reagent exhibiting greater molar absorptivity was examined.

5.3.3. Determination of Iron(III) Using Ferene S

Initial investigations on the use of ferene S in an FI method for iron(III), were centred around an AutoAnalyser method proposed by Artiss et al. [147]. A sample injection FI manifold, type D, was used to analyse a series of standards in the range 200 - 1000 μg l^{-1}. The experimental conditions for this manifold during the investigation are given in Table 5.8, the sample-injection volume was fixed at 300 μl and a detector with a yellow LED was used. The response was linear (r = 0.9981) across the calibration range and was described by the regression equation:

Signal (mV) = 0.03 [Fe] (μg l^{-1}) - 0.77

The baseline obtained with this manifold was very steady, in addition the detector noise was low but so too were the standard responses. Thus, the sensitivity of the

method was poor and the practical limit of detection, twice the peak-to-peak noise, was calculated to be 145 $\mu g\ l^{-1}$.

TABLE 5.8

Conditions for Initial Ferene S FI Manifold.

Stream	Composition	Flow Rate ($ml\ min^{-1}$)
C	Deionised Water	1.45
R1	100 $g\ l^{-1}$ HYD	0.31
R2	2 $g\ l^{-1}$ ferene S	0.31
R3	3.86 $g\ l^{-1}$ NH_4Ac + 28 $ml\ l^{-1}$ HAc	0.99

Investigation of the Use of a Selective Reducing Agent

An alternative FI manifold was based on the manual method of Mehra et al. [148]. In this manual method ferene S was used in conjunction with a selective reducing agent for iron(III), pentacyanoamine ferroate (PCAF), which was reported to have an almost instantaneous action with no initiation or warming period required. The experimental conditions for this FI manifold, type C, are given in Table 5.9, the sample-injection volume was fixed at 160 μl. Using this manifold a series of standards (0 - 1000 $\mu g\ l^{-1}$) were analysed and the performance of the manifold with red, yellow and green LEDs fitted in the solid-state detector is summarised in Table 5.10. The response using each of the detectors was linear across the range and was described by the following regression equations:

Red, Signal (mV) = 0.22 [Fe] ($\mu g\ l^{-1}$) - 5.14 (r = 0.9988)

Yellow, Signal (mV) = 0.030 [Fe] ($\mu g\ l^{-1}$) - 0.421 (r = 0.9985)

Green, Signal (mV) = 0.092 [Fe] ($\mu g\ l^{-1}$) - 3.759 (r = 0.9980)

TABLE 5.9

Conditions for Ferene S/PCAF FI Manifold.

Stream	Composition	Flow Rate ($ml\ min^{-1}$)
C	Deionised water	1.5
R1	5 g l^{-1} ferene S	0.20
R2	0.3 g l^{-1} PCAF	0.20
R3	20.5 g l^{-1} NaAc + 15.2 ml l^{-1} HAc	0.50

TABLE 5.10

Comparison of Solid-State Detectors for FI Ferrozine Determination of Iron(III).

	Red		Yellow		Green	
Iron(III) ($\mu g\ l^{-1}$)	Signal[a] (mV)	RSD (%)	Signal[a] (mV)	RSD (%)	Signal[a] (mV)	RSD (%)
0	0	0	0	0	0	0
50	7.4	14.3	-	-	-	-
100	16.2	7.3	2.1	10.9	2.6	9.5
200	30.7	2.9	4.7	6.4	12.3	4.1
400	85.4	2.3	11.9	2.8	33.3	1.5
600	130.3	2.1	17.9	1.3	51.5	1.1
800	175.5	1.0	23.6	1.4	70.3	2.4
1000	217.5	1.4	28.5	3.5	87.5	2.9

[a] n = 10

From these regression equations it was obvious that the most sensitive detector was that which incorporated the red LEDs. This was confirmed by the practical detection limits, twice the peak to peak noise, which were calculated to be 36, 97 and 66 $\mu g\ l^{-1}$ using the red, yellow and green LEDs respectively.

This experiment also illustrated that the sensitivity of the method was not only dependent on the wavelength "match" between the LED and the coloured complex, but also on the intensity of the LED. In this experiment, the detector fitted with LEDs exhibiting maximum intensity closest to the ferene S complex gave the lowest responses. Whereas the detector with red LEDs, with an intensity maximum furthest from the ferene S complex, gave the highest responses. The size of the response from the detectors increased with increasing LED intensity: yellow < green < red. Therefore the detector fitted with red LEDs was used for all other experiments.

Optimisation of the Manifold to Maximise Iron Response

A simplex optimisation procedure was used to maximise the response for a 200 $\mu g\ l^{-1}$ iron(III) standard solution. The manifold, with the solid-state detector fitted with red LEDs, remained unchanged from the previous experimental investigation. The simplex matrix is given in Table 5.11, together with the starting and finishing conditions. The simplex response variable was defined as the mean signal for six injections of the standard solution.

A graphical illustration of the optimisation procedure is given in Fig. 5.4, where a plot of response verses experiment number is given. The simplex procedure was terminated after 20 experiments, when a 43 % increase in the response had been achieved. It was not possible to correlate the increase in response with any particular variable, but it is likely that a significant contribution to this improvement was due to the increase in sample volume. To assure that the linearity of the method remained at higher iron concentrations, a 30 cm reaction coil was included in the manifold flow tubing immediately prior to the detector to ensure the homogeneity of the sample with the reagents.

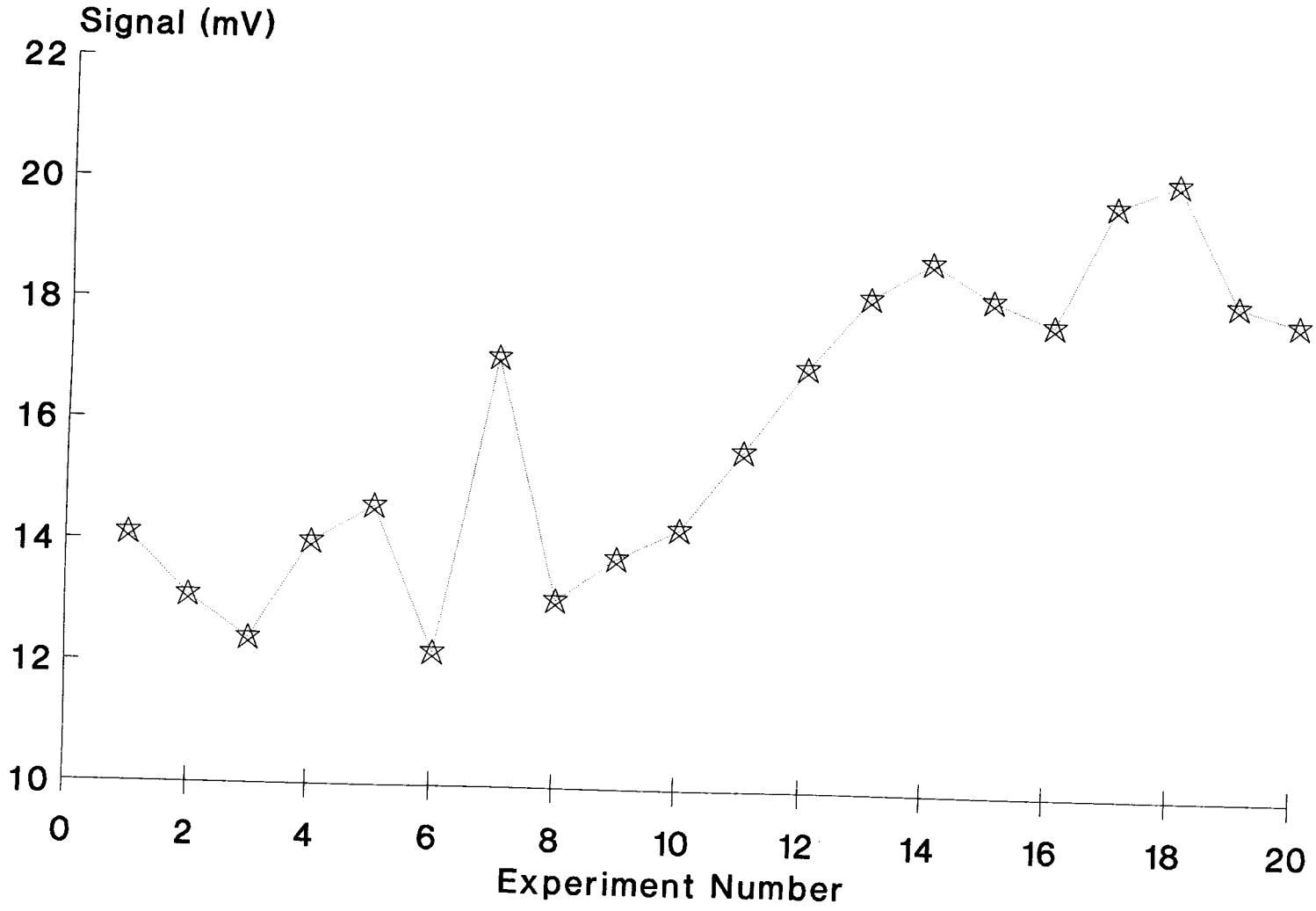

Fig. 5.4 Simplex Optimisation to Maximise Iron Response.

TABLE 5.11

Optimisation of Ferene S FI Manifold with Respect to Iron Response.

Variable	Range	Precision	Conditions	
			Initial	Final
R1 (g l^{-1})	1 - 10	1	5	5
R2 (g l^{-1})	0.1- 1.0	0.1	0.3	0.5
R3 (pH)	3 - 6	0.5	5	6
SV (μl)	80 - 300	20	200	280
LC (cm)	0 - 200	10	30	0

Optimum Manifold and Detector Performance

The performance of the method, and of the original detector in comparison to the modified detector was assessed in two experiments.

Detector Sensitivity: The first experiment compared the performance of the two detectors with and without glass capillary flow cells; for comparison purposes detectors fitted with both red and yellow LEDs were used, to confirm that the intensity of the LED was a contributing factor to the sensitivity of the method. The information summarised in Table 5.12 serves to illustrate the improved sensitivity that was achieved firstly by the correct choice of LED, and secondly by the replacement of the PTFE flow cells.

The modifications improved the sensitivity of both detectors without losing linearity across the calibration range, 0 - 1000 μg l^{-1}. The responses were described by the following regression equations:

Yellow LED - unmodified detector

$$\text{Signal (mV)} = 0.031\ [\text{Fe}]\ (\mu\text{g } l^{-1}) + 0.108 \quad (r = 0.9997)$$

Red LED - unmodified detector

$$\text{Signal (mV)} = 0.40\ [\text{Fe}]\ (\mu\text{g } l^{-1}) - 6.04 \quad (r = 0.9997)$$

TABLE 5.12

Detector Comparison Ferene S FI Determination of Iron(III).

Fe (III) ($\mu g\ l^{-1}$)	Yellow LED Signal[a] (mV)	Yellow LED RSD (%)	Red LED Signal[a] (mV)	Red LED RSD (%)
PTFE "Flow Cells"				
0	0	0	0	0
50	-	-	8.8	8.5
100	3.0	10.7	30.8	3.8
200	6.6	5.7	72.9	1.4
400	12.6	1.6	154.2	0.8
600	19.5	2.3	237.1	0.4
800	25.0	1.8	311.7	1.0
1000	31.3	1.7	390.8	0.9
Glass "Flow Cells"				
0	0	0	0	0
50	5.2	7.9	20.0	7.4
100	19.2	2.1	70.8	2.9
200	47.5	-	175.8	1.2
400	99.2	1.3	369.2	1.0
600	151.7	0.9	561.7	0.7
800	197.5	0.8	742.5	0.8
1000	241.7	0.8	921.7	1.3

[a] n = 6

Yellow LED - modified detector

Signal (mV) = 0.25 [Fe] (μg l^{-1}) - 2.78 (r = 0.9993)

Red LED - modified detector

Signal (mV) = 0.94 [Fe] (μg l^{-1}) - 13.62 (r = 0.9996)

The most sensitive detector was the one fitted with red LEDs and glass capillary flow cells, where the modification resulted in an increase in the signal of $\approx$ 127 % at 50 μg l^{-1}. With this detector, a practical limit of detection, twice the peak-to-peak noise, was calculated to be 31 μg l^{-1}.

Reagent Stability: The second experiment was used to determine the short term stability of the reagents. A range of standards, prepared freshly for each analysis, were analysed with the same batch of reagents at the beginning and end of a ten day period. The responses from an unmodified detector (Red LED) are given in Table 5.13, and were described by the following regression equations:

Day (1) Signal (mV) = 0.40 [Fe] (μg l^{-1}) - 6.04 (r = 0.9997)

Day (10) Signal (mV) = 0.39 [Fe] (μg l^{-1}) + 1.06 (r = 0.9999)

The variation in the response between Day (1) and Day (10) did not vary significantly, indicating that the reagents were stable for a period of at least ten days with no loss in analytical performance.

Method Sensitivity

To confirm the practical limit of detection for the FI method, a series of iron(III) calibration standards covering the range 0 - 600 μg l^{-1} were freshly prepared and analysed using the optimum manifold, conditions and modified detector fitted with red LEDs.

TABLE 5.13

Ferene S FI Manifold, Reagent Stability Trial.

Fe (III) ($\mu g\ l^{-1}$)	Day (1) Signal[a] (mV)	Day (1) RSD (%)	Day (10) Signal[a] (mV)	Day (10) RSD (%)
0	0	0	0	0
50	8.8	8.5	20.8	9.2
100	30.8	3.8	39.5	4.2
200	72.9	1.4	78.4	6.0
400	154.2	0.8	161.7	2.5
600	237.1	0.4	235.8	1.3
800	311.7	1.0	314.6	0.9
1000	390.8	0.9	391.3	0.3

[a] n = 6

The response across the range 20 - 600 $\mu g\ l^{-1}$ was linear (r = 0.9998), Table 5.14, and was described by the regression equation:

$$\text{Signal (mV)} = 0.77\ [\text{Fe}]\ (\mu g\ l^{-1}) - 2.51$$

It was not possible to measure the response for a 10 $\mu g\ l^{-1}$ standard above the background noise, but the limit of detection, at twice the peak-to-peak noise, was calculated as 11 $\mu g\ l^{-1}$. It was concluded that the practical LOD was < 20 $\mu g\ l^{-1}$, which is sufficiently below the GL for iron of 50 $\mu g\ l^{-1}$ for the determination of iron as a residual coagulant in treated waters.

TABLE 5.14

Ferene S FI Manifold, Determination of Limit of Detection.

Fe (III) ($\mu g\ l^{-1}$)	Signal[a] (mV)	RSD (%)
0	0	0
10	-	-
20	10.5	10.0
30	20.2	8.5
40	26.3	5.2
50	32.5	6.9
100	75.8	2.7
200	155.8	1.3
400	311.7	2.2
600	455.8	0.8

[a] n = 6

This calibration procedure highlighted the problem of assuming linearity across a wide concentration range. Fig. 5.5 graphically illustrates the regression equations for the concentration ranges 0 - 50 and 100 - 600 $\mu g\ l^{-1}$. The linear

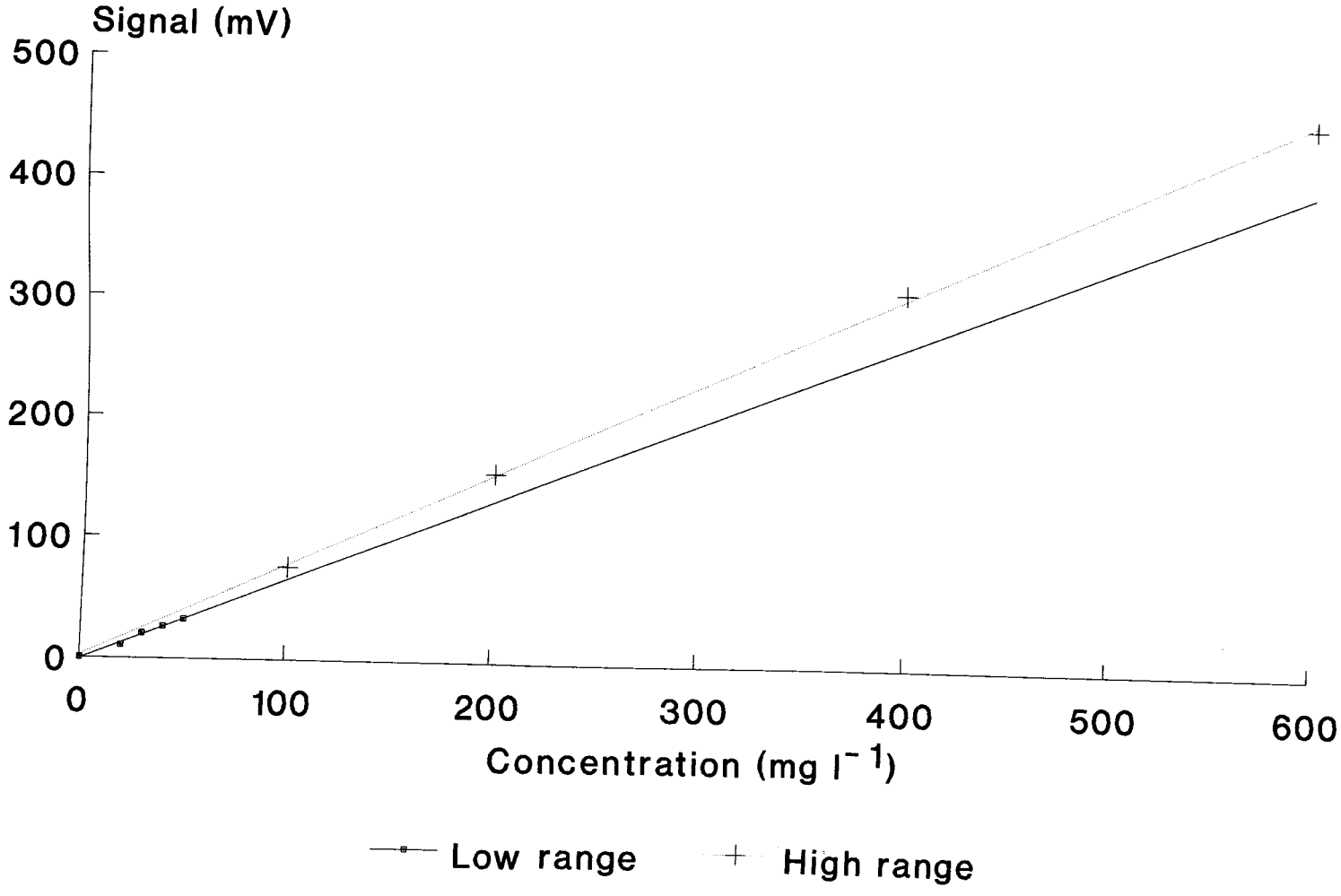

Fig. 5.5 Iron (III) Calibration.

responses over these two ranges were not comparable, and therefore it would not be possible to use a high calibration standard in the automated monitor without avoiding a negative bias at lower analyte concentrations.

5.3.4. Field Trials

The monitor was operated with two versions of the control software, the difference between them being the standard concentration value. This parameter was set to 50 and 200 $\mu g\ l^{-1}$ for RLB25(A) and RLB25(B) respectively, all the user defined parameters are given in Table 5.15.

Monitor Accuracy and Performance

The accuracy of the analytical result was assessed by replacing the "sample" solution with one of known iron concentration. In trials, it was found that to meet the required accuracy [24] at the GL level (50 $\mu g\ l^{-1}$) a 50 $\mu g\ l^{-1}$ standard had to be used; using a 100 $\mu g\ l^{-1}$ standard against a 50 $\mu g\ l^{-1}$ "sample" gave a result with a negative bias ($\approx$ 20 % low). Summaries of two trials with "samples" at both the GL and MAC levels are given in Table 5.16. The performance at both these levels was acceptable, however an improvement in the initial success rate would be desirable. During the trial it was found that the detector was being affected by electrical noise. This had the most significant effect over the response at the lower end of the calibration range, where the smallest analogue signals were measured. Any extraneous noise had a significant effect on the signal-to-noise ratio for these small signals and led to the rejection of a higher number of results, where the defined threshold limits were exceeded.

Monitor Performance

The overall performance characteristics are summarised in Table 5.17. These compare favourably with the water industry specifications [24] for a dissolved iron analyser for clarified water monitoring.

TABLE 5.15

User-Defined Parameters Included in FI Iron Monitor Software, Version RLB25(A/B).

Parameter	Unit	Setting
sampint%	min	30
cycletime%	min	11
flushdel%	s	50
filldel%	s	45
injdel%	s	20
sensthresh	--	0.75
maxfails%	--	3
mvdiff	mV	10
maxexpect	$\mu g\ l^{-1}$	250
minexpect	$\mu g\ l^{-1}$	0
standconc	$\mu g\ l^{-1}$	50 (A) 200 (B)

TABLE 5.16

Dissolved Iron FI Monitor Performance Trial.

Parameter	RLB25(A)[a]	RLB25(B)[b]
Number of measurements	141	128
Calculated concentration	47.9	194.3
Standard deviation ($\mu g\ l^{-1}$)	3.6	7.0
RSD (%)	7.5	3.6
Total number of failures	14	5
Initial success rate (%)	90.1	96.1
Overall success rate (%)	100	100

[a] 50 μg Fe l^{-1} "sample" and standard solutions
[b] 200 μg Fe l^{-1} "sample" and standard solutions

TABLE 5.17

Dissolved Iron FI Monitor Specification and Performance.

Parameter	Industry specification	Proposed monitor
Overall accuracy	± 10 %	± 4 % (at 50 $\mu g\ l^{-1}$)[a] ± 3 % (at 200 $\mu g\ l^{-1}$)[b]
Repeatability	± 10 %	± 8 % (at 50 $\mu g\ l^{-1}$)[a] ± 4 % (at 200 $\mu g\ l^{-1}$)[b]
Response time	< 15 min	10 min
Nominal range	0-1000 $\mu g\ l^{-1}$	0-1000 $\mu g\ l^{-1}$
Limit of detection		20 $\mu g\ l^{-1}$
Reliability		> 93 %
Unattended operation	35 days	35 Days

[a] n = 141, 50 $\mu g\ l^{-1}$ standard
[b] n = 128, 200 $\mu g\ l^{-1}$ standard

For this application the response time is less critical and trend information is more important. If the calibration frequency was reduced a sample response could be generated within five minutes and this would allow the automated system to be applied to control applications, where a rapid response is essential. Reagent consumption figures and operational costs were calculated for a 35 day operational cycle, Table 5.18, allowing for a 5 % repeat of the measurement cycle. This assumes that the monitor provides valid results on a first determination basis for 95 % of the operational period. The operation of the monitor with the current protocol would prove to be very economical, but further reductions in reagent consumption would be possible by reducing the frequency of the measurement cycle and/or the frequency of the calibration procedure.

TABLE 5.18

Reagent Consumption and Running Costs.

Reagent	Consumption (l)
Ferene S	3.0
PCAF	3.0
Buffer	6.2
Carrier	20.9
Standard	5.8
Costs	**£**
Reagent cost:	79
Pump tubing:	3
Total Cost:	82

Tap Water Trial: The automated monitor was set-up to monitor the iron concentration of tap water from the public supply, details of sample delivery to the

monitor were given in Chapter 4. However, during a period of > 48 hours, it was found that the iron concentration was below the LOD of the FI method and the trial was abandoned.

5.4. CONCLUSIONS

The FI iron monitor meets industry specifications for the monitoring of clarified water after treatment, and could be readily modified to provide the rapid response required for treatment process control.

The monitor showed high reliability during the short term trials, but further extended trials would be required to fully validate the system.

Chapter Six

FI Determination of Dissolved Organic Carbon

6.1. INTRODUCTION

Total carbon can be defined as a series of fractions including: inorganic (IC), total organic (TOC), dissolved organic (DOC), non-dissolved organic (NDOC), purgeable organic carbon (POC) and non-purgeable organic (NPOC) [21]. DOC is defined as that fraction of TOC which passes through a 0.45 μm pore-diameter filter [158] and therefore may contain fine particulate and colloidal matter.

A variety of indices have been used to measure the total organic content of water, for example biological oxygen demand (BOD) and chemical oxygen demand (COD), but generally there is little or no correlation between them [66]. The measurement of DOC, is however, regarded as an important component of water quality studies [159], representing the degradation products of aquatic plant or animal life and pollution from domestic sewage or industrial effluent.

6.1.1. Why is Dissolved Organic Carbon Important ?

DOC is a very complex mixture of chemicals that are constantly subject to chemical and biological change. It consists of a continuum of compounds ranging from relatively simple species of short residence time, e.g. glucose, to stable high molecular weight geopolymers and colloids. Approximately 50 % of the DOC in uncoloured US surface waters consists of humic substances, while in coloured waters this humic fraction can be as high as 80 % [160]. Humic substances are defined as high molecular weight polyelectrolytes, containing both aromatic and aliphatic carbon with phenolic, alcoholic, carbonyl, acidic, and amino functional groups [159]. The universal feature of these organic compounds is that they contain oxidisable carbon [161].

In the aquatic ecosystem it is likely that the biomass of living organisms accounts for only a small proportion of the TOC present. Most will occur as the decaying and partially digested remains of living tissues or as dissolved organic compounds derived from living and decaying organisms [162]. The measurement of POC and DOC is of considerable importance in elucidating the carbon and

energy budget of the global or local aquatic environment. These components, common to all trophic levels, can be used to assess the flow of energy through the ecosystem, and to determine a carbon balance for the measurement of bacterially degradable organics [163]. In addition the solubility and mobility of chemical micropollutants have been observed to increase with their association or bonding to non-polar highly hydrophobic compounds.

DOC is also commonly measured to assess the performance of water treatment processes and to prevent the abstraction of water high in organic carbon, which may interfere with or inhibit the treatment process. For example, the influence of DOC on the efficiency of a granular activated carbon (GAC) unit to remove smaller organic molecules, which may prove to be a health hazard. Essentially, the lower the influent DOC content, typically 2 - 6 mg l^{-1}, to a GAC unit the more efficient the treatment process will be [159]; suspended organic material is usually removed by simple coagulation and flocculation processes. It is desirable to achieve a reduction in the organic content of water before distribution to the consumer, thus reducing the concentration of organic micropollutants and taste and odour problems. In addition this reduction will prevent the formation of potentially hazardous by-products from the treatment process, for example during chlorine disinfection [66,164].

The measurement of DOC should provide the most useful information for the evaluation of treatment process efficiency and the amount of additional treatment required [165]. In addition, DOC can be measured with more precision at lower concentrations than TOC [166]. It is also more useful in predicting trends that may not be apparent, due to the presence of particulate carbon and therefore sample inhomogeneity, for example while a river is in spate. DOC is therefore regarded as being more indicative of water quality changes than TOC over a long period of time [166]. No quantitative guidelines have been established for the acceptable concentration range of DOC in drinking water, but the cause of rising levels of TOC above the normal concentration must be investigated [12].

6.1.2. The Determination of Dissolved Organic Carbon

Considerable effort has been directed towards the determination of DOC in both fresh and seawaters. All the analytical procedures rely upon the oxidation of the dissolved organic fraction to carbon dioxide and its subsequent quantification, either directly or indirectly. Early methods for the determination of organic matter in biological matrices centred on wet chemical oxidation techniques, and usually employed potassium persulphate as the oxidising agent [167,168]. Elevated temperatures were often used to promote and accelerate this oxidation process, for example the determination of organic carbon in fermented liquors [169] and biological material [170]. Menzel and Vaccaro [171] used this oxidation procedure in a manual batch method for the rapid determination of DOC in seawater, the carbon dioxide produced being measured directly with an infra-red (IR) analyser. Baldwin and McAtee [172] used a silver catalyst for the simplified room-temperature persulphate oxidation and determination of DOC in water, where they observed higher oxidation efficiencies for some samples. This method was modified by Strickland and Parsons [173] and was used as a standard method for the determination of DOC in sea-water. Alternative oxidation procedures have been suggested, including: The use of potassium peroxide as an alternative chemical oxidant [174]; a high temperature air oxidation procedure [175]. More recently a hydrogenolysis process [176] has been proposed for the determination of DOC.

Major advances were made by Ehrhardt [177] who developed an automatic analytical procedure for DOC in sea-water based on a Technicon AutoAnalyser. This method used an UV irradiation procedure for the oxidation of organic material with persulphate as the oxygen source, the carbon dioxide being determined conductometrically. The use of automatic analysers for DOC measurements has proliferated during the past twenty years, with a variety of modifications suggested to enhance oxidation efficiency and the general performance of the method. The most common detection system employed in these automatic methods being non-dispersive IR for the direct measurement of

the liberated carbon dioxide [159,178-180]. An indirect detection method has also been successfully applied; the carbon dioxide produced diffuses across a gas diffusion membrane into a buffered pH indicator stream, and the resulting colour change is measured [181-183]. Alternative detection procedures for these automatic methods include the conversion of carbon dioxide to methane prior to FID detection [184]. These methods have been compared to determine the best possible system configuration for the efficient, rapid and accurate determination of DOC [164,185]. However, recent developments in the high temperature catalytic determination of DOC in seawater [186] has made the effectiveness of traditional procedures to oxidise all the DOC present questionable. Recommended water industry instrumental methods for the determination of TOC, total oxygen demand (TOD) and other related determinands, include most of these oxidation procedures and detector systems [158].

Because of the presence of inorganic carbon in natural waters, typically 0.1 - 0.4 mg l^{-1} for river water [71], it is necessary to remove this fraction of the total dissolved carbon prior to the determination of DOC. This has usually been achieved by means of an acidification step, which liberates gaseous carbon dioxide, followed by a nitrogen purging step to remove any dissolved carbon dioxide from the solution. This acidification process was also used for the AutoAnalyser determination of carbon dioxide in plasma [187] and inorganic carbon in freshwater [188,189]. In these AutoAnalyser methods the carbon dioxide liberated was diffused through a microporous membrane into a buffered indicator stream, either cresol red, phenolphthalein or thymol blue. Baadenhuijsen and Seuren-Jacobs [190] developed an automated FI method for total carbon dioxide in plasma, this used a similar gas diffusion and cresol red indicator detection system to that of Kenny and Cheng [187]. A cresol red indicator system was also used in the method proposed by Motomizu et al. [191], who used a tubular microporous membrane as opposed to a PTFE sheet membrane.

Simple FI Determination of Dissolved Organic Carbon

The principal aim in the development of a robust method for DOC in natural waters is to maintain the simplicity and speed of the FI method and the automated monitor. A traditional wet chemical oxidation procedure for the organic carbon fraction and a simple acidification process for the inorganic carbon fraction were selected. The wet chemical process selected was that of Goulden and Brooksbank [159], who utilised a silver catalysed persulphate procedure with possible enhancement of the oxidation process by the use of a low power UV source. The simple indirect method of Kenny and Cheng [187] and Motomizu et al. [191] was selected for the determination of the liberated carbon dioxide, whereby the diffusion of carbon dioxide through a microporous membrane into a weakly buffered alkaline cresol red indicator stream causes a colour change, which can be measured using a solid-state detector. Cresol red was selected because of the proximity of the absorption maximum of the alkaline form (570 nm) to the wavelength of maximum intensity of a green LED (565 nm). Alternative indicators, with suitable pK values, including phenolphthalein, thymolphthalein, thymol blue and α-naptholphthalein, have alkaline forms with absorption maxima insufficiently close to the intense wavelengths of the available LEDs. The carbon dioxide was quantified on the basis of the decreasing colour intensity of the alkaline form of the indicator. Fig. 6.1 illustrates the change in absorbance at 570 nm of the alkaline form of cresol red with changing pH.

The range of interest for DOC was set at 1-10 mg l^{-1}, the concentration range generally expected in river water. The development procedure for the method was simplified by separation into two parts: (1) Development and optimisation of the FI method for the determination of carbon dioxide, and (2) Optimisation of a FI procedure for the quantitative and efficient oxidation of organically derived dissolved carbon. The aim of this work was to develop an FI system for the sequential determination of dissolved inorganic and organic carbon, without separation of the fractions prior to analysis.

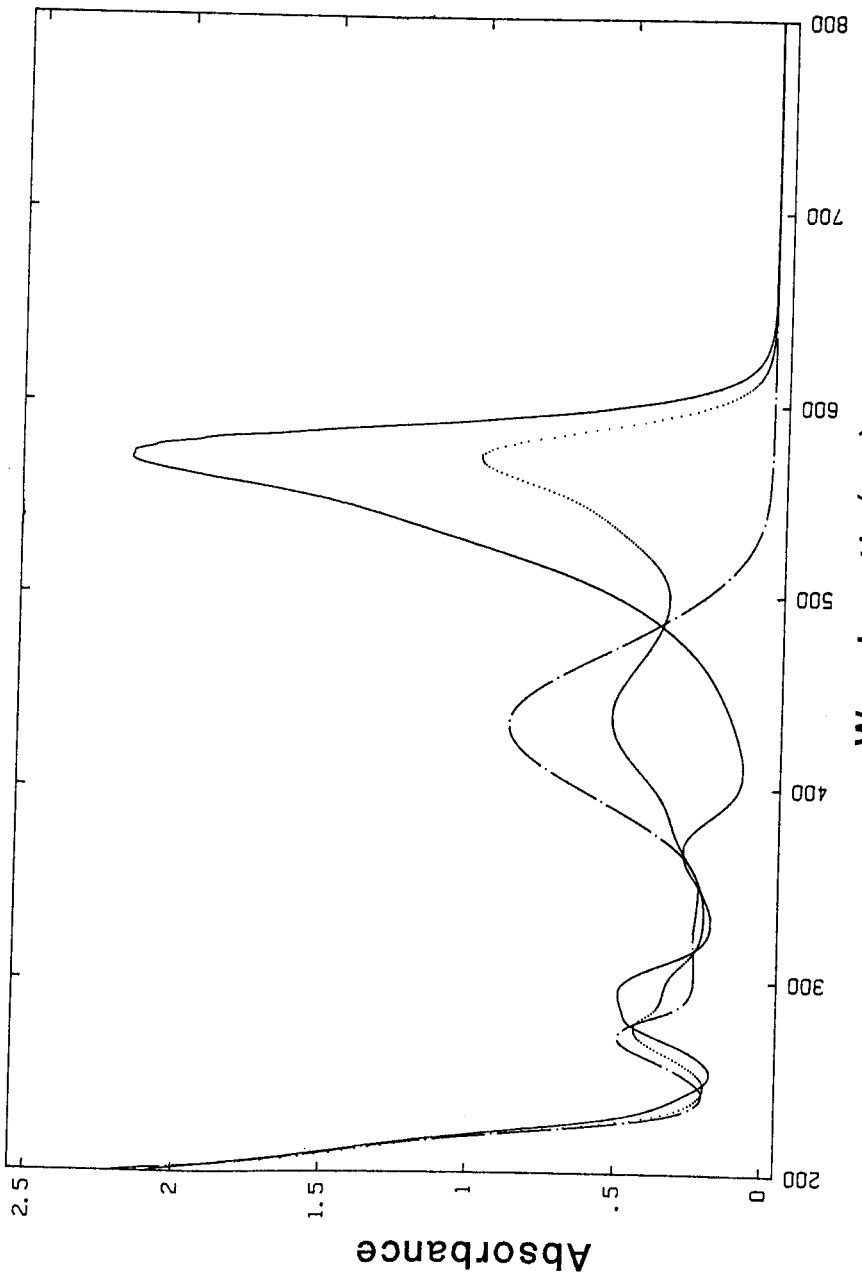

Fig. 6.1 Cresol Red Absorbance Spectra at Varying pH.

Key: —·—·— pH 3.2
..... pH 7.6
——— pH 8.6

6.2. EXPERIMENTAL

6.2.1. Reagents

All solutions were prepared in Milli-Ro or Milli-Q water, in glassware. All reagents were of GPR (or equivalent) grade unless otherwise stated. The four reagent streams were as follows: R1, a mixture of cresol red (BDH) (CR), sodium hydrogen carbonate (AnalaR, BDH) ($NaHCO_3$) and 0.03% (w/v) Brij 35 (Sigma), adjusted to the required pH with 0.1 M hydrochloric acid (AnalaR, BDH); R2, dilute sulphuric acid (BDH); R3, potassium persulphate (Aldrich); R4, silver nitrate (Johnson Matthey and Hogg Laboratory Supplies). Reagent concentrations are given in the Results and Discussion Section. Inorganic carbon stock solutions, 1000 mg C l^{-1}, were prepared from sodium hydrogen carbonate ($NaHCO_3$), sodium carbonate (Na_2CO_3) and potassium hydrogen carbonate ($KHCO_3$) (AnalaR, BDH), all dried overnight at 105 °C. The organic carbon stock solutions, 1000 mg C l^{-1}, were prepared from AnalaR (BDH) (or equivalent) grade reagents unless otherwise stated. Working standards were prepared by dilution of these stock solutions immediately prior to analysis.

Simple organics:

S1 Sucrose

S2 Glucose (Fisons)

S3 Succinic acid

S4 Ethylenediaminetetra-acetic acid (EDTA)

S5 Potassium hydrogen phthalate

Carboxylic acids:

S6 Methanoic (> 90%)

S7 Ethanoic

S8 Propanoic

S9 Butanoic (Fluka)

S10 Pentanoic

Phenols:

S11 Phenol

S12 4-Nitrophenol

S13 2,4-Dichlorophenol

6.2.2. Instrumentation

A manual system was used for the development, optimisation and calibration of the FI manifolds. The indicator colour changes were measured with a solid-state detector incorporating green LEDs. The construction details and specifications of the manual system and the detector were given in Chapter 2. The reaction coil(s) were heated where necessary by means of a thermostatically controlled water bath (Grant Instruments Ltd., Cambridge).

The in-line gas diffusion cells were machined (in-house) from two solid Perspex blocks, each with a channel 240 mm long, 1.5 mm wide and 0.4 mm deep (total surface area $\approx$ 360 mm^2). These two channels, with a volume of $\approx$ 145 μl each, were separated by a gas diffusion membrane such that donor and acceptor solutions flowed parallel to each other. An illustration of one of these gas diffusion cells is given in Fig. 6.2. Unless otherwise stated PTFE thread seal tape (572-238, RS Components Ltd., Corby) was used in the gas diffusion cell as the membrane.

A low power UV source (Thorn EMI FLJ 1008, 300 mm, 8 W, mercury vapour discharge tube) in an EPROM eraser unit (Watford Electronics Ltd.) was used to investigate the enhancement of the oxidation process by UV irradiation, the sample passing through a 100 cm coil of PTFE tubing (0.8 mm i.d.) wrapped directly around the UV tube.

6.2.3. Procedures

Univariate and simplex optimisation procedures were used to maximise the response associated with carbon dioxide passage through the membrane and the oxidation of the organic carbon compounds.

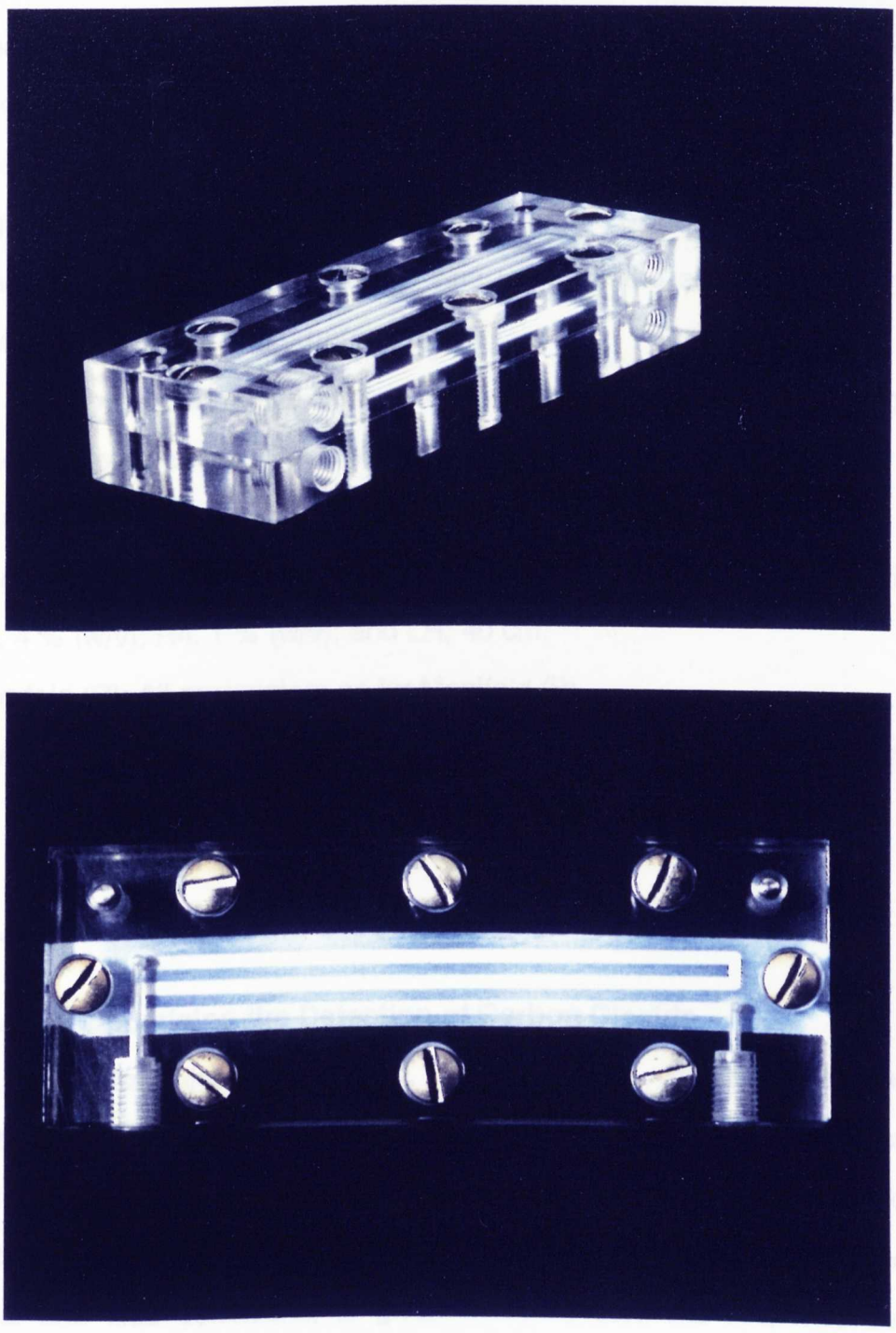

Fig. 6.2 Gas Diffusion Cell.

All experiments were based around one of four FI manifolds, three of these are schematically illustrated in Figs. 6.3(a)-(c). Manifold (A) was used for the determination of dissolved inorganic carbon, the optimisation of carbon dioxide measurement and for a study of different membranes; (B) and (C) were used to investigate the potential FI determination of dissolved organic carbon. Manifold (C) was also used to study the efficiency of the oxidation process for a range of organic compounds, and the enhancement of the oxidation process by UV sample irradiation. Manifold (D), Fig. 6.4, was used for the sequential determination of dissolved inorganic and organic carbon.

The experimental parameters for the manifolds were as follows, unless otherwise stated in the Results and Discussion section.

Manifold (A): R1, composition and flow rate variable; R2, 0.18 M.

Manifold (B): R1, conditions as established by optimisation procedure; R2, 0.54 M; R3, 4 % (w/v); R4, 1 % (w/v); and LR, 40 cm.

Manifold (C): All parameters as for Manifold (B).

Manifold (D): Experimental conditions as established by optimisation procedures.

6.3. RESULTS AND DISCUSSION

6.3.1. Optimising the Detection of Carbon Dioxide

A flow-injection manifold, type (A), with conditions as described by Motomizu et al. [191] was used for the determination of inorganic carbon. The manifold was optimised by a simplex procedure to maximise the response to the carbon dioxide liberated from inorganic carbon. The simplex matrix, including initial and final conditions, is given in Table 6.1. The response variable was defined as the mean response for 5 injections of a 4 mg C l^{-1} standard solution ($NaHCO_3$) into a 0.18 M sulphuric acid stream (R2). The optimisation procedure was terminated after 12 experiments at which point an increase of > 400 % for the response variable had been achieved. Six carbon standard solutions ($NaHCO_3$),

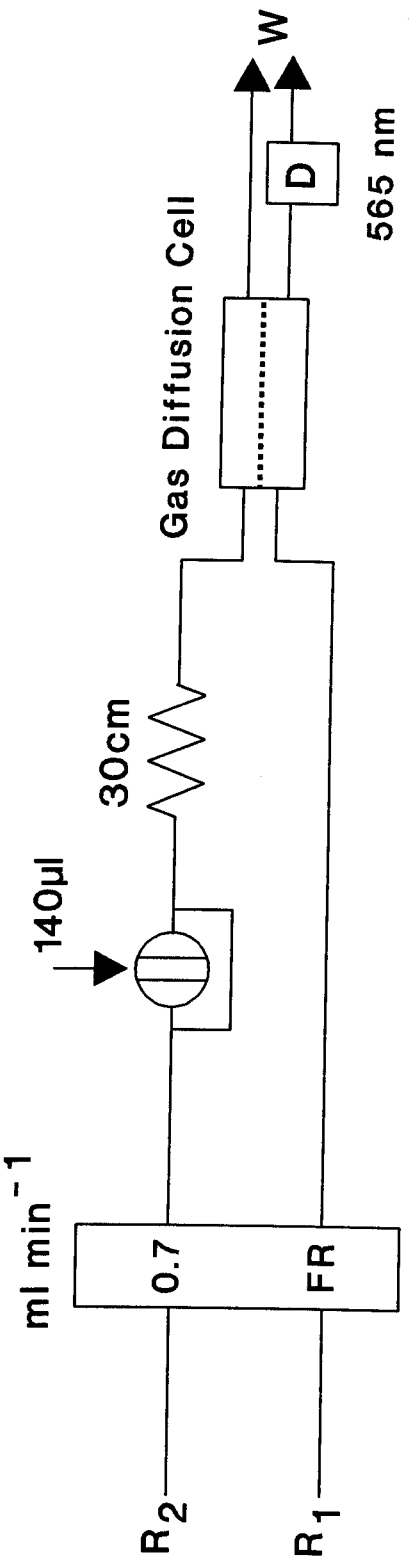

Fig. 6.3(a) FI Manifold for the Determination of Inorganic Carbon.

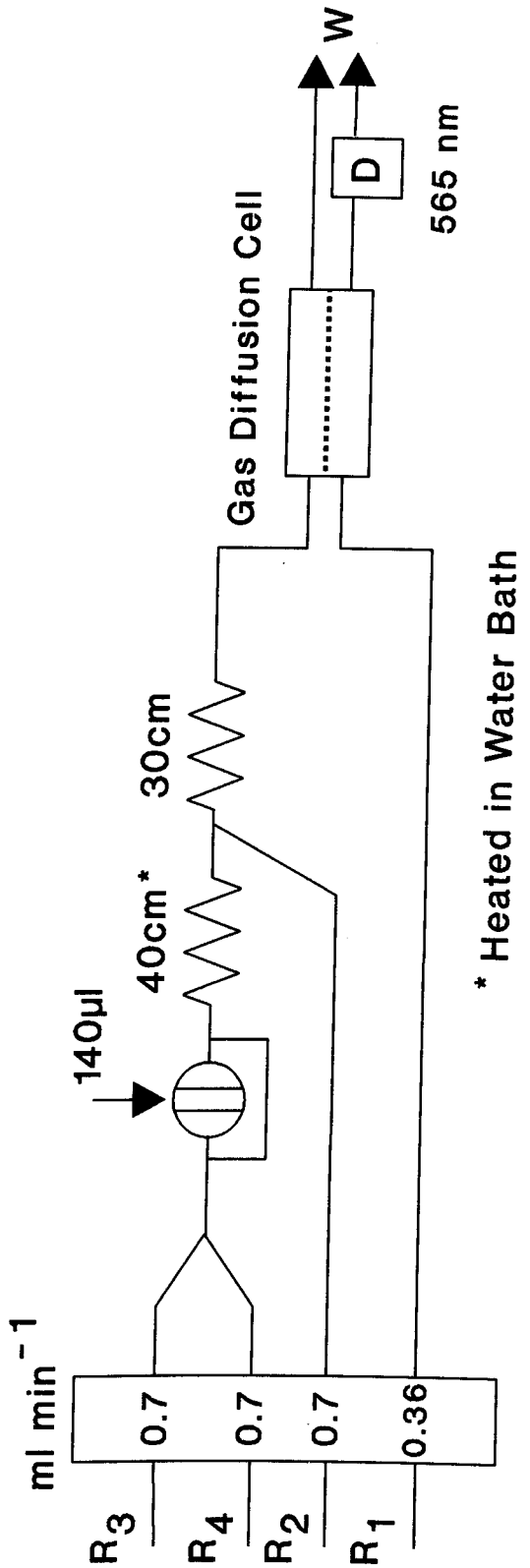

Fig. 6.3(b) FI Manifold for the Determination of Organic Carbon.

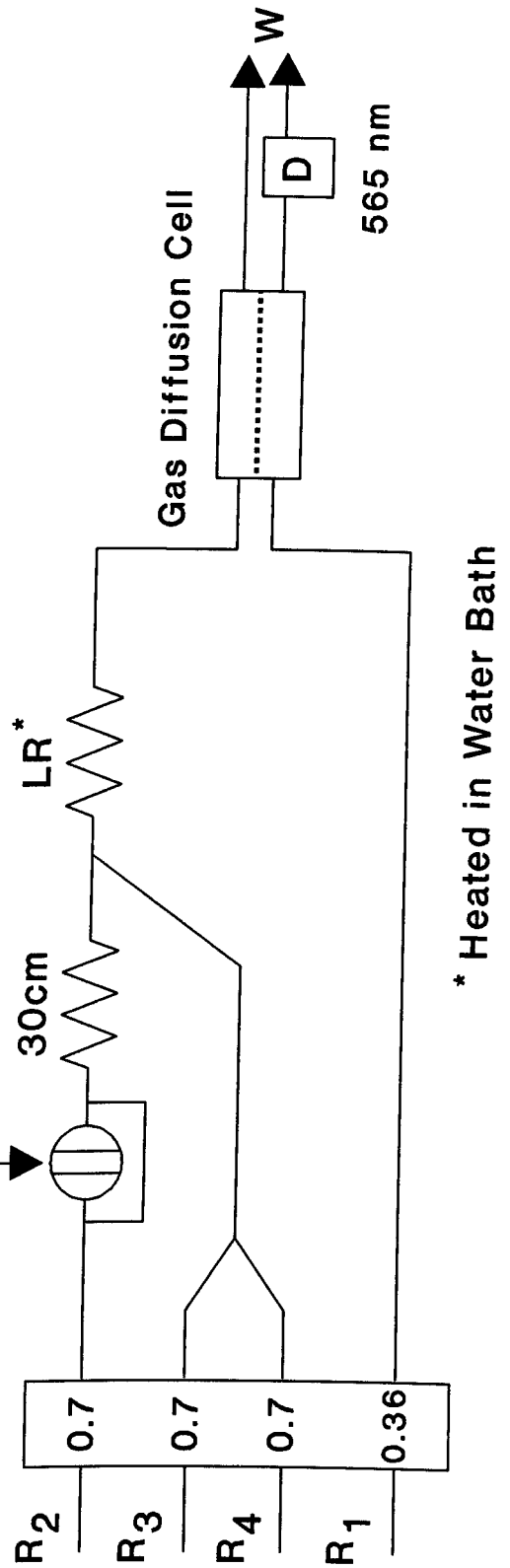

Fig. 6.3(c) FI Manifold for the Determination of Organic Carbon.

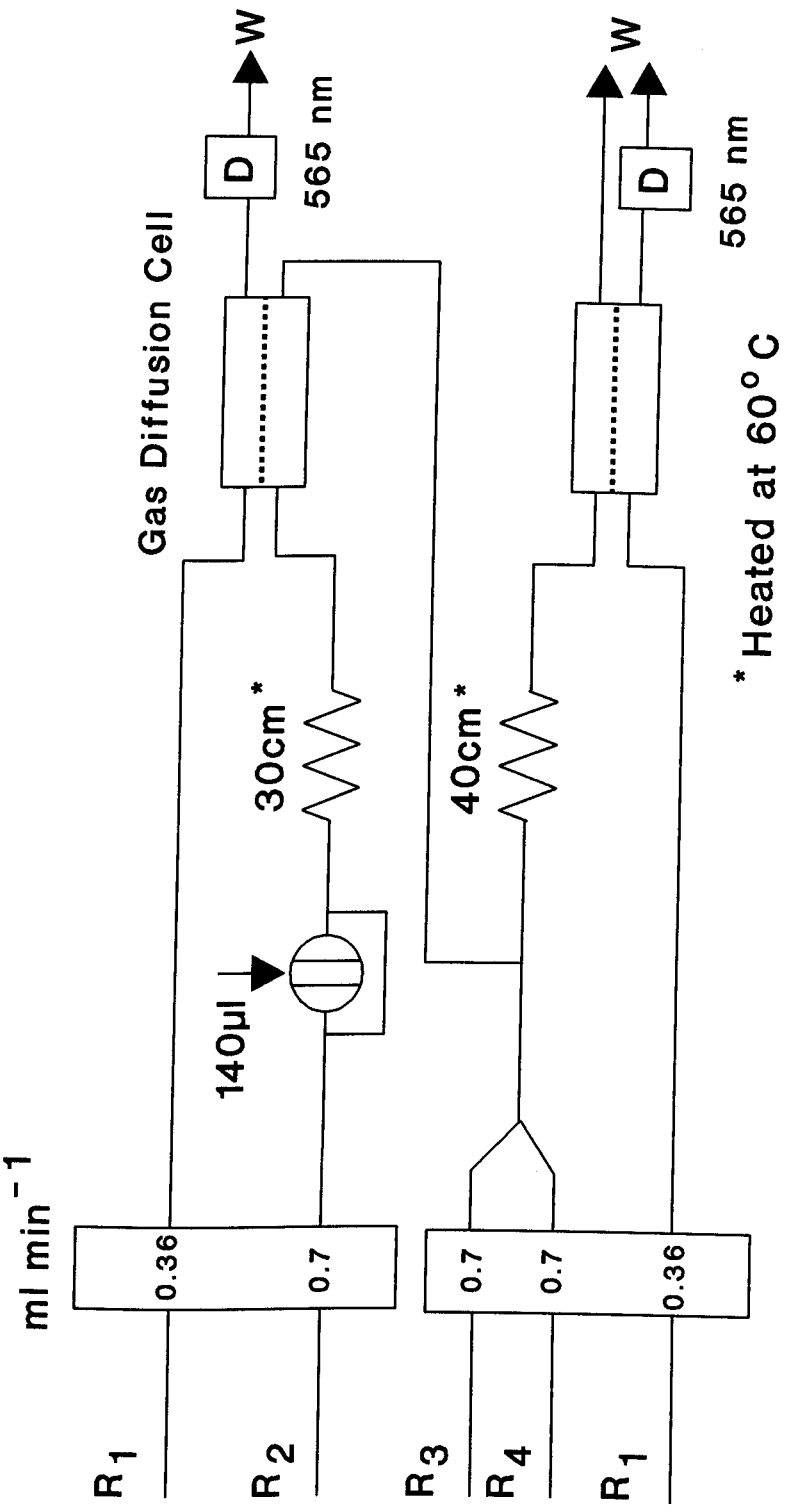

Fig. 6.4 FI Manifold for the Sequential Determination of Inorganic and Organic Carbon.

0 - 10 mg l^{-1}, were analysed using the final manifold conditions; the response was linear (r = 0.9993) across this range and was described by the following regression equation:

$$\text{Signal (mV)} = 10.77\ [C]\ (\text{mg } l^{-1}) + 1.39$$

The theoretical limit of detection, defined as the response for the blank signal + 3 σ, was calculated to be 0.1 mg C l^{-1}, which was an improvement over the unoptimised manifold where the LOD was calculated to be 0.4 mg C l^{-1}. The final conditions for the composition of the buffered colour reagent (R1) were used in all other experiments unless otherwise stated.

TABLE 6.1

Optimisation of Carbon Dioxide Measurement.

Variable	Range	Precision	Conditions	
			Initial	Final
[CR] (M x10^{-5})	5 - 20	1.25	10	7.5
[$NaHCO_3$] (M x10^{-3})	1.6 - 6	0.4	3	1.6
R1 (pH)	8.8 - 10.2	0.1	9	8.8
FR (ml min^{-1})	0.36 - 1.44	0.09	0.72	0.36

A second simplex optimisation procedure, Table 6.2, was used in an attempt to lower the LOD for inorganic carbon. After 12 experiments the simplex was terminated when an improvement of > 160 % had been achieved for the response variable (see definition above). Six carbon standards ($NaHCO_3$) in the range 0 - 10 mg l^{-1} were then analysed using the modified conditions, the response was non-linear across the range. However, the response was linear over the smaller range 0 - 4 mg C l^{-1} (r = 0.9998) and was described by the regression equation:

$$\text{Signal (mV)} = 38.64\ [C]\ (\text{mg } l^{-1}) + 3.98$$

The theoretical limit of detection, blank + 3 σ, was calculated to be 0.05 mg C l^{-1}. These manifold conditions could be used for analyses where greater sensitivity was required rather than a wide linear range. These modified conditions were not used in any of the following experiments.

TABLE 6.2

Reoptimisation of Carbon Dioxide Measurement.

Variable	Range	Precision	Conditions	
			Initial	Final
[CR] (M x10^{-5})	1.25 - 10	1.25	7.5	8.75
[$NaHCO_3$] (M x10^{-4})	8 - 20	2	16	16
R1 (pH)	7.2 - 9	0.1	8.8	7.7
FR (ml min^{-1})	0.27 - 0.54	0.05	0.36	0.32

6.3.2. Membrane Performance

The sensitivity of the detection system was limited partly by the diffusion efficiency of the microporous membrane in the diffusion cell; i.e. the quantity of carbon dioxide that diffuses through the membrane whilst the sample slug is "exposed" to the membrane. In the first of two studies, six different membranes were compared using the same standards and reagents; the latter were prepared according to the previously described optimised manifold conditions. Each of these membranes, Table 6.3, were used in turn in the diffusion cell during the analysis of 5 carbon standards, 0 - 50 mg C l^{-1} ($NaHCO_3$). The mean response for each standard from four injections was recorded, in both ascending and descending order.

TABLE 6.3

Microporous Membranes Tested for Suitability.

Type	Pore Size / (μm)	Porosity (%)	Thickness (mm)	Supplier (Stock No.)
Microporous PTFE	0.45	64	0.225	(FP301315) Goodfellows, Cambridge
	1.0	91	0.075	(FP301220)
	3.0	95	0.025	(FP301150)
	5.0	91	0.025	(FP301040)
Thread Seal Tape (PTFE)	--	--	--	(512-238) RS Components Ltd., Corby
Latex Rubber	--	--	--	London Rubber Company
Gortex	0.45	--	--	W.L. Gore & Associates

The responses are illustrated graphically in Fig. 6.5, from which it can be seen that best overall performance was obtained using the PTFE tape membrane (M1) and the characterised 1 μm pore-diameter membrane (M2). At carbon concentrations < 30 mg l^{-1} M2 was more efficient, whereas at higher carbon concentrations M1 exhibited more efficient diffusion properties. The other membranes did not offer comparable performance and for practical and economic reasons it was decided to use M1 in preference. A major disadvantage of M2 was the thinness of the material which made mounting it, avoiding tears and "ridges", very difficult. M1 was easy to handle and mount without causing obvious visible damage to the PTFE material. Secondly, each characterised membrane, M2, was one hundredfold more expensive than each PTFE tape membrane, M1, at £4.80 and £0.04 respectively.

Reproducibility of PTFE Tape Membranes

During the previous trial of the different membranes, three different PTFE tape membranes (from the same roll of thread seal tape) were mounted in the diffusion cell, and used in the same analytical procedure. The responses obtained with each of these membranes is illustrated illustrated in Fig. 6.6. Although there are differences in the responses recorded for each of the three membranes, the trend over the concentration range is consistent.

Gortex Membrane Trial

In this second trial, a 0.45 μm-pore-diameter Gortex membrane was compared with a PTFE tape membrane. The manifold and conditions remained unchanged from the previous trial except that the acid stream concentration, R2, was increased to 0.54 M. Six inorganic carbon standards (Na_2CO_3), 1 - 50 mg l^{-1}, were analysed and the calibration data recorded given in Table 6.4. The response using the PTFE tape was found to be linear over the range 0 - 8 mg C l^{-1}, and the response using the Gortex was linear over the range 0 - 10 mg C l^{-1}. These responses were described by the following regression equations:

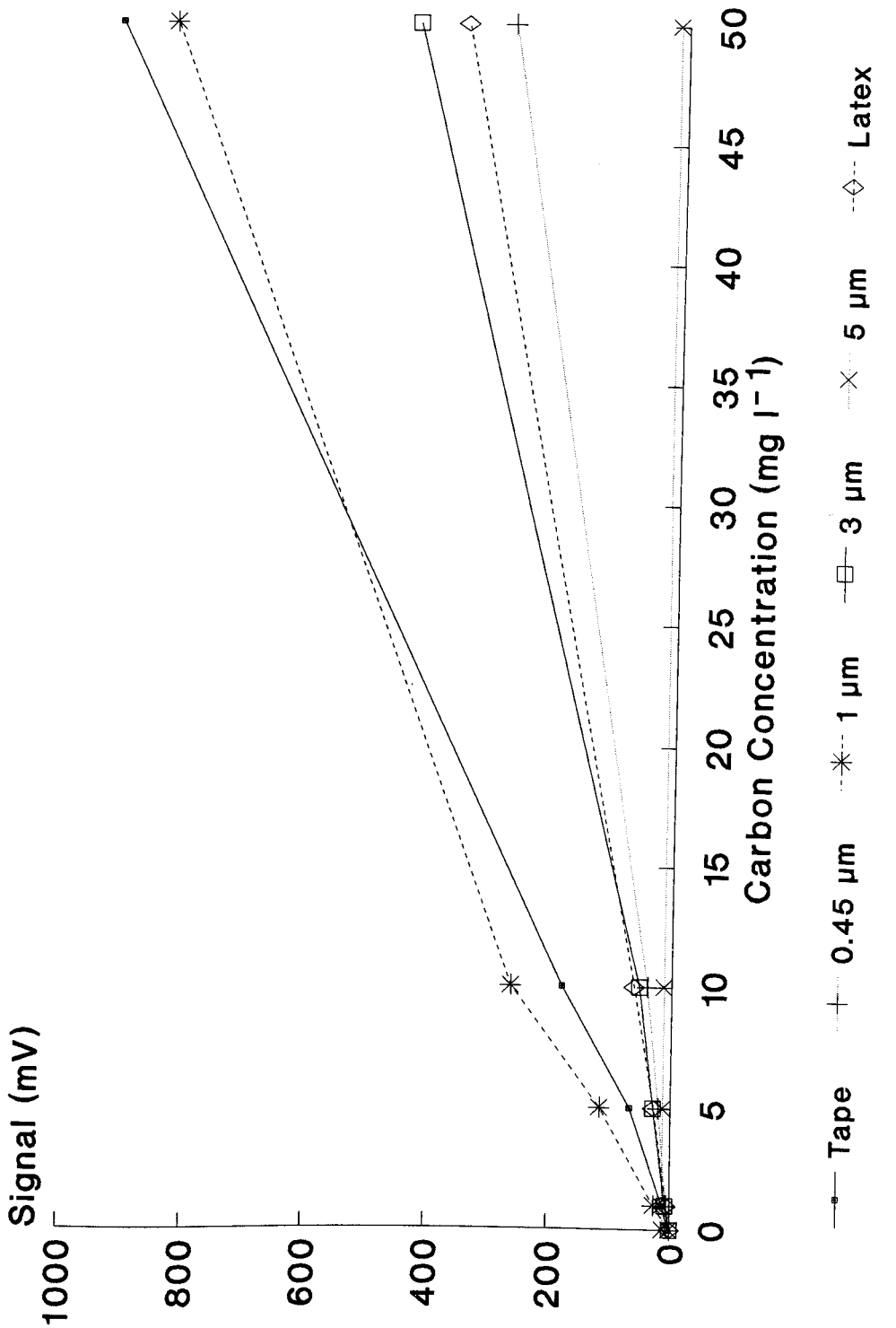

Fig. 6.5 Membrane Performance Trial.

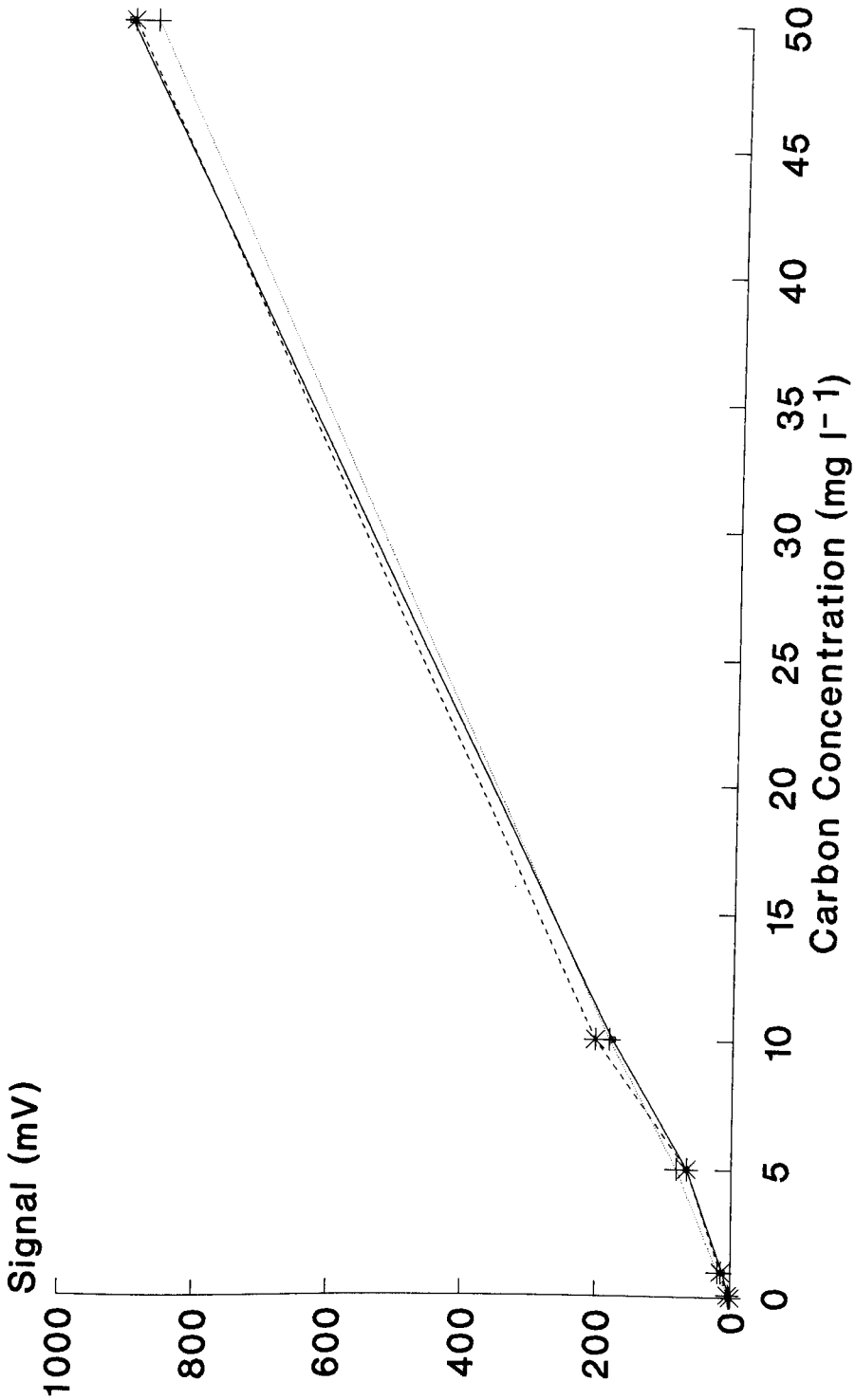

Fig. 6.6 Reproducibility of PTFE Tape.

PTFE Tape: Signal (mV) = 24.49 [C] (mg l^{-1}) - 2.05

($r = 0.9997$, 0 - 8 mg l^{-1})

Gortex: Signal (mV) = 27.81 [C] (mg l^{-1}) + 1.22

($r = 0.9999$, 0 - 10 mg l^{-1})

TABLE 6.4

Comparison of PTFE Tape and Gortex Membranes.

C (mg l^{-1})	PTFE Tape Signal[a] (mV)	PTFE Tape RSD (%)	Gortex Signal[a] (mV)	Gortex RSD (%)
0	0	0	0	0
1	22.9	12.7	31.1	17.8
2	44.3	7.3	57.4	20.3
6	142.9	8.2	165.0	15.8
8	195.9	6.0	224.4	12.0
10	262.7	4.3	280.3	7.9
50	631.6	4.4	465.4	8.4

[a] n = 8

It was concluded from this trial that Gortex offered greater sensitivity, with an increase in the signal of between 7 and 36 % being observed. This would indicate that the Gortex membrane has a greater efficiency for carbon dioxide transfer, and should therefore be used in situations where greater sensitivity at lower carbon levels is required. However, it was decided on economic grounds to continue using the low-cost PTFE tape in all the development investigations, where it was unlikely that this minor increase in sensitivity would be of significance.

A further trial to investigate the potential of improved precision using a Gortex membrane for the determination of organic carbon is described later in this chapter.

Electron microscopic examination of the different membranes did not show any significant structural differences that could account for the performance variations or the varying transport properties. From the comparative trials with the membranes it was not possible to correlate transfer efficiency with pore size, but the degree of crystallinity (or the degree of regular ordering of the atoms within the material) of the PTFE will have a direct bearing on its observable porosity to carbon dioxide; the permeability of the membrane decreasing with increasing crystallinity [192]. A quantitative description of the membrane transport process in a flow-through unit and its dependence on the characteristic membrane properties is given by van der Linden [193].

6.3.3. Determination of Dissolved Organic Carbon Using a Chemical Oxidation Procedure

A FI manifold, type (B), based on the AutoAnalyser method of Goulden and Brooksbank [159] was used to investigate the efficiency of the on-line chemical oxidation process for a series of organic carbon species. The manifold conditions were unchanged from those detailed in the Experimental section. A lower concentration of the silver nitrate solution (R4) than used in the original procedure was adopted because of the high cost of the reagent. The effect of silver nitrate concentration on the oxidation process was included as part of a further investigation.

Temperature Effect on Oxidation Efficiency

The variation in oxidation efficiency with temperature was investigated for two organic compounds over the range 20 - 80 °C. The response for 6 and 10 mg C l^{-1} $NaHCO_3$, succinic acid and potassium hydrogen phthalate standards were recorded while the temperature at which the reaction coil (LR) was held was increased in 10 °C increments. The observed oxidation efficiencies for the organic

compounds with increasing temperature are illustrated graphically in Fig. 6.7. These were calculated by comparison to the response for inorganic carbon assuming 100 % conversion. These calculated values indicate complete conversion of the organic species at moderate temperatures between 60 - 80 °C. At lower temperatures, oxidation of the organic standards at the lower concentration was more efficient, whereas at higher temperatures there was no difference across the concentration range.

With the oxidant and catalyst streams replaced with Milli-Q water no oxidation of the organic species was observed below 60 °C, while at this temperature only limited oxidation of the succinic acid was observed (20 - 45 %).

Temperature Effect on Inorganic Carbon Calibration

A series of inorganic standards, 0 - 10 mg C l^{-1} ($NaHCO_3$), were analysed with unchanged conditions from the previous experiment. The responses remained linear with increasing temperature, Fig. 6.8, with a uniform increase of ≈ 240 % across the concentration range. This experiment shows that with the increasing temperature of the sample, more carbon dioxide permeates through the membrane. This is either due to enhanced transport properties of the membrane at higher temperatures, or the fact that more dissolved carbon dioxide (produced by the acidification step) is liberated from solution and is readily available for transfer across the membrane.

Alternative Inorganic Carbon Standards

It was decided to investigate why the theoretical oxidation efficiencies for the organic compounds were greater than 100 %. It was considered that the inorganic standard used, sodium hydrogen carbonate, was either contaminated with sodium carbonate or that it was not purified sufficiently for use as a primary standard. A two line manifold, type (A), with the optimum conditions for the indicator stream (R1) and a 0.54 M sulphuric acid stream (R2), was used to quantify standards made up from $NaHCO_3$ and $KHCO_3$ by comparison to Na_2CO_3. Five Na_2CO_3 standards, 0 - 10 mg C l^{-1}, were analysed and the

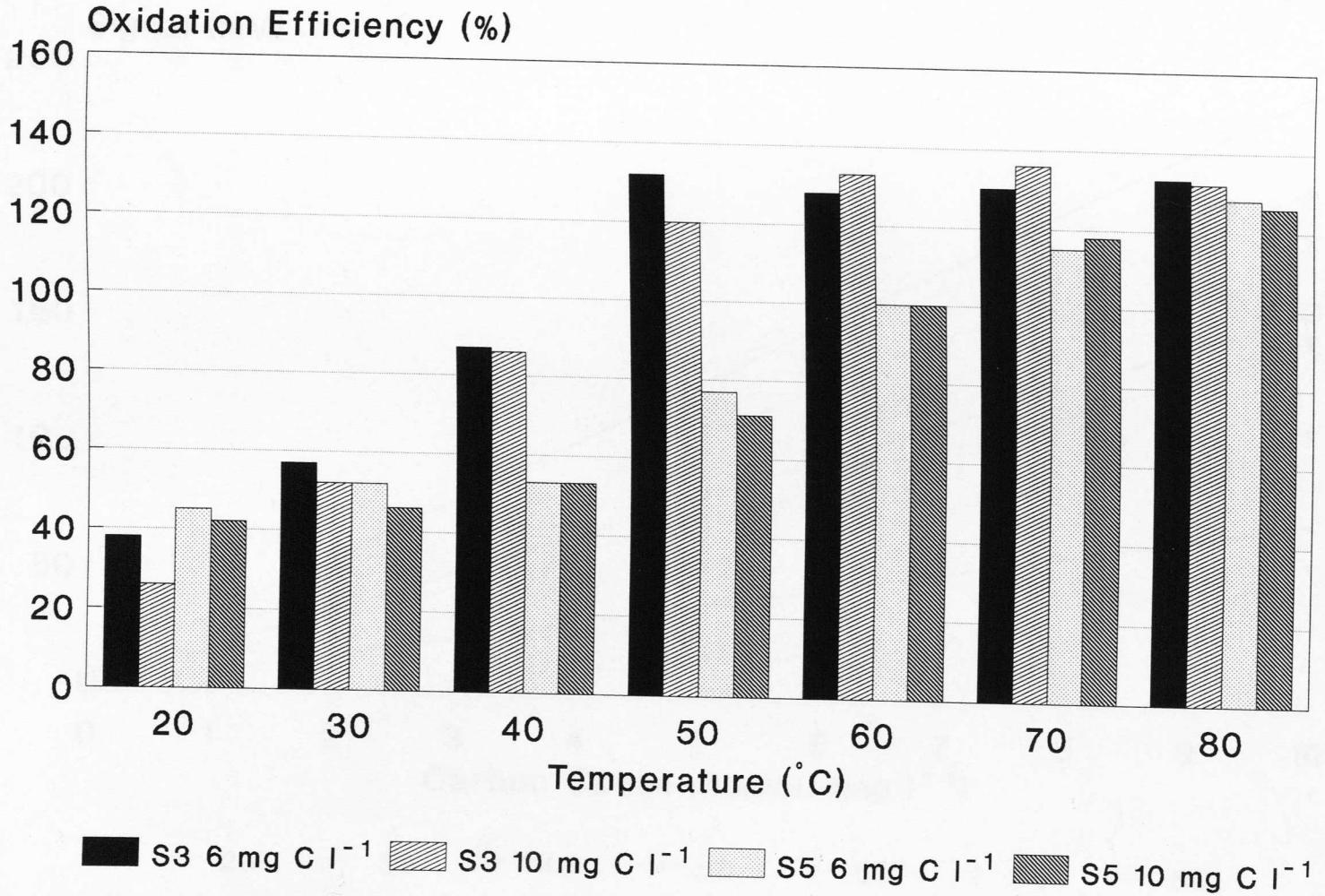

Fig. 6.7 Temperature Effect on Oxidation Efficiency.

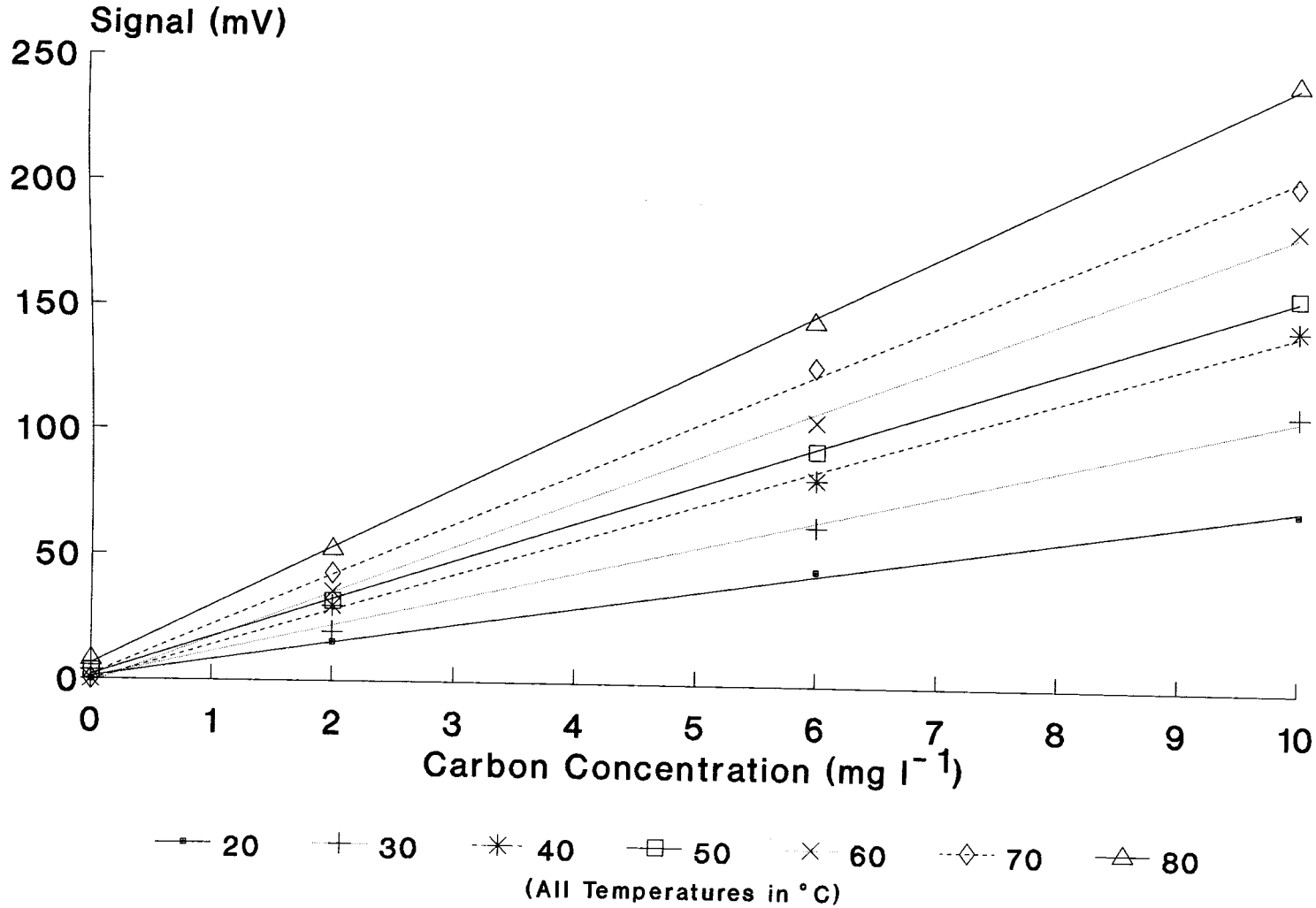

Fig. 6.8 Signal Variation with Temperature (Inorganic C).

response, Table 6.5, was found to be linear (r = 0.9999) across the range and was described by the following regression equation:

$$\text{Signal (mV)} = 17.65\ [C]\ (\text{mg l}^{-1}) + 0.48$$

From this regression equation the actual carbon content of the 5 mg C l^{-1} $NaHCO_3$ and $KHCO_3$ standards were calculated. These were less than 5 mg l^{-1}, at 4.0 and 4.8 mg l^{-1} for the sodium and potassium compounds respectively.

TABLE 6.5

Calibration Data for Alternative Inorganic Carbon Standard: Sodium Carbonate.

C (mg l^{-1})	Signal[a] (mV)	RSD (%)
0	0	0
2	37.3	2.7
4	70.3	2.7
6	105.5	4.4
8	142.1	1.7
10	177.2	1.1

[a] n = 8

Using a manifold, type (B), unchanged from the study of temperature effect and with the reaction coil (LR) heated to 60 °C, the following organic compounds were analysed: S1, sucrose; S2, glucose; S4, EDTA; and S5, potassium biphthalate. The oxidation efficiencies for these compounds were calculated against the responses obtained for two different inorganic carbon standards, 1/ $NaHCO_3$ and 2/ Na_2CO_3. The efficiencies at four different carbon concentrations are illustrated in Fig. 6.9, the apparent efficiencies achieved relative to the Na_2CO_3 standards are lower at every sample concentration. This explained the theoretical oxidation efficiencies of > 100 % calculated by

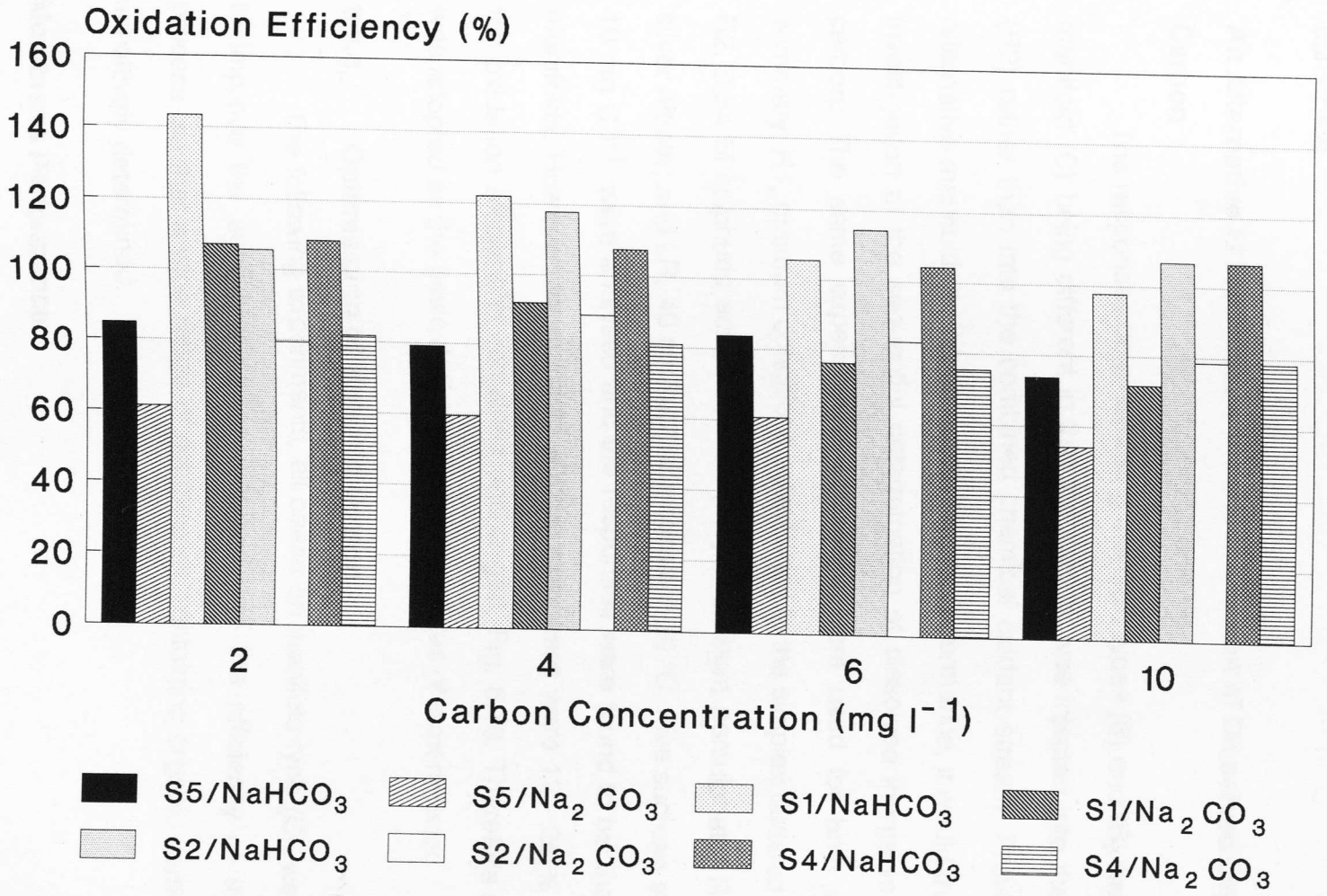

Fig. 6.9 Comparison of Inorganic Carbon Standards.

comparison to $NaHCO_3$ standards. Consequently it was decided that all future experiments would use inorganic carbon standards prepared from sodium carbonate.

An Alternative FI Manifold for the Determination of Dissolved Organic Carbon

The responses obtained using manifold types (B) and (C) were compared, manifold (C) being different in that the sample was injected into the acid stream (R2) rather than into the combined chemical oxidant stream. Provided that this alternative manifold design gave satisfactory performance, it would then permit the investigation of the sequential determination of dissolved inorganic and organic carbon. The same experimental conditions were used for both manifolds, in summary: R1, optimum conditions established in the simplex detailed in Table 6.1; R2, 0.54 M sulphuric acid; R3, 4 % (w/v) potassium persulphate; R4, 1 % (w/v) silver nitrate; and LR, 40 cm kept at a constant 20 °C. Five sucrose standards, 1 - 10 mg C l^{-1}, were analysed and the responses were found to be linear with both manifolds. However, for manifold (C) the responses were 12 - 25 % smaller, but the oxidation efficiencies remained unchanged, Fig. 6.10. Therefore manifold (C) was adopted as the basic design for a further series of experiments.

6.3.4. Optimisation of Manifold Design

The following experiments, all based on manifold type (C), were designed to improve the sensitivity of the manifold and the efficiency of the oxidation process, so that a wide range of compounds containing organic carbon could be sensitively determined.

Membrane Performance

The performance of PTFE tape and Gortex membranes were examined at two temperatures, 25 and 60 °C. Table 6.6 summarises the responses to three sucrose solutions at differing concentrations. This trial confirmed the findings of an earlier investigation, where increased responses were observed using the Gortex

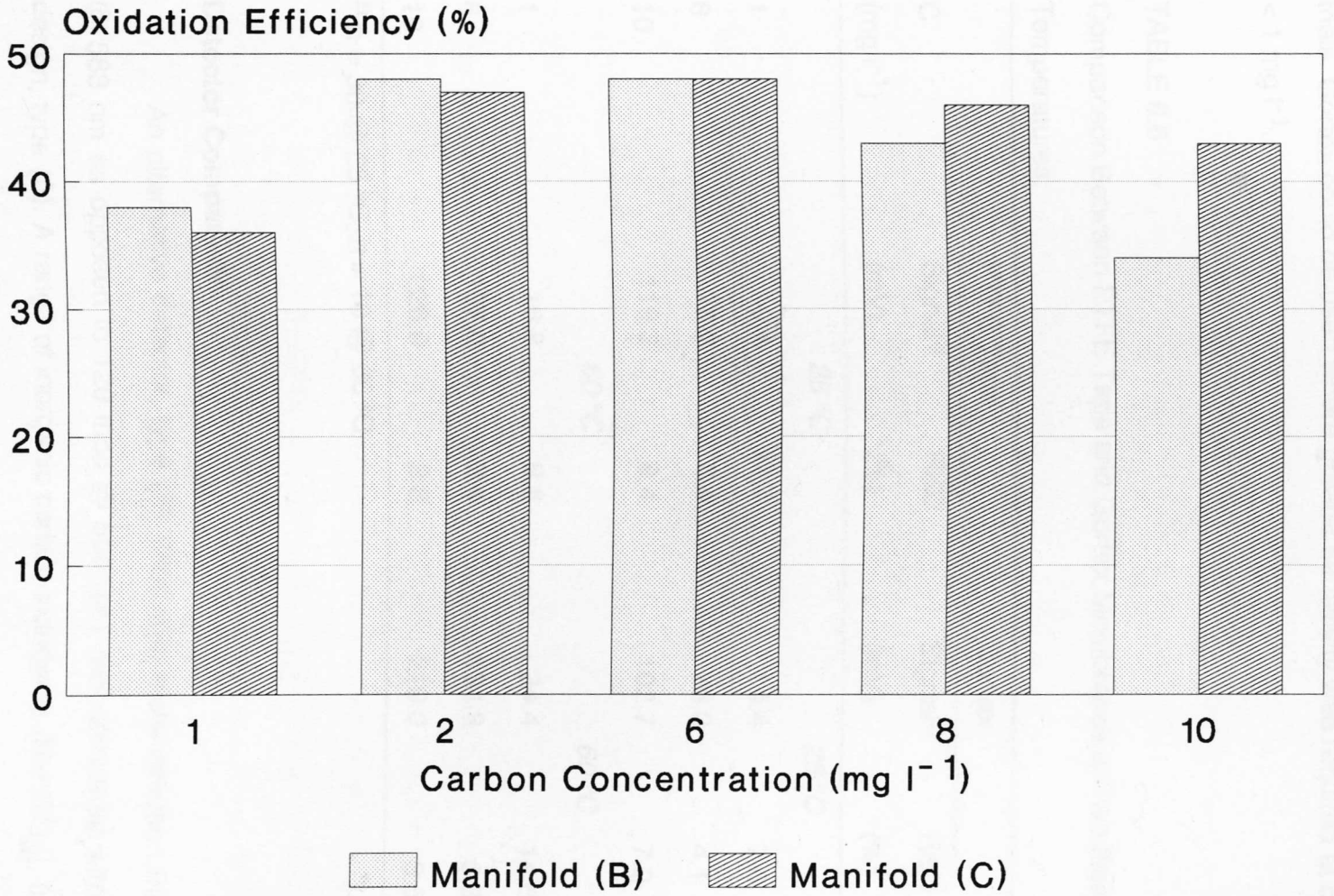

Fig. 6.10 Oxidation Efficiency of Two FI Manifolds.

membrane for carbon standards at the low end of the concentration range. However, the increases were not sufficient to warrant the use of Gortex in further trials. Gortex could be used where greater sensitivity was required at carbon levels < 1 mg l^{-1}.

TABLE 6.6

Comparison Between PTFE Tape and Gortex Membranes at Two Reaction Temperatures.

	PTFE Tape		Gortex	
C (mg l^{-1})	Signal[a] (mV)	RSD (%)	Signal[a] (mV)	RSD (%)
	25 °C		*25 °C*	
1	10.4	11.7	14.4	7.0
6	77.2	8.4	78.0	4.1
10	119.3	9.4	102.7	7.0
	60 °C		*60 °C*	
1	10.8	9.6	24.4	14.5
6	137.0	3.4	134.8	5.3
10	226.0	2.8	219.0	6.6

[a] n = 30 @ 25 °C, n = 10 @ 60 °C

Detector Comparison

An alternative detector, type (B), fitted with more intense LEDs (250 mcd @ 563 nm as opposed to 120 mcd @ 565 nm) was compared with the original design, type (A). A range of inorganic carbon standards ($NaHCO_3$), 0 - 10 mg l^{-1}, were analysed with a fixed temperature of 20 °C for reaction coil, LR, and all other conditions unchanged from the previous experiment. The responses from both detectors were non-linear over the full range, but linear over the smaller range of 0 - 8 mg C l^{-1} and were described by the following regression equations:

Type (A), Signal (mV) = 13.34 [C] (mg l^{-1}) + 0.29 (r = 0.9998)

Type (B), Signal (mV) = 14.59 [C] (mg l^{-1}) - 1.18 (r = 0.9995)

With type (B) a modest (5 - 10 %) increase in the response was achieved and because no reduction in the linear range was observed, it was decided to use this detector for all future investigations.

Reinvestigation of Temperature Effect on Oxidation Efficiency

Figs. 6.11(a) and 6.11(b) illustrate the increasing oxidation efficiency of the chemical oxidation process with temperature. The four organic carbon compounds, at two concentrations 1 and 10 mg C l^{-1}, were analysed using a manifold, type (C), and conditions unchanged from the previous experiment. Complete oxidation was observed for most of these compounds at 60 or 80 °C. The blank value increased with increasing temperature, indicating that some dissolved carbon (either inorganic or organic in nature) was present in the Milli-Q water used to prepare the standard solutions.

Univariate Optimisation of Manifold to Maximise Oxidation Efficiency

Three parameters were individually varied over a defined range while all other conditions were kept constant, and the responses for 10 mg C l^{-1} inorganic (Na_2CO_3) and organic (glucose and EDTA) standards recorded. Manifold (C) was used with the optimum conditions for R1, and the temperature of reaction coil, LR, fixed at 60 °C for each of the three following trials:

1. The concentration of potassium persulphate (R3) and silver nitrate (R4) were fixed at 4 % and 1 % (w/v) respectively, the length of the knitted reaction coil (LR) was varied between 20 and 100 cm.

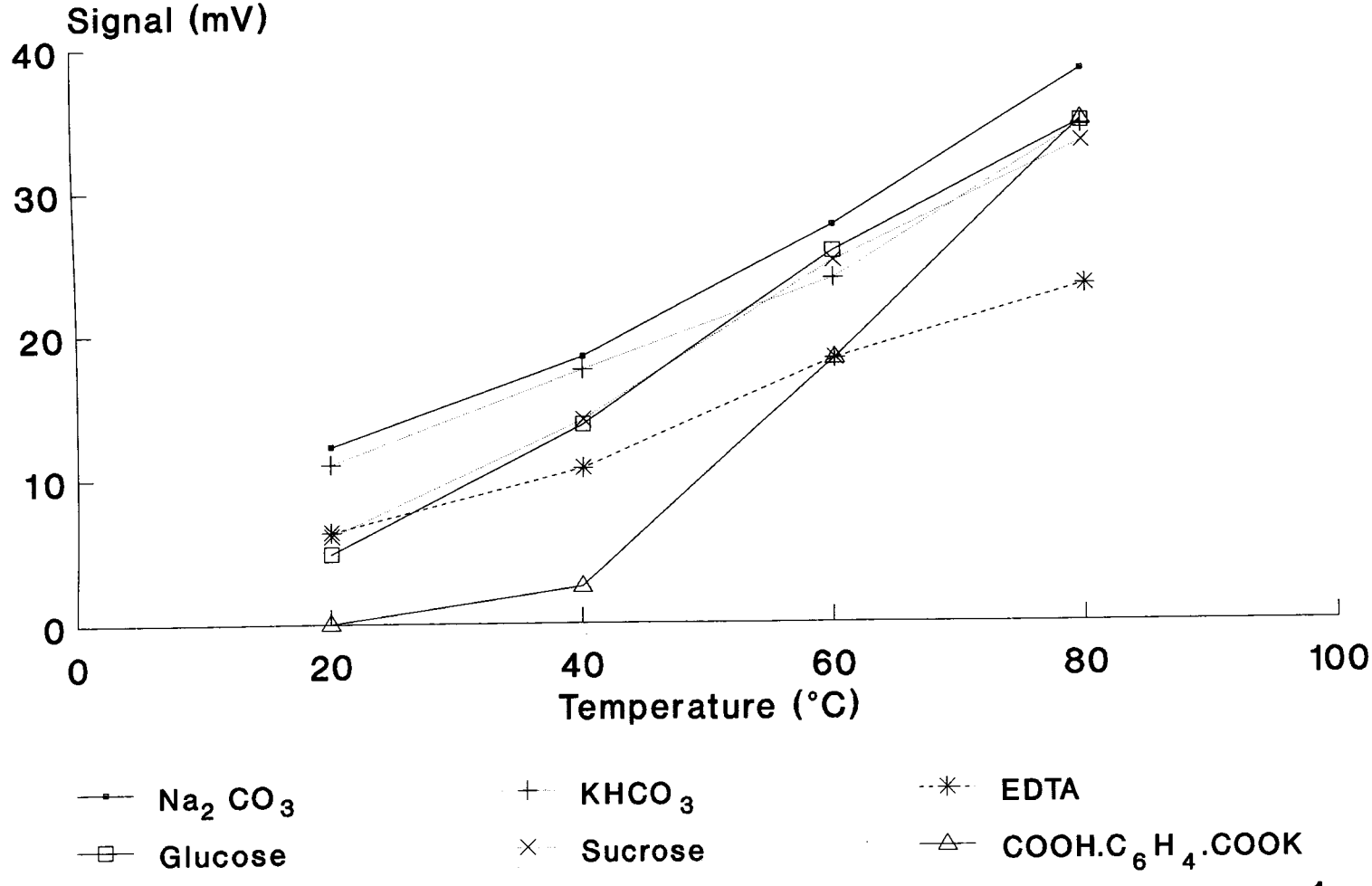

Fig. 6.11(a) Temperature Effect on Oxidation (1 mg C l^{-1}).

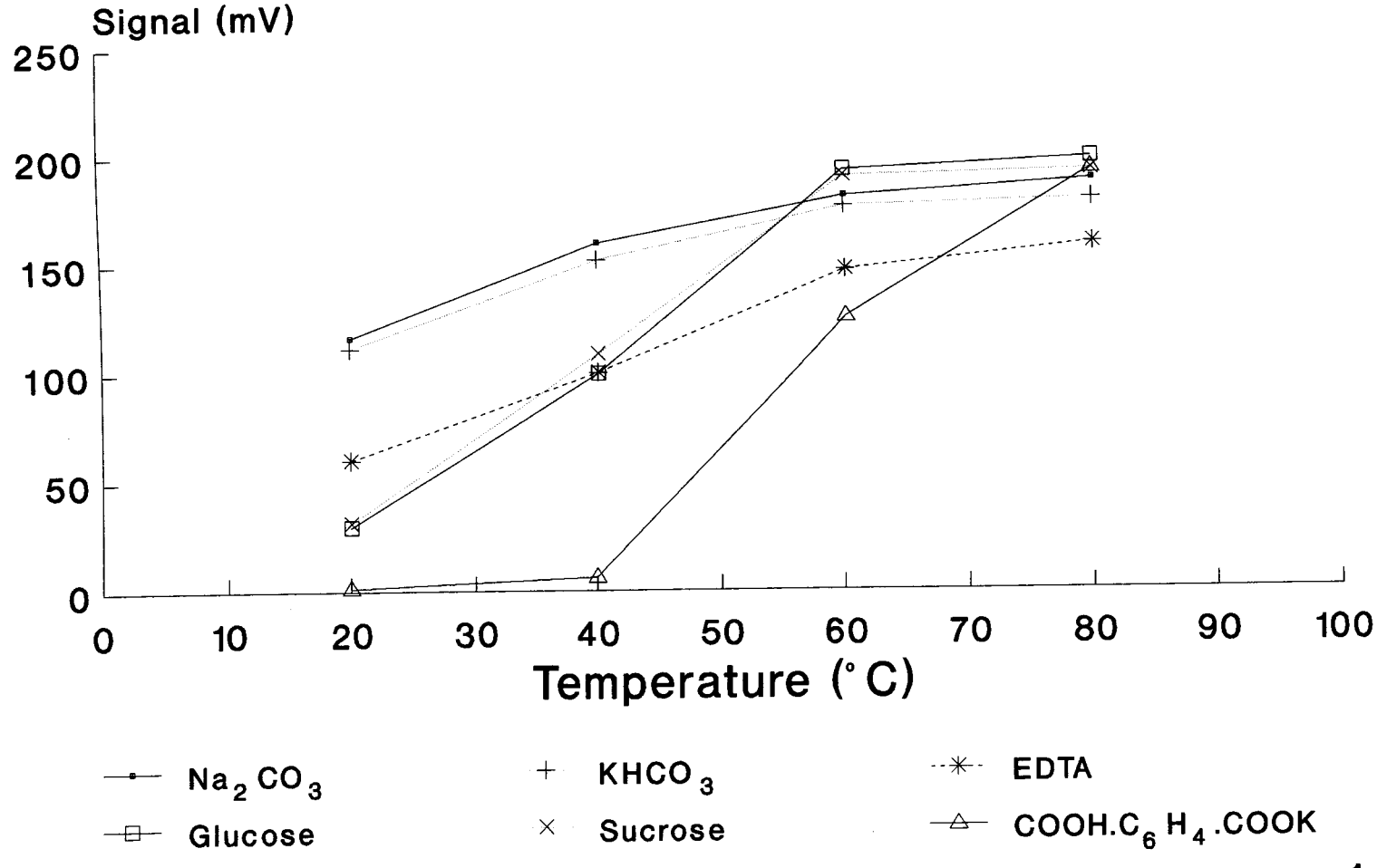

Fig. 6.11(b) Temperature Effect on Oxidation (10 mg C l^{-1}).

2. The silver nitrate concentration was fixed at 1 % (w/v) and the length of LR at 40 cm, the potassium persulphate concentration was varied between 1 and 5 % (w/v).

3. The potassium persulphate concentration was fixed at 4 % (w/v) and the length of LR at 40 cm, the silver nitrate concentration was varied between 0.1 and 1.5 % (w/v).

The effect of varying these parameters is illustrated graphically in Figs. 6.12(a)-(c). The variation in coil length had little effect on either signal size or oxidation efficiency. A length of 40 cm was chosen so as to maintain maximum response at low carbon concentration, whilst maintaining efficient oxidation and also minimising sample dispersion. Increasing the persulphate concentration above 2 % (w/v) made little difference to the oxidation efficiency or response, however a concentration of 4 % (w/v) was chosen to ensure that an excess of the "oxygen source" was available for the oxidation process. Silver nitrate concentration had a significant effect on the size of the response but not oxidation efficiency, a concentration of 0.5 % (w/v) was chosen. At this concentration the response was at a maximum and therefore sensitivity was maintained at low carbon concentrations.

Performance of Optimum FI Manifold

A range of organic compounds (S1 - S13) were analysed with a modified version of Manifold (C), which included an additional 20 cm coil. This coil was placed in the flow system after the merging point of the oxidising agent and catalyst to ensure thorough mixing. The following optimum conditions were used:

Reagent streams: R1, [CR] $\equiv 7.5 \times 10^{-5}$ M, [$NaHCO_3$] $\equiv 1.6 \times 10^{-3}$ M, pH $\equiv$ 8.8; R2, 0.54 M; R3, 4 % (w/v); and R4, 0.5 % (w/v).

Manifold conditions: LR, 40 cm; and HB, 60 °C.

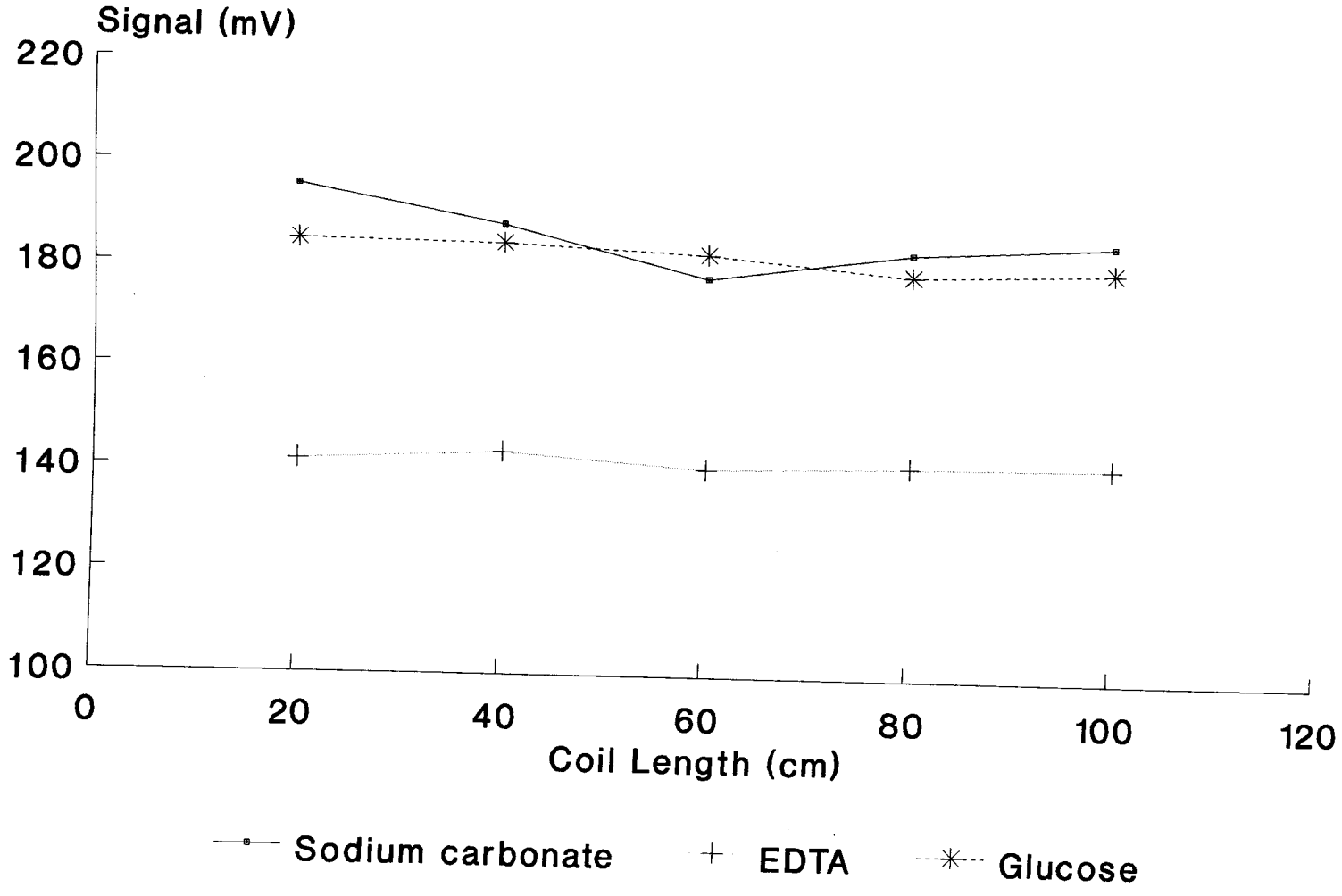

Fig. 6.12(a) Effect of Coil Length on Response.

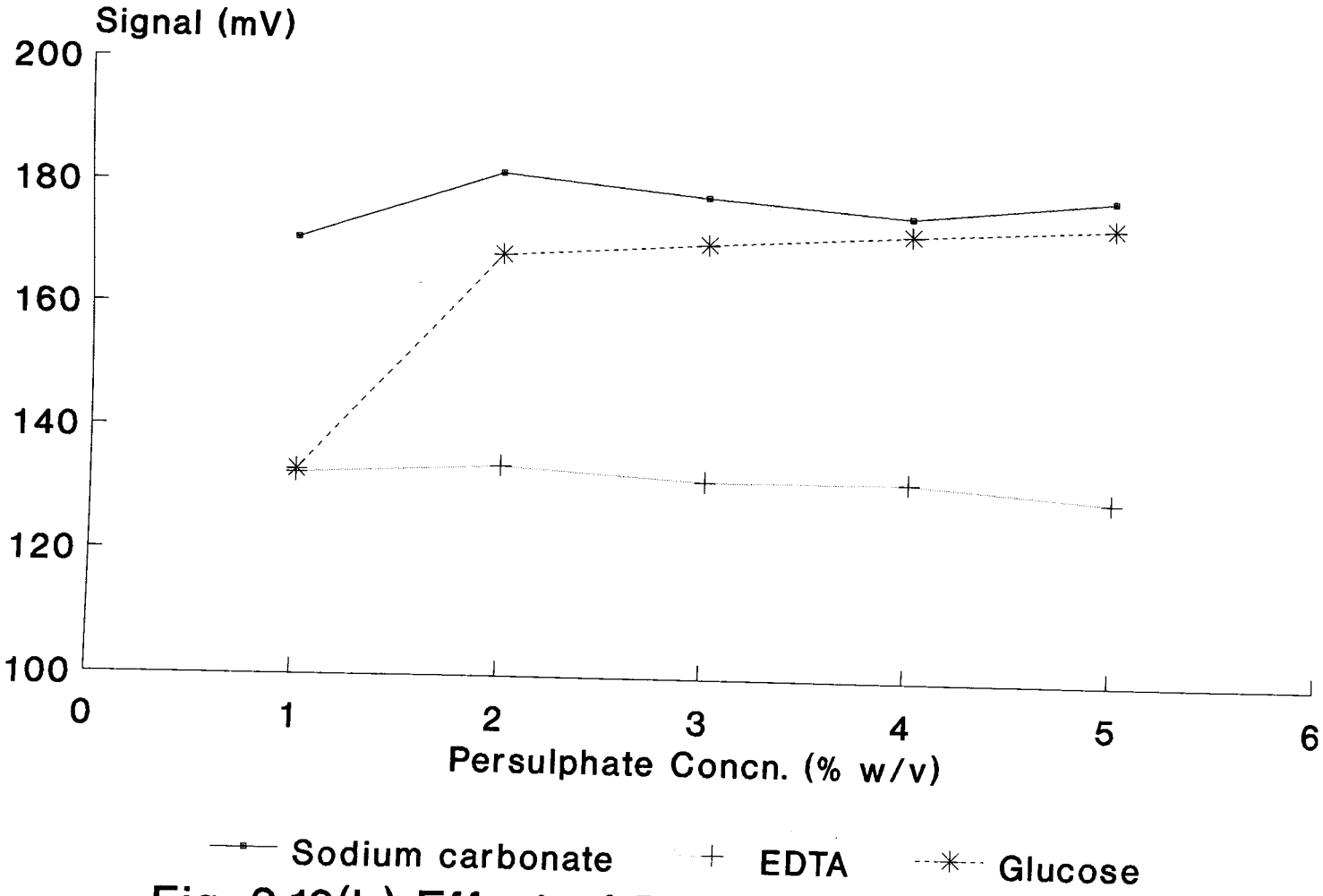

Fig. 6.12(b) Effect of Persulphate Concentration on Response.

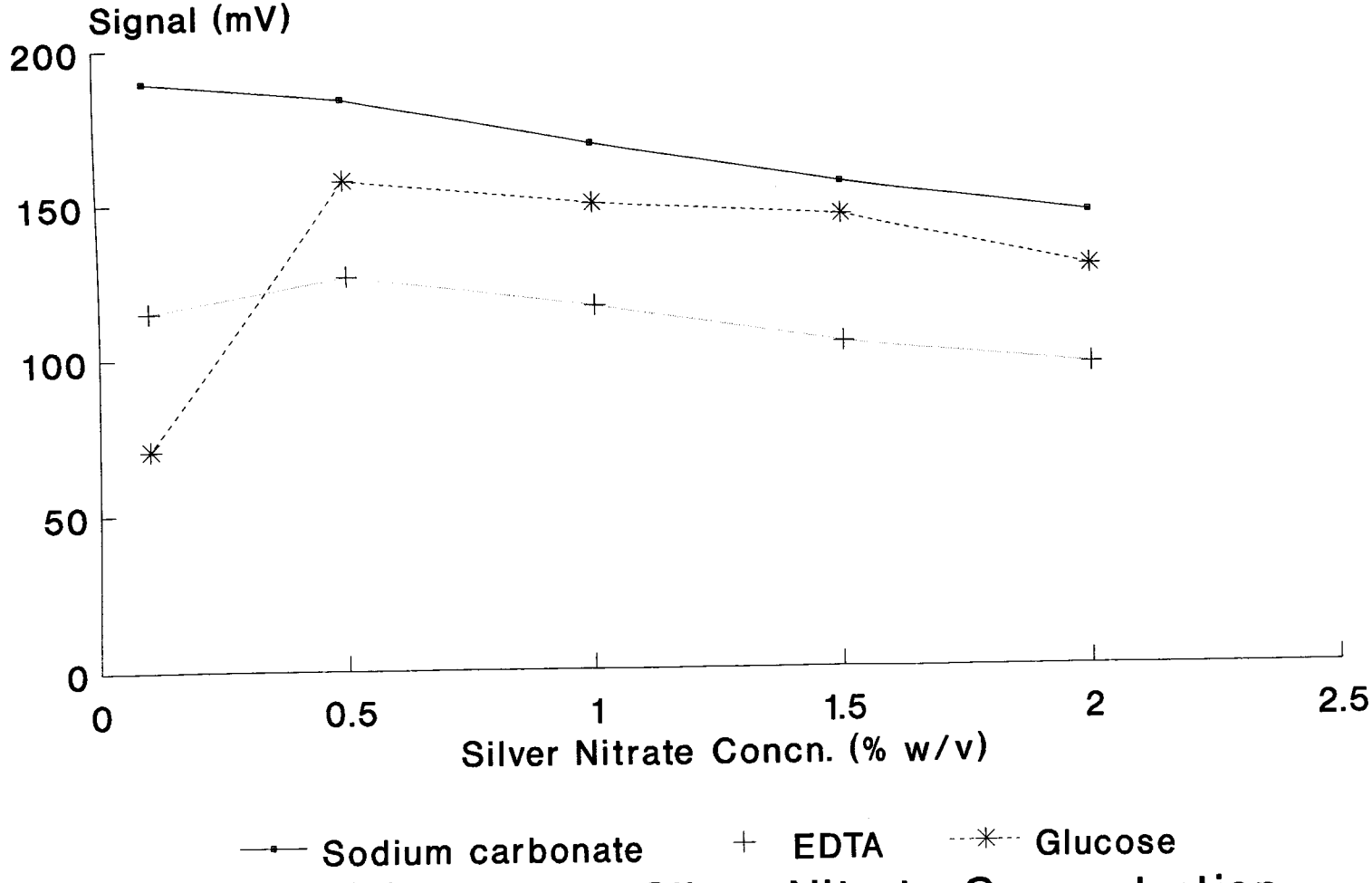

Fig. 6.12(c) Effect of Silver Nitrate Concentration on Response.

The oxidation efficiencies for each of these organic compounds at two concentrations, 2 and 10 mg C l^{-1}, were calculated with respect to the response for inorganic carbon (Na_2CO_3).

Fig. 6.13 represents graphically the efficiency of the oxidation process. This shows that most of the simple organics and all the carboxylic acids are oxidised > 80 %, and that there was little difference in oxidation efficiency at the two concentration levels.

The calculated oxidation efficiency for methanoic acid shows a recovery of significantly > 100 %. The working standard solution was prepared assuming that the stock solution was 90 % pure, and therefore from the calculated recovery it would appear that it was of higher purity.

The oxidation process was less efficient for the phenols, with recoveries of < 64 %. Consequently, it was decided to investigate enhanced oxidation with the inclusion of a UV irradiation step.

6.3.5. Combined Chemical and UV Oxidation of Organic Carbon

An irradiation step was included in the analytical procedure to improve the efficiency of the oxidation process, in particular the oxidation of organic compounds more resistant to chemical attack. The oxidising power of persulphate is enhanced when it is allowed to decompose in the presence of UV irradiation [194], the persulphate generating sulphate free radicals. These, in turn, react with water molecules to produce hydroxyl radicals, which under certain conditions initiate chain reactions leading to the decomposition of organic molecules.

A 100 cm coil, wound directly around the envelope of a very low power UV source (8 W), was inserted into the manifold (type (C)) immediately after the 40 cm heated reaction coil, and prior to the gas diffusion cell. The phenol standards were reanalysed with and without the UV source activated, the results are illustrated graphically in Fig. 6.14. A low power UV source was chosen so as to minimise the heat "build-up" in the monitor housing, and to keep the electrical power requirements to a minimum.

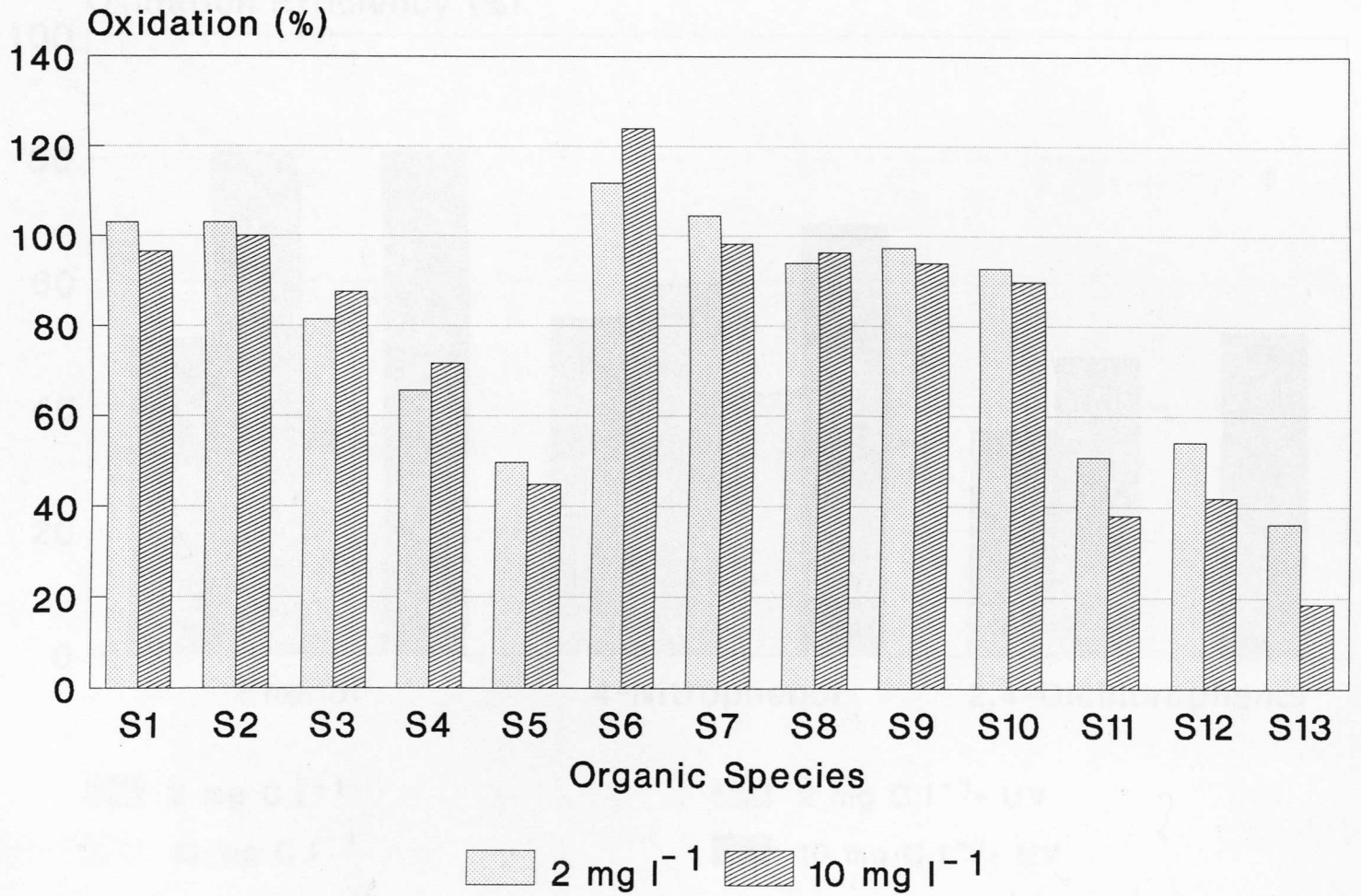

Fig. 6.13 Oxidation of Organic Carbon Species.

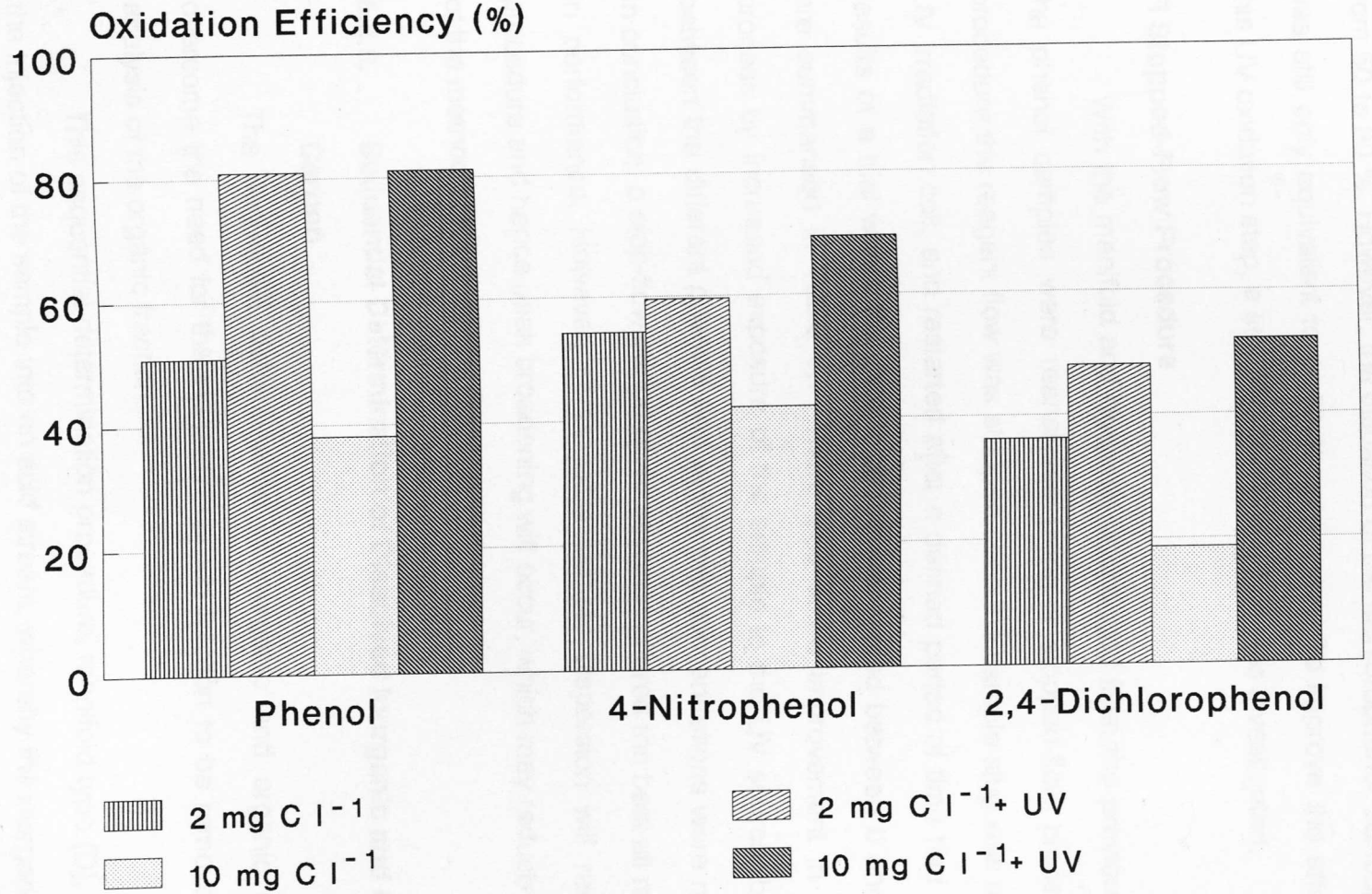

Fig. 6.14 Effect of UV Irradiation on Oxidation Efficiency.

It was clear from these analyses that the inclusion of the UV source had a significant effect on the oxidation process, the recovery of phenol being increased from 50 to 80 %. However, the oxidation of the dichlorophenol, although improved, was still only equivalent to ≈ 50 % conversion. To improve the effectiveness of this UV oxidation step, a stopped-flow procedure was investigated.

FI Stopped-Flow Procedure

With the manifold and reagents unchanged from the previous experiment the phenol samples were reanalysed using a stopped-flow procedure. In this procedure the reagent flow was stopped once the sample slug was resident in the UV irradiation coil, and restarted after a defined period of time had elapsed. The results of a trial where this "stop" period was varied between 0 and 60 seconds are summarised in Table 6.7. There was some improvement in the oxidation process by increased exposure of the sample to the UV source, but the results between the different phenols and at the two concentrations were not consistent. In conclusion, a stop-flow period of 40 seconds offered the best all round increase in performance. However, some extra sample dispersion will result from this procedure and hence peak broadening will occur, which may reduce the sensitivity of the method at lower concentrations.

6.3.6. Sequential Determination of Dissolved Inorganic and Organic Carbon

The sequential determination of inorganic and organic carbon would overcome the need for the inorganic carbon fraction to be removed prior to the analysis of the organic fraction.

This sequential determination procedure, manifold type (D), was based on the injection of the sample into an acid stream, whereby the inorganic fraction was oxidised and the carbon dioxide quantified at Detector (1), (D1). The eluent from this first diffusion cell was then mixed with the chemical oxidants and passed to a second diffusion cell where carbon dioxide from the organic fraction was quantified at Detector (2), (D2).

TABLE 6.7

Oxidation Efficiency of FI Stopped-Flow Procedure.

Sample		Stop-Flow Period (S)			
(mg l^{-1})		0	20	40	60
			Oxidation (%)		
S11:	2	62.2	76.4	80.7	59.4
	10	84.4	121.0	112.6	112.4
S12:	2	77.7	76.4	73.6	61.3
	10	78.9	90.3	95.7	94.1
S13:	2	44.0	56.1	64.3	64.4
	10	62.5	64.4	71.5	69.6

In practice, because the carbon dioxide transfer across the membrane was less than 100 % efficient, carbon dioxide quantified at the second cell was from both the inorganic and organic fractions.

Preliminary Investigation

A FI manifold with dual gas diffusion cells and solid-state detectors, type (A), was used for the analysis of two series of inorganic and organic carbon standards. The optimum conditions for the oxidation of organic carbon were used except that the concentration of R3 was fixed at 2 % (w/v). Fig. 6.15 illustrates the responses observed at D1 and D2. The responses for the organic carbon standards at D2 are smaller than those for comparable inorganic carbon standards at D1. This observation can be explained in terms of the difference in dispersion of the sample slug at the first and second diffusion cells; this dispersion was calculated to be 3.2 and 10.4 at the first and second diffusion cells respectively.

The effect of a 10 mg l^{-1} inorganic carbon spike on the response of a range of organic carbon standards is illustrated in Fig. 6.16; this spike showed an additive effect.

Characterisation of the Dual Detector System

Twenty five mixed inorganic (Na_2CO_3) and organic (glucose) carbon standards were prepared according to the matrix given in Table 6.8. These standards were analysed using the same manifold and conditions as used in the preliminary experiment, except that the concentration of R3 was increased to 4 % (w/v) to ensure complete oxidation of the organic standards. Fig. 6.17 illustrates the recorded responses at D2 for the individual inorganic and organic carbon standards, confirming the dispersion effect observed in the earlier investigation. The simple additive effect of the organic carbon on the organic response is illustrated graphically in Fig. 6.18, where the responses for organic carbon with increasing inorganic carbon spikes, 2.5 - 10.0 mg l^{-1}, are plotted against detector response.

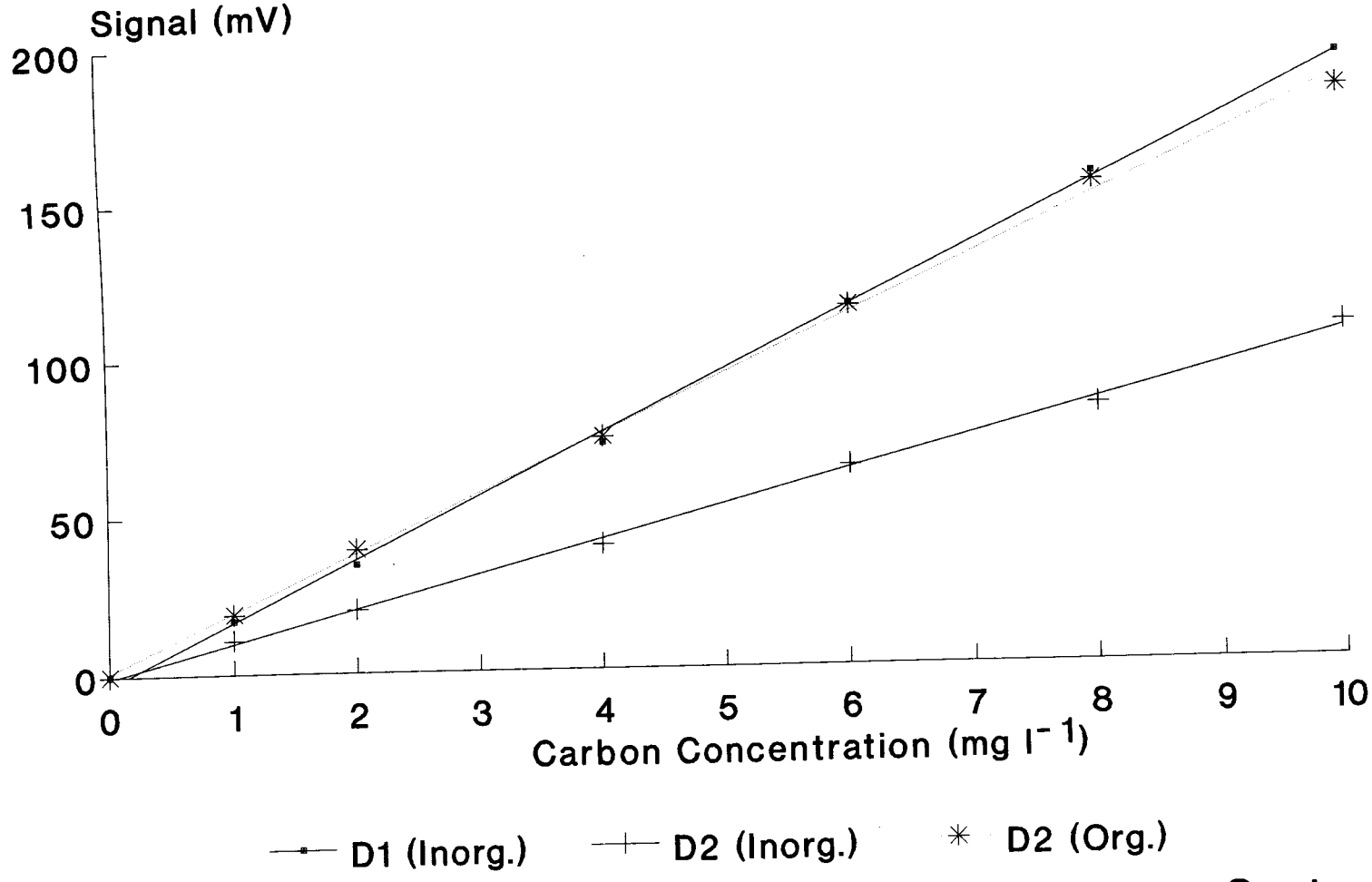

Fig. 6.15 Responses Observed with Dual Detector System.

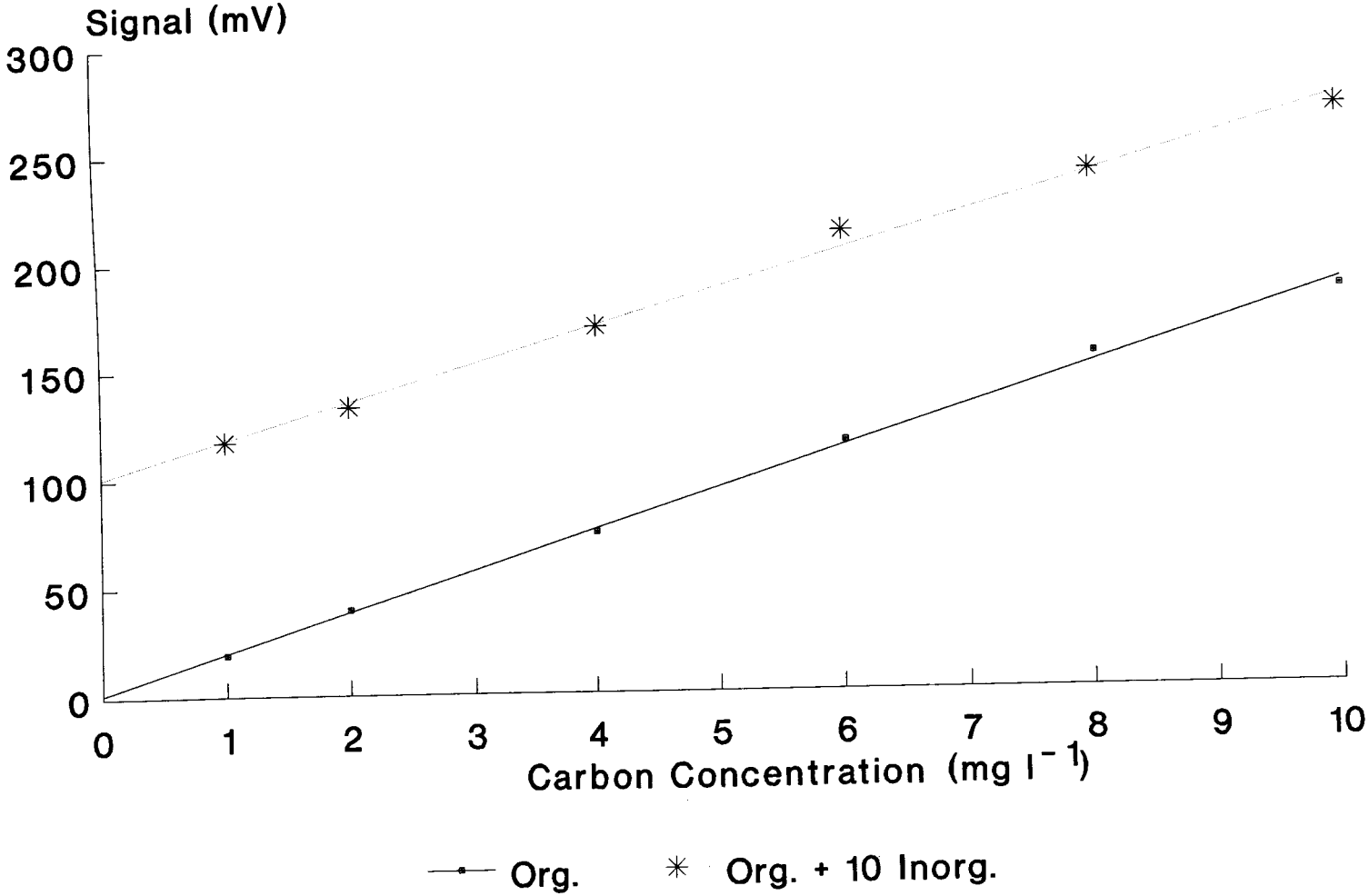

Fig. 6.16 Additive Effect of Inorganic Carbon.

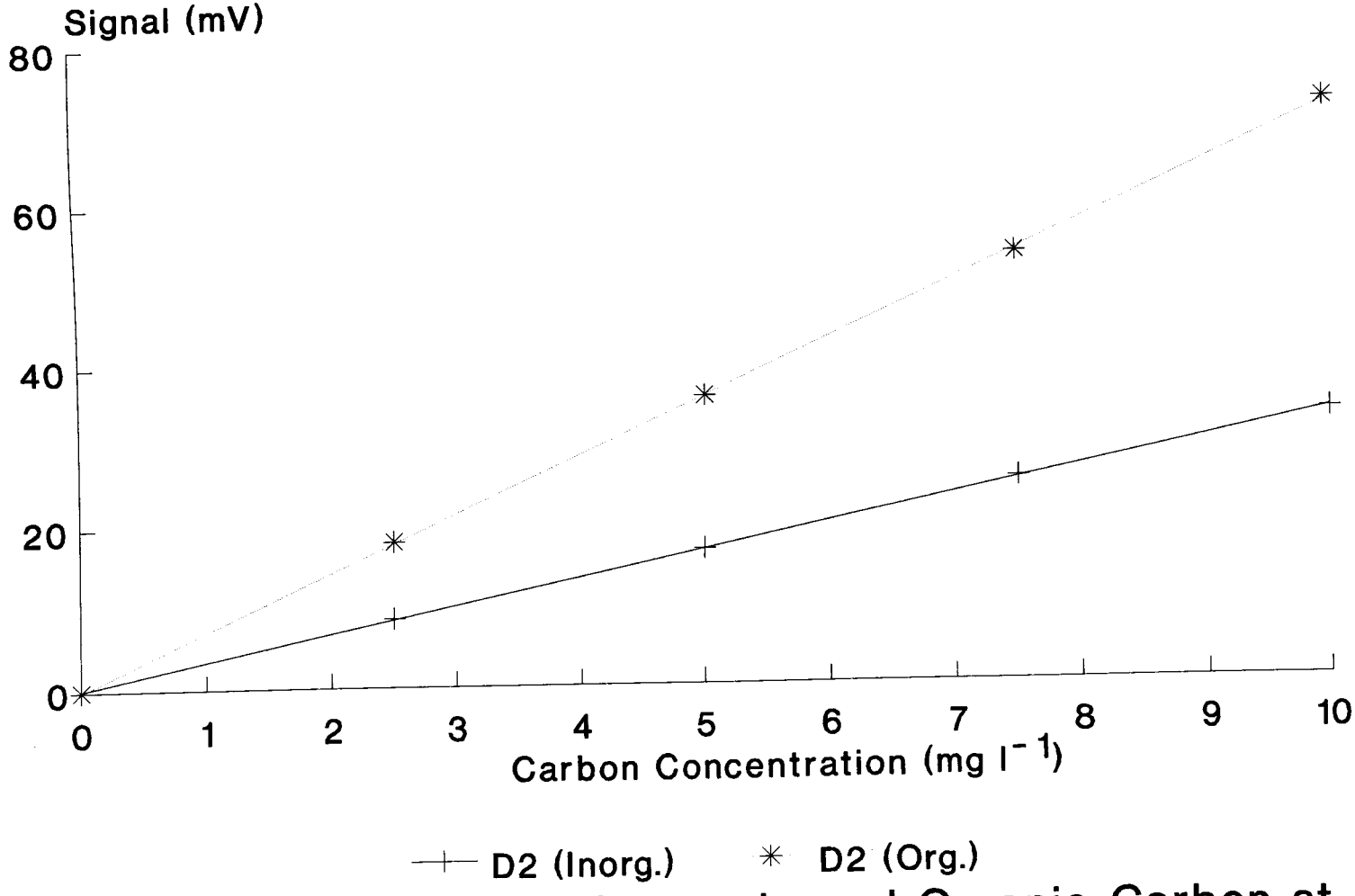

Fig. 6.17 Response for Inorganic and Organic Carbon at Second Detector.

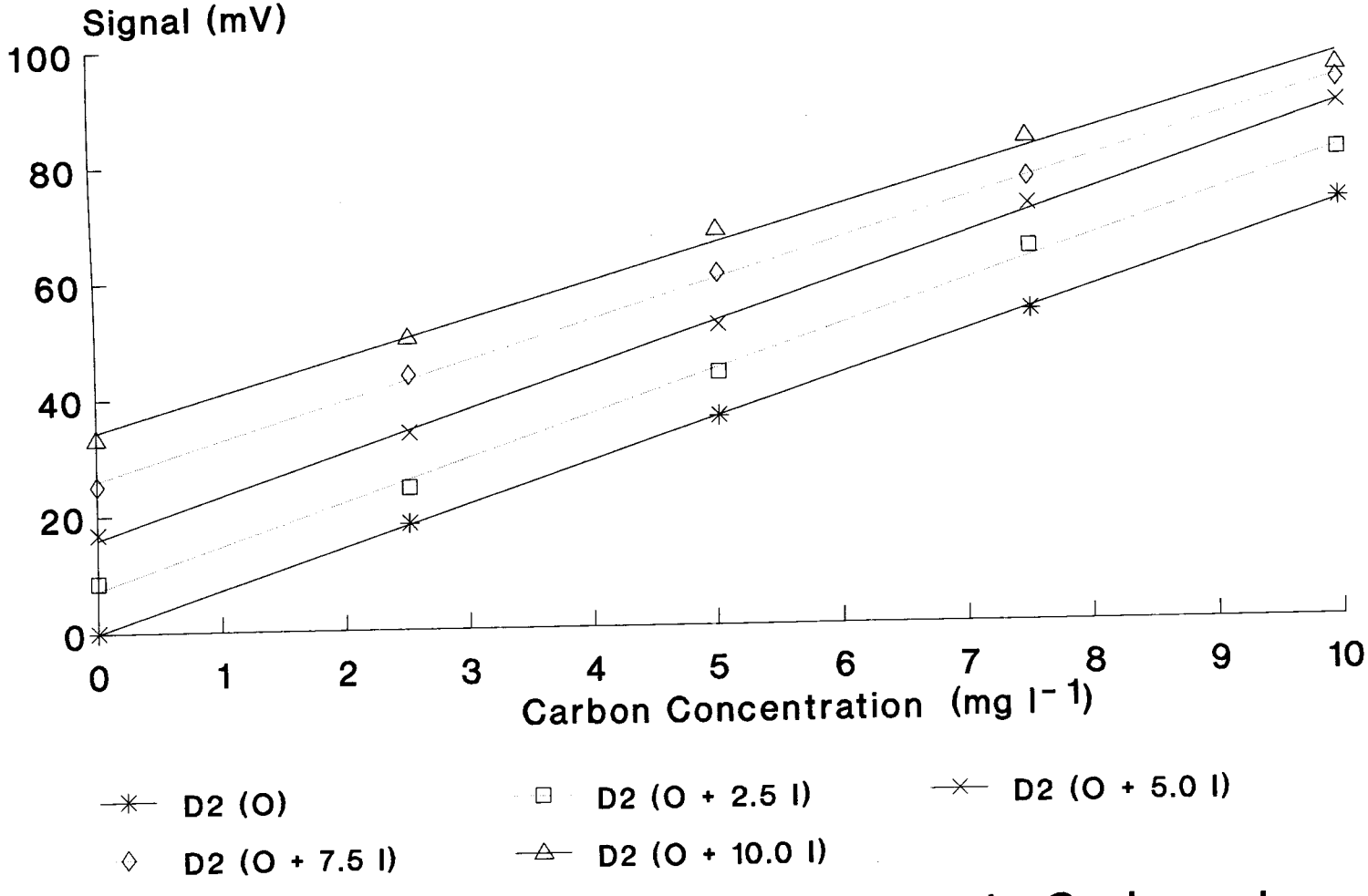

Fig. 6.18 Additive Effect of Inorganic Carbon at Second Detector.

TABLE 6.8

Matrix for Mixed Inorganic and Organic Carbon Standards.

Inorganic ($mg\ l^{-1}$)	Organic / Solution No. ($mg\ l^{-1}$)				
	0	2.5	5.0	7.5	10.0
0	1	2	3	4	5
2.5	6	7	8	9	10
5.0	11	12	13	14	15
7.5	16	17	18	19	20
10.0	21	22	23	24	25

The difference in the responses for the range of inorganic carbon standards at D1 and D2 were calculated and the results summarised in Table 6.9, the mean difference over the concentration range was 42.0 %. This calculated mean value was used to correct the responses for the spiked organic carbon standards. The theoretical inorganic response at D2, calculated as 42.0 % of the response observed at D1, was subtracted from the response observed for the spiked organic standard at D2. This corrected response was then substituted into the regression equation calculated for the unspiked organic carbon standards:

$$\text{Signal} = 7.17\ [C]\ (mg\ l^{-1}) - 0.06$$

The results of this calculation procedure are summarised in Table 6.10.

TABLE 6.9

Responses for Inorganic Carbon at Detectors (1) and (2).

C	Signal (mV)		Difference
(mg l^{-1})	D(1)	D(2)	(%)
2.5	17.8	8.5	47.8
5.0	38.7	16.7	43.2
7.5	62.8	25.1	40.0
10.0	89.3	33.1	37.1

TABLE 6.10

Correlation of Actual and Calculated Organic Carbon Concentrations in a Known System.

Composition of Standard		Calculated Concentration
Organic C ($mg\ l^{-1}$)	Inorganic C ($mg\ l^{-1}$)	Organic C ($mg\ l^{-1}$)
2.5	2.5	2.3
5.0	2.5	5.0
7.5	2.5	7.9
10.0	2.5	10.2
2.5	5.0	2.4
5.0	5.0	4.9
7.5	5.0	7.7
10.0	5.0	10.1
2.5	7.5	2.5
5.0	7.5	5.7
7.5	7.5	7.0
10.0	7.5	9.2
2.5	10.0	1.9
5.0	10.0	4.4
7.5	10.0	6.8
10.0	10.0	8.6

Although at higher inorganic spike concentrations some deviation from the true organic concentration was observed, there was a correlation between the calculated and actual organic carbon concentration.

Assuming the difference in response between D1 and D2 for inorganic carbon is constant or through a simple calibration procedure can be calculated, a response for organic carbon alone can be calculated and quantified by comparison to a simple organic carbon calibration.

This hypothesis was tested by spiking five organic carbon standards at two concentrations, 2.5 and 7.5 mg l^{-1}, with increasing quantities of inorganic carbon. The size of the unquantified spike gave inorganic carbon concentrations in the range 1 - 10 mg l^{-1}. These spiked standards were analysed together with unspiked organic and inorganic carbon standards, from the later the response differences between D1 and D2 for the inorganic fraction was calculated. The response difference varied between 55.6 and 64.9 %, with a mean value of 60.8 %; this mean value was used to correct the responses observed at D2 for the spiked organic carbon standards. These corrected responses were then substituted into the regression equation calculated for the unspiked organic carbon standards:

$$\text{Signal (mV)} = 7.55\ [C]\ (\text{mg } l^{-1}) - 3.78$$

The calculated organic carbon concentrations, Table 6.11, are consistent with the findings of the previous experiment, where higher concentrations of inorganic carbon gave a negative bias to the calculated organic carbon concentration. However, the expected levels of inorganic carbon in natural waters are < 1 mg l^{-1} and therefore in practice this bias should not be observed.

When applied to the automated monitor, it should be possible to use only one inorganic and one organic carbon standard to calibrate the detectors; the concentration of the standards selected on the basis of the likely concentration of each of the fractions in river water.

TABLE 6.11

Correlation of Actual and Calculated Organic Carbon Concentrations in an Unknown System.

Solution[a]	Organic C ($mg\ l^{-1}$)	Calculated ($mg\ l^{-1}$)	Difference ($mg\ l^{-1}$)
1	2.5	2.4	- 0.1
2	2.5	2.1	- 0.4
3	2.5	2.0	- 0.5
4	2.5	1.9	- 0.6
5	2.5	0	- 2.5
6	7.5	7.7	+ 0.2
7	7.5	7.5	0
8	7.5	6.8	- 0.7
9	7.5	6.3	- 1.2
10	7.5	5.0	- 2.5

[a] Inorganic carbon spike increasing in concentration from $\approx$ 1 - 10 mg C l^{-1} in the solution sets 1 - 5 and 6 - 10.

6.4 CONCLUSIONS

FI coupled with solid-state photometric detection offers a cheap and simple means for the quantitative determination of inorganic and organic carbon. The use of a low power UV source for sample irradiation and stopped-flow procedure greatly enhanced the oxidation ability of the FI procedure for complex organic species. A dual detector system provides a convenient method for the quantitative determination of inorganic and organic carbon without separation of the species.

Chapter Seven

Conclusions and Future Work

7.1. FINAL CONCLUSIONS

FI has been successfully applied to the on-line monitoring of water quality parameters and the following general conclusions can be drawn:

1. Automated FI instruments with solid-state detection systems are rugged and reliable during extended continuous on-line operation.

2. Commercial industrial control computers have been successfully applied to the automation of the FI systems.

3. The EuroBEEB Cube computer system offers low cost automation for simple dedicated instrumentation.

4. The STEbus based computer system offers powerful control, processing and communication facilities, and also simplifies monitor construction. It is fully PC compatible and easily expanded. Simple maintenance and repair is facilitated by the wide availability of replacement cards.

In addition specific conclusions can be made about the solid-state detectors and the FI methods:

1. The performance of the solid-state detector is greatly enhanced by simple modification. Replacement of the PTFE flow cells with glass capillaries, and substitution of the LEDs with more intense versions significantly increase the sensitivity of the detector.

2. The FI methods for aluminium and iron using the modified solid-state detectors are sensitive and selective. The FI procedure for aluminium has a limit of detection of 13 $\mu g\ l^{-1}$, and at the GL level (50 $\mu g\ l^{-1}$) a twenty-fold

excess of iron(III) gives rise to only a small positive bias of < 20 %. The method for iron has a limit of detection of 11 $\mu g\ l^{-1}$.

It can be concluded from the operation and performance trials of the STEbus based automated FI monitors for residual coagulants (aluminium and iron) that:

1. They are very reliable, providing valid results, on a first determination basis, for > 95 % of the operational period and 100 % overall.

2. They are economical to operate, consuming < 21 l of any one reagent during the 35 day unattended period when operated on a twice hourly measurement cycle. The consumable cost per analysis is one pence and five pence for the aluminium and iron monitors respectively.

3. The aluminium monitor provides reliable trend information by determination of the dissolved, uncomplexed monomeric fraction.

4. They meet all water industry specifications for accuracy, precision and all general operational requirements for aluminium and iron analysers applied to clarified water monitoring.

5. They are suitable as prototypes for commercialisation, with the aluminium and iron FI methods as standard procedures.

The conclusions from the investigation into the use of FI for the on-line determination of dissolved organic carbon are as follows:

1. The on-line chemical oxidation procedure is 100 % efficient for simple organic species, and is enhanced for certain more complex organic species

by the inclusion of a low power UV irradiation and stopped-flow step; for example > 95 % for nitrophenol and > 70 % for dichlorophenol.

2. A simple dual detector FI method shows promise as the basis of a procedure to provide rapid semi-quantitative information for dissolved inorganic and organic carbon, without prior separation of the fractions.

7.2. SUGGESTIONS FOR FUTURE WORK

One area where significant improvement in the sensitivity and versatility of the system could be made, is in the design of the solid-state detector. Modifications could include:

1. Simplification of the design by revision of the optical arrangement to remove the reference channel.

2. Pulsing of the LED sources to enhance the signal-to-noise ratio.

3. The use of alternative flow cell materials to enhance light throughput, but retaining the robustness of the detector design.

4. Changes to the flow cell configuration to give a longer path length, coupled with the use of more intense LEDs and/or laser diodes.

5. The use of LED arrays for simultaneous multi-wavelength detection.

The future development of the automated FI monitoring system can be divided into short, medium and long term aims.

Short Term:

1. The linking of several individual "wet chemistry" modules, to provide multi-parameter systems.

2. The reduction of maintenance requirements to extend operational periods and reduce overall costs, for example by the use of syringe pumps in place of peristaltic pumps.

3. To fully validate the FI method for the determination of dissolved organic carbon (DOC), and quantify the interference from inorganic carbon in the dual detector system.

4. The construction of an automated system for the on-line determination of DOC, with due consideration given to the difficulties associated with the inclusion of heating elements and UV sources in the monitor.

4. The development of automated instrumentation for alternative parameters and applications; both for wider environmental monitoring, for example nutrient cycling in the marine environment and the continuous monitoring of soil leachates, and also for industrial process control.

Medium Term:

1. Development of self-contained battery operated systems for remote sampling locations, with a fully submersible version for deployment in coastal waters and estuaries.

2. Production of a low cost version for use in large water quality monitoring networks and in developing countries.

3. Application of the on-line oxidation procedures for the determination of other organic species including phosphorus and nitrogen compounds.

Long Term:

1. The use of mixed chromogenic reagents with LED array detectors and multivariate calibration procedures for simultaneous analyte determinations.

2. Extension of the current range of parameters by the use of alternative FI procedures, for example the use of enzymatic methods for total pesticide analysis and chemiluminescence detection systems.

References

1 J. R. Mather, Water Resources: Distribution, Use and Management, John Wiley and Sons, New York, 1984.

2 Water Data, Water Data Unit, Department of the Environment, Reading, 1978.

3 Digest of Environmental Protection and Water Statistics, Department of the Environment, HMSO, London, 1991.

4 W. Howarth, Water Pollution Law, Shaw and Sons, London, 1988.

5 Water Act 1973, HMSO, London, 1973.

6 R. Macrory, Water Law, Principles and Practice, Chapter 3, 17-43, Longman, London, 1985.

7 Halsbury's Statutes of England and Wales, 4th Edn., Current Statutes Service: Volume 49, Butterworth, London, 1988.

8 N. Haigh, European Community Enviromental Policy in Practice, Vol. 1, "Comparative Report: Water and Waste in Four Countries", Graham Trotman, London, 1986.

9 Masons, Water Law, Chapter 5, 113-130, Woodhead-Faulkner, London, 1990.

10 European Environment Policy, European Communities Economic and Social Committee, Brussels, 1987.

11 N. Haigh, EEC Environmental Policy & Britain, 2nd Edn., Longman, Harlow, 1989.

12 J. Gardiner and G. Mance, UK Water Quality Standards Arising From European Community Directives, WRc Technical Report TR 204, WRc, Medmenham, 1984.

13 Guidelines for Drinking Water Quality, Vol. 1, World Health Organisation, Geneva, 1984.

14 Guidance on Safeguarding the Quality of Public Water Supplies, Department of the Environment, Welsh Office, HMSO, London, 1989.

15 P. D. Abel, Water Pollution Biology, Ellis Horwood, Chichester, 1989.

16 D. T. E. Hunt and A. L. Wilson, The Chemical Analysis of Water, 2nd Edn., The Royal Society of Chemistry, London, 1986.

17 P. L. Brezonik, C. Hendry and H. Prentice, Jnl. Water Pollution Control Federation (Eng.), 49 (1977) 986-992.

18 F. M. Garfield, J. Assoc. Off. Anal. Chem., 72 (1989) 405-411.

19 General Principles of Sampling and Accuracy of Results: Methods for the Examination of Water and Associated Materials, HMSO, London, 1980.

20 Sample Collection, Preservation and Storage, Technical Report TR 214, WRc, Medmenham, 1984.

21 L. S. Clesceri, A. E. Greenberg and R. R. Trussell (Eds.), Standard Methods for the Examination of Water and Wastewater, 17th Edn., American Public Health Association, 1989.

22 C. P. Hensley, W. J. Keffer, C. McKensie and M. D. Lair, Jnl. Water Pollution Control Federation (Eng.), 50 (1978) 1061-1066.

23 R. L. Jolley and A. L. Rivera, Jnl. Water Pollution Control Federation (Eng.), 61 (1989) 782-785.

24 Water Industry Specifications Information and Guidance Notes, WAA Process Systems Committee, WRc, Medmenham, 1989.

25 The Water Industry Steering Group on Instrumentation Control and Automation - Guideline Four, WRc, Medmenham, 1989.

26 M. J. Beckett, Ion-Selective Electrodes, Technical Report T.P. 99, WRA, Medmenham, 1973.

27 M. D. Stewart, Ultrapure Water, 5 (1988) 24-38.

28 M. J. Beckett, The Ammonia Sensitive Membrane Electrode, Technical Report T.P. 104, WRA, Medmenham, 1973.

29 P. L. Bailey, Analysis with Ion-Selective Electrodes, 2nd Edn., Heydon, London, 1980.

30 E. H. Hansen, C. G. Lamm and J. Ruzicka, Anal. Chim. Acta, 59 (1972) 403-426.

31 D. S. Gruber and J. M. Diamond (Eds.), Automated Biomonitoring: Living Sensors as Environmental Monitors, Ellis Horwood, Chichester, 1988.

32 J. Cairns and W. H. Van Der Schalie, Water Research, 14 (1980) 1179-1196.

33 W. S. G. Morgan, P. C. Kuhn, B. Allais and G. Wallis, Water Science & Technology, 14 (1982), 151-161.

34 T. Yoshida, Water Science & Technology, 14 (1982) 897-899.

35 W. Sloof, Aquatic Toxicology, 3 (1983) 127-139.

36 T. J. Hall and D. L. Borton, Tappi, 70 (1987) 57-59.

37 G. Kraus and S. Kornder, Tappi, 70 (1987) 62-66.

38 C. F. Mason, Biology of Freshwater Pollution, Longman, Harlow, 1981.

39 R. W. Brandon, Water Services (London), 92 (1988) 432.

40 F. D. Snell (Ed.), Photometric and Fluorometric Methods of Analysis, John Wiley & Sons, New York, 1978.

41 Z. Marczenko, Separation and Spectrophotometric Determination of Elements, 2nd Edn., Ellis Horwood, Chichester, 1986.

42 L. D. Mee, Sci. Total Environ., 49 (1986) 27-87.

43 J. Ruzicka and E. H. Hansen, Flow Injection Analysis, 2nd Edn., John Wiley and Sons, New York, 1988.

44 M. Valcarcel and M. D. Luque de Castro, Flow Injection Analysis: Principles and Applications, Ellis Horwood, Chichester, 1987.

45 B. Karlberg in Chemical Derivatization in Analytical Chemistry, Vol. 2, R. W. Frei and J. F. Lawrence (Eds.), Plenum Press, New York, 1982.

46 J. Ruzicka, Fresenius Z. Anal. Chem., 329 (1988) 653-655.

47 C. B. Ranger in Automated Stream Analysis for Process Control, Vol. 1, D. P. Manka, (Ed.), Academic Press, New York, 1982.

48 W. E. van der Linden, Anal. Chim. Acta, 179 (1986) 91-101.

49 J. Ruzicka, Anal. Chim. Acta, 190 (1986) 155-163.

50 M. Gisin and C. Thommen, Anal. Chim. Acta, 190 (1986) 165-176.

51 J. B. Callis, D. L. Illman and B. R. Kowalski, Anal. Chem., 59 (1987) 624A-637A.

52 M. Gisin and C. Thommen, TrAC, 8 (1989) 62-66.

53 M. Trojanowicz, P. J. Worsfold and J. R. Clinch, TrAC, 7 (1988) 301-305.

54 P. J. Worsfold, J. R. Clinch and H. Casey, Anal. Chim. Acta, 197 (1987) 43-50.

55 J. R. Clinch, P. J. Worsfold and H. Casey, Anal. Chim. Acta, 200 (1987) 523-531.

56 J. R. Clinch, P. J. Worsfold and F. W. Sweeting, Anal. Chim. Acta, 214 (1988) 401-407.

57 H. Flaschka, C. McKeithan and R. Barnes, Anal. Lett., 6 (1973) 585-594.

58 D. J. Hooley and R. E. Dessy, Anal. Chem., 55 (1983) 313-320.

59 D. Betteridge, E. L. Dagless, B. Fields and N. F. Graves, Analyst, 103 (1978) 897-908.

60 D. Betteridge, Anal. Chem., 50 (1978) 832A-846A.

61 D. Betteridge, W. C. Cheng, E. L. Dagless, P. David, T. B. Goad, D. R. Deans, D. A. Newton and T. B. Pierce, Analyst, 108 (1983) 1-16.

62 K. S. Johnson and R. L. Petty, Limnol. Oceanogr., 28 (1983) 1260-1266.

63 M. Trojanowicz, W. Augustyniak and A. Hulanicki, Mikrochim. Acta, II (1984) 17-25.

64 K. S. Johnson, C. L. Beehler and C. M. Sakamoto-Arnold, Anal. Chim. Acta, 179 (1986) 245-257.

65 J. R. Clinch, PhD Thesis, University of Hull, 1988.

66 F. N. Kemmer (Ed.), The NALCO Water Handbook, 2nd Edn., McGraw-Hill, New York, 1988.

67 R. F. Packham, Cationic Polyelectrolytes as Primary Coagulants, Technical Paper TP. 100, WRA, Medmenham, 1973.

68 A. M. Ure and M. L. Berrow, The Elemental Constituents of Soils, in H. J. M. Bowen (Ed.), Environmental Chemistry, Vol. 2, RSC, London, 1982, Chapter 3.

69 F. A. Cotton and G. Wilkinson, Advanced Inorganic Chemistry, 4th Edn., John Wiley and Sons, New York, 1980.

70 D. Carroll, Rock Weathering, Plenum Press, New York, 1970.

71 W. Stumm and J.J. Morgan (Eds.), Aquatic Chemistry, 2nd Edn., John Wiley and Sons, New York, 1981.

72 N. M. Johnson, C. T. Driscoll, J. S. Eaton, G. E. Likens and W. H. McDowell, Geochim. et Cosmochim. Acta, 45 (1981) 1421-1437.

73 A. J. Rubin (Ed.), Aqueous-Environmental Chemistry of Metals, Ann Arbor Science Publishers, Ann Arbor, Michigan, 1974.

74 K. R. Bull and J. R. Hall, Chemical Analysis in Environmental Research, ITE Symposium Series No. 18, (1987) 6-11.

75 J. D. Hem, Aluminium Species in Water, in Trace Inorganics in Water, Advances in Chemistry Series No. 73, American Chemical Society, 1968.

76 W. K. Stewart, Aluminium Toxicity in Individuals with Chronic Renal Disease, in R. C. Massey and D. Taylor (Eds.), Aluminium in Food and the Environment, RSC, London, 1989.

77 D. R. Crapper McLachlan and U. De Boni, Neurotoxicology, 1 (1980) 3-16.

78 P. O. Ganrot, Environ. Health Perspectives, 65 (1986) 363-441.

79 D. P. Perl and A. R. Brody, Science, 208 (1980) 297-299.

80 L. L. Heston, A. R. Mastri, V. E. Anderson and J. White, Arch. Gen. Psychiatry, 38 (1981) 1085-1090.

81 D. R. Crapper McLachlan and M. F. A. Van Berkum, Prog. Brain Res., 70 (1986) 399-410

82 J. M. Candy, J. Klinowski, R. H. Perry, E. K. Perry, A. Fairbairn, A. E. Oakley, T. A. Carpenter, J. R. Atack, G. Blessed, J. A. Edwardson, Lancet, I (1986) 354-356.

83 J. K. Marquis, Neurotoxicity of Aluminium, in T. E. Lewis (Ed.), Environmental Chemistry and Toxicolgy of Aluminium, Lewis Publishers, Chelsea, Michigan, 1989, Chapter 16.

84 R. B. Martin, Clin. Chem., 32 (1986) 1797-1806.

85 A. Prescott, New Scientist, 21st January 1989, 58-62.

86 L. Liss, J. Long and D. Thornton, Aluminium Neurotoxicity, Alzheimer Disease and Alcoholic Encephalopathy, in T. E. Lewis (Ed.), Environmental Chemistry and Toxicolgy of Aluminium, Lewis Publishers, Chelsea, Michigan, 1989, Chapter 18.

87 R. U. Schenk, J. Bjorksten and L. Yeager, Composition and Consequences of Aluminium in Water, Beverages and Other Ingestibles, in T. E. Lewis (Ed.), Environmental Chemistry and Toxicolgy of Aluminium, Lewis Publishers, Chelsea, Michigan, 1989, Chapter 14.

88 C. N. Martyn, An Epidemiological Approach to Aluminium and Alzheimer's Disease, in R. C. Massey and D. Taylor (Eds.), Aluminium in Food and the Environment, RSC, London, 1989.

89 P. MacCarthy and R. W. Klusman and A. J. Rice, Anal. Chem., 59 (1987) 308R-337R.

90 O. Royset, A. O. Stuanes, G. Ogner and G. Sjotveit, Intern. J. Environ. Anal. Chem., 29 (1987) 141-149.

91 C. A. Coutinho, E. Cosenza Arruda, M. J. Mundin and W. P. de Araujo, Steel Res., 61 (1990) 201-203.

92 J. A. Kennedy and H. K. J. Powell, Anal. Chim. Acta, 184 (1986) 329-333.

93 A. C. Edwards and M. S. Cresser, Talanta, 30 (1983) 702-704.

94 A. D. Wilson and G. A. Sergeant, Analyst, 88 (1963) 109-112.

95 Acid Soluble Aluminium in Marine, Raw and Potable Waters, HMSO, London, 2nd Edn., 1988.

96 P. Jones, Intern. J. Environ. Anal. Chem., 44 (1991) 1-10.

97 A. Anton, Anal. Chem., 32 (1960) 725-726.

98 C. Wyganowski, S. Motomizu and K. Toei, Anal. Chim. Acta, 140 (1982) 313-317.

99 E. Kaneko, H. Tanno, and T. Yotsuyanagi, Mikrochim. Acta, III (1988) 333-340.

100 W. K. Dougan and A. L. Wilson, Analyst, 99 (1974) 413-430.

101 O. Royset, Anal. Chim. Acta, 178 (1985) 223-230.

102 O. Royset, Anal. Chim. Acta, 185 (1986) 75-81.

103 J. M. Henshaw, T. E. Lewis and E. M. Heithmar, Intern. J. Environ. Anal. Chem., 34 (1988) 119-135.

104 D. L. Massart, B. G. M. Vandeginste, S. N. Deming, Y. Michotte and L. Kaufman, Chemometrics: A Textbook, Elsevier, Amsterdam, 1988, Chapter 18.

105 R. G. Brereton, Chemometrics: Applications of Mathematics and Statistics to Laboratory Systems, Ellis Horwood, Chichester, 1990.

106 C. T. Driscoll, Intern. J. Environ. Anal. Chem., 16 (1984) 267-283.

107 R. J. Mitchell, Microcomputer Systems Using the STE Bus, Macmillan, London, 1989.

108 D. Stevenson and K. Miller, Microprocessor Applications, ACOL, John Wiley and Sons, Chichester, 1987.

109 F. M. M. Morel, Principles of Aquatic Chemistry, John Wiley and Sons, New York, 1983.

110 Proposed Environmental Quality Standards for List II Substances in Water: Iron, Technical Report TR 258, WRc, Medmenham, 1988.

111 J. Rodier, Analysis of Water, John Wiley and Sons, New York, 1975.

112 H. Fadrus and J. Maly, Anal. Chim. Acta, 77 (1975) 315-316.

113 H. L. Golterman, R. S. Clymo and M. A. M. Ohnstad (Eds.), Methods for Physical and Chemical Analysis of Fresh Waters, 2nd Edn., Blackwell Scientific, Oxford, 1978.

114 Analytical Methods Committee, Analyst, 103 (1978) 391-396.

115 R. A. Leach, J. Ruzicka and J. M. Harris, Anal. Chem., 55 (1983) 1669-1673.

116 B. P. Bubnis, M. R. Straka and G. E. Pacey, Talanta , 30 (1983) 841-844.

117 J. L. Burguera and M. Burguera, Anal. Chim. Acta, 161 (1984) 375-379.

118 A. T. Faizullah and A. Townshend, Anal. Chim. Acta, 167 (1985) 225-231.

119 J. Mortatti, F. J. Krug, L. C. R. Pessenda, E. A. G. Zagatto and S. S. Jorgenson, Analyst, 107 (1982) 659-663.

120 T. Yamane and E. Goto, Anal. Sci., 5 (1989) 221-223.

121 T. Aita, T. Odashima and H. Ishii, Analyst, 109 (1984) 1139-1145.

122 H. Ishii, M. Aoki, T. Aita and T. Odashima, Anal. Sci., 2 (1986) 125-129.

123 D. P. Poe, A. D. Eppen and S. P. Whoolery, Talanta, 27 (1980) 368-370.

124 R. D. Perry and C. L. San Clemente, Analyst, 102 (1977) 114-119.

125 A. Rios, M. D. Luque de Castro and M. Valcarcel, Analyst, 110 (1985) 227-281.

126 W. K. Dougan and A. L. Wilson, The Determination of Iron in Water, Technical Report T.P. 83, WRA, Medmenham, 1972.

127 W. K. Dougan and A. L. Wilson, Water Treat. Exam., 22 (1973) 100-113.

128 C. Hammerton, Proc. Soc. Water Treat. Exam., 11 (1967) 293-295.

129 Iron in Raw and Potable Waters by Spectrophotometry, Methods for the Examination of Waters and Associated Materials, HMSO, London, 1977.

130 M. C. Mehra, M. Satake, L. F. Chang and H. B. Singh, Microchem. J., 31 (1985) 392-395.

131 L. L. Stookey, Anal. Chem., 42 (1970) 779-781.

132 V. V. S. E. Dutt and H. A. Mottola, Anal. Chem., 49 (1977) 319-321.

133 M. K. Gadia and M. C. Mehra, Mikrochim. Acta, II (1977) 413-418.

134 J. R. Duffy and J. Gaudin, Clin. Biochem., 10 (1977) 122-123.

135 M. M. Gibbs, Water Res., 13 (1979) 295-297.

136 P. D. Carpenter and J. D. Smith, Anal. Chim. Acta, 159 (1984) 299-308.

137 J. C. Thompsen and H. A. Mottola, Anal. Chem., 56 (1984) 755-757.

138 V. Kuban and D. B. Gladilovich, Coll. Czech. Chem. Commun., 53 (1988) 1461-1475.

139 M. V. Dawson and S. J. Lyle, Talanta, 37 (1990) 1189-1191.

140 M. L. Balconi, F. Sigon, M. Borgarello, R. Ferraroli and F. Realini, Anal. Chim. Acta, 234 (1990) 167-173.

141 A. A. Schilt and W. C. Hoyle, Anal. Chem., 39 (1967) 114-117.

142 M. K. Gadia and M. C. Mehra, Microchem. J., 22 (1977) 27-33.

143 F. E. Smith, J. Herbert, J. Gaudin, D. J. Hennessey and G. R. Reid, Clin. Biochem., 17 (1984) 306-310.

144 A. A. Schilt and M. R. Di Tusa, Talanta, 29 (1982) 129-132.

145 T. Higgins, Clin. Chem., 27 (1981) 1619-1620.

146 D. J. Hennessey, G. R. Reid, F. E. Smith and S. L. Thompson, Can. J. Chem., 62 (1983) 721-724.

147 J. D. Artiss, D. R. Stranbergh and B. Zak, Microchem. J., 28 (1983) 275-284.

148 M. C. Mehra, B. Francoeur and M. Katyal, Jnl. Bangladesh Acad. Sci., 9 (1985) 47-54.

149 N. D. Seudeal, R. J. Thibert and B. Zak, Microchem. J., 34 (1986) 131-139.

150 D. J. Leggett, N. H. Chen and D. S. Mahadevappa, Indian J. Chem., 20A (1981) 1051-1053.

151 M. J. Whittaker and M. F. Bryant, Jnl. Coal Qual., 4 (1985) 68-71.

152 D. C. Goswani and H. Kalita, Def. Sci. J., 38 (1988) 177-182.

153 T. P. Lynch, N. J. Kernoghan and J. N. Wilson, Analyst, 109 (1984) 839-842.

154 T. P. Lynch, N. J. Kernoghan and J. N. Wilson, Analyst, 109 (1984) 843-846.

155 J. W. Dieker and W. E. van der Linden, Anal. Chim. Acta, 114 (1980) 267-274.

156 V. A. Elrod, K. S. Johnson and K. H. Coale, Anal. Chem., 63 (1991) 893-898.

157 Application Note, ASN 72-01/84, Tecator Ltd., Perstop Analytical, Bristol, 1984.

158 The Instrumental Determination of Total Organic Carbon, Total Oxygen Demand and Related Determinands, HMSO, London, 1980.

159 P. D. Goulden and P. Brooksbank, Anal. Chem., 47 (1975) 1943-1946.

160 I. H. Suffet and P. MacCarthy (Eds.), Aquatic Humic Substances, Influence on Fate and Treatment of Pollutants, American Chemical Society, Washington, 1989.

161 P. J. Statham and P. J. LeB. Williams in, Methods of Seawater Analysis, 2nd Edn., K. Grasshoff, M. Ehrhardt and K. Kremling (Eds.), Verlag Chemie, Weinheim, 1983, Chapter 13.

162 C. D. Baker, P. D. Bartlett, I. S. Farr and G. I. Williams, Freshwat. Biol., 4 (1974) 467-481.

163 A. W. Busch in, Chemical Environment in the Aquatic Habitat, H. L. Golterman and R. S. Clymo (Eds.), N. V. Noord-Hollandsche, Amsterdam, 1967.

164 R. J. Oake, A Review of Photo-Oxidation for the Determination of Total Organic Carbon in Water, Technical Report TR 160, WRc, Medmenham, 1981.

165 Y. Takahashi, J. Environment. Pathol. Toxicol. Ancol., 7 (1987) 373-391.

166 A. Jirka and M. J. Carter, Alternatives for Measuring Organic Carbon in Water, Advances in Automated Analysis, 7th Technicon International Conference, 1976, 27-31.

167 J. Katz, S. Abraham and N. Baker, Anal. Chem., 26 (1954) 1503-1504.

168 E. H. Battley, J. Bio. Chem., 226 (1957) 237-240.

169 O. L. Osburn and C. H. Werkman, Indust. Eng. Chem., Anal. Edn. (US), 4 (1932) 421-423.

170 S. L. Chen and K. J. H. Lauer, Anal. Chem., 29 (1957) 1225-1226.

171 D. W. Menzel and R. F. Vaccaro, Limnol. Oceanogr., 9 (1964) 138-142.

172 J. M. Baldwin and R. E. McAtee, Microchem. J., 19 (1974) 179-190.

173 J. D. H. Strickland and T. R. Parsons, A Practical Handbook of Seawater Analysis, Bulletin 167, 2nd Edn., Fisheries Research Board of Canada, Ottawa, 1972.

174 R. F. Wilson, Limnol. Oceanogr., 6 (1961) 259-261.

175 C. E. Van Hall and V. A. Stenger, Anal. Chem., 39 (1967) 503-507.

176 B. V. Stolyarov and E. E. Galev, Sov. J. Water Chem. Technical, 10 (1988) 57-62.

177 M. Ehrhardt, Deep-Sea Research, 16 (1969) 393-397.

178 K. J. Collins and P. J. LeB. Williams, Mar. Chem., 5 (1977) 123-141.

179 R. A. Van Steenderen, W. D. Basson and F. A. Van Duuren, Water Res., 13 (1979), 539-543.

180 R. A. Van Steenderen and J. -S. Lin, Anal. Chem. 53 (1981) 2157-2158.

181 W. Schreurs, Hydrobio. Bull., 12 (1978) 137-142.

182 L. R. Gravelet-Blondin, H. R. Van Vliet and P. A. Mynhardt, Water SA, 6 (1980) 138-143.

183 S. A. Mostert, S. Afr. J. Mar. Sci., 1 (1983) 57-60.

184 G. Cauwet, Mar. Chem., 14 (1984) 297-306.

185 J. M. Sharp, Mar. Chem., 1 (1973) 211-229.

186 Y. Sugimura and Y. Suzuki, Mar. Chem., 24 (1988) 105-131.

187 M. A. Kenny and M. H. Cheng, Clin. Chem., 18 (1972) 352-354.

188 J. Crowther and W. B. Moody, Anal. Chim. Acta, 120 (1980) 305-311.

189 L. R. Gravelet-Blondin, H. R. Van Vliet and B. W. H. Schoones, Water SA, 6 (1980) 135-137.

190 H. Baadenhuijsen and H. E. H. Seuren-Jacobs, Clin. Chem., 25 (1979) 443-445.

191 S. Motomizu, K. Toei, T. Kuwaki and M. Oshima, Anal. Chem. 59 (1987) 2930-2932.

192 C. Hall, Polymer Materials, 2nd Edn., Macmillan Education, London, 1989.

193 W. E. van der Linden, Anal. Chim. Acta, 151 (1983) 359-369.

194 R. B. Roy, J. Jansen and A. Conetta in, Automated Stream Analysis for Process Control, Vol. 1, D. P. Manka (Ed.) Academic Press, New York, 1982.

Appendices

APPENDIX A

Circuit Diagrams for Solid-State Detector

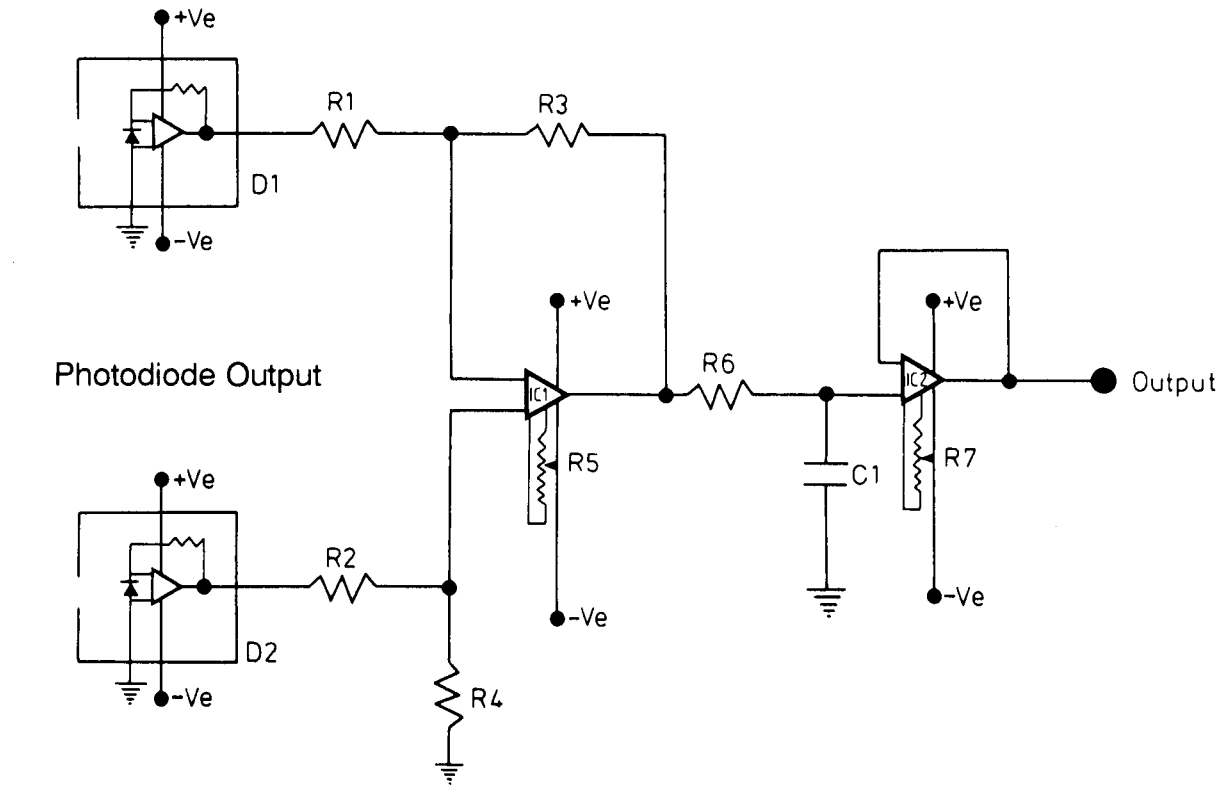

LED Power Supply

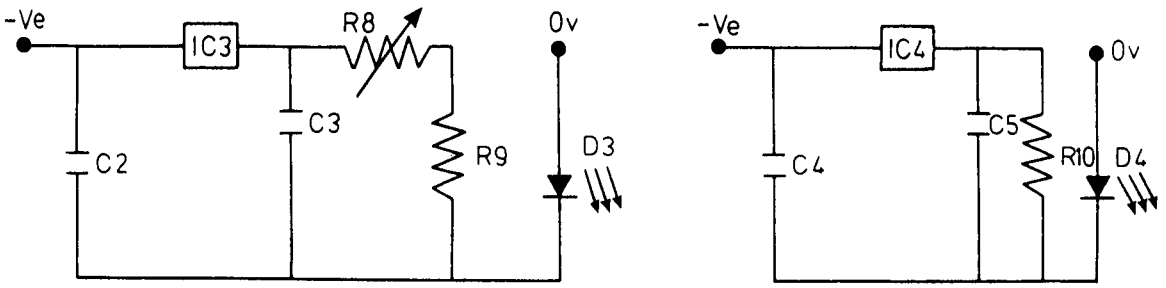

Reference Sample

Key to Components:

Resistors:	R1/R2	4K7	Capacitors:	C1	2.2 μF
	R3/R4	100K		C2/C4	220 nF
	R5	10K		C3/C5	470 nF
	R6	470K			
	R7	25K			
	R8	1K			
	R9	1K2			
	R10	1K5			

Diodes:	D1/D2 (Photo)	RS Cat. No. 308-067
	D3/D4 (LED)	RS Cat. No. 588-263
Integrated circuits:	IC1/IC2	741N
	IC3/IC4	79LO5

Flow Cell Design

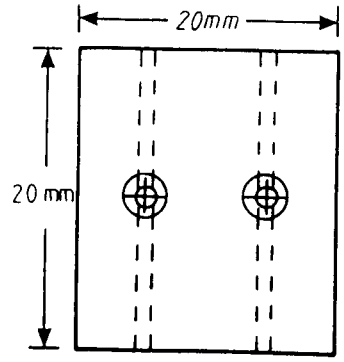

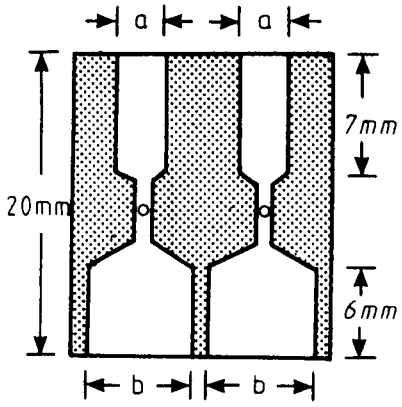

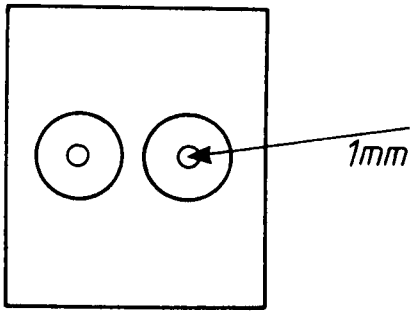

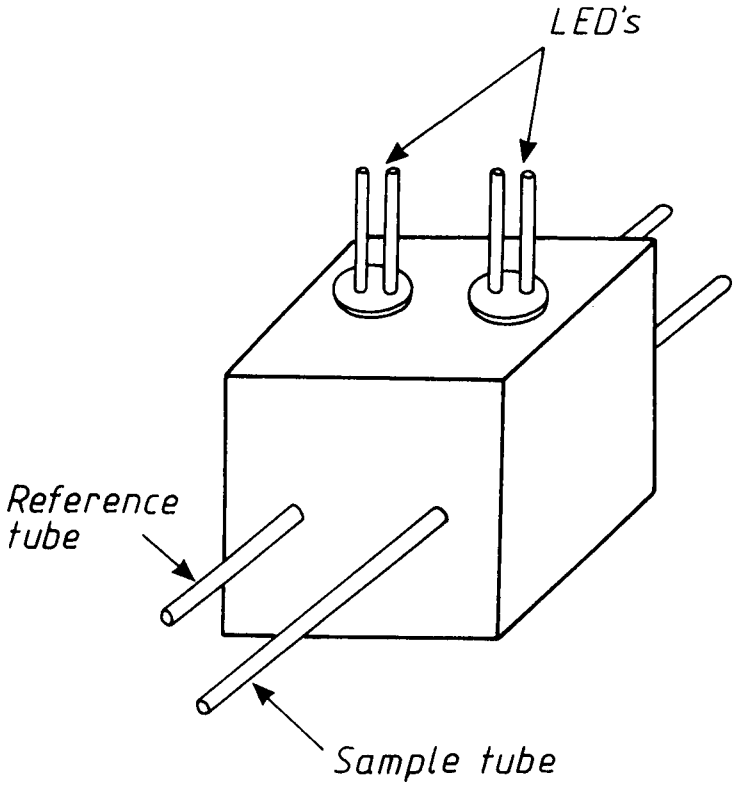

Key: (a) 5 mm to fit LED
(b) 8 mm to fit photodiode

APPENDIX B

Listing of Example Software for FI Monitor Control and Operation.

```
 10REM "ALMON66E"
 15REM ****AUTOBOOT****
 20HIMEM=&2000:LOMEM=&E00
 30DIM MV(6):DIM CS(2):CH=0:PE=0
 40OUTCH 0 TO 15
 45REM****TIME FOR ANALYSIS ?****
 50ZZ$=MID$(CLOCK$,4,2)
 60PE=0
 70GOTO 110
 80ZZ$=MID$(CLOCK$,4,2)
 90ZZ$=VAL(ZZ$)
 95REM****MONITOR CONTROL & INJECTION SEQUENCES****
 96REM****CHANNEL 0 = INJECTION VALVE****
 97REM****CHANNEL 1 = SWITCH VALVE****
 98REM****CHANNEL 4 = REAGENT PUMP****
 99REM****CHANNEL 5 = SAMPLE PUMP****
100IF ZZ=0 OR ZZ=30 THEN 110 ELSE 80
110TURNON 5,0
120DELAY 12000
130TURNON 4
140DELAY 20000
145REM****INITIATE DATA CAPTURE****
150SAMPLE 4000,300000,&4000,32
160TURNOFF 0,5
170DELAY 3000
180TURNON 0,5:DELAY 3000
190TURNON 0:TURNON 1
200DELAY 3000:TURNON 0
210DELAY14000
220DELAY 3000:TURNOFF 0,5
230DELAY 3000
240TURNON 0,5:DELAY 3000
250TURNOFF 0,1
260DELAY 8000
270TURNOFF 0 TO 6
280PROCPEAKFIND
```

```
290IF PE=1 THEN 50
300PROCSTD
310IF CH=1 THEN 330
320PROCSAM
330CH=0:GOTO 80
340END
345REM****PEAK FINDING ROUTINE****
350DEFPROCPEAKFIND
360SAMPLE 0,0,0,0
370I=0
380I=I+1
390REAING=SAMPLE I,32
400FOR J=1 TO 4
410I=I+1:IF I>4000 THEN 630
420PREVIOUS=REAING:REAING=SAMPLE I,32
430IF REAING<PREVIOUS OR REAING=PREVIOUS THEN 410
440MIL=PREVIOUS
450I=I+1:IF I>4000 THEN 630
460PREVIOUS=REAING:REAING=SAMPLE I,32
470IF REAING>PREVIOUS OR REAING=PREVIOUS THEN 450
480MAL=PREVIOUS:MVL=(MAL-MIL)/8
490IF MVL<5 THEN 410
500MV(J)=MVL
510NEXT J
520SAM=(MV(1)+MV(2))/2:REF=(MV(3)+MV(4))/2
530AL=(SAM/REF)*200:AL=INT(AL)
540V=INT(REF)
550TIMES$=LEFT$(CLOCK$,3)
560TIMES$=TIMES$+ZZ$
565REM****OUTPUT INFORMATION****
570*FX3,0
580VDU2
590PRINT DATE$;" ";TIMES$;" ";AL;"(";V;")"
600VDU3
610*FX3,7
620GOTO 710
630TIMES$=LEFT$(CLOCK$,3)
640TIMES$=TIMES$+ZZ$
645REM****OUTPUT ERROR MESSAGE****
650*FX3,0
```

```
660VDU2
670PRINT DATE$;" ";TIMES$;" ERROR"
680VDU3
690*FX3,7
695REM****LESS THAN FOUR PEAKS, REPEAT ANALYSIS****
700PE=1
710ENDPROC
715REM****STANDARD PEAK CHECK****
720DEF PROCSTD
730DIFF=ABS(MV(3)-MV(4))
740IF DIFF<10 THEN 810
750CH=1
760*FX3,0
770VDU2
780PRINT DATE$;" ";TIMES$;" EST"
790VDU3
800*FX3,7
810ENDPROC
815REM****SAMPLE PEAK CHECK****
820DEF PROCSAM
830 DIFF=ABS(MV(1)-MV(2))
840IF DIFF<10 THEN 1310
845REM****SAMPLE INJECTION REPEAT ON FAILURE****
850TURNON 0,4,5
860DELAY 3000
870SAMPLE 2000,300000,&4000,32
880DELAY 1000:TURNOFF 0,5
890DELAY 3000:TURNON 0,5
900DELAY 3000:TURNOFF 0,5
910DELAY 7000:TURNOFF 0 TO 6
920SAMPLE 0,0,0,0
925REM****FIND NEW SAMPLE PEAK VALUES****
930I=0
940I=I+1
950REAING=SAMPLE I,32
960FOR SA=1 TO 2
970I=I+1:IF I>2000 THEN 1250
980PREVIOUS=REAING:REAING=SAMPLE I,32
990IF REAING<PREVIOUS OR REAING=PREVIOUS THEN 970
1000MIL=PREVIOUS
```

```
1010I=I+1
1020PREVIOUS=REAING:REAING=SAMPLE I,32
1030IF REAING>PREVIOUS OR REAING=PREVIOUS THEN 1010
1040MAL=PREVIOUS:MVL=(MAL-MIL)/8
1050IF MVL<5 THEN 970
1060CS(SA)=MVL
1070NEXT SA
1075REM****REPEAT SAMPLE CHECK****
1080DIFF=ABS(CS(1)-CS(2))
1090IF DIFF>10 THEN 1190
1100SAM=(CS(1)+CS(2))/2
1110AL=(SAM/REF)*200:AL=INT(AL)
1120RIMES$=LEFT$(CLOCK$,5)
1125REM****OUTPUT INFORMATION****
1130*FX3,0
1140VDU2
1150PRINT DATE$," ";RIME$;" ";AL;"(";V;")"
1160VDU3
1170*FX3,7
1180GOTO 1310
1185REM****OUTPUT ERROR MESSAGE****
1190*FX3,0
1200VDU2
1210PRINT DATE$;" ";TIMES$;" ESA"
1220VDU3
1230*FX3,7
1240GOTO 1310
1250TIMES$=LEFT$(CLOCK$,5)
1260*FX3,0
1270VDU2
1280PRINT DATE$;" ";TIMES$;" SRE"
1290VDU3
1300*FX3,7
1310ENDPROC
1320PROCTIME
1330TIMES$=LEFT$(CLOCK$,3)
1340TIMES$=TIMES$+ZZ$
1350ENDPROC
```

APPENDIX C

Listing of STEbus FI Monitor Control Software

```
10 REM PROGRAM ="RLB" [STE Water Quality Monitoring]
20 REM Version
30 REM Creation Date
35 REM ************************************************
40 REM PROGRAM STARTUP and COUNTDOWN
50 adelements%=512:DIM ad%(512),flag%(5)
70 initialise
80 count%=0:REM number of analyses done
90 lt%=100:REM last clock reading
100 t%=(minutes% MOD sampint%)
105 REM countdown to next analysis
110 IF lt%<>t% THEN lt%=t%
120 IF t%=0 THEN analyse
150 delay(1)
160 IF INP(&FE1)=0 THEN pumpson
170 l1$="*** WAITING TO ANALYSE ***"
180 DScreen
200 GOTO 100
210 REM ************************************************
1999 REM SYSTEM INITIALISATION
2000 DEF initialise
2010 REM set SPIBB port A for output and B for input
2020 OUT &FE3,&82:OUT &FE7,&80:OUT &FE6,&1D
2030 rflag%=0:OUT &FE0,rflag%:REM all relays open
2035 REM Define pump & valve channels
2040 p1%=1:p2%=0:v1%=6:v2%=7
2050 REM User-defined parameters
2050 sampint%= ? :REM time between analyses
2060 cycletime%= ?
2070 true=1:false=0
2090 REM timing parameters
2100 flushdel%= ? :filldel%= ? :injdel%= ?
2190 REM error conditions
2200 sensthresh= ? :maxfails%= ? :mvdiff= ?
2210 maxexpect= ? :minexpect= ?
```

```
2215 REM calibration standard value
2220 standconc= ?
2250 REM initialisation of strings for LCD
2251 l1$="                    "
2252 l2$="                    "
2300 ENDPROC
2310 REM
2400 DEF Dinit
2405 REM initialise LCD
2410 FOR i=1 TO 3
2420 OUT 190,56
2430 NEXT i
2440 OUT 190,12
2450 OUT 190,6
2460 OUT 190,128
2470 OUT 190,1
2480 ENDPROC
2485 REM
2600 DEF DScreen
2605 Dinit
2610 x%=LEN(l1$):y%=LEN(l2$)
2620 FOR i=1 TO 20-x%/2:OUT 191,32:NEXT i
2630 FOR i=1 TO x%:c$=MID$(l1$,i-1,1):OUT 191,ASC(c$):NEXT i
2640 x%=40-x%-(y%-x%)/2
2650 FOR i=1 TO x%:OUT 191,32:NEXT i
2660 FOR i=1 TO y%:c$=MID$(l2$,i-1,1):OUT 191, ASC(c$):NEXT i
2670 ENDPROC
2672 REM ************************************************
2675 REM MONITOR CONTROL and TIMING
3000 DEF setrelay(no%,st%)
3010 LOCAL i%:i%=255-2**no%:i%=i% AND rflag%
3020 IF st%>0 THEN i%=i% OR 2**no%
3030 rflag%=i%:OUT &FE0,rflag%
3040 ENDPROC
3045 REM
3100 DEF delay(time)
3110 LOCAL i%:i%=time*16
3120 OUT 138,&2C:REM register &A=16Hz
3130 OUT 139,&46:REM register &B
3140 WHILE i%>0
```

```
3150  IF INP(140)>191 THEN i%=i%-1
3160 WEND
3170 OUT 138,&20:OUT 139,&6:i%=INP(140)
3175 REM
3200 DEF minutes%
3210 =INP(132)*60+INP(130)
3215 REM
3300 DEF gettime
3320 t$=STR$(INP(135))+":"+STR$(INP(136))+":"+STR$(INP(137))
3330 t$=t$+"   "+STR$(INP(132))+":"+STR$(INP(130))
3340 ENDPROC
3345 REM
3499 REM
3500 DEF pumpson
3505 l1$="*** PURGING ***":DScreen
3510 setrelay(p1%,true):setrelay(p2%,true)
3520 delay(1)
3530 IF INP(&FE1)=0 THEN GOTO 3520
3540 setrelay(p1%,false):setrelay(p2%,false)
3600 ENDPROC
4000 DEF adval(chan%)
4010 LOCAL i%,j%
4020 OUT &EE,chan%:OUT &EE,chan%+&80:REM start conversion
4030 WHILE INP (&EE) < 128 : WEND
4035 delay(0.5)
4040 i%=INP(&EC):j%=INP(&ED)
4050 i%=i%+&100*(j% AND &F): IF (j% AND 63)<32 THEN i%=-i%
4060 OUT &EE,chan% : REM stop the converter
4100 =i%
4110 REM
5000 DEF capture(chan%,Hz%)
5001 l2$="CAPTURING SIGNAL":DScreen
5010 LOCAL counter%,i%,z%
5020 counter%=0 : i%=15
5030 WHILE 2**(16-i%)<Hz% : i%=i%-1 : WEND
5040 IF i% < 11 THEN i%=11 : REM max of 32 Hz
5050 OUT 138,&20+i% : OUT 139, &46
5100 REPEAT
5200 WHILE INP(140)<192 : WEND
5220  OUT &EE,chan% : OUT &EE,chan%+&80
```

```
5225 FOR i%=1 TO 10 : NEXT i%
5230  WHILE INP(&EE) < 128 : WEND
5240  z%=INP(&EC)+&100*((INP(&ED)) AND &F)
5300  ad%(counter%)=z% : counter%=counter%+1
5400 UNTIL counter% >= adelements%
5500 OUT 138,&20 : OUT 139, &6 : i%=INP(140)
5600 ENDPROC
5605 REM ************************************************
5610 REM ANALYSIS
6000 DEF initanalysis
6010 setrelay(v1%,1)
6015 l2$="FLUSHING WITH SAMPLE":DScreen
6020 setrelay(p1%,1)
6030 delay(flushdel%)
6090 ENDPROC
6095 REM
6100 DEF initstand
6110 setrelay(v2%,1):setrelay(v1%,1)
6120 l2$="FLUSHING WITH STANDARD":DScreen
6130 setrelay(p1%,1)
6140 delay(flushdel%)
6150 ENDPROC
6155 REM
7000 DEF getpeak
7010 setrelay(p1%,1):setrelay(p2%,1)
7011 l2$="FILLING LOOP":DScreen
7020 setrelay(v1%,1)
7030 delay(filldel%)
7040 setrelay(v1%,0)
7050 setrelay(p1%,0)
7051 l2$="INJECTING":DScreen
7060 delay(injdel%)
7065 REM sampling channel & frequency
7100 capture(1,8)
7200 setrelay(p2%,0)
7201 l2$="PROCESSING DATA":DScreen
7300 =findpeak
7310 REM Processing Data
7500 DEF findpeak
7590 REM background = first 8 elements
```

```
7600 t=0
7610 FOR i=0 TO 7:t=t+ad%(i):NEXT i
7620 bgd=t/8
7625 REM find position of max value
7630 max%=-1:p%=10
7640 FOR i=4 TO adelements%-5
7650  IF ad%(i)>max% THEN max%=ad%(i):p%=i
7660 NEXT i
7668 REM peak = mean 0.5 sec either side of max
7670 t=0
7680 FOR i=p%-4 TO p%+4
7690   t=t+ad%(i)
7700 NEXT i
7710 peak=t/9
7800 =peak-bgd
7810 REM
8000 DEF analyse
8005 count%=count%+1:l1$="*** ANALYSING ***"
8008 fails%=0:gettime
8010 FOR i%=1 TO 5:flag%(i%)=false:NEXT i%
8015 l1$="*** ANALYSING ***"
8120 IF sampint%-(minutes MOD sampint%)<cycletime% THEN
       flag%(1)=true:GOTO 8700
8200 initanalysis
8210 u1=getpeak:u2=getpeak
8250 initstand
8260 s1=getpeak:s2=getpeak
8265 IF s1=0 OR s2=0 THEN flag%(1)=true
8266 IF s1=0 OR s2=0 THEN flag%(2)=true
8267 IF s1=0 OR s2=0 THEN GOTO 8370
8290 setrelay(v2%,0):REM deactivate switch valve
8291 l1$="ANALYSIS CYCLE COMPLETE":l2$="=====":DScreen
8300 IF ABS(1-s1/s2)>0.1 THEN flag%(2)=true
8370 s1=s1+s2
8380 IF (s1>maxpeak) AND (flag%(2)=false) THEN maxpeak=s1
8390 IF s1<maxpeak*sensthresh THEN flag%(1)=true
8400 IF ABS(u1-u2)>mvdiff THEN flag%(3)=true
8450 u1=(u1+u2)*standconc/s1
8460 IF u1>maxexpect THEN flag%(4)=true
8470 IF u1<minexpect THEN flag%(5)=true
```

```
8500 pr$=t$+" ("+STR$(count%)+") Al Concn. "+STR$(u1)+" ppb"
8501 REM ************************************************
8502 REM OUTPUT
8503 output
8505 OUT 188,10
8600 err%=false
8610 FOR i=1 TO 5:err%=err%+flag%(i):NEXT i
8620 IF err%=0 THEN ENDPROC
8700 fails%=fails%+1
8705 pr$="ERROR CODE: "
8710 output
8720 code
8750 IF fails%<maxfails% THEN GOTO 8010
8800 ENDPROC
8810 DEF output
8820 FOR op=1 TO LEN(pr$)
8830 st=INP(189) AND 8
8840 IF st=8 THEN GOTO 8830
8850 byt$=MID$(pr$,op-1,1)
8860 OUT 188,ASC(byt$)
8870 NEXT op
8890 ENDPROC
9000 REM ERROR CODES
9010 REM flag 1 = low standard reading
9020 REM flag 2 = standard reproducibility
9030 REM flag 3 = sample reproducibility
9040 REM flag 4 = value higher than expected
9050 REM flag 5 = value lower than expected
9055 REM Printer Output Control
9060 DEF code
9070 FOR ec=1 TO 5
9080 st=INP(189) AND 8
9090 IF st=8 THEN GOTO 9080
9100   IF flag%(ec)=true THEN OUT 188,88
9110   IF flag%(ec)=true THEN GOTO 9130
9120   OUT 188,79
9130 NEXT ec
9140 OUT 188,10
9150 ENDPROC
```

APPENDIX D

Presentations

1. Spectrophotometric FI Techniques for Process Monitoring. Poster presentation, Research and Developments Topics Meeting, Dublin City University, Dublin, 21/3/89.
2. The On-Line Determination of Residual Coagulants in Potable and Treated Waters by FIA. Poster presentation, Anatech '90, Noordwijkerhout, The Netherlands, 4/4/90.
3. The On-Line Determination of Residual Coagulants in Potable and Treated Waters by FIA. Poster presentation, Research and Developments Topics Meeting, ICI C & P Ltd., Runcorn, Cheshire, 16/7/90.
4. On-Line Spectrophotometric Techniques for Water Quality Monitoring. Lecture Presentation, Research and Developments Topics Meeting, University of Aberdeen, Aberdeen, 9/7/91.
5. Remote Spectrophotometric Water Quality Monitoring. Poster presentation, Flow Analysis V, Kumamoto, Japan, 23/8/91.
6. On-Line Determination of Aluminium and Other Determinands. Lecture presentation, Metal Speciation in Natural Waters, RSC Western Region, Polytechnic South West, Plymouth, 17/9/91.

Publications

1. Spectrophotometric FI Techniques for Process Monitoring, Anal. Proc., 26 (1989) 385-387.
2. On-Line Determination of Residual Aluminium in Potable and Treated Waters by FIA, Anal. Chim. Acta, 238 (1990) 177-182.
3. Recent Developments in Water Quality Monitoring by FIA, TrAC, 10 (1991) 11-17.
4. A FI Approach to the Continuous Monitoring of Residual Coagulants (Aluminium and Iron) in Potable and Treated Waters, Sci. Tot. Environ., in press.